THE UNIVERSITY OF HULL

GENETIC ANALYSIS OF SQUAMOUS CELL CARCINOMA OF THE HEAD AND NECK

Being a thesis submitted for the degree of

Doctor of Philosophy

in the University of Hull

By

James Nicholas Edmund Ashman, B.Sc. (Hons) University of Nottingham

May 2002

Synopsis

Head and neck squamous cell carcinoma (HNSCC) is the sixth commonest cancer worldwide with an increasing incidence in developing countries. Despite numerous advances in surgery, radiotherapy and chemotherapy over the past few decades the overall survival rate for patients with HNSCC has changed little. Currently, the management of HNSCC patients is based on the assessment of a variety of clinical and pathological parameters. However, in many instances, these factors fail to accurately predict the clinical behaviour of an individual patients tumour. HNSCC therefore, is a tumour entity that would benefit from a greater insight into the chromosomal alterations underlying the disease. Knowledge of such alterations would be expected to provide many benefits to the HNSCC clinician in terms of diagnostic and prognostic markers and may eventually identify novel molecular targets for therapeutic intervention.

This thesis was aimed at characterising the chromosomal abnormalities involved in the tumourigenesis of HNSCC, principally using the powerful molecular cytogenetic technique of comparative genomic hybridisation (CGH), and the clinical applications of such data. Firstly, the technique was optimised and initially applied to specimens of primary HNSCC and surrounding uninvolved mucosa from 19 patients in order to investigate the phenomenon of 'field cancerization'. Specimens of primary HNSCC and histologically normal mucosa taken from 1cm and 5cm distant to the primary site were analysed from each patient in order to characterise the chromosomal abnormalities associated with malignant tissue and attempt to identify aberrations underlying the 'field change'. CGH of the primary tumour specimens revealed numerous chromosomal aberrations with a relatively consistent pattern. Frequent deletions of DNA were identified on chromosome 3p, 4p, 8p, 9p, 11q, 13q and 18q and frequent gains on chromosomes 2q, 3q, 5p, 7q, 8q, 9q and 11q. The histologically normal mucosa did not show chromosomal abnormalities within the cells analysed. Therefore, if molecular abnormalities were present in the mucosa surrounding a primary HNSCC they would be below the resolution of CGH, such as subtle point mutations, or only present in a minority of cells.

In order to investigate the genetic relationship between primary HNSCC and lymph node metastases, matched pairs of primary and metastatic tumours were obtained from 18 patients and analysed by CGH. Whilst the overall frequency of genetic alterations was similar between primary and metastatic tumours, a surprising degree of discordance was identified between each individual's matched pair of tumours. At least one common aberration was identified in all cases studied, however the percentage of aberrations detected in the lymph node metastases that were shared with the primary tumour varied greatly, ranging from 100% - 8.3%. Several chromosomal regions were found to be altered at similar frequencies in both the primary and metastatic tumours. Most interestingly, regions of the genome found to be altered at a higher frequency in the population of metastatic HNSCC included deletion of 4p15.3-pter and 17q22-qter and gain of 6qcen-q15 and 13q21-22. In addition, both gains and deletions of material from chromosome 22 were found at a higher frequency in the metastatic tumours. These chromosomal regions may contain genes important in the process of metastasis in HNSCC. The level of discordance identified between matched pairs of tumours also suggests that a linear progression model may not satisfactorily explain the progression to metastases in all HNSCC.

This thesis also addressed the important clinical question of resistance to radiotherapy demonstrated by a significant fraction of laryngeal tumours. No markers that reliable predict the response of an individual tumour to radiotherapy are currently available. The expression of a panel of markers involved in DNA damage recognition, cell cycle arrest,

DNA repair and apoptosis were evaluated in 23 glottic laryngeal tumours (8 radio-resistant and 13 radio-sensitive). Of these, the expression of bcl-2, an anti-apoptotic marker, was specifically associated with the resistant phenotype. This statistically significant association provides preliminary evidence for the dysregulation of apoptosis as a mechanism by which resistant tumours can evade radiotherapy induced tumour regression.

Overall, CGH analysis of primary HNSCC identified a relatively consistent pattern of DNA alterations with several distinct regions of DNA deletion and gain identified. Frequent deletions of DNA were identified on chromosomes 1p, 2q, 3p, 4p, 4q, 5q, 7q, 8p, 9q, 10q, 11p, 11q, 13q, 17p, 18q, 19 and 21 and frequent gains of DNA on chromosomes 1q, 2q, 3q, 4q, 5p, 6q, 7p, 7q, 8q, 11q, 12p, 13q, 18p and 18q. Chromosome 3 was the most frequent site of both deletions and gains. Follow up data was obtained for all patients analysed by CGH and Kaplan-Meier survival analysis demonstrated a significant correlation between gain of DNA on 3q25-27 and reduced overall survival. This finding highlights the necessity for further, high resolution, characterisation of this region in order that the specific genetic marker can be identified. This thesis demonstrates that molecular analysis of tumours is able to offer new, and valuable information for the understanding of HNSCC carcinogenesis and that these data can be used to compliment existing methodology. Further work is required to isolate specific genes and to understand their interactions.

Acknowledgements

This thesis was undertaken whilst working in the Academic Department of Otolaryngology and Head and Neck Surgery, part of the Academic Surgical Unit, University of Hull. I am indebted to many people for their help and guidance during the course of my studies, the most important of whom I will endeavour to recognise here.

I am deeply indebted to Dr John Greenman for his supervision and guidance throughout my PhD and for his great enthusiasm for research that kept me going whilst facing the many technical challenges encountered during my course of study. Without this constant support and encouragement I would not have been able to complete this thesis. I would also like to express my thanks for the many hours of spent reviewing this manuscript and the valuable criticisms and comments received.

Secondly, I owe immeasurable thanks to Professor Nicholas Stafford for employing me and for giving me the opportunity to undertake this research. I am also immensely grateful for all his help and for providing me with the clinical specimens without which I would not have had the opportunity to carry out this research.

I would like to acknowledge the help of the many members of the Department of Histopathology, Hull and East Yorkshire Hospitals, for their assistance in obtaining archival specimens. Special thanks go to Dr Alistair MacDonald, Consultant Histologist, for his patient assistance in reviewing the many pathological specimens involved in this thesis.

I would also like to thank Mr Luke Condon for all his help in obtaining the clinical and pathological information relating to the patients studied in this thesis. For this help in mining the masses of patient notes, databases and pathology reports I am truly thankful. For deeming the finding of this thesis worthy of pursuing I am flattered, and for keeping me involved and for agreeing to aid in presenting the findings I am grateful.

My thanks also go to the many members of the Departments of Surgery, Medicine and Oncology, past and present, whom I have worked with closely over the last few years. Without this rich source of scientific knowledge and the active social calendar my time in Hull would have been far more difficult. I would especially like to thank Dr Lynn Cawkwell for employing me after finishing the experimental phase of my PhD and continuing to support me during the writing of this thesis.

Finally, all my love and thanks go to my parents without who's love and support this thesis, and many other things, would never have been possible.

Contents

Chapter 4 – Establishment of CGH

Chapter 5 – Results

Chapter 6 – Results

Chapter 7 – Results

List of Figures

List of Figures (continued)

List of Tables

Thesis associated publications

Publications relating directly to this Thesis

Papers

Genetic analysis of field cancerization of squamous cell carcinoma of the head and neck using comparative genomic hybridization. Stafford ND, Ashman JNE, MacDonald AW, Ell SR, Monson JRT, Greenman J.
Archives of Otolaryngology-Head and Neck Surgery, **125**(12):1341-1348 (1999).

Multiple cell populations in colorectal carcinomas: analysis by 3-colour fluorescence in situ hybridization. Greenman J, Ashman JNE, Brankin V, McDonald AW, Duthie GS, Lee PWR, Kerin MJ, Monson JRT.
International Journal of Oncology, **12**(1):75-80 (1998).

Overexpression of Bcl-2 in Squamous Cell Carcinoma of the Larynx: A marker of Radioresistance. Condon LT, Ashman JNE, Cawkwell L, Ell SR, Greenman J, Stafford ND.
International Journal of Oncology (in press)

Manuscripts in preparation

Comparison of primary head and neck squamous cell carcinomas and lymph node metastases: Discordance between matched pairs.

Genetic aberrations in head and neck squamous cell carcinoma identified by comparative genomic hybridisation – Association of gain of 3q25-27 and reduced survival.

Published Abstracts

Chromosomal changes in squamous cell carcinoma of the head and neck and involved lymph nodes: Identification of a metastatic genotype. Ashman JN, Ell SR, Greenman J, Stafford ND.
British Journal of Cancer, **80**:12 (1999).

Genetic analysis of head and neck squamous cell carcinoma and surrounding uninvolved mucosa by comparative genomic hybridization. Ashman JNE, Greenman J, Ell SR, Stafford ND.
British Journal of Cancer, **78**(2):153-153 (1998).

Overexpression of bcl-2 in squamous cell carcinoma of the larynx: A marker of radio-resistance. Condon LT, Ashman JNE, Cawkwell L, Ell SR, Greenman J, Stafford ND.
European Journal of Surgical Oncology, **27**(8):815 (2001).

Role of 3q gain in solid tumour formation. Loveday RL, Ashman JNE, Mehigan BJ, Rogers C, Grundy C, Stafford ND, Greenman J, Monson JRT.
British Journal of Surgery, **88**(5):755-755 (2001).

Colorectal tumours are highly heterogenous in chromosome number at the single cell level.
Greenman J, Ashman J, Brankin V, Duthie GS, Lee PWR, Kerin MJ, Monson JRT.
British Journal of Surgery, **85**(5):710-710 (1998).

Other Presentations

Evidence for the 'field cancerization' theory is not seen by comparative genomic hybridization of squamous cell carcinoma of the larynx. Ell SR, Ashman JNE, Greenman J, Stafford ND.
Oral presention at the Otolaryngological Research Society , Autumn 1997.

A comparison of CGH analysis from laryngeal and breast tumours:- variation between countries.
Greenman J, Ashman JNE, Loveday R.
Oral presentation at the 5th Smart Capture users meeting September 1998

Other Publications related to this thesis

Manuscripts in preparation

A comparison of three colour fluorescence in-situ hybridisation and comparative genomic hybridisation in primary colorectal cancer. Mehigan BJ, Greenman J, Ashman JN, Topping K, Kerin MJ, Monson JRT.

Genetic aberrations in colorectal primary tumours identified using comparative genomic hybridisation. Mehigan BJ, Greenman J, Ashman JN, Loveday RL, McDonald A, Kerin MJ, Monson JRT.

Influence of mismatch repair and p53 status on genetic aberrations as detected by comparative genomic hybridization. Mehigan BJ, Cawkwell L, Bedford KJ, Baker RP, Ashman JN, Greenman J, Monson JRT.

Published Abstracts

Influence of mismatch repair and p53 status on genetic aberrations as detected by comparative genomic hybridization. Mehigan BJ, Cawkwell L, Bedford KJ, Baker RP, Ashman JN, Greenman J, Monson JRT.
British Journal of Surgery, **88**(5):754-755 (2001).

Identification of the isoform-specific vascular endothelial growth factor receptor, neuropilin 1, and enhanced vascular endothelial growth factor receptor production in colorectal carcinoma. Easterbrook JR, Greenman J, Ashman JNE, MacDonald AW, Monson JRT.
British Journal of Surgery, **88**(5):753-754 (2001).

Genetic analysis of colorectal cancer primary tumours and cell lines using comparative genomic hybridisation. Mehigan B J, Loveday R L, Ashman J N, Malone C, Greenman J, Hartley JE, Kerin MJ, Monson JRT.
Colorectal Disease, **1**(Suppl. 1):18 (1999).

Novel colorectal oncogenes and tumour suppressor genes identified using comparative genomic hybridisation. Mehigan B J, Ashman J N, Malone C, Greenman J, Hartley JE, Kerin MJ, Monson JRT.
Irish Journal of Medical Science, **168**(Suppl. 6):59 (1999).

Other presentations

The expression of vascular endothelial growth factor (VEGF) and VEGF-C in early glottic laryngeal squamous cell carcinoma and their relationship with radioresistance. Homer JJ, Ashman J, Greenman J, Stafford ND.

Oral presentation at the British Association of Otalryngologists-Head and Neck Surgeons, Nottingham 7-8 September 2000.

Identification of genetic aberrations in colorectal tumours using comparative genomic hybridisation. Mehigan BJ, Ashman JN, Loveday RL, Greenman J, Hartley J, Kerin MJ, Monson JRT.

Oral Presentation at the 3rd Nottingham International Colorectal Cancer Symposium, University of Nottingham, October 1999.

Genetic analysis of colorectal cancer primary tumours and cell lines using comparative genomic hybridisation. Mehigan BJ, Loveday RL, Ashman JN, Malone C, Hartley JE, Greenman J, Monson JRT.

Oral presentation at the Royal Academy of Medicine in Ireland. Registrars Prize meeting. RCSI Dublin, January 1999. 2nd prize.

Chapter 1

Head and Neck Squamous Cell Carcinoma
Clinical Aspects

1.1 Introduction - Squamous cell carcinoma of the head and neck

Head and neck squamous cell carcinoma (HNSCC) comprise a heterogenous group of tumours of the head and neck region including those arising in the oral cavity, nose, pharynx and larynx (Figures 1.1 and 1.2). Tumours of the brain and central nervous system are excluded and considered a separate speciality. The majority of head and neck cancers arise in the mucosa lining the upper aero-digestive tract (UADT) comprising the lips, oral cavity, pharynx, larynx, and cervical oesophagus. The approximate distribution of HNSCC is as follows: oral cavity, 44%; larynx, 31% and pharynx, 25%. Other tumour sites that traditionally come under the definition of head and neck cancer are the nose, parasinuses, salivary glands, thyroid, parathyroid and skin. Squamous cell carcinoma, originating in the epithelial cells that constitute the mucosa of the UADT, accounts for 95% of all head and neck tumours (Figure 1.3; Jafek and Stark, 1996). The remaining 5% are almost all adenocarcinoma, with mucoepidemoid and adenocystic carcinomas presenting rarely.

Cancer of the head and neck conveys major social repercussions on the individual patient. Many aspects of normal, daily life are affected both by the disease and the therapy employed. These include breathing, chewing, speech, swallowing and, perhaps most importantly, the confidence of the patient. HNSCC patients face significant reductions in their quality of life after surgical resection as reconstruction is challenging due to the complex anatomy of the region. Despite advances in reconstructive surgery and rehabilitation patients who have undergone major resections such as laryngectomy or glossectomy can be left with significant cosmetic and functional disabilities. Management of the HNSCC patient requires a multi-disciplinary approach involving not only the surgeon and radiotherapist but also the speech therapist and dietician.

Head and neck cancer continues to be a major disease with significant morbidity and mortality. Significant benefit would be gained from a better understanding of its molecular basis and pathogenesis. The identification of novel molecular markers would be valuable in the management of HNSCC patients and potentially lead to exciting developments in novel therapeutic strategies.

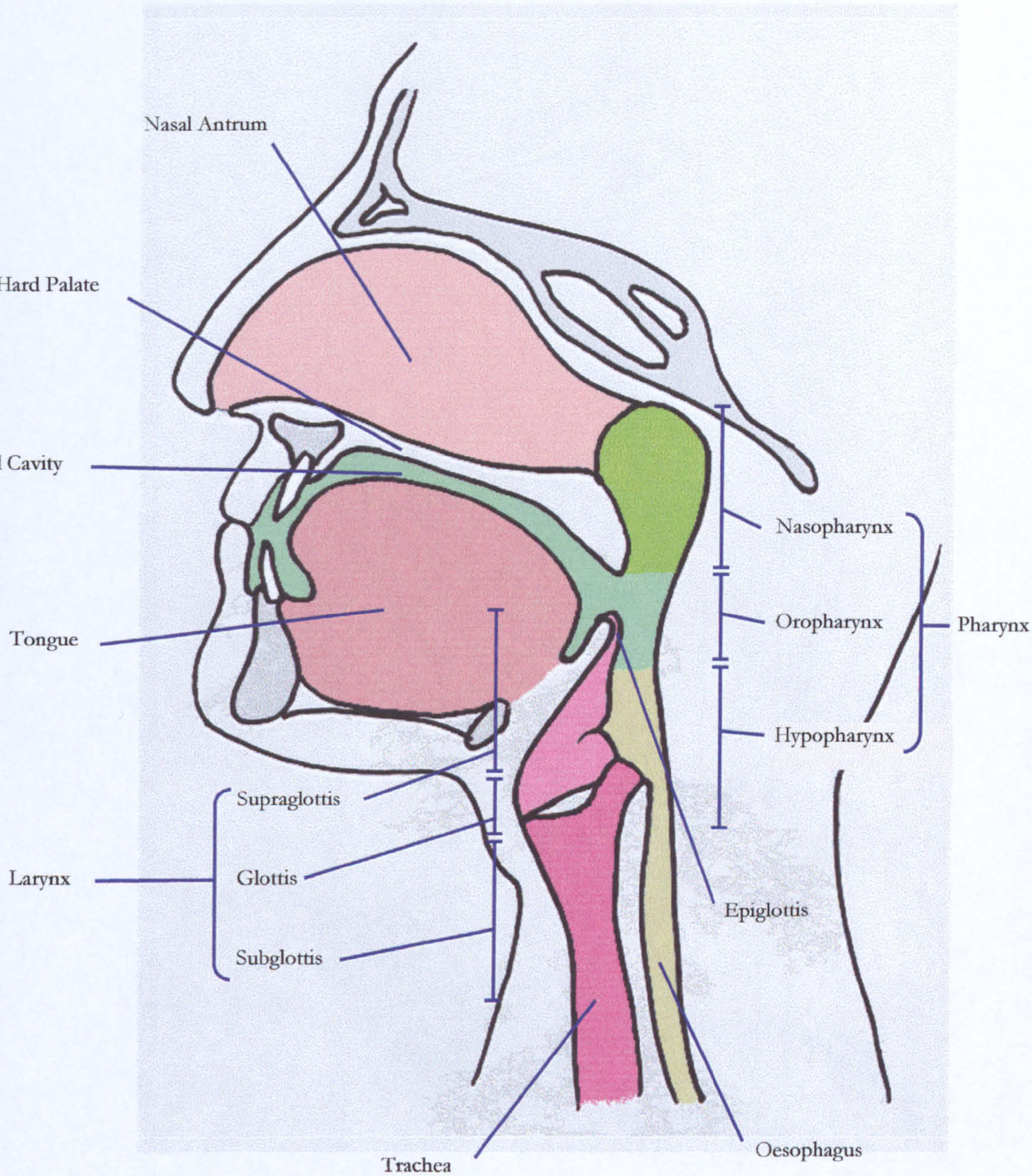

Figure 1.1 – Anatomy of the Head and Neck region. Head and neck squamous cell carcinoma encompasses a diverse group of tumours arising in the epithelium lining the structures depicted above.

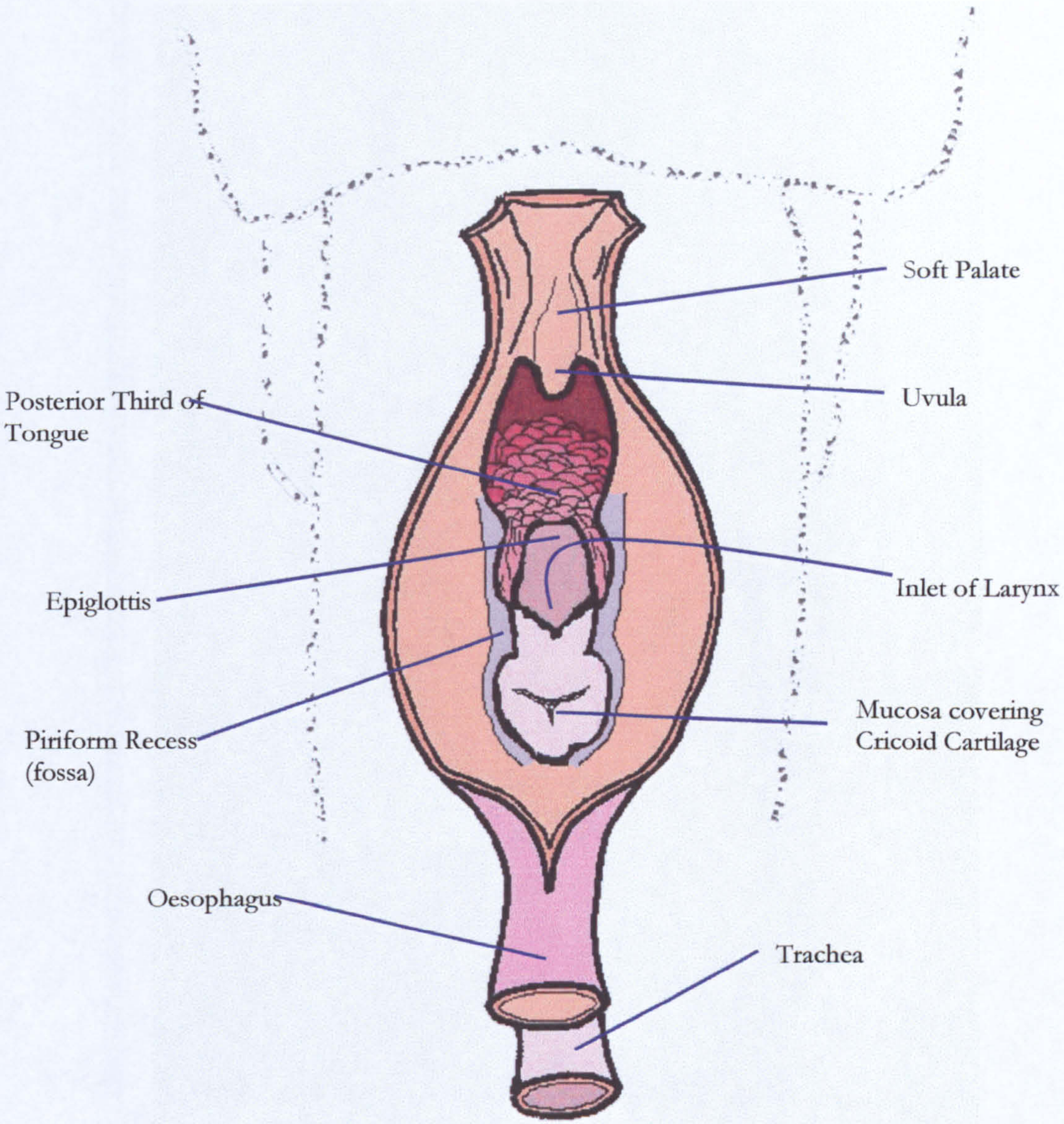

Figure 1.2 – Anatomy of the larynx/pharynx. Posterior view adapted from Agur and Lee (1999).

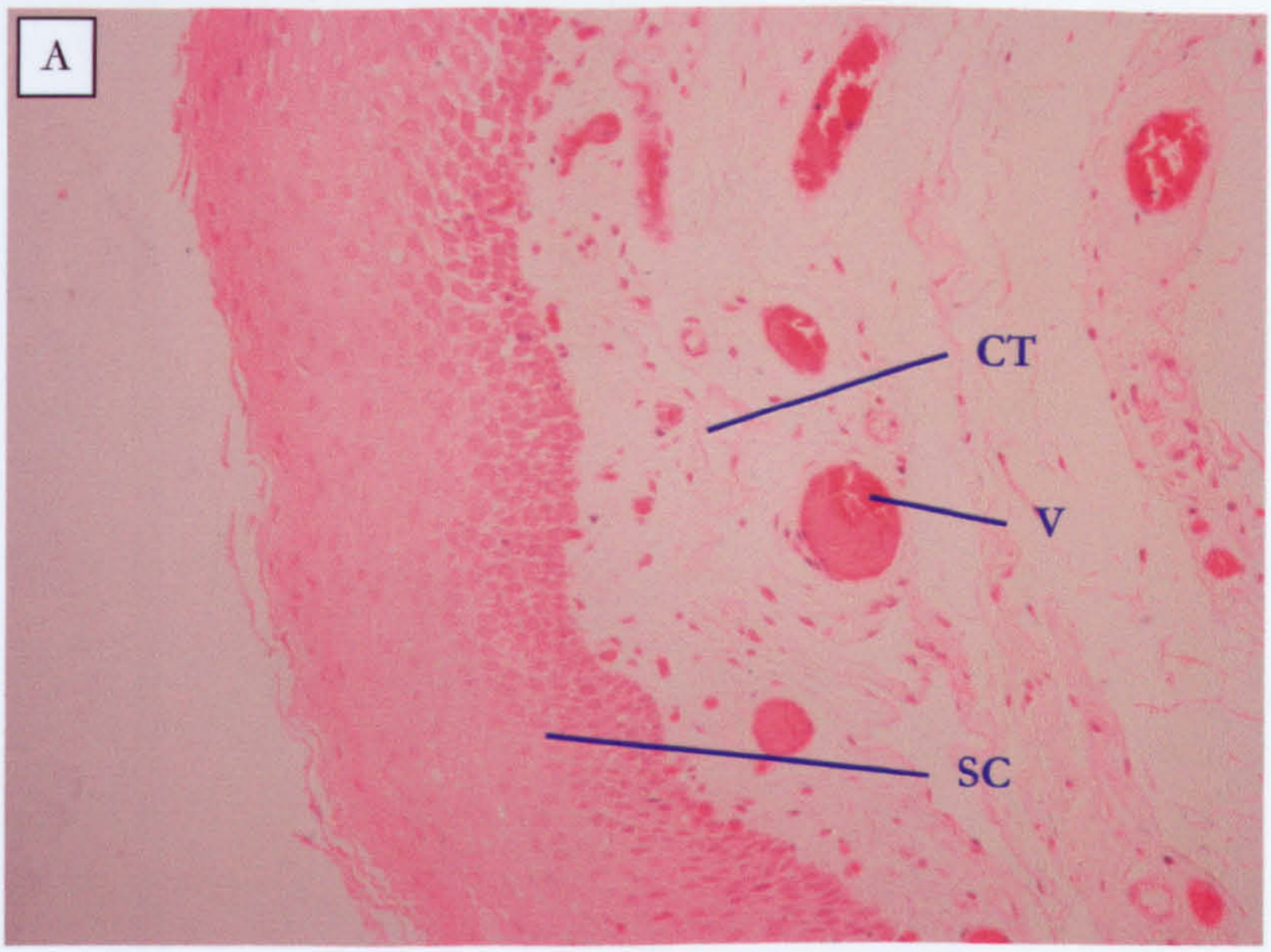

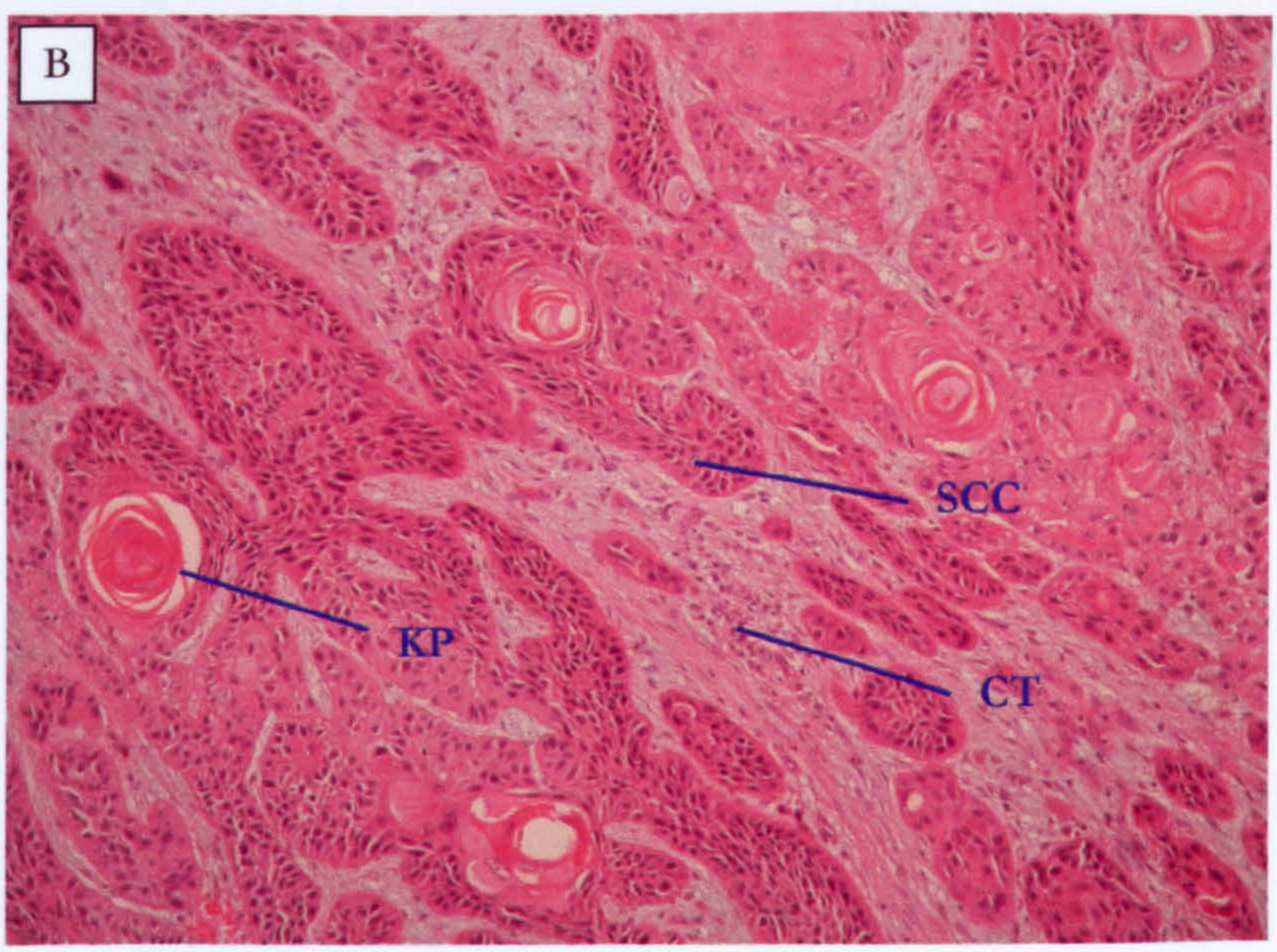

Figure 1.3 – Histology of Head and Neck Squamous Cell Carcinoma. Haemotoxylin and Eosin stained tissue sections (Magnification x400). Figure 1.3(A) depicts the appearance of normal, stratified squamous epithelium of a human uvula removed from a chronic snorer. A regular layer of stacked squamous cells (SC) can be with underlying connective tissue (CT). Blood vessels (V) are also visible in the connective tissue. Figure 1.3(B) depicts an H&E stained section of invasive SCC. 'Nests' of malignant squamous cell carcinoma (SCC) are visible invading into the surrounding connective tissue. Characteristic Keratin pearls (KP), whorls of accumulated keratin, are also visible.

1.1.1 Incidence of HNSCC

Current figures indicate an incidence of approximately 500,000 newly diagnosed cases world-wide per year, making HNSCC the sixth most common cancer constituting 5% of cancers in the developed world (Vokes *et al*, 1993). Globally, there is a marked variation reflecting the different aetiological risk factors associated with the disease. In the East and Far East, incidences of oral and pharyngeal cancers are far greater and account for nearly half of all cancers. This relates to local habits of betel quid consumption and the practice of reverse smoking of homemade cigars (Squire *et al*, 1984). Incidence in the UK shows a slight regional variation between 15.3 cases per 100 000 population in Wales to 7.7 per 100 000 in South-East Thames (Effective Head and Neck Cancer Management, Second Consensus Document – 2000). Within the Northern and Yorkshire region approximately 500 cases are diagnosed each year, the disease constituting 2.8% of all malignancies (Northern and Yorkshire Cancer Registry Information service). The incidence of HNSCC increases with age, and patients are typically over the age of 50. There is also a strong association with socio-economical profile. Whilst male to female ratios of HNSCC vary widely depending on tumour site and geography, at all but one site there is a preponderance of cases in men. The only exception being cancer of the hypopharynx, where a female preponderance of post cricoid cancer is association with Paterson-Brown-Kelly syndrome (characterized by iron deficiency anaemia, glossitis and upper oesophageal webbing; Morton and McIvor, 1997).

Despite advances in surgical technique, radiotherapy and chemotherapy, over the last 20 years, only marginal improvements have been seen in the 5-year survival rate, which is still among the lowest of the major cancers. Early stage HNSCC (T1/T2 tumours without lymph node involvement), especially those situated in the oral cavity and larynx, have a high cure rate (approximately 80%; Effective Head and Neck Cancer Management, Second Consensus Document – 2000). However, at presentation, over 60% of cases are advanced, resulting in a considerable worse prognosis. Survival rates in Yorkshire (for the period 1986-1990) were 63% at 2 years and 53% at five years reflecting the high incidence of advanced cases. (Northern and Yorkshire Cancer Registry Information service).

1.1.2 Anatomical site of HNSCC

One of the major difficulties involved in the interpretation of studies and trials on HNSCC results from the grouping together of patients with tumours arising from a variety of sites with only a relatively small number of patients having tumours at a specific anatomical site.

Patterns of tumour growth, extension and metastases vary significantly depending on the anatomical site of the primary tumour, and this must be taken into account when interpreting data. The majority of the work in this thesis is concerned with laryngeal cancer, the most common form of HNSCC in the UK (Effective Head and Neck Cancer Management, Second Consensus Document – 2000).

1.1.3 Staging of laryngeal cancer

Optimal therapy for any cancer depends upon the proper identification of the primary tumour as well as determining the local, regional, and distant extent of disease. Staging of squamous cell carcinoma attempts to classify the local extent and spread of the tumour by histological assessment of resected specimens. Staging of all cancers is based on the tumour, nodal metastases and distant metastases system (TNM) devised jointly by the Union Internationalle Contre le Cancer (UICC) and the American Joint Committee on Cancer (AJCC) and revised in 1997. Staging assists in the planning of a patient's treatment and provides limited prognostic information. In addition, a universally adopted staging system allows the comparison and exchange of information between researchers from different institutions.

Staging is only a rough guide to prognosis and does not overcome the difficulty in predicting the behaviour of individual tumours. The diversity of anatomical sub-sites of HNSCC is reflected in the clinical behaviour of each tumour and consequently TNM definitions vary depending on the location of the tumour. As the majority of the tumours investigated in this thesis were laryngeal, the laryngeal staging system is detailed in below. Staging of both laryngeal and non-laryngeal will be referred to extensively in this thesis and a complete explanation of the staging system for all head and neck cancer can be found in Effective Head and Neck Cancer Management (Second Consensus Document, 2000)

1.1.3.1 Anatomy of the larynx

The larynx, or voice box, consists of a cartilaginous framework covered by mucosa attached above to the hyoid bone by the thyrohyoid membrane and below to the trachea. The larynx is divided into three anatomical regions (Figure 1.4), the supraglottis, the glottis and the subglottis. Tumours of these sub-sites have significantly different behaviours. Staging varies depending on the anatomical location of the tumour within the larynx and is detailed below.

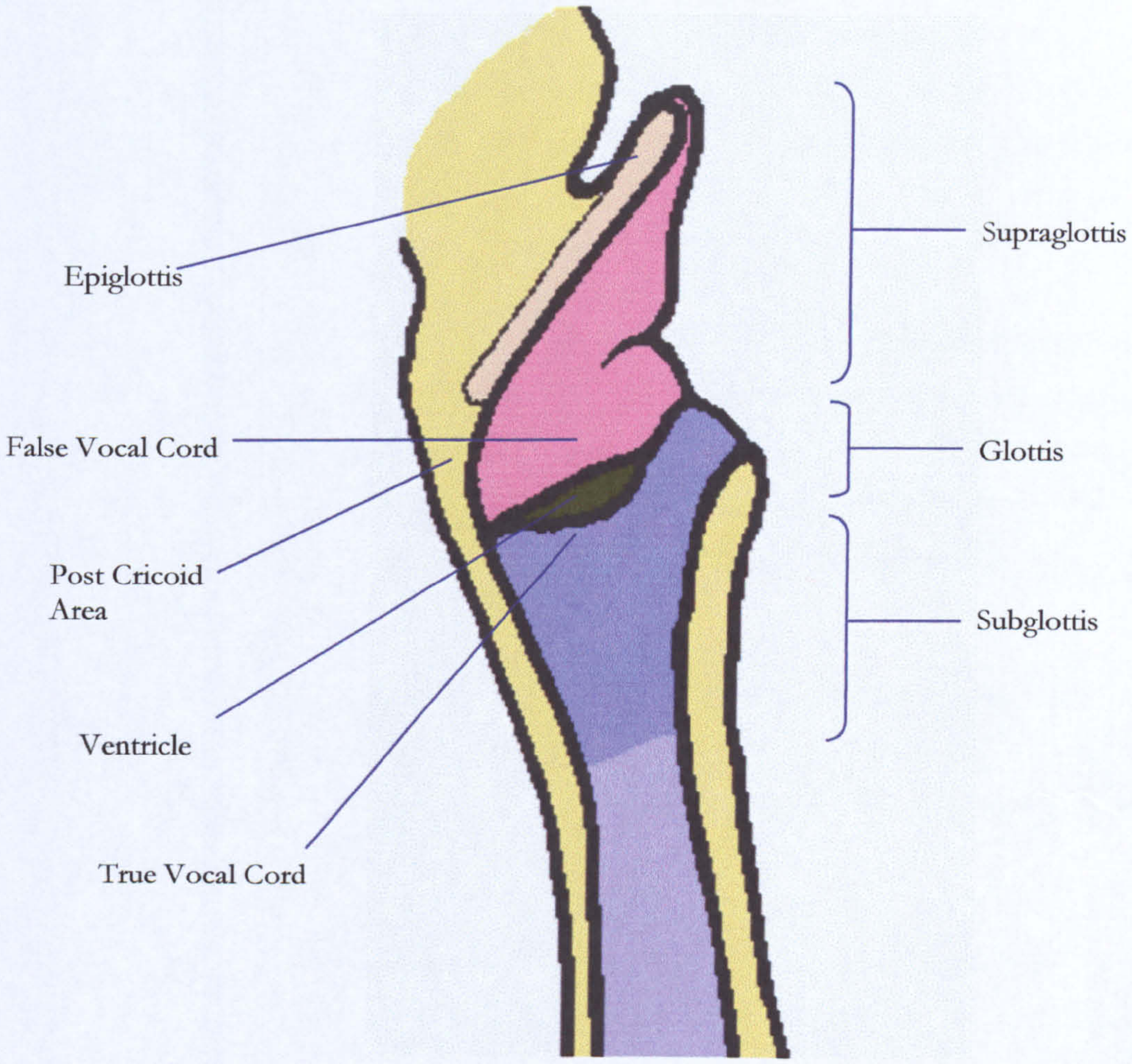

Figure 1.4 – Anatomy of the Larynx. The larynx consists of three distinct anatomical areas, the supraglottis, the glottis (encompassing the region of the vocal cords), and the subglottis. Tumours arising within the different areas have differing biological characteristics – including the propensity to metastasise, due to differences in lymphatic drainage.

Supraglottic larynx

This is the largest region of the larynx extending up to the base of the tongue and including the epiglottis, the aryepiglotic folds, the arytenoids and the false vocal cords. In a Western population, supraglottic cancers account for 30% of laryngeal cancers and tend to produce few symptoms, accounting for the advanced stage at which most patients cancers present (O'Connor and Lund, 1998). The supraglottic area is rich in lymphatic drainage resulting in a tendency for early spread, and approximately 25-50% of patients present with involved lymph nodes (Magnano *et al.*, 1997).

Glottic larynx

The glottis consists of the two true vocal cords, the narrow fibrous bands which vibrate to produce sound. Cancers of the glottis tend to produce early symptoms, usually an alteration in voice, and account for the majority of laryngeal tumours (approximately 65%). The true vocal cords have very poor lymphatic drainage and tumours that have not extended above or below the cords rarely present with involved lymph nodes (Stell, 1987).

Subglottic larynx

This constitutes the region bounded by the vocal cords and the superior limit of the trachea. Cancers of the subglottis are rare (less than 5% of laryngeal cancer) and tend to be poorly differentiated. Most present as advanced lesions and metastases occur in approximately 20% of patients (Stell, 1987).

The TNM staging system for laryngeal cancer (Table 1.1) allows for the allocation of stage into 24 possible sub-categories. A more simple classification system for head and neck cancer has been devised to group different tumours with similar prognosis into a single stage group (Table 2.2). This combines the individual TNM stages and gives an overall measure of tumour advancement.

Early cancers are defined as stage I and II, these are localised cancers without detectable spread to regional lymph nodes. Prognosis for early cancers is good for all sites within the larynx with cure rates of 50-95% (Stell, 1987; Hoffman *et al*, 1998).

Site	T Stage	Description
Common to all sites	Tx	The primary tumour cannot be assessed
	T0	No evidence of primary tumour
	Tis	Carcinoma *in-situ*
Supraglottis	T1	Tumour limited to one subsite, normal vocal cord mobility
	T1a	Tumour limited to one true vocal cord
	T1b	Tumour involves both vocal cords
	T2	Tumour invades more than one subsite, normal vocal cord mobility
	T3	Tumour limited to larynx; vocal cord fixation or invasion of post cricoid area, medial wall of piriform sinus, or pre-epiglotic space
	T4	Tumour invades adjacent structures
Glottis	T1	Tumour limited to vocal cords, normal mobility
	T1a	Tumour limited to one cord
	T1b	Tumour involves both cords
	T2	Tumour extends to supraglottis/subglottis, impaired vocal cord mobility
	T3	Tumour limited to larynx, vocal cord fixation
	T4	Tumour invades adjacent structures
Subglottis	T1	Tumour limited to subglottis
	T2	Tumour extends to glottis, normal or impaired mobility
	T3	Tumour limited to larynx, vocal cord fixation
	T4	Tumour invades adjacent structures

N Stage	N0	No regional metastases
	N1	Metastases in single ipsilateral node and <3cm in size
	N2a	Metastases in single ipsilateral node 3-6cm
	N2b	Metastases in multiple nodes <6cm
	N2c	Metastases in bilateral nodes <6cm
	N3	Metastases > 6cm

M Stage	Mx	Presence of distant metastases cannot be assessed
	M0	No distant metastases
	M1	Distant metastases

Table 1.1 – The TNM classification system for laryngeal cancer.

T- Tumour; N- Node; M- Metastasis

Stage group	TNM	5-year Survival
Stage 0:	Tis, N0, M0	90%+
Stage I:	T1, N0, M0	65-90%
Stage II:	T2, N0, M0	50-80%
Stage III:	T3, N0, M0 T1-T2-T3; N1, M0	35-60%
Stage IV:	T4, N0 or N1, M0 Any T, N2 or N3, M0 Any T, any N, M1	10-30%

Table 1.2 Staging of Laryngeal cancer. From (Stell, 1987; Hoffman *et al*, 1998). Tis – carcinoma *in-situ*.

1.1.4 Histological assesment

Histological examination of tumour biopsies grades HNSCC into 3 categories depending on the level of keratinization. Well-differentiated tumours are characterised by a high level (>75%) of keratinization, including the formation of keratin pearls (Microscopic whorls of abnormal keratin; Figure 1.3B), and display an ordered stratification. Moderately differentiated tumours contain about 25-50% keratinization and demonstrate some stratification along with characteristic 'prickle' cells (a fixation artifact caused by shrinkage of cells which remain joined by their desmosomes). Poorly differentiated tumours have a low level of keratinization and demonstrate prominent nuclear polymorphism with atypical mitoses. These tumours tend to have the worst prognosis and are generally more aggressive with a higher incidence of metastases. However predicting the behaviour of individual tumours is difficult and differentiation grade does not always reflect the biological aggresiveness of HNSCC (Crissman *et al*, 1984).

1.2 Aetiology of HNSCC

1.2.1 Tobacco and alcohol

Approximately 90% of cases of HNSCC can be linked with prolonged exposure to environmental factors of which the two major risk factors are tobacco and alcohol (Blot *et al*, 1988). Tobacco smoke consists of a potent mix of more than 4000 known chemicals

many of which act as carcinogens capable of initiating and promoting cancer development. Currently 43 carcinogens have been identified in tobacco smoke including polynuclear aromatic hydrocarbons, nitrosamines, heterocyclic hydrocarbons and radioactive polonium-210 (US Department of Health and Human Services publication CDC-89-8411, 1989). Tobacco is used in various forms around the world and the differing methods of consumption are reflected in the marked global variations in the incidence and site of HNSCC. In the West the method of choice for tobacco users is smoking. However in many Asian countries chewing tobacco, or its derivatives, is more common. For example, in Bombay a mixture of chewing tobacco called Pan (consisting of betel nut, catechu, tobacco and areca nut) is very popular and is believed to contribute to the high incidence of HNSCC of the oral cavity and hypopharynx. These cancers make up 50% of all cancers in Bombay but account for only 3% of all cancers in the West where smokeless consumption is much less popular (Squire *et al*, 1984). HNSCC of the hard palate, uncommon in most of the world, is another example of the link between the method of tobacco use and site of cancer. A high incidence of hard palate cancer is seen in parts of India, Venezuela and Panama where the practice of reverse smoking (in which the burning end of the homemade cigar is held inside the mouth) is prevalent (Blot *et al*, 1988; Squire *et al*, 1984). Cannabis smoking also appears to confer a higher risk of HNSCC than tobacco smoking. This is probably due to the higher tar burden and greater concentrations of aromatic hydrocarbons found in marijuana smoke (Donald, 1986; Carriot and Sasco, 2000).

Alcohol, or more accurately, ethanol, is not a carcinogen *per se*, but it is thought to potentiate tobacco-related carcinogenesis synergistically. The majority of HNSCC patients are heavy drinkers and smokers. Ethanol, in its role as a solvent, may exert its influence by enhancing the contact of tobacco carcinogens with the mucosa of the upper aero-digestive tract (Blot *et al.*, 1988). The biological mechanisms of the ethanol effect are still unclear, although recent *in-vitro* experiments have demonstrated the induction of proliferation and downregulation of the p21 cell cycle inhibitor in HNSCC cell lines treated with this solvent (Hager *et al*, 2001). Ethanol may also exert its influence by interfering with the synthesis of retinoids, derivatives of vitamin A, implicated in the chemoprevention of HNSCC (Wang *et al*, 1998). A large scale European study (>28,000 patients) has demonstrated a relative risk of developing oropharyngeal cancer of 3.0 in subjects who consumed 7-21 units/week of beer or spirit as opposed to non-drinking controls (Gronbank *et al*, 1998). The same study demonstrated a lower relative risk (1.7) in subjects who also consumed wine as a significant

part of their alcohol intake, presumably due to the chemopreventative activity of resveratrol, a natural product derived from grapes (Jang *et al*, 1997).

Head and neck cancer is most common in male tobacco users aged between 50 and 65. Despite this knowledge, the incidence of smoking in the UK has recently begun to increase again after dramatic falls in the late seventies and eighties (Department of Health Publication – Statistics on Smoking: England 1976-1996). Public education, by surgeons and health care workers, appears to have failed to educate individuals choosing to put themselves at risk. This may reflect the failure to provide a medical or scientific explanation for the fact that many smokers and drinkers do not develop cancer. The risks posed by tobacco and alcohol use are likely to depend on the degree of exposure (duration more than intensity) and the inherent susceptibility of the individual. Identification of a molecular or genetic explanation for the inter-individual differences in susceptibility to carcinogen exposure would allow for closer monitoring of patients at risk from developing cancer, as well as for more influential health education programmes.

1.2.2 Viral agents

Two virus have been implicated in HNSCC tumourigenesis with the majority of evidence coming from epidemiological studies identifying viral genomes at a high frequency in certain tumours.

1.2.2.1 Epstein-Barr virus

The strongest evidence linking HNSCC and viral infection has been established between the Epstein-Barr virus (EBV) and the development of nasopharyngeal cancer. EBV is a Herpes virus that has been associated with several forms of malignancy (Burkitt's lymphoma, Hodgkin's disease, leiomysarcoma; Griffin, *et al*, 2000). Nasopharyngeal cancer has a distinct ethnic predilection and is endemic in southern China and northern Africa and this is thought to reflect a combination of genetic predisposition and, more importantly, exposure to the Epstein-Barr virus as a child. Whilst the EBV genome is also detected in other HNSCC, its genome is most frequently detected in nasopharyngeal tumours in South-east Asia (Vasef *et al*, 1997). Immigration studies suggest that differences in incidence are more strongly associated with environment than they are with genetic predisposition, as the incidence of nasopharyngeal cancer in American Chinese is halfway between native Chinese and American whites (Henderson *et al.*, 1977). Another major risk factor for nasopharyngeal cancer is the consumption of salted fish as a dietary standard (Yu, 1990). Salted fish constitutes a major part of the diet in China and has been identified

as an independent risk factor for nasopharyngeal cancer (Fedder and Gonzalez, 1985). Changes in diet between native and American Chinese may partly account for the reduction in the incidence of nasopharyngeal cancer in the latter group.

EBV infection has been shown to induce several proto-oncogenes (bcl-2, bcl-10, jun/fos and c-fgr) as well as coding for oncogenic proteins itself (EBNA1, EBNA 2, EBNA-LP, LMP1; Wattre and Hober, 1996). The nuclear antigen EBNA-LP is believed to play an important role in malignant transformation by interfering with the function of tumour suppressor genes p53 and pRB. These genes (see below for detailed explanation of function) are responsible for monitoring the cells' DNA for damage and thus diverting cells with abnormal genomes to either repair damaged DNA or undergo apoptosis (programmed cell death). Loss of this function in cells with a latent viral infection compromises the cells ability to monitor DNA mutations and therefore allows infected cells to propagate acquiring further mutations along the way.

1.2.2.2 Human papilloma virus

Another family of viruses that can override the protective mechanisms of p53 and pRB is the human papilloma virus (HPV). HPV is believed to play a central role in the aetiology of squamous cell carcinoma of the cervix (Giannoudis and Herrington, 2001) and has also been implicated in HNSCC (Snijders *et al*, 1996). Over 77 types of HPV have been identified to date, all of which have tropism for squamous epithelial cells. By far the most common types of HPV are the 'high risk' types 16 and 18 and these have been detected in HNSCC at a frequency of the 35-60% with the highest frequency in tumours of the oral cavity (Anwar *et al*, 1993, Clayman *et al*, 1994, McKaig *et al*, 1998). HPV type 16 and 18, amongst others, code for three proteins with oncogenic properties, E5, E6 and E7. E6 and E7 inhibit components of cell cycle regulation by binding to p53 and pRB respectively whereas E5 has been shown to stimulate growth factor activation, enhancing cellular proliferation (Flaitz and Hicks, 1998).

1.2.3 Genetic factors associated with HNSCC

To a large extent, head and neck cancer is a preventable disease, with the vast majority of cases occurring in individuals with a history of exposure to the carcinogens mentioned above. However not all HNSCC patients have been exposed to environmental carcinogens and, indeed, some individuals go through life enjoying extensive tobacco and alcohol habits and never develop the disease. First degree relatives of head and neck cancer patients appear to have a higher incidence of UADT cancer than do the relatives of cancer free

controls that can not convincingly be explained by similar environmental exposure alone (Copper *et al.*, 1993). This evidence suggests that genetic factors are likely to contribute to HNSCC risk.

The majority of ingested carcinogens are not dangerous themselves. It is the intermediate metabolites, created as the body attempts to metabolise the compounds, which are carcinogenic, therefore the manner in which the individual manages the removal of toxic compounds is crucial in understanding the risk posed. Detoxification of these carcinogenic intermediates requires an efficient enzyme system. If a particular intermediate is allowed to accumulate, due to insufficient levels of a particular enzyme in the metabolic pathway, then it is free to exert its effects in the local environment. The active metabolites of many chemical carcinogens can covalently bind to DNA, causing the formation of DNA adducts leading to genetic mutations. Polymorphisms (the presence of subtly different versions of one enzyme in different individuals) of several enzymes involved in the metabolism of carcinogens have been examined (Jahnke *et al.*, 1996). A study on a Japanese population of oral squamous cell carcinomas identified an increased risk for individuals with a particular polymorphism of N-acetyltransferase 1 (Katoh *et al.*, 1998). This enzyme is responsible for acetylating a variety of carcinogenic aromatic amines. A variety of polymorphic genotypes have been identified with differing rates of metabolic activity. Katoh *et al* identified a significantly increased risk of oral squamous cell carcinoma associated with the NAT1*10 allele.

Another important enzyme involved in the detoxification of carcinogenic nitrosamines and aromatic amines found in cigarette smoke is Glutathione S-transferase (GST). Four GST families have been identified, GST α, μ (M), π (P), and θ (T), all of which catalyse the conjugation of carcinogens to glutathione (Tsuchida and Sato, 1996). The metabolism of these carcinogens shows considerable inter-individual variability related to genetic polymorphism. Polymorphisms in several members of the GST family of detoxifying enzymes have been analysed in HNSCC and putatively protective and risk genotypes have been identified. Preliminary studies have indicated that the GSTM1 AB genotype may be associated with a lower risk for all HNSCC, whilst the GSTM3 BB genotype and GSTP1 AA genotype are specifically associated with a lower risk of laryngeal and oral/pharyngeal cancers respectively (Jahnke *et al*, 1999). Individuals lacking the GSTM1 gene (the 'null' genotype) have been shown to be at an increased risk for all types of HNSCC (Cheng *et al*, 1999).

Genetic polymorphism within key detoxification enzymes may explain the increased susceptibility to mutagens exhibited by lymphocytes from HNSCC patients when compared to healthy controls (Spitz *et al*, 1993). This abnormal sensitivity to bleomycin induced chromosomal damage *in vitro* in the lymphocytes of HNSCC patients has been postulated to reflect an inherent chromosomal instability in the genomes of cancer patients (Cloos *et al.*, 1996). The influence of GSTM1 genotype on the induction of bleomycin induced DNA breaks has been examined and an higher frequency of chromatid breaks and gaps was suggested in the GSTM1 null group however the small study cohort (n=18) rendered this finding statistically non-significant (Kocabas *et al*, 2000). This relationship between enzyme variants and cancer incidence may also explain, in part, the increase in relative risk identified in first-degree relatives (who will share many of the same genes) of patients with multiple head and neck cancers. Identification of genetic polymorphisms associated with differing levels of DNA adduct formation may eventually allow clinicians to predict an individual's response to exposure to these carcinogens and identify individuals at an increased risk of cancer formation.

1.3 Diagnosis and prognosis of HNSCC

Currently the prognosis for HNSCC patients is determined by a combination of patient, tumour and treatment factors. The age, sex and general health of the patient have all been shown to affect outcome. However the TNM classification system is currently the most important determinate for prognosis. For the majority of sites within the head and neck, patients with a stage I tumour can expect a 5-year survival rate of more than 80%. The survival rate for patients with advanced tumours (stage III and IV) drops to about 40%. The single most important prognostic factor for head and neck cancer is the presence of lymph node metastases and it is generally accepted that the detection of involved lymph nodes decreases survival by 50% (O'Brien *et al*, 1986). The number of involved lymph nodes also effects prognosis, as does the presence of extra-capsular spread (the extension of metastatic cells outside of the lymph node capsule). The presence of pathologically proven neck metastases is therefore of paramount importance in predicting the prognosis of HNSCC patients, however this information is only available to the pathologist after a neck dissection. The incidence of regional metastases varies greatly, reflecting the diverse biological behaviour of HNSCC, from about 1% for glottic tumours up to 80% for some nasopharyngeal tumours (Snow *et al*, 1992). Clinical nodal status has been shown to be an independent prognostic marker for survival and locoregional recurrence (Cerezo *et al*, 1992). However, clinical assessment of nodal status can differ widely from pathological

nodal status. Up to 50% of clinically positive necks can be pathologically negative and up to 40% of clinically negative necks will be positive after pathological examination (Ali *et al*, 1985), emphasising the difficulty in accurately identifying local metastasis without a formal neck dissection.

The TNM classification system provides clinicians with a guideline for planning therapy, although there is always difficulty in predicting the behaviour of individual tumours. Patients with similar stage tumours often have extremely varied clinical outcomes (Snow *et al*, 1989), with TNM staging failing to predict the biological properties of the individual tumours. Cure rates for HNSCC have changed little in the past few decades and new prognostic markers are urgently needed. Markers are required to fully characterise tumours with regard to their aggressiveness, invasiveness and metastatic potential, in order to plan efficient therapeutic strategies. In addition, head and neck surgeons are also looking for prognostic markers which can predict the response of individual tumours to the different therapeutic options allowing treatment to be tailored to the individual tumour, thereby preventing ineffective, unnecessary treatment.

1.3.1 Presentation and diagnosis

Early diagnosis is of paramount importance in reducing mortality (Kendall *et al*, 1996). Stage I and II tumours can be readily treated by either radiotherapy or surgery with an 80% chance of 5-year survival for most sites. Early warning symptoms, which should always be investigated, include a persistent sore throat, pain or difficulty when swallowing, hoarseness, earache and the presence of a neck lump, lasting for more than two weeks (Effective Head and Neck Cancer Management - Second Consensus Document, 2000). Any of these symptoms warrant a physical examination involving palpitation of the neck, examination of oral mucosa and examination of the nasopharynx, hypopharynx and larynx. Radiological techniques such x-ray, CT or MRI imaging may also be employed. Suspicious abnormalities are likely to be biopsied for histological assesment.

1.4 Natural history of HNSCC

1.4.1 Histological overview of Head and Neck cancer formation

Animal studies have led to the categorisation of epithelial carcinogenesis into three phases: initiation, promotion and progression. Current understanding of HNSCC has identified several key steps in the neoplastic pathway: genetic alteration; abnormal proliferation and altered differentiation; altered regulatory responses; invasion and/or metastasis. A pathway

to invasive malignancy has been postulated and HNSCC is recognised to progress through a series of distinct histopathological stages.

1.4.1.1 Normal epithelia - Structure and function

Epithelial tissue covers both the external surfaces of the body and lines the tubes and spaces within the body. It consists of sheets of cells and serves a number of different functions including secretion, absorption and general protection of underlying tissues and organs. Epithelial tissues are avascular – entirely devoid of blood vessels. Nutrition is acquired by diffusion from capillaries located in the underlying connective tissue. Epithelial tissues attach to a mucopolysaccharide-containing basement membrane, which separates them from the connective tissue. The classification of epithelial tissue depends on several morphological characteristics: whether the cells occur as a single layer or stacks; the shape of the cells; the presence or absence of specialised structures on the surface of the cells such as microvilli or cilia. The UADT consists mainly of stratified (stacked) squamous (flat) epithelia (see Figure 1.3). The vast majority of the UADT is comprised of non-keratinised squamous epithelia with the only exceptions being the gingiva and the dorsal surface of the tongue (Young and Heath, 2000). HNSCC is thought to arise when mutations in an epithelial cell (or in a field of cells) increase the propensity of the cell to proliferate. The altered cell and its progeny initially retain the appearance of normal epithelial cells but they reproduce at an abnormally high rate resulting in hyperplasia of the epithelium (see Figure 1.5).

1.4.1.2 Dysplasia

The two main clinically recognisable, potentially pre-malignant, lesions in oral head and neck cancer are leukoplakia (a whitish patch on the mucosa resulting from keratinization of the cells) and erythroplakia (a reddish patch). Both types of pre-malignant lesion exhibit dysplasia – abnormal cellular changes identifiable by histopathological analysis. Dysplastic cells tend to be of more primitive appearance than normal squamous mucosa demonstrating nuclear hyperplasia (enlarged nuclei with an increased nuclear/cytoplasmic ratio), hyperchromatin (dark staining nuclei), prominent nucleoli and an increased cellular density. Progression from hyperplasia to dysplasia is likely to involve the acquisition of further mutations. Other features more indicative of pre cancerous changes include pleomorphism (variation in the cellular and nuclear shape) and increased mitotic activity demonstrated by the presence of mitotic figures (Speight *et al*, 1996). Dysplastic tissue is graded into mild, moderate and severe according to the combination of tissue and cellular changes present. Mild dysplasia demonstrates proliferation of atypical or immature basal

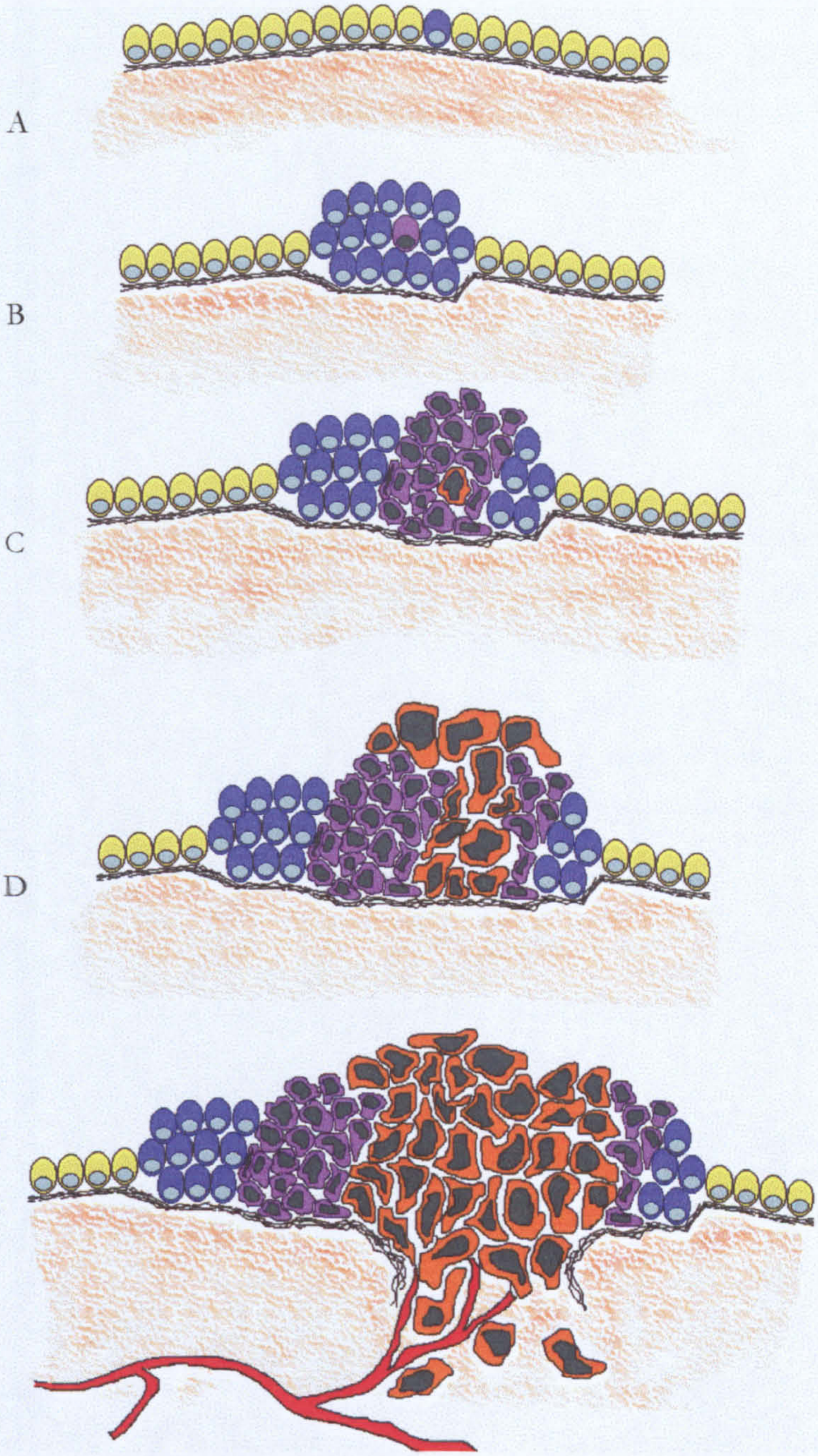

Figure 1.5 – Schematic representation of the multi-step process of tumour development.

A genetic mutation occurring in a cell (blue) within a normal population (yellow) increases its propensity to proliferate (A). The descendants of this altered cell still appear normal but proliferate more than the surrounding tissue – Hyperplasia (B). A subsequent mutation (or mutations) within one of these cells (purple) triggers further proliferation and the cells begin to look abnormal – Dysplasia (C). Further mutation(s) in any of these cells (orange) results in the formation of a mass of even more abnormal cells. If the mass of cells remains confined by the basement membrane the tumour is termed carcinoma *in situ* (D). If cells acquire the ability to breach the basement membrane, invading the underlying tissue (probably after acquiring still further mutation(s)) the tumour has become malignant (E) and has the potential to penetrate blood and lymph vessels allowing the tumour cells to metastasise to local lymph nodes and/or distant sites throughout the body. Multiple genetic aberrations within key regulatory genes must occur for tumour formation, usually over a period of years. Adapted from Weinberg, 1996.

cells above the parabasal region but not extending beyond the lower third of the epithelium. Moderate dysplasia exhibits similar proliferation but extends into the middle third of the epithelium whereas severe dysplasia exhibits abnormal proliferation extending into the upper third of the epithelium.

Both leukoplakia and erythroplakia are commonly associated with tobacco and alcohol use. Several large-scale studies have monitored patients with clinically diagnosed leukoplakia in an attempt to assess the likelihood of malignant transformation in this lesion. Bouquet and colleagues summarised data from 10 such studies and identified a malignant transformation rate of 4-20% representing an annual transformation rate of just under 1% each year (Bouquet and Whitaker, 1994). Erythroplakia is much less common than leukoplakia but thought to have a much higher propensity to become malignant. Both are theoretically reversible although it is assumed that with continued exposure to the etiological causative factors, and if the lesion is not removed, it will progress along a path to invasive HNSCC. Progression of these dysplastic lesions to an invasive phenotype may be associated with a reduction in the laminin and type IV collagenase content of the sub-epithelial basement membrane (Tosios *et al*, 1998)

1.4.2 Recurrent disease

Tumour cells left behind after surgery are one cause of recurrence and the failure to obtain clear margins after resection indicates the necessity for post operative radiotherapy. For stage I and II cancers, negative margins predict a high probability of control but histological assessment of excision margins of higher stage tumours is more difficult. Even with negative margins about 40% of patients with late stage cancers are likely to develop local recurrence (Looser *et al*, 1978). Frozen section analysis of tumour resection margins at the time of surgery has identified microscopic foci of tumour cells up to 1cm away from clinical disease at a frequency of 70% in one study of 93 cases (Davidson *et al.* 1987). Conventional assessment of tumour margins consists of identifying tumour cells by histological appearance alone. More recently, attempts have been made to identify aberrant cells in surgical margins by other methods. Brennan et al (1995) used molecular analysis of surgical margins to identify p53 mutations in histologically negative margins in over 50% (n=13/25) of p53 positive HNSCC tumours (Brennan *et al*, 1995). Of the thirteen tumours with margins positive for p53 mutations, 38% (n=5) went on to recur locally, whilst none of the tumours with margins negative for p53 mutations recurred at the primary site.

1.4.3 Field cancerization or micro-metastatic spread?

Multiple primary tumours in HNSCC patients is a well-recognised phenomenon (Licciardello *et al*, 1989) and have an important influence on the survival rate for head and neck cancer patients. Second primaries, either synchronous or metachronous, occur with a frequency around 4% and the prognosis of these patients is poor, especially if the second tumour arises in the lungs (Leon *et al*, 1999; Jones *et al*, 1995). Conventionally, second tumours are defined as independent if they arise separated from the original primary by more than 2cm of histologically normal mucosa or arise after an interval of at least 3 years. Two, non-mutually exclusive, theories have been formed to explain multiple primary tumours. Firstly, that multiple and unrelated transforming events occur giving rise to unrelated tumour clones from within a field of abnormal tissue (Slaughter *et al*, 1953) and secondly, that any transforming event is rare and a single cell is transformed from which all tumours arise through mucosal or micro-metastatic spread of the abnormal clone (Sidransky *et al*, 1992).

In 1953 Slaughter *et al* proposed the theory of field cancerization to explain the high incidence of synchronous and asynchronous second primary tumours. This work was based on the observation of multi-focal squamous cell carcinomas in the oral cavity and was put forward to explain the presence of several distinct lesions within the same resected specimen and, more interestingly, the observation of normal mucosa surrounding a tumour with other areas of non-contiguous dysplasia. Based on the fact that most of the epithelia of the UADT is subjected to the same carcinogenic insult, Slaughter proposed that multiple oral SCC arise in a multi-focal fashion within a field of mucosa with an increased risk of cancer development. Several studies have offered support for field cancerization including the observation that histopathological abnormalities can be detected in the epithelia of the respiratory tract of most smokers and lung cancer patients (Auerbach *et al*, 1961). The recent identification of molecular abnormalities in histologically normal mucosa distant from the primary tumour also supports the field change theory. Such abnormalities include loss of heterozygosity (Tabor*et al*, 2001; Lydiatt *et al*, 1997), p53 over-expression (Nees *et al*, 1993), and chromosomal polysomies (Hittleman *et al*, 1993). These findings are also consistent with the multistep paradigm for colorectal carcinogenesis proposed by Fearon and Vogelstein (1990) and the similar model proposed for HNSCC carcinogenesis (Califano *et al*, 1996).

An alternative theory, based on the premise that any transforming event is a rare occurrence, proposes that multiple primary tumours arise following the spread of cells from the original primary (either submucosally or through re-implantation at distant sites of cells shed from the initial primary). The evidence for this theory is more limited. Several papers have analysed multiple primary tumours in an attempt to identify a clonal origin. However in order to establish whether second primary tumours arise from cells from the original tumour a suitable marker of clonality must be identified. Bedi *et al.* examined the pattern of X chromosome inactivation in a small group of female patients (n=8) and found the same X chromosome to be inactivated in four out of four informative cases, indicating these tumours may have arisen from a common clone (Bedi *et al*, 1996). In addition, this study demonstrated identical patterns of loss of heterozygosity in a third of patients and hypothesised that, in at least a proportion of patients with head and neck cancers, multiple primary tumours arise from a single clone. p53 mutational status within multiple tumours has been analysed, based on the assumption that recurrent or clonally related tumours are expected to share identical p53 mutations and that independently arising tumours would display different p53 gene mutations. However, the presence of abnormal p53 in apparently normal mucosa questions the validity p53 mutations as a marker of clonal relationship. p53 mutations have been detected in approximately half of late or severe HNSCC dysplasias and have been shown to precede tumour invasion (Boyle *et al*, 1993; Sauter *et* al, 1994). Gasperotto *et al* (1995) identified 4 identical p53 mutations out of 9 informative multiple tumour patients, with 3 local tumours and 2 lung tumours containing different mutations to the initial primary. However, Chung *et al* (1993) detected p53 mutations in 21 out of 31 patients and identified discordant mutations between the initial and second primaries in all 21 informative cases. The discordance between p53 mutations in multiple primary tumours identified in both these studies suggests an independent origin for multiple primary tumours.

The concept of field cancerization is further confused by the frequent failure of studies which identify markers of clonality between multiple tumours to distinguish whether additional tumours arise from the spread of a fully malignant cell or independently from histologically normal cells which contain early genetic mutations. Most studies have concentrated on aberrations, which are detected at a high frequency in invasive HNSCC, based on the assumption that such common aberrations are likely to be important and early events in the progression of HNSCC. However, identical aberrations found within

multiple primary tumours do not necessarily indicate the metastases or migration through the epithelium of malignant cells i.e. the clonal origin theory of field cancerization.

Both theories for the origin of multiple tumours explain the fact that histologically normal mucosa may contain genetic abnormalities, as well as the fact that distant lesions are seen to be separated by normal mucosa. If multiple primary tumours do arise from migration of clonally related cells, then patients should be considered to have micrometastatic spread at the time of presentation. If second primary tumours arise independently from a field of tissue predisposed to cancer formation then removal of carcinogenic stimulus is essential to minimise the chance of further tumours developing. The identification of patients at an increased risk of developing second primary tumours would be very useful in planning treatment protocols for HNSCC patients following surgery.

1.4.3.1 Screening

The high success rate when treating early stage head and neck tumours has raised the question of screening for symptoms and early precursors. No evidence is available to indicate whether the evaluation of asymptomatic individuals will lead to a decrease in the mortality rate from HNSCC but a screening program may yet prove to be effective in countries such as India with a high incidence of oral cancer. Field cancerization of the UADT would suggest that altered mucosa with a propensity for tumour formation may allow for the development of a screening tool. However, at present, little is known about the initial changes that may be occurring in the mucosa of individuals with a high level of exposure to known risk factors. Further characterisation of the mucosa surrounding primary tumours is important and potentially holds the key to the early identification of individuals at risk of developing head and neck cancer.

1.4.4 Metastases

The ability of solid tumours to metastasise requires the tumour to overcome formidable obstacles. Cells must first break away from neighbouring cells at the primary site and breach the basement membrane. This requires the loss of adhesion molecules binding the tumour cells to the remainder of the tissue. Several families of enzymes, the most well characterised being the matrix metalloproteinases (MMP) and their inhibitors (TIMP), are important in this loss of cell adhesion. Cells have to invade through the stroma and penetrate either the blood or lymphatic vessels (intravasation). If a cell avoids destruction during transit it must then be able to reverse this process at the remote site (extravasation) and continue proliferating (Petruzzelli, *et al*, 1998). To ensure that the newly formed

metastases can continue to grow (above a size of approximatley $1mm^3$) angiogenic factors also need to be secreted to initiate neovascularisation (Homer *et al.*, 2000).

Squamous cell carcinoma of the UADT is the most common tumour to metastasise to the cervical lymph nodes. Approximately 35-40% of all HNSCC patients will have lymphatic metastases at the time of presentation (Jones *et al*, 1998). Whilst metastasis to the lymph nodes is more likely in patients with larger primary tumours, the site of the primary also affects the chance of metastasis. Tumours arising at sites with poor lymphatic drainage, for example tumours confined to the glottis, rarely metastasise, whereas tumours arising just a few millimetres away in the supraglottis, with its rich lymphatic drainage, have a much higher frequency of local nodal metastasis (O'Connor and Lund, 1998).

Distant metastases are relatively infrequent in head and neck cancer although the high incidence of second primary tumours can make the differentiation of the two difficult, particularly when the lungs are involved. Distant metastasis is usually to the lungs, bones and liver and is detected at a frequency of 10-30% at the time of death (O'Connor and Lund, 1998).

1.5. Therapy of HNSCC

The main goal of curative treatment is the gross removal of tumour cells with minimal damage to normal tissue and, in the case of HNSCC especially, with minimal cosmetic and functional impairment. Choice of treatment depends on many factors including staging of the tumour, the location of the tumour, nodal status and the general health of the patient including their psychosocial status. Approximately one third of patients present with an early stage disease (stage I or II) which is usually treated and cured with single modality surgery or radiation therapy. Patients presenting with more advanced disease, stages III and IV with involved lymph nodes, account for the majority of HNSCC cases. Treatment of these patients usually consists of surgery with post-operative radiotherapy.

1.5.1 Radiotherapy resistance in laryngeal HNSCC

The less mutilating therapy of external beam radiation is the treatment of choice for small volume tumours of the larynx. 5-year survival rates of around 95% are achieved in glottic tumours with no evidence of micrometastatic spread (Staplers *et al*, 1987). However, approximately 10% of T1 laryngeal tumours and up to 30% of T2 tumours treated in this way prove to be resistant to radiotherapy resulting in recurrence at the primary site within 12 months of treatment (Terhaard *et al*, 1991; Harwood *et al*, 1981). Such radio-resistant

patients have a subsequently worse prognosis as a result of technically more difficult salvage surgery with associated complications, a delay in the treatment of the original tumour, and the psychological effects to the patients of the original therapy having failed (Stoeckli *et al*, 2000). Prediction of radio-resistance based on molecular analysis of pre-treatment tissue biopsies would allow surgery to be performed as the primary therapy for patients with suitable, radio-resistant tumours. At present there are no clinically available markers of radioresistance.

1.6 Summary

HNSCC remains a major disease carrying considerable morbidity and mortality. Current clinical and pathological characterisation fails to satisfactorily predict the biological behaviour of individual tumours. As a result of this, a significant number of patients undergo unnecessary or ineffective therapy during the management of their disease. The discrimination of critical genetic events in head and neck tumourigenesis will not only increase our understanding of this group of tumours but also allow greater prediction of tumour behaviour, monitoring of therapy, identification of residual disease and eventually result in novel therapeutic strategies.

Chapter 2

Genetic Basis of Head and Neck Squamous Cell Carcinoma

2.1 Cancer as a genetic disease

Cancer is probably as old as mankind itself and has been documented since the time of the Egyptians (Breasted, 1970). The increasing prevalence of the disease is mainly due to two independent factors, increased life span and an increase in the spectrum of environmental compounds encountered in every day life. The term cancer refers to a diverse collection of different diseases with many varied causes and symptoms but all are characterised by - unregulated cell growth, invasion of surrounding tissues and potential for metastatic spread to other parts of the body. A normal healthy human body consists of approximately 30 trillion cells growing and dividing in a complex interdependent relationship. Tissue architecture is maintained by the strict regulation of proliferation with cells reproducing only when instructed. Cancer cells are able to evade the normal mechanisms of control of cell growth and proliferation (King, 2000).

2.1.1 Genetic basis of cancer

Head and neck tumourigenesis, like other malignant neoplasms, is a multi-step process believed to be driven by the accumulation of genetic damage in genes critical for the normal choreography of the cell cycle (Figure 2.1). These regulatory genes have been termed oncogenes and tumour suppressor genes and, in their normal configuration, expression of these genes intricately control the growth and proliferation of individual cells in response to the requirements of the tissue as a whole. Malignant transformation occurs after the accumulation of genetic changes in these genes. It is these mutations which account for the uncontrolled proliferation of abnormal cells which is characteristic of neoplasia. Several mechanisms leading to mutations in these genes have been identified including point mutations, deletions, amplifications and chromosomal rearrangements (Figure 2.2).

2.1.2 How many mutations are required for cancer?

No single mutational event can trigger malignancy in a normal cell (Kinzler and Vogelstein, 1996) and the pattern of mutations varies from cancer to cancer (Kinzler and Vogelstein, 1997). It has been estimated that HNSCC requires approximately 6-10 genetic alterations (Renan, 1993), however the spontaneous mutation rate in normal cells has been estimated to be between 10^{-6} and 10^{-5} mutations/gene/generation (Stein, 1991). This suggests that spontaneous mutations are relatively rare occurrences and insufficient to account for the large number of aberrations seen in cancer cells. In the average human lifetime spontaneous mutations could not accumulate to the level seen in the genome of cancer

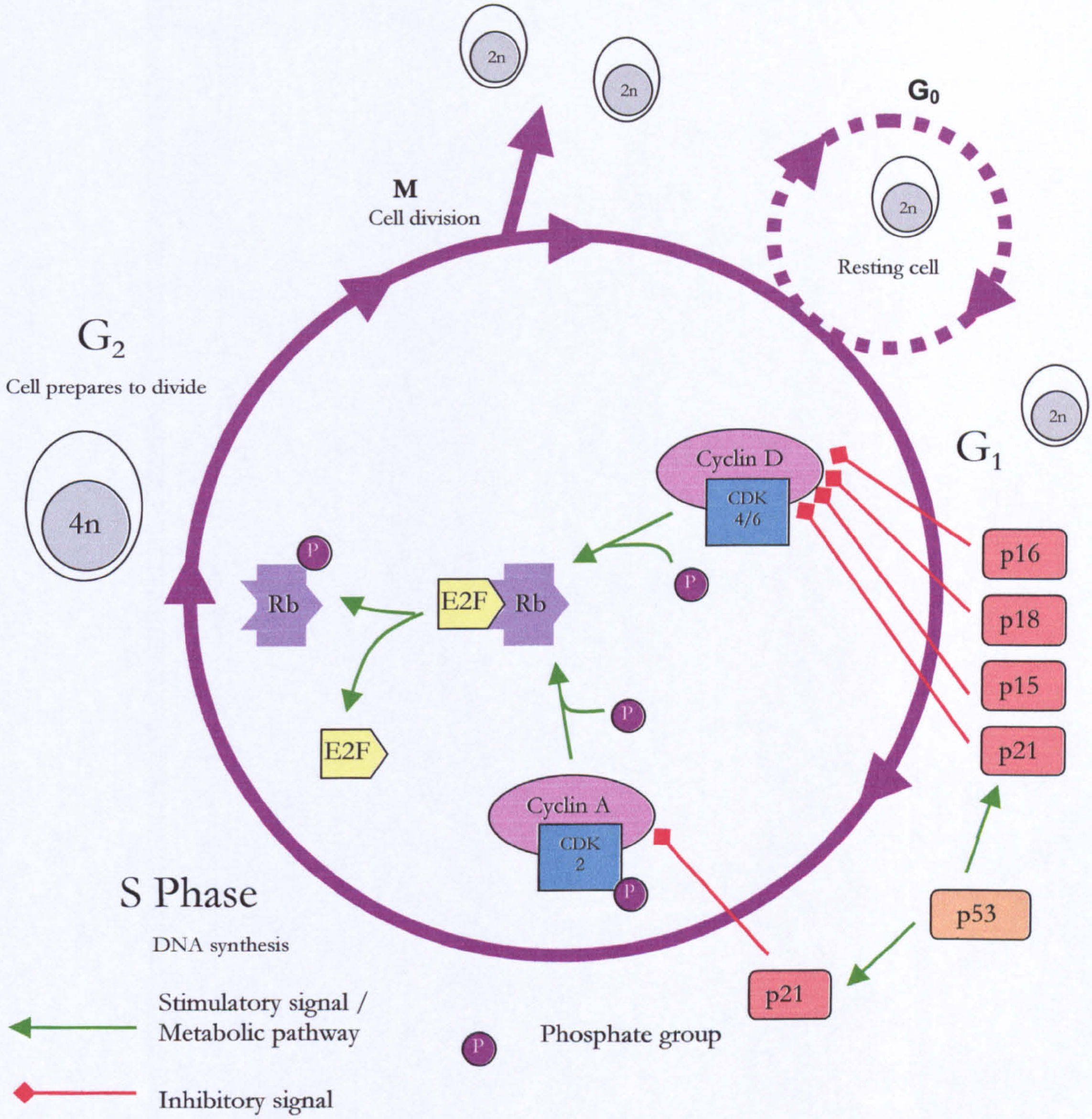

Figure 2.1 – Schematic representation of the cell cycle

Inappropriate growth of cancer cells occurs through the disruption of critical signalling pathways interfering with the cell cycle clock. A multitude of proteins are involved in the control of the cell cycle and mutations in genes coding for many of these growth stimulatory and inhibitory signal transducers generate the tumour suppressor genes and oncogenes underlying tumour progression.
Phosphorylation of the Retinoblastoma (pRb) suppressor protein ('the master brake') by the cyclin-D / cdk4/6 complex releases and activates the transcription factor E2F. E2F migrates to the nucleus where it stimulates the transcription of proteins involved in growth regulation including cdc2, myc and DNA polymerase α. Growth is inhibited by repression of the cyclin/cyclin dependant kinase complexes. The ink_4 family of inhibitors (p15, p16, p18, and p19) inhibit cdk4 and 6 complexes whilst p21 acts directly on the cyclin/cdk complex. p53 'monitors' DNA for damage and blocks cell proliferation, through p21, to prevent the proliferation of cells with damaged DNA and induces either DNA repair or apoptosis. Adapted from Weinberg, 1996

G_0 – Gap 0; G_1 – Gap 1; G_2 – Gap 2; S Phase – Synthesis phase; M – Mitosis; cdk – cyclin dependant kinase; 2n – Diploid DNA content; 4n – Tetraploid DNA content.

DNA Rearrangements – Chromosomal level

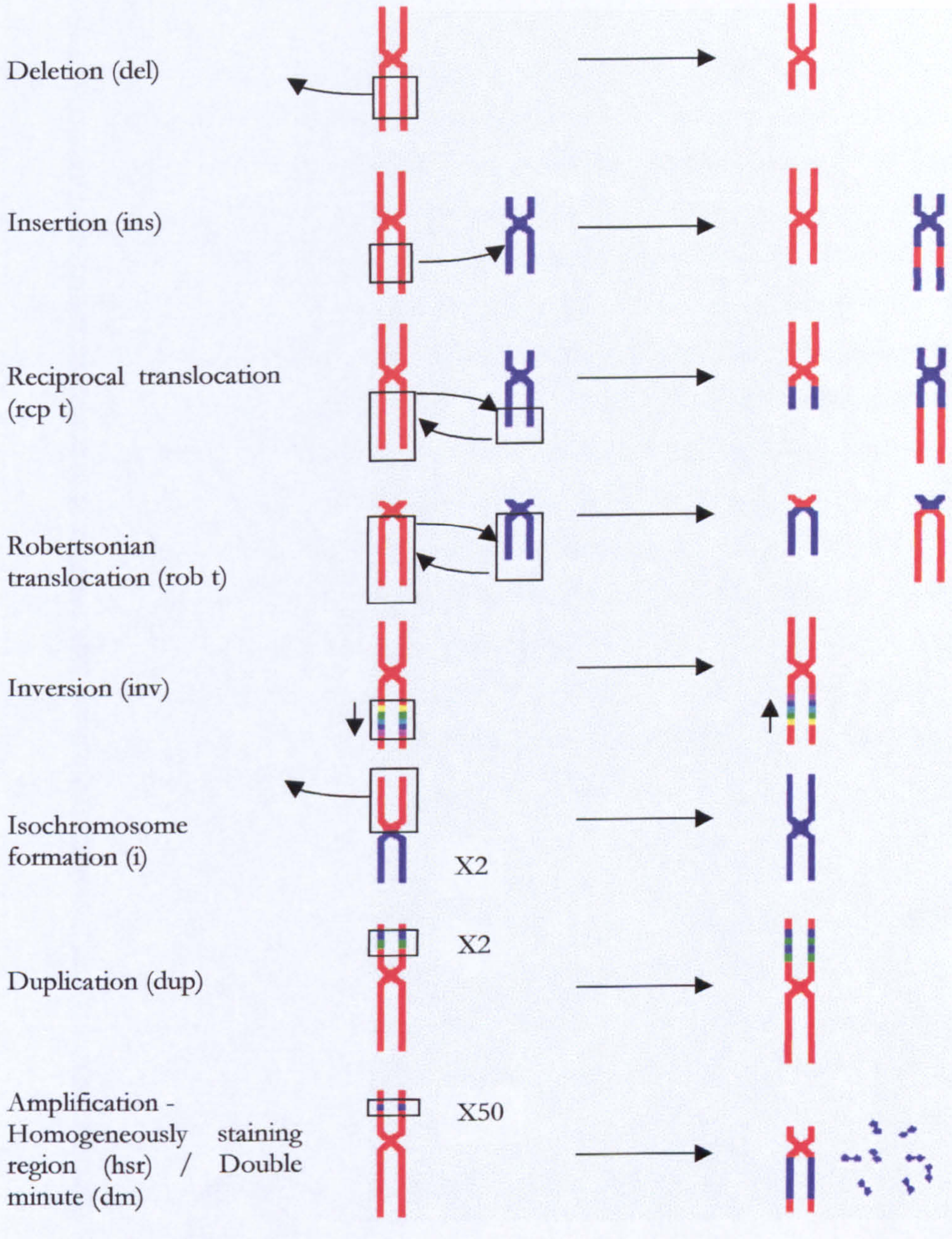

DNA Rearrangements – Nucleotide level

Normal	ABCDEFGHIJKLM
Point mutation	ABCDEQGHIJKLM
Insertion	ABCDEQRSTFGHIJKLM
Deletion	ABCD| IJKLM
Inversion	ABCDHGFEIJKLM
Substitution	ABCDXYZHIJKLM
Duplication	ABCDEFGHIJKLMABCDEFGHIJKLM
Amplification	ABCDEFGHIJKLMABCDEFGHIJKLMABCDEFGHIJKLMABCDEFGHIJKLM

Figure 2.2 – Manifestation of DNA aberrations.

cells. Therefore the mutation rate in cancer cells must be far greater than that of normal cells.

A variety of protective mechanisms are active in normal cells to recognise and repair DNA mutations and chromosomal damage before they are allowed to propagate through cell division (Carothers, 1997). Loeb *et al* (1991) proposed that tumourigenesis can only occur if the genomes of pre-malignant cells are far more mutable than their normal counterparts and that cancer cells exhibit a mutator phenotype caused by alteration of genes involved in DNA replication, DNA repair and chromosomal segregation. Compelling evidence for one example of a mutator phenotype has been demonstrated in studies on hereditary non-polyposis colorectal carcinoma (HNPCC), a form of familial cancer characterised by microsatellite instability. Microsatellites are short stretches of repeated base sequences, a common site of DNA alterations, thought to be due to DNA polymerase slippage errors during DNA replication (Kunkle, 1995). The proof reading system of the DNA replication enzymes is not responsible for repairing these errors, this duty falls to a family of proteins that make up the mismatch repair system (Strauss *et al*, 1997). Germline mutations in these mismatch repair genes prevent effective repair of replication errors and as a result these tumours exhibit a dramatic increase in genetic instability displaying elevated mutation rates at selected loci (Glaab *et al*, 1997; Baross-Francis *et al*, 1998).

However, most colorectal cancers, as well as the vast majority of HNSCC, show no microsatellite instability but instead exhibit abnormal chromosome numbers and loss of heterozygosity suggesting an alternative mutagenic mechanism (Blons *et al*, 1999; Piccinin *et al*, 1998). This phenotype has been termed Chromosomal Instability (CIN) and is associated with defects in the genes that regulate the segregation of chromosomes during the mitotic process (Cahill *et al*, 1998).

2.2 Chromosomal abnormalities associated with HNSCC

The cells that make up a cancer have long been known to exhibit abnormal phenotypic characteristics. The somatic mutation theory of cancer was first proposed by Theodor Boveri in 1914 who hypothesised that the phenotypic characteristics of tumour cells could be passed onto their daughter cells through permanent mutations of the tumour cell's genome. This theory proposed that the genomes of cancer cells contain chromosomal abnormalities and it is these changes that are responsible for the neoplastic properties of the tumour cells. Over the last few decades numerous chromosomal abnormalities have

been identified in HNSCC by techniques including DNA ploidy analysis, classical karyotyping, loss of heterozygosity (LOH) and, more recently, comparative genomic hybridization (CGH). These techniques have demonstrated that HNSCC, like other cancers, is characterised by apparently non-random chromosomal alterations.

2.2.1 DNA ploidy

DNA ploidy is defined as the amount of genetic material within the nuclei of the cells. Normal human somatic cells contain 46 chromosomes (equating to approximately 7.18pg of DNA) and are termed diploid (2n). The majority of cells within normal tissue are in the diploid, G_0 phase of the cell cycle (Figure 2.1). During cell division cells enter S phase and begin to duplicate their DNA content until they have double the normal DNA complement (4n, or tetraploid). DNA ploidy has been studied extensively in most cancers and HNSCC, like other tumours, are known to exhibit DNA instability with a large proportion of tumours demonstrating aneuploidy (an abnormal DNA content greater than 2n). DNA ploidy has been quantified by two different methods: image analysis and flow cytometry, with a high degree of correlation between the two techniques (Cope *et al*, 1991). Both methods apply a stoichiometric DNA specific stain to the cells of interest. Normal cells, of known DNA content, are included in every batch and calibrate the system allowing optical or fluorescent measurements to be converted to absolute concentrations. Several papers have associated a diploid DNA content with increased survival in HNSCC (Zatterstrom *et al*, 1991; Milroy *et al*, 1997). The correlation appears to be strongest when oral cancers are analysed alone. A large study of 429 oral cancer patients identified DNA aneuploidy as an independent prognostic factor of locoregional recurrence and as a predictor of metastases to the neck (Hemmer *et al*, 1999). Other studies have supported these findings and also suggested that aneuploid oral tumours respond better to radiotherapy (Tytor *et al*, 1989; Tytor *et al*, 1992).

The clinical usefulness of ploidy measurement in laryngeal HNSCC has yet to be determined with conflicting data so far reported (Milroy *et al*, 1997; Janot *et al*, 1996). Intra-tumoural heterogeneity may result in sampling errors, although ploidy measurements of incisional biopsies have been shown to be representative of corresponding surgical resection specimens (Hemmer *et al*, 1998).

2.2.2 Classical cytogenetics

Cytogenetics is the study of the relationships between chromosomes (particularly number, structure and function) and the phenotypic characteristics of cells. The term 'chromosome' was first introduced by Waldeyer in 1888, however the number of human chromosomes remained unknown until the technical development of chromosome arrest in mitosis (Levan, 1938) and improvements in chromosome spreading techniques (Hsu, 1952) allowed direct visualisation of good quality chromosome preparations under the microscope. The diploid human complement was finally determined to be 46 by Tjio and Levan in 1956 (and not 48 as was thought for several years) and this lead the way for the identification of chromosomal abnormalities underlying many human diseases. These included, amongst others, trisomy 21 in Down syndrome (Lejeune, 1959), monosomy X in Turner syndrome (Ford *et al*, 1959) and the first neoplasia associated chromosomal abnormality identified – the Philadelphia chromosome in Chronic Myelogenous Leukaemia (CML; Nowell and Hungerford, 1960). The Philadelphia chromosome was identified before the development of chromosomal banding techniques on the basis that one of the G group of chromosomes (the smallest human chromosomes later categorised as chromosomes 21, 22 and Y) was much shorter than the others. The identification of the Philadelphia chromosome was the first evidence supporting Boveri's hypothesis that the neoplastic characteristics of a cancer cell could be attributed to chromosomal abnormalities within the nucleus of that cell.

In the 1960s Caspersson developed the first method of producing characteristic chromosome banding patterns by identifying the distribution of GC rich regions along the lengths of the chromosomes using an alkylating agent conjugated to the fluorochrome Quinacrine mustard (QM) (Caspersson *et al*, 1970). This method of 'Q' banding chromosomes was later superseded by the now familiar 'G' banding of chromosomes developed by Gustav Giemsa, a non-fluorescent technique that produces more permanent, higher resolution bands than Q banding and still remains the standard tool for cytogenetic analysis of metaphase chromosomes (Czepulkowski, 2001).

With the advent of chromosomal banding techniques the Philadelphia chromosome was identified as a shortened chromosome 22 arising from a reciprocal translocation between chromosome 9 and chromosome 22 [t(9;22)(q34;q11)]. This translocation is consistently found in about 95% of adults with (CML), and at a lower frequency in other leukaemias,

and is the only cytogenetic abnormality detected in the majority of CML cases (Rowley *et al.*, 1990). This translocation results in the transfer of the Abelson (*abl*) oncogene to an area of chromosome 22q11 termed the breakpoint cluster region (*bcr*) (Kurzrock *et al*, 1988) and transcription of this *bcr-abl* fusion gene produces an abnormal tyrosine kinase protein. CML patients lacking the Philadelphia chromosome abnormality are pathologically indistinguishable from Ph+ patients, however Ph- patients generally have a poorer response to therapy and a shorter overall survival (Martiat *et al*, 1991) highlighting the clinical usefulness of cytogenetic analysis in complementing standard pathological procedures. Over the last few decades a multitude of studies has provided evidence to support the idea of cancer resulting from mutations in the genomes of somatic cells and other abnormal fusion gene products have since been identified in many forms of tumours (reviewed by Mitelman *et al*, 1997). Interest has begun to focus on identifying recurrent and consistent abnormalities, specific to individual tumour types. The Catalogue of Chromosomal Aberrations in Cancer was first published in 1983 and reported on 3,144 neoplasms with abnormal karyotypes. At the last update of the Mitelman database of chromosome aberrations in cancer (May 2002) this number had risen to 41,361 cases of neoplasm with karyotyped abnormalities (Mitelman *et al*, 2001). Although solid tumours are responsible for the majority of mortality and morbidity of cancer, the vast body of this data (75%) relates to leukemias and lymphomas. This is due to both the technical difficulties involved in culturing solid tumours, and the complex karyotypes generated which makes accurate identification of the origin of chromosomal material using conventional G-banding difficult and often impossible. A recent compilation of karyotypic data from 3,185 malignant solid tumours clearly demonstrates the non-random nature of chromosomal changes in solid tumours and highlights the characteristic distribution of chromosomal imbalances in different tumour types (Mertens *et al*, 1997). Therefore it appears that similar processes are occurring in solid tumours, highlighting the need for new methods of genomic analysis.

From the few studies that have been undertaken on HNSCC, classical cytogenetic analysis of both short-term primary cultures and established cell lines has revealed complex karyotypes with numerous and frequent structural chromosomal abnormalities (Jin *et al.*, 1995; Jin *et al.*, 2000; Osella *et al*, 1992; Carey *et al*, 1993; Van Dyke *et al*, 1994; Sreekentaiah *et al*, 1996). Common abnormalities including chromosomal aneuploidy, deletions, translocations, isochromosome (i) formation (most frequently - i(3q), i(5p), i(8q)) and homogeneous staining regions, have all been described, with unbalanced translocations

being the most common aberration (Van Dyke *et al*, 1994). Jin *et* al (2000) demonstrated that the majority of break points occurred in the centromeric regions of chromosomes, accounting for 43% of the total breakpoints in the largest study of laryngeal cancers (n=105). Deletions of chromosomal material from chromosomes Y, 1p, 3p13-p24, 4p, 5q12-q23, 7q22-q34, 8p11-p23, 9p21-p24, 10p, 11q23-qter, 13p11-p13, 18q22-q23 and 21 have been detected frequently along with gains of 3q21-qter, 5p, 7, 8q13-q24.3 and amplification of 11q13-q23 (Van Dyke *et al*, 1994; Jin *et al.*, 1995; Mertens *et al*, 1997; Jin *et al.*, 2000). Several consistent breakpoints have been identified including 1p11-12, 1p22, 3p, 3q27-29, 7p22, 7q22, 11q13, 12q13 and 18q21, indicating regions of the genome disrupted by translocation events. Although the effect of culture conditions on karyotypic data still remains debatable (Yin *et al*, 1993), karyotypic aberrations identified in HNSCC cultures have been confirmed by fluorescence *in-situ* hybridisation studies on histological sections of the original primary tumour in a limited number of cases (Worsham *et al*, 1999). Karyotypic data have demonstrated extensive intra-tumour heterogeneity in HNSCC identifying both multiple related and unrelated clones in HNSCC and the clonal evolution of multiple sub-clones within a tumour (Carey *et al*, 1993; Jin *et al*, 2000). Additional studies are required to investigate the clonality of HNSCC tumours.

In a large meta-analysis of 11 tumour types, HNSCC and breast cancer were the only two tumour entities which failed to demonstrate a characteristic gain or loss that was not present in any of the other tumour types (Mertens *et al*, 1997). This is an indication of the karyotypic complexity and general genetic instability of these tumour types and, in the case of HNSCC, may also reflect sub-site diversity. Few clinical correlations between karyotypic data and prognosis have so far been demonstrated, again possibly reflecting the complexity of this tumour type. The strongest correlation of chromosomal alteration and poor prognosis in HNSCC tumourigenesis is demonstrated by the 11q13 locus and is described in detail below. Loss of material from 18q has also been associated with a poor prognosis, being identified more frequently in patients who died of disease in one study (Van Dyke *et al*, 1994), a similar finding to LOH analysis of this region (Pearlstein *et al*, 1998). Comparison of radio-resistant and radio-sensitive HNSCC cell lines identified an association between breakpoints at bands 1p22, 3p24, 8p11.2 and deletion of 14q, with *in vitro* radio-resistance and 11q13 break point and gain of 14q with radio-sensitivity, although the genes responsible for this relationship, and the *in vivo* relevance still remain to be identified (Cowan *et al*, 1993).

2.2.3 Comparative Genomic Hybridization

Classical karyotyping is a technically demanding technique requiring skilled staff and trained cytogeneticists. Not all tumours can be cultured sufficiently to generate chromosomes for analysis, and findings are subject to potential selection of particular sub-clones that have the propensity to grow in an artificial environment *in vitro*. The desire to overcome many of the technical limitations of conventional cytogenetics led to the development of comparative genomic hybridization (CGH). CGH is a relatively new and powerful cytogenetic technique first described by Kallioniemi *et al* in 1992. CGH analysis allows the detection of DNA sequence copy number alterations (CNA) throughout the genome of interest in a single experiment, making it possible to screen the entire genome for chromosomal loci deleted or amplified in cancer. CGH utilises whole genomic DNA from the cell population of interest, circumventing the difficulties of obtaining metaphase preparation from tumour cells, and eliminates the potential selection of tumour sub-clones during the culturing of tumour cells. CGH is based on the competitive, co-hybridization of differentially labelled tumour and normal DNA samples to preparations of normal human metaphase chromosomes. In a typical CGH experiment, tumour DNA is labelled by the incorporation of a green fluorochrome (FITC, Spectrum Green) and normal DNA with a red fluorochrome (TRITC, Spectrum Red, Rhodamine). The two, labelled, DNA samples are mixed and hybridised onto chromosome preparations generated from normal human lymphocytes (a much easier process than preparing chromosomes from a solid tumour). Images of the binding of the two sets of fluorochromes are captured using an epifluorescent microscope equipped with appropriate filters and a cooled, charged coupled device (CCD) digital camera. Image analysis of the signal intensities of the two fluorochromes, down the axis of each of the chromosomes, indicates regions of chromosomal imbalance in the test DNA. These chromosomal regions of gained and deleted DNA are mapped directly onto normal chromosomes, allowing easy identification of the loci of chromosomal loss and the origins of amplified DNA. CGH is a global technique that requires no prior knowledge of the chromosomal loci under investigation unlike LOH and FISH that are limited to previously characterised aberrations (James, 1999; Nacheva *et al*, 1998).

Since its introduction, CGH has been applied rapidly to many tumour types and has allowed CNAs to be detected in each tumour. At the time of initiation of this thesis, several small studies had been published applying CGH to head and neck tumours (Brzoska *et al*, 1995 - n=10; Speicher *et al.*, 1995 - n=13; Bockmühl *et al*, 1996 - n=30).

Since then several other groups have added to the literature and these initial studies have been expanded (Bockmühl *et al*, 1998 - n=50; Gebhart *et al*, 1998 - n=23; Wolff *et al*, 1998 - n=20; Bergamo *et al*, 2000 - n=19; Bockmühl *et al*, 2000 - n=113; Hermesen *et al*, 2001 - n=42). These studies have identified many regions of chromosomal losses and gains including both sites of known oncogenes and tumour suppressor genes and regions to which no known tumour genes have yet been mapped. Copy number alterations have been reported on every chromosomal arm and the pattern of gains and losses detected by CGH is consistent with karyotypic data. Both techniques frequently identify the same pattern of involved chromosomal regions, however CGH tends to report deletions, and especially gains of genetic material at a higher frequency than karyotyping does (Merten *et al.*, 1997; Gebhart and Liehr, 2000). This reflects the ability of CGH to detect accurately the origin of gained chromosomal regions and highlights the limitations of conventional G-banding in identifying the origin of inserted material.

Deletion of 3p and gain of 3q are the two most commonly reported aberrations in HNSCC and suggest an important role for this chromosome in HNSCC progression. Other regions deleted in >30% of cases (when the individual studies were combined) include 1p, 4, 5q, 6q, 8p, 9p, 11p, 11q, 13q, 18q, and 21. DNA gains have been reported at a frequency of >30% on 3q, 5p, 8q, 9q, 11q13 (repeatedly reported as the site of high level amplifications), 16p, 17, 19, 20, 22 (reviewed by Gebhart and Liehr, 2000).

2.3 Oncogenes implicated in HNSCC

Oncogenes were originally discovered through studies on virally induced cancers in animals. The *v-src* oncogene was the first to be identified as the gene responsible for the sarcoma inducing properties of the Rous sarcoma virus in chickens. A cellular homologue of the viral gene was subsequently discovered on chromosome 20 in normal cells coding for a protein with tyrosine kinase activity involved in the transduction of growth signals to the cell nuclei.

The normal cellular counterparts of oncogenes are termed proto-oncogenes and are classified into several categories depending on their function within the normal cell including transcription factors, growth factors and signal transduction molecules. All proto-oncogenes have one common function, the promotion of cellular growth and proliferation. These molecules make up the molecular communication system which transmits growth signals from outside the cell into the cell's nucleus. Mutations within

these molecules cause the deregulation of these growth stimulatory pathways by keeping the signal to proliferate constitutively active.

The identification of consistent chromosomal breakpoints and regions of DNA gain and amplification in human cancer led Heim and Mitelman (1987) to hypothesise that such regions were the sites of novel oncogenes. They compared the distribution of chromosomal breakpoints in a variety of cancers with the chromosomal loci of 26 cellular known oncogenes and identified a highly significant clustering ($p = 0.0000012$), indicating that chromosomal aberrations underlie the activation of oncogenes in solid tumours. Genetic aberrations within proto-oncogenes can result in either the production of an abnormal molecule (by point mutations or translocation events) with oncogenic properties or increased levels of the normal, growth stimulatory, product (through gene amplification or translocation induced altered transcriptional control of the gene). Characterisation of the chromosomal loci associated with HNSCC has implicated the involvement of several oncogenes.

2.3.1 Oncogenes of the 11q13 locus

Amplification of the chromosomal band 11q13 has been identified in 30-60% of HNSCC and has been associated with a poor prognosis in a number of studies (Meredith *et al*, 1995; Akerval *et al*, 1995). This region contains several putative oncogenes (Table 2.1) that are co-amplified and much interest has recently focussed on identifying the specific gene (or genes) involved in HNSCC tumour progression and any possible interactions between them.

Gene	Protein	Function	Reference
ccnd-1	Cyclin D1 (Prad1)	cell cycle	Hinds *et al*, 1994
hst-1	a fibroblast growth factor	growth signal	Yoshida *et al*, 1988
ems-1	cortacin	actin binding cytoskeletal associated protein	Schuuring *et al*, 1993
gst-π-1	glutathione S transferase π 1	cellular detoxification / prevention of oxidative damage	Silberstein and Shows, 1982
int-2	fibroblast growth factor 3	growth signal	Yoshida *et al*, 1988

Table 2.1 – Oncogenes of the 11q13 locus

Amplification of the 11q13 locus has demonstrated a strong correlation with over-expression of the Cyclin D1 protein in HNSCC (Sidransky, 1995). Cyclin D1 is a 295

amino acid, 33 kDa protein encoded by the *ccnd-1* gene (also know as *prad1* and *bcl-1*). Cyclin D1 is a rate-limiting controller of the G1 phase progression in the cell cycle acting as a molecular switch preventing the cells from entering S phase until levels of the Cyclin D1 protein have reached a certain level. Cyclin D1 combines with and activates the Cyclin-dependant kinases cdk4 and cdk6 allowing them to phosphorylate the 'major brake' of the cell cycle clock, the RB protein (Figure 2.1). When sufficiently phosphorylated RB releases the growth promoting transcription factor E2F. Over-expression of Cyclin D1 may increase the aggressiveness of HNSCC by shortening the G1 interval and accelerating growth and proliferation.

To date, *ccnd1* is the only gene of the 11q13 locus that has demonstrated oncogenic properties. Amplification of *ccnd1* has been correlated with poor overall survival in several studies (Bellacosa *et al*, 1996; Akerval *et al*, 1997; Fortin *et al*, 1997; Kyomoto *et al*, 1997), as has over-expression of the protein product Cyclin D1 (Pignataro *et al*, 1998; Callender *et al*, 1994). *ccnd1* amplification has been demonstrated predominantly in high-grade, high-stage and aneuploid HNSCC suggesting it may be important in tumour progression (Callender *et al*, 1994). A recent study of 45 cases of HNSCC identified a significantly reduced 5-year survival in patients with either gene amplification (22%) or protein over-expression (53%). However, with multivariate analysis, only amplification of the *ccnd-1* gene demonstrated independent prognostic value (P=0.0018) (Kyomoto *et al*, 1997). HPV infection has been implicated in the amplification of the *ccnd1* gene through the oncoproteins E6 and E7 from high-risk HPV types known to cause genomic instability (Cattani *et al*, 1998). In this analysis of 75 laryngeal tumours *ccnd-1* amplification was present in 20% of tumours and was significantly associated with HPV infection, predominately the highly oncogenic HPV-16 and 18 genotypes.

Analysis of *int-2*, *hst-1*, *ems-1* and *gst-π-1* has failed to identify a prognostic correlation in HNSCC suggesting these genes are merely co-amplified alongside other genes involved in the progression of the disease (Rubin *et al*, 1995; Callander *et al*, 1994). Other, as yet unidentified genes involved in HNSCC tumourigenesis may still remain to be identified in the 11q13 locus.

2.3.2 *c-erbB*

Another oncogene implicated in the development of HNSCC is *c-erbB*. The *c-erbB* oncogene was initially discovered as a result of its homology with the viral oncogene of the

avian erythroblastosis virus (Vennstrom *et al*, 1982). It is located on chromosome 7p12, a region of frequent gain in HNSCC, and codes for the Epidermal Growth Factor Receptor (EGFR), a 170 kDa surface membrane-associated tyrosine kinase. EGFR stimulates proliferation of target cells through the interaction with its ligand Epidermal Growth Factor (EGF), a potent mitogenic polypeptide. EGFR also mediates signal transduction for transforming growth factor-α (TGF-α). Amplification and over-expression of *c-erbB* in HNSCC have been detected in the majority of HNSCC (Santini *et al*, 1991, Ishitoya *et al*, 1989) and found to occur early in carcinogenesis (Uhlman *et al*, 1996). Univariate analysis of EGFR levels (determined by a radioligand receptor assay – an alternative assay to immunohistochemistry for quantifying specific receptors) in 140 laryngeal patients identified a significant relationship between EGFR status and survival. When a cut-off value of 20fmol EGF/mg protein was used to stratify tumours into EGFR negative and EGFR positive tumours the 5 year survival was 81% and 25% respectively (Maurizi *et al*, 1996). Over-expression of EGFR may reflect the development of an autocrine growth loop as most epithelial cells require EGF. High levels of the receptor may allow tumour cells to respond to concentrations of EGF which are non-mitogenic to normal cells.

A recent study of 91 HNSCC patients has identified increased expression of EGF and TGF-α (as measured by immunohistochemistry) as statistically significant predictors of disease-free survival (Grandis *et al*, 1998). Multivariate analysis identified high levels of these proteins as statistically significant predictors of reduced disease free survival and the levels of these two growth factors predicted clinical outcome as accurately as cervical lymph node dissection. In order to determine whether EGFR expression contributed to tumour growth Grandis' group then suppressed EGFR expression in tumour xenografts through *in situ* expression of antisense oligonucleotides (He *et al*, 1998). This 'anti-sense' therapy effectively inhibited tumour growth and resulted in cancer cell death suggesting a potential role for blocking overproduction of EGFR and TGF-α as a therapeutic option for HNSCC.

EGFR over-expression, as well as being very common, may also be one of the early events in HNSCC tumourigenesis and a potential biomarker of 'field cancerization'. Two studies have identified abnormalities in EGFR in histologically normal mucosa of HNSCC patients (Shin *et al*, 1994; Grandis and Tweardy, 1993). Shin *et al* identified significantly greater expression of EGFR by immunohistochemistry in 'normal' mucosa adjacent to 36 HNSCC patients compared with mucosa of healthy controls who had not been exposed to tobacco

or alcohol. In addition EGFR expression increased with histological grade in these patients suggesting up-regulation of EGFR expression was involved at an early stage in the multistep process of tumourigenesis. Grandis and Tweardy, examined EGFR and TGF-α mRNA production in histologically normal mucosa of HNSCC patients and found essentially the same, that EGFR expression was increased (by an average of 29-fold) in the mucosa of HNSCC patients when compared with normal controls.

2.3.3 *c-erbB-2*

Another member of the EGFR family is the oncogene *c-erbB-2* (also named *neu* and *Her-2*) is located on chromosome 17 and codes for a 185 kDa protein with tyrosine kinase activity (Schecter *et al*, 1984). Over-expression of c-erbB-2 has been identified in many tumour types (Gutman *et al*, 1989), most notably in breast cancer where approximately 20-30% of tumours demonstrate over-expression (Schnitt, 2001). Elucidation of the role c-erbB-2 in breast cancer growth led to the development of a humanised monoclonal antibody directed against the c-erbB-2 protein as a therapeutic agent (Herceptin™) (Pegram *et al*, 2000). Application of Herceptin™ blocks the over-expressed receptor molecules and is believed to inhibit the growth stimulatory signals of c-erbB-2. A high level of c-erbB-2 expression within the membrane of tumour cells is seen in approximately 50% of HNSCC (Xia *et al*, 1997; Craven *et al*, 1992). Protein over-expression, detected by immunohistochemistry, has shown a strong correlation with decreased survival in oral SCC (Xia *et al*, 1997) and an association with poor prognosis in tumours of the salivary glands (Press *et al*, 1994). The c-erbB2 protein has also been postulated as a target for therapy in HNSCC and recombinant short chain antibody toxins directed against the protein have been shown to inhibit the *in vitro* growth of head and neck cells lines (Azemar *et al*, 2000). However, the role of c-erbB-2 in HNSCC remains controversial with other studies failing to identify a correlation between c-erbB-2 expression and patient survival (Craven *et al*, 1992; Kearsley *et al*, 1991).

2.3.4 *c-myc*

Located on chromosome 8q24, the *c-myc* proto-oncogene codes for a 62 kDa nuclear protein. The myc protein dimerises with another protein, max, to form an activated transcription factor that binds to DNA altering the regulation of many genes including those responsible for DNA replication (Atchley and Fitch, 1995). Over-expression of the myc protein leads to increased amounts of the active myc-max heterodimer (Bouchard *et al*, 1998). Over-expression of myc has been reported in many tumour types, including HNSCC (Schraml *et al*, 1999). The most widely described oncogenic role of *c-myc* is in Burkitt's lymphoma where the t(8;14) translocation dissociates *c-myc* from its normal

Burkitt's lymphoma where the t(8;14) translocation dissociates *c-myc* from its normal promoter and regulatory sequences and places it under the regulatory control of the immunoglobulin heavy chain switch recombination region (mu or alpha) promoter (Adams *et al*, 1993). Over-expression of the myc protein has been demonstrated in upto 48% of primary head and neck cancers and high levels of the myc protein have been associated with shorter overall survival (Field *et al*, 1989)

2.3.5 The *ras* gene family

The three *ras* oncogenes, *h-ras*, *k-ras* and *n-ras* all encode 21 kDa guanine nucleotide – binding proteins involved in the intracellular transduction of growth and differentiation signals from activated membrane receptors (Wong-Staal *et al*, 1981). Mutation of the *ras* genes and subsequent over-expression of the protein product have been reported in a number of solid tumour types including breast, colon and lung (Field and Spandidos, 1990). A number of studies of HNSCC have failed to demonstrate significant involvement of *ras* mutations (less than 5%) in HNSCC in the Western world (Kiaris *et al*, 1995, Clark *et al*, 1995, Rizos *et al*, 1999). The incidence of *ras* mutation is much higher in Indian oral cancer, with approximately 35% of cancers demonstrating mutation suggesting a specific mutagenic effect of tobacco and betel nut chewing on the *ras* oncogenes (Saranath, 1991; Das *et al*, 2000).

2.4 Tumour suppressor genes implicated in HNSCC

The counterparts to the growth stimulatory components of the cell cycle are termed tumour suppressor genes (TSG). These genes, when expressed, have an inhibitory effect on cellular growth and are normally reversibly inactivated in order for proliferation to occur. Repression of growth is achieved by the binding of repressor molecules to stimulatory molecules within the cell blocking their growth promoting activity. These genes contribute to carcinogenesis when they become constitutively inactivated resulting in an unrestrained signal for cell growth and it is for this reason these proteins are sometimes referred to as the 'brakes' of the cell cycle. Other genes now implicated in a suppressor role include DNA repair genes, adhesion molecules and genes involved in cellular apoptosis (Reviewed by King, 2000).

The vast majority of TSGs are recessive, i.e. as long as the cell retains one normal allele tumour suppression continues, as opposed to the dominant role of oncogenes where a single mutation can predispose the cell to cancer formation. Much of the early understanding of TSG function resulted from studies on retinoblastoma, a childhood

cancer of the retina that exists in both familial and sporadic forms. Based on the statistical analysis of retinoblastoma in children, Knudson (1971) proposed that two genetic events were required to inactivate the gene underlying the development of retinal tumours. In the hereditary form of the disease, which usually develops in the first weeks of infancy, one of the germline alleles already contains a mutated gene and a single somatic event in the other allele is sufficient to give rise to the cancer. The sporadic form of the disease tends to develop later in life and reflects the requirement for two somatic mutations in the gene. This became known as Knudson's 'two hit' hypothesis and became the model for all subsequent investigations into tumour suppressor genes. Several mechanisms for revealing a recessive mutation have now been identified including deletion, point mutation, translocation and more recently transcriptional inactivation of the gene by hypermethylation of 5' CpG islands in the promotor of the gene (Merlo *et al*, 1995). Several TSGs have been implicated in the tumourigenesis of HNSCC (see below). Much of the evidence for the involvement of these genes, as well as the identification of genetic loci likely to harbour additional genes has come from the detection of allelic loss in HNSCC tumours. Deletion of specific chromosome material is one of the most common genetic events in solid tumours and the deleted regions are believed to contain potential tumour suppressor genes.

2.4.1 Loss of Heterozygosity

Loss of Heterozygosity (LOH) analysis has been applied extensively to many cancers and has identified allelic imbalance at multiple chromosomal loci harbouring known and putative tumour suppressor genes (Lasko and Cavenee, 1991). LOH represents the structural deletion of chromosomal regions ranging in size from a single gene to the loss of the whole chromosome (or chromosome arm) carrying that gene. LOH analysis exploits the polymorphisms within microsatellites, non-coding sequences of DNA found throughout the genome (approximately every 100 kb). These microsatellite markers consist of short sequences (2 or 3 base pairs) of DNA repeated many times. Normal cells contain two sets of alleles (one derived maternally and one paternally) and are heterozygous at many microsatellite loci. The number of repeats within any given microsatellite varies between individuals, and also between the two alleles in a particular person, giving rise to alleles of different lengths. These alleles can be visualised through PCR amplification of the chosen microsatellite and subsequent electrophoretic separation of the PCR products (Weber and May, 1989). If the individual is heterozygous for the particular microsatellite, the PCR amplification will yield two PCR products of differing lengths, visualised as two bands on the electrophoretic gel. Analysis of both tumour and normal DNA samples from

LOH when two bands of a heterozygous loci are seen in the normal DNA and reduced to one band in the tumour DNA. Not all samples are informative as for some loci / patients the normal DNA will be homozygous by nature.

Table 2.2 details some of the more frequently reported regions of LOH in HNSCC. Reported frequencies of LOH can be seen to vary reflecting the differences in the choice of markers examined in each study as well as the different tumour subtypes examined. These differences may also hint at subtle geographical variations in the genetics of HNSCC, an area requiring further investigation. Not all studies specified the type of tumours included in their cohort making direct comparison difficult. Despite the variation of LOH frequency between different studies, LOH has been identified at a high frequency (>30%) at several chromosomal loci including 3p, 5q, 8p, 9p, 11q, 13q, 17p, 17q and 18q. These chromosomal loci are consistent with the findings of classical karyotyping studies, however the frequency of LOH tends to be higher than the frequency of regions of deletion identified by classical karyotyping. This is a reflection of the higher resolution of LOH and also indicates that discrete regions of loss more frequently affect some chromosomal loci than gross chromosomal deletion. Most notable are 9p (LOH – 70-80%; karyotypic data ~10%) and 17p (LOH – 40-55%; karyotypic data 5-10%) (Table2.2). Some studies reported significant differences in the frequency of LOH in particular tumour subtypes e.g. 3p and 17p losses were seen most frequently in tumours of the hypopharynx in two studies (Field *et al*, 1995; Rowley *et al*, 1996). The body of LOH data for HNSCC is growing, although so far there have only been a handful of large-scale global analyses. Tumour suppressor genes have been linked to some of these chromosomal sites however speculation remains as to the target gene(s) on many other regions of chromosomal loss.

2.4.1.1 Chromosome 3p

Allele loss on chromosome 3p is also a common event in HNSCC and a study of a pure population of 48 oral cancers has significantly associated LOH at 3p with poor prognosis, late stage and impairedsurvival in oral cancer (Partridge *et al*, 1996). Re-introduction of 3p into oral tumours has been shown to suppress tumourigenicity in cell lines *in-vitro* (Uzawa *et al*, 1995) providing strong evidence for tumour suppressor genes on 3p. Three discrete regions of loss have been identified in several studies, 3p24-p26, 3p21 and 3p12-p14. LOH of the same regions of 3p have been reported in lung cancer (Hibi *et al*, 1992) possibly reflecting the similar causative agents of the two diseases, however loss of material on 3p is

Chromosome	No of loci analysed	Tumour type (s)	% LOH	No. of Tumours	Reference	Correlation/Comments
1p	2	Not Specified	30	29	Nawroz *et al*, 1994	
	1	Not Specified	14	28	Ah See *et al*, 1994	
	6	Not Specified	27	80	Field *et al*, 1995	Main region of loss 1p21-p22.1
	1	Or(40),Ph(19),La(17), Ot(2)	30	78	Ransom *et al*, 1996	
3p	32	Oral		48	Partridge *et al*, 1999	5 areas of LOH identified, *VHL* and *FHIT* not affected
	3	BSH(35), Dy(31), CIS(21), SCC(70)	16/52/60/67	83	Califano *et al*, 1996	High incidence of LOH in pre-invasive lesions suggests an early event
	2	Not Specified	67	29	Nawroz *et al*, 1994	
	3	Not Specified	44	28	Ah See *et al*, 1994	
	18	Not Specified	52	80	Field *et al*, 1995	Main regions of loss 3p24-p25, 3p13 and 3p21
	4	Or(40),Ph(19),La(17),Ot(2)	26	78	Ransom *et al*, 1996	
	6	Hy(16),Or(12),La(8),Op(6),Sa(3),Sk(1)	48	46	Rowley *et al*, 1996	Minimum region of loss 3p24-p25.1, LOH more common in Hypopharyngeal tumours (63%)
			74	38	Maestro *et al*, 1993	Identified three discrete regions of loss: 3p24-pter, 3p21.3, 3p12-cen
	4		100	26	Waber *et al*, 1996	LOH identified in regions surrounding, but not including, the *VHL* gene. No evidence for mutation of *VHL*
	15	Oral	71	48	Partridge *et al*, 1996	Identified three distinct regions of loss: 3p24-26, 3p21.3-22.1, 3p12.1-14.2. Correlated with late stage and survival
3q	2	Not Specified	50	29	Nawroz *et al*, 1994	
	1	Not Specified	0	28	Ah See *et al*, 1994	
	2	Not Specified	13	80	Field *et al*, 1995	
4q	2	BSH(35), Dy(31), CIS(21), SCC(70)	4/9/21/47	83	Califano *et al*, 1996	
	1	Not Specified	37	29	Nawroz *et al*, 1994	
	1	Not Specified	11	28	Ah See *et al*, 1994	
	3	Not Specified	13	80	Field *et al*, 1995	

Table 2.2 – Loss of Heterozygosity studies on HNSCC reported in the literature.

Chromosome	No of loci analysed	Tumour type (s)	%age LOH	No. of Tumours	Reference	Correlation/Comments
5q	1	Not Specified	25	29	Nawroz *et al*, 1994	
	1	Not Specified	43	28	Ah See *et al*, 1994	Common region of loss included the *APC/MCC* region
	8	Not Specified	29	80	Field *et al*, 1995	Main region of loss 5q21-q22
	1	Or(40),Ph(19),La(17), Ot(2)	56	78	Ransom *et al*, 1996	
	1	Oral	73	28	Uzawa *et al*, 1994	Site of the *APC* gene analysed (5q21). Nucleotide substitutions also identified in 3 (12.5%) patients
6p	3	BSH(35), Dy(31), CIS(21), SCC(70)	8/20/19/38	83	Califano *et al*, 1996	
	3	Not Specified	38	29	Nawroz *et al*, 1994	
	1	Not Specified	9	28	Ah See *et al*, 1994	
	3	Not Specified	21	80	Field *et al*, 1995	
7q	1	Not Specified	29	29	Nawroz *et al*, 1994	
	1	Not specified	38	?	Resto *et al*, 2000	Identified an oncogenic role for MPP11 locus (7q22-31.1)
	1	Not Specified	0	28	Ah See *et al*, 1994	
	2	Not Specified	7	80	Field *et al*, 1995	
8p	1	BSH(35), Dy(31), CIS(21), SCC(70)	14/13/21/40	83	Califano *et al*, 1996	
	1	Not Specified	40	29	Nawroz *et al*, 1994	
	1	Not Specified	11	28	Ah See *et al*, 1994	
	5	Not Specified	35	80	Field *et al*, 1995	Main regions of loss 8p11.22-p21.3 and 8p12
	1	Or(40),Ph(19),La(17), Ot(2)	16	78	Ransom *et al*, 1996	
	4	19 La-SCC, 13 Benign La lesions	47	32	Rizos *et al*, 1998	
	14	Oral	63	32	Ono *et al*, 1999	Main regions of loss 8p12 and 8p22
8q	2	Not Specified	38	29	Nawroz *et al*, 1994	
	1	Not Specified	9	28	Ah See *et al*, 1994	
	6	Not Specified	21	80	Field *et al*, 1995	

Table 2.2 – Loss of Heterozygosity studies on HNSCC reported in the literature.

Chromosome	No of loci analysed	Tumour type (s)	%age LOH	No. of Tumours	Reference	Correlation/Comments
9p	3	BSH(35), Dy(31), CIS(21), SCC(70)	20/57/80/73	83	Califano *et al*, 1996	High incidence of LOH in pre-invasive lesions suggests an early event.
	3	Not Specified	72	29	Nawroz *et al*, 1994	
	1	Not Specified	25	28	Ah See *et al*, 1994	
	11	Not Specified	62	80	Field *et al*, 1995	Common region of loss 9p22-p23
	24	Oral	53	34	Nakanishi *et al*, 1999	Identified three regions of loss, two within 9p22 (*INFA*), and 9p21
	8	Not Specified	45	42	Lydiatt *et al*, 1998	9p21-p22 main region of loss, correlated with recurrence. Suggested additional TSG close to *p16*
	7	Laryngeal	82	17	Kiaris *et al*, 1995	Main region of loss at 9p22 (distinct from *p16*)
		Pre-invasive and invasive HNSCC	28/72	20	El-Naggar *et al*, 1995	9p LOH most frequent LOH in pre-invasive lesions
	7	19 La-SCC, 13 Benign La lesions	78	32	Rizos *et al*, 1998	
		Pre-invasive and invasive HNSCC	71/72	17/29	van der Riet *et al*, 1994	Analysed region 9p21-p23.3. Similar frequency in pre-invasive and invasive lesions suggests an early event
9q	2	Not Specified	13	29	Nawroz *et al*, 1994	
	2	Not Specified	35	28	Ah See *et al*, 1994	
	3	Not Specified	20	80	Field *et al*, 1995	Associated with nodes at pathology (P=0.020)
11q	2	Not Specified	61	29	Nawroz *et al*, 1994	
	2	Not Specified	45	28	Ah See *et al*, 1994	
	4	Not Specified	23	80	Field *et al*, 1995	
	3	Not Specified	25	56	Lazar *et al*, 1998	LOH of 11q23 associated with recurrent disease
	4	Or(40),Ph(19),La(17), Ot(2)	8	78	Ransom *et al*, 1996	
12q	1	Not Specified	25	29	Nawroz *et al*, 1994	
	1	Not Specified	12	28	Ah See *et al*, 1994	
	2	Not Specified	15	80	Field *et al*, 1995	Associated with histopathological grading (P=0.022)

Table 2.2 – Loss of Heterozygosity studies on HNSCC reported in the literature.

Chromosome	No of loci analysed	Tumour type (s)	%age LOH	No. of Tumours	Reference	Correlation/Comments
13q	2	BSH(35), Dy(31), CIS(21), SCC(70)	**3/32/35/52**	83	Califano *et al*, 1996	
	2	Not Specified	**54**	29	Nawroz *et al*, 1994	
	1	Not Specified	**0**	28	Ah See *et al*, 1994	
	6	Not Specified	**27**	80	Field *et al*, 1995	Associated with histopathological grading
	2	Or(40),Ph(19),La(17), Ot(2)	**29**	78	Ransom *et al*, 1996	
	10		**52**	59	Yoo *et al*, 1994	94% LOH at marker telomeric to *Rb* gene, *Rb* gene lost in only 19% suggesting additional TSG at 13q14
	18	Oral	**68**	34	Ogawara *et al*, 1998	minimal region of deletion mapped at 13q14.3, telomeric to the RB1 locus, correlated with nodal metastases
	13	Or(18), Op(9), Hp(10), La(31), Ot(2)	**61**	70	Lee *et al*, 1994	LOH identified at multiple sites – suggested chromosome instability of chromosome 13. LOH identified in 63% of 'normal' mucosa
	?	Oral and supraglottic	**69**	145	Gupta *et al, 1999*	3 minimal regions of LOH identified: 13q34; 13q14.3; 13q12.1. Suggested two new TSG's
	4	Not Specified	**48%**	44	Sanchez-Cespedes *et al*, 2000	4 common regions of loss, *ing1* possibly not a TSG target in HNSCC
14q	2	BSH(35), Dy(31), CIS(21), SCC(70)	**3/23/32/44**	83	Califano *et al*, 1996	
	1	Not Specified	**39**	29	Nawroz *et al*, 1994	
	1	Not Specified	**5**	28	Ah See *et al*, 1994	
	3	Not Specified	**11**	80	Field *et al*, 1995	
17p	2	BSH(35), Dy(31), CIS(21), SCC(70)	**11/33/47/55**	83	Califano *et al*, 1996	High incidence of LOH in pre-invasive lesions
	3	Not Specified	**52**	29	Nawroz *et al*, 1994	
	2	Not Specified	**40**	28	Ah See *et al*, 1994	
	6	Not Specified	**50**	80	Field *et al*, 1995	Main region of loss 17p11.1-p12. 77% LOH seen in Hypopharyngeal tumours
	2	Or(40),Ph(19),La(17), Ot(2)	**45**	78	Ransom *et al*, 1996	

Table 2.2 – Loss of Heterozygosity studies on HNSCC reported in the literature.

Chromosome	No of loci analysed	Tumour type (s)	%age LOH	No. of Tumours	Reference	Correlation/Comments
17q	2	Not Specified	31	29	Nawroz *et al*, 1994	
	1	Not Specified	20	28	Ah See *et al*, 1994	
	4	Not Specified	30	80	Field *et al*, 1995	
	1	Or(40),Ph(19),La(17), Ot(2)	50	78	Ransom *et al*, 1996	
	4	19 Laryngeal SCC, 13 Benign laryngeal lesions	56	32	Rizos *et al*, 1998	
18q	1	Not Specified	23	29	Nawroz *et al*, 1994	
	42	Not Specified	70-75%	57	Takebayashi *et al*, 2000	Identified 3 regions of loss ; 18q21.1, 18q22.2, 18q23
	1	Not Specified	0	28	Ah See *et al*, 1994	
	8	Not Specified	49	80	Field *et al*, 1995	Main region of loss 18q21.1-21.3, not the site of DCC
	1	Or(40),Ph(19),La(17), Ot(2)	20	78	Ransom *et al*, 1996	
	10	Hy(15), Or(14), La(6), Or(6)	49	41	Rowley *et al*, 1995	Main region of loss 18q 21.1-q21.3. Low frequency of DCC loss
			40	67	Pearlstein *et al*, 1998	18q LOH correlated with poorer 2-year survival (P=0.008)
	18	Not Specified	52	17	Jones *et al*, 1997	Main regions of loss 18q11.1-q12.3 and 18q21.1-q23
22q	1	Not Specified	29	29	Nawroz *et al*, 1994	
	1	Not Specified	16	28	Ah See *et al*, 1994	
	1	Not Specified	0	80	Field *et al*, 1995	
	3	Not Specified	8-28	50	Poh-Fredenco *et al*, 2000	LOH higher in laryngeal tumours; region of loss 22q11.2-q12.3 may play a role in aggressive stage III/IV tumours
	1	Or(40),Ph(19),La(17), Ot(2)	18	78	Ransom *et al*, 1996	

Table 2.2 – Loss of Heterozygosity studies on HNSCC reported in the literature. This table represents the results of multiple studies and is restricted to the chromosomal arms demonstrating a high frequency of LOH. The data in this table was gathered from a Medline search (1993-2000) therefore only data presented in the abstract was available. As a consequence of this the histological type of many of the tumours studied was not specified.

Hy – Hypopharyngeal, La – Laryngeal, Op – Oropharyngeal, Or – Oral, Ph – Pharyngeal, Sa – Salivary Gland, Sk – Skin, Ot – Other., BSH – Benign Squamous Hyperplasia, Dy – Dysplasia, CIS – Carcinoma *in situ*, SCC – Invasive SCC.

also seen in most major cancers (Mertens *et al*, 1997). Despite the high prevalence of 3p deletions, only two serious candidate tumour suppressor genes have been identified, *FHIT* and *VHL*. The fragile histidine triad gene (*FHIT*) is a recently identified tumour suppressor gene located at 3p14.2 (Gotte *et al*, 2000). Abnormal transcripts of *FHIT* have been detected in over 50% of cases and reduced expression have been detected in 66% of (n=32) oral SCC (Mao *et al*, 1996; van Heerden *et al*, 1999). However, the mechanisms for inactivating the gene are not well understood and abnormal transcription does not always correlate with genetic alterations. Methylation of the 5' CpG island of the *FHIT* gene has been demonstrated to be closely linked to transcriptional inactivation in oesophageal cancers (Tanaka *et al*, 1998) and it is suggested that a similar mechanism may be responsible for transcriptional repression in HNSCC.

The Von-Hippel Lindau (*VHL*) TSG maps to the region 3p25-p26 and is commonly mutated in renal cancer, however this may not be the target gene for HNSCC. Waber *et al* (1996) identified losses in regions surrounding the *VHL* gene but found no evidence for mutation of *VHL* in HNSCC, when analysed by single-strand conformation polymorphism, dideoxyfingerprint and direct DNA sequence analysis.

2.4.1.2 Chromosome 8p

No candidate TSG have been put forward for chromosome 8p that has shown LOH for a range of loci at frequencies of 16-63%. Two regions have been identified as loci of minimal loss: 8p12, and 8p22. 8p22 is also postulated to be the site of a TSG important in colorectal cancer (Cunningham *et al*, 1993).

2.4.1.3 Chromosome 9p

LOH on chromosome 9p is commonly observed with the majority of studies reporting frequencies in the range 70-80%. The most common region of loss on 9p occurs within the band 9p21-p22, the site of the *p16* TSG. $p16^{ink4a}$ codes for the p16 protein, an inhibitor of the cyclin D1/cyclin dependant kinase complex. Wild type p16 interacts strongly with cdk 4 and cdk 6 (inhibiting the kinases ability to interact with cyclin D1), arresting normal diploid cells in late G1 phase whereas abnormal p16 cannot (Lukas *et al*, 1995)(Figure 2.1). However wild type p16 is unable to induce cell cycle arrest in cells lacking a functional Rb protein indicating loss of p16 and loss of Rb protein may form a common path to tumourigenesis (Lukas *et al*, 1995). Deletions and mutations of p16 have been found at frequencies of over 75% in melanoma cell lines (Kamb *et al*, 1994) and some work suggests that genetic abnormalities in *p16* may underlie familial susceptibility to melanoma (Hussein

et al, 1994). Loss of active p16 has been shown in a large number of tumour types, including HNSCC (Merlo *et al*, 1995; Lai and El-Naggar, 1999). LOH at the 9p21 locus is a common event in HNSCC, however point mutations, determined by DNA sequencing, appear not to be the major method of inactivation of the remaining allele. Methylation of the 5' CpG island of the *p16* gene has been identified as a method of tumour suppressor gene deactivation (El-Naggar *et al*, 1997a; Riese *et al*, 1999; Merlo *et al*, 1995) and Sidransky's group demonstrated that this methylation pattern was associated with a complete transcriptional block which was reversible with treatment of 5-deoxyazacytidine (Merlo *et al*, 1995). This has lead to the interesting question posed by Little and Wainright (1995): Could this methylation be overcome *in vivo* and could *p16* be specifically demethylated? The high prevalence of *p16* alterations detectable in HNSCC indicates an important role for this tumour suppressor gene in the development of HNSCC.

Several studies have identified additional discrete regions of loss distinct from p16 suggesting the involvement of other TSG in this region (Nakanishi *et al*, 1999; Kiaris *et al*, 1995). Allelic loss of the interferon-α cluster tumour suppressor gene (*INFA*) has been identified as a frequent genetic occurrence as well as loss of a region telomeric to both the *INFA* and *p16* loci.

LOH of 9p21 has been shown to occur in the absence of histological change (Lydiatt *et al.*, 1998). This study of 21 oral and oropharyngeal tumours comparing available samples of histologically normal mucosa, dysplasia and adjacent invasive identified LOH at 9p21 (13 informative patients) in 6/13 normal mucosa specimens, increasing to 8/13 in dysplastic lesions and 11/13 in invasive cancer. Analysis of other markers believed to be involved in HNSCC tumourigenesis (3p21 and 3p14) identified LOH in only 1/17 informative dysplastic specimens and none of the histologically normal mucosal specimens. This finding of 9p LOH early on in HNSCC tumourigenesis has been reported in several other studies at frequencies of 28-72% (Califano *et al.*, 1996; El-Naggar *et al.*,1995; van der Reit *et al*,1994 – See Table 2.2). The high incidence of LOH on 9p along with frequent LOH in pre-invasive lesions suggests that loss of gene(s) on 9p is an early event in HNSCC progression. Exactly which gene(s) are involved remains to be fully elucidated.

2.4.1.4 Chromosome 13q

Two distinct regions of loss have been mapped to 13q33-34 and 13q14.2-q14.3 (Maestro *et al*, 1996, Yoo *et al*, 1994, Ogawara *et al*, 1998). Despite frequent LOH on 13q, there does not appear to be inactivation of the retinoblastoma tumour suppressor gene in HNSCC,

instead a region telomeric to this locus at 13q14.3 is likely to contain additional, as yet unidentified, TSG important to HNSCC. LOH in this region has also been identified in histological mucosa adjacent to tumours and correlated with nodal metastases in two studies (Ogawara *et al*, 1998; Lee *et al*, 1994). Recently *ing1* has been suggested as a target tumour suppressor gene for the 13q33-34 locus (Garkavtsev *et al*, 1997). The *ing1* gene encodes the p33(ING1) nuclear protein, an inhibitor of cell growth thought to act through physical interaction with p53 (Garkavtsev, 1996). Whilst germline polymorphisms have been demonstrated in approximately 20% of HNSCC tumours (Sanchez-Cespedes *et al*, 2000; Krishnamurthy *et al*, 2001), the few reports in the literature to date have so far failed to identify *ing1* as a site of significant somatic mutation in HNSCC.

2.4.1.5 Chromosome 17p

The locus of the *p53* gene on 17p13 is a common site for allelic imbalance in HNSCC (40-55%) although higher frequencies of LOH have been reported at loci distal to this at 17p11.1-p12 with particularly high frequency of loss in hypopharyngeal tumours (77% - Field *et al*, 1995). LOH analysis reports chromosomal loss on 17p at a much greater frequency than does conventional karyotyping (Mertens *et al*, 1997) demonstrating that regions of loss on 17p are relatively small deletions, beyond the resolution of G banding karyotyping.

Mutations of the *p53* tumour suppressor gene are the most frequent genetic alteration detected in human cancers (Greenblatt *et al*, 1994). The *p53* gene encodes a 53 kDa nuclear phosphoprotein that has been described as the 'guardian of the genome'. A key function of the protein appears to be the prevention of the propagation of genetic errors acquired during DNA replication by either inducing G1 growth arrest and stimulating DNA repair or by triggering apoptosis. *p53* mutations can be identified either by sequencing analysis of the gene or detection of the abnormal protein product by immunohistochemistry. Wild type p53 protein has a very short half-life (6-20 minutes) and is not normally detectable by immunohistochemistry, however mutant forms of p53 are far more stable with half lives of up to 6 hours allowing accumulated abnormal p53 to be detected by immunohistochemistry (Gannon *et al*, 1990). However, in general, immunohistochemistry fails to detect frame shift mutations that lead to the production of a truncated protein. Mutation frequencies for *p53* in head and neck tumours, as detected by immunohistochemistry, have been quoted as between 37% and 88% (Smith and Haffty, 1999) with incidence increasing with disease progression (Boyle *et al*, 1993). The frequency of mutation has also been demonstrated to be higher in HNSCC patients who use tobacco

and alcohol compared to the minority group of non-drinkers and non-smokers (Brennan *et al*, 1995).

Point mutations are the most common abnormality of *p53* in HNSCC and have been described in many codons of the gene with mutational hotspots identified within the evolutionary conserved region of the gene at codons 149, 274, 288, 296 and 298 (El-Naggar *et al*, 1995). Analysis of the entire coding region of *p53*, by sequencing all 11 exons, has identified *p53* mutations in 42-91% of HNSCC patients (Kropveld *et al*, 1999; van Oijen *et al*, 2000; Saunders *et al*, 1999). Interestingly, van Oijen *et al* demonstrated the high variability of p53 mutations with no mutation occurring more than twice in a sample of 69 HNSCC. This full length sequencing of the gene may be of significance as many previous studies had analysed only the core domain of the gene (exons 5-9) as it was suggested that mutations outside of this region were rare (Hollstein *et al*, 1991). These full length sequencing studies (136 patients in total) identified mutations outside the traditionally examined region in 20-33% of cases indicating that analysis of the evolutionary conserved region of the gene is likely to underestimate the frequency of *p53* gene mutation. However the significance of these mutations outside the core domain of the protein remains to be elucidated. Differentiating the types of mutation within the core domain of the p53 protein has identified correlation between mutations in the DNA binding site of the p53 protein and loss of chromosomal alleles, higher tumour stage, lymph node metastases and survival (Erber *et al*, 1998). This would suggest that mutations interfering with the binding of p53 to DNA have the greatest effect on the ability of p53 to monitor the genome for DNA damage, however additional studies are required to confirm this.

A large-scale study of archival specimens of HNSCC has identified mutant p53 expression in 56% of dysplastic lesions (n=190), 60% of carcinoma *in-situ* (n=102) and 53% carcinomas (n=493) (Pavelic *et al*, 1994). These figures demonstrated that p53 mutations did not increase with progression of the lesions and strongly suggest that p53 alterations occur early in HNSCC tumourigenesis. Other studies have reported the finding of mutant p53 expression in pre-invasive lesions (Raybaud-Diogene *et al*, 1996; Ahomadegbe *et al*, 1995).

A recent analysis of resection margins in 25 HNSCC patients demonstrating a p53 mutation demonstrated a significantly higher frequency of recurrence in patients (n=13) with surgical margins positive for p53 mutations (5/13 recurred) compared with patients

whose margins were negative (0/12 recurred) (Brennan *et al*, 1995). This study also identified neoplastic cells in 21% of lymph nodes initially classified as negative by histological assessment. A similar studied on 18 oral cancer patients with conventionally clear margins comprehensively assessed p53 status (by p53 phage plaque assay, immunocytochemistry and mutational analysis) and identified tumour positive surgical margins in 6/11 assessable patients (Partridge *et al*, 2000). Of the 5 patients who subsequently developed locoregional recurrence (follow up >36 months) 4 had tumour positive margins, as assessed by molecular analysis of p53, at time of resection. Both these studies demonstrate how molecular analysis can augment standard histopathological assessment and may improve the prediction of local recurrence.

Mutations of p53 have been implicated in radio-resistance of tumours of the oral cavity/oropharynx (Raybaud-Diogene *et al.*, 1997). Functional p53 is required for radiation induced apoptosis following DNA damage therefore it was hypothesised that tumours lacking a functional *p53* gene will become radio-resistant. Tumours with detectable p53 expression and a low growth fraction (as measured by immunostaining for ki-67 – a marker of proliferation) demonstrated a significant probability (P=0.000004) of not responding to radio therapy, whilst absence of p53 expression, and a high rate of cellular proliferation, predicted an excellent response to radiotherapy even in advanced disease. Univariate and multivariate analysis of the simultaneous detection of bcl-2 over-expression and *p53* gene mutation has also been associated with a greater risk of locoregional failure (n=85; p=0.002 and p=0.001 respectively) (Gallo *et al*, 1999). The relationship of *p53* mutations and laryngeal radio-resistance is less well understood.

The central role of the p53 in human cancer has identified the *p53* gene as a potential candidate for gene therapy. Transfection of a functional *p53* gene into a p53 deficient human HNSCC cell line has been shown to result in a dose-dependant increase in radio-sensitivity and restoration of the apoptotic pathway (Pirollo *et al*, 1997). Phase I/II trial are underway evaluating the safety and tolerability of adenovirus-mediated *p53* gene transfer in both HNSCC and lung cancer (Clayman *et al*, 1998; Nemunaitis *et al*, 2000). Clayman *et al* have demonstrated no dose-limiting toxicity or serious adverse effects and limited clinical efficacy in 17 of the 33 patients with non-resectable tumours.

2.4.1.6 Chromosome 18q

LOH on 18q has identified two main regions of loss, 18q1.1-12.3 and 18q21.1-q21.3 (Jones *et al*, 1997; Field *et al*, 1995). The region affected by the loss at 18q21.1-21.3 appears to be

distinct from the site of the *DCC* (Deleted in Colorectal Carcinoma) gene suggesting the presence of additional TSG at this locus. LOH at 18q has been correlated with poor 2-year survival in one study (Pearlstein *et al*, 1998).

2.5 Genetic progression model for HNSCC

The multistep process of cancer development has been best described for colorectal cancer by Vogelstein (1992). Information obtained from classical cytogenetics and LOH studies has begun to identify many of the key genetic aberrations underlying the development of squamous cell cancer of the head and neck. These studies have demonstrated that HNSCC is characterised by loss of genetic material at many loci, including the sites of known TSGs. Analysis of invasive HNSCC, as well as early pre-malignant lesions and histologically 'normal' mucosa surrounding a lesion, has led to attempts at establishing the order of many of these frequently found aberrations and to relate this to the histological progression of the disease. Several attempts have been made at defining a multi-step carcinogenesis model for HNSCC based on the frequencies of genetic abnormalities in different stages of malignant progression (Califano *et al*, 1996; Mao and El-Naggar, 1999; Myers, 1996). These proposed models are essentially the same and are based on the elegant demonstration of LOH analysis of 10 loci previously shown to be involved in HNSCC (Califano *et al*, 1996). This study demonstrated a progressive increase in the spectrum of chromosomal loss at each histopathological step from benign hyperplasia through to invasive cancer (Figure 2.3).

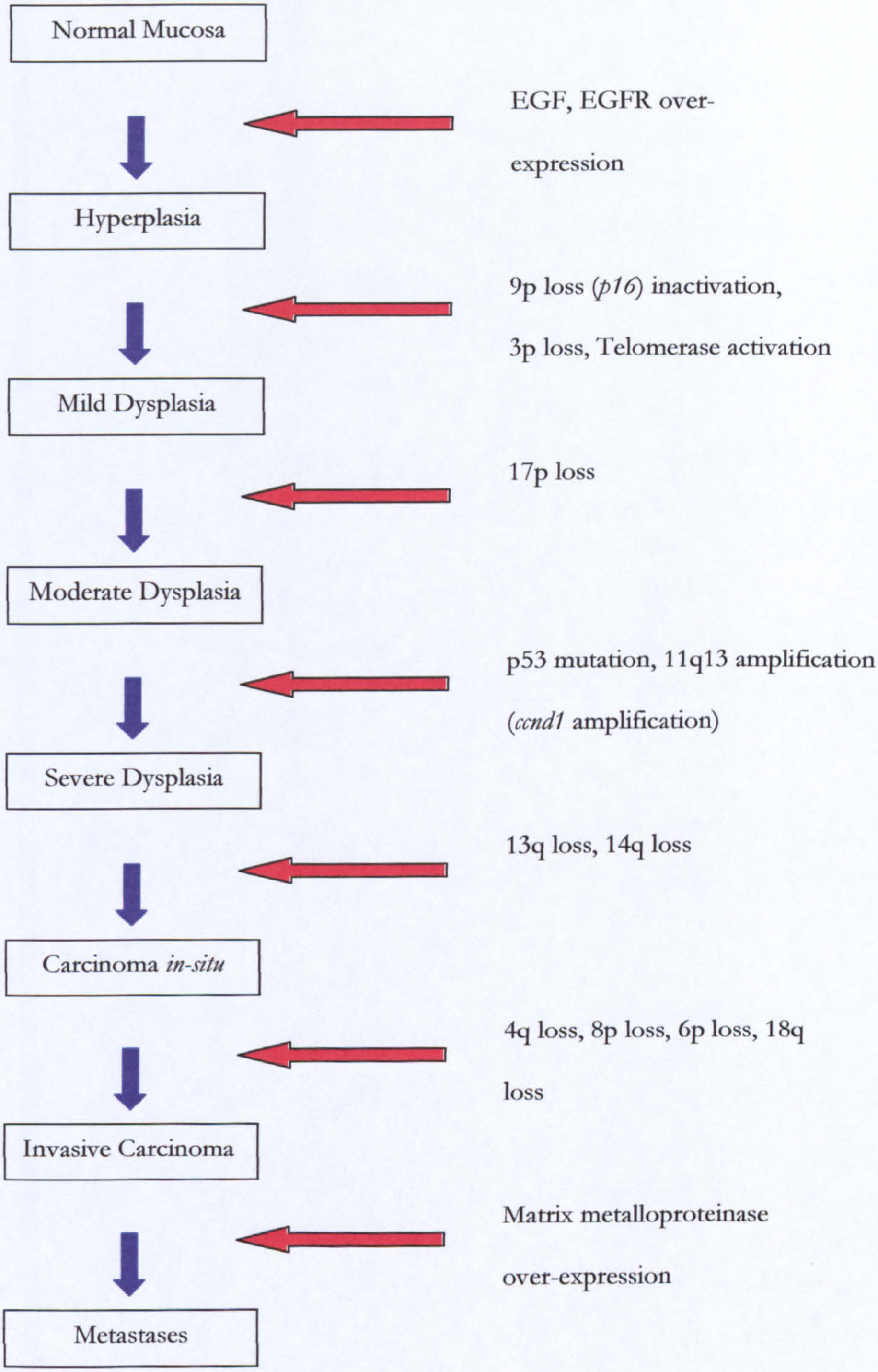

Figure 2.3 – Preliminary genetic progression model for HNSCC. Genetic events associated with the progression from normal mucosa to invasive and metastatic HNSCC are depicted. The relative order of aberrations is inferred from the frequencies of these aberrations in different stages of histopathological malignant progression. Adapted from Califano *et al*, 1996, Mao and El-Naggar, 1999 and Myers, 1996.

2.6 Aims

The aim of this thesis was to apply the new technology of CGH to head and neck squamous cell tumours to identify regions of chromosomal gains and losses responsible for the biological behaviour of the disease. As genomic technology advances it is envisaged that such technology may become increasingly important to the head and neck oncologist and therefore the work of this thesis was aimed at establishing modern molecular techniques in a clinical environment. Several questions were addressed to evaluate the clinical usefulness of this technique.

Can CGH be established in a clinical laboratory setting? Optimisation of the key stages in the methodology and evaluation of the influence of each stage on the accuracy of the technique (Chapter 4).

Can CGH provide evidence of a field change effect occurring in the mucosa surrounding a primary head and neck tumour? Are gross chromosomal aberrations detectable in histologically normal mucosa? (Chapter 5).

What is the genetic relationship between primary head and neck tumours and corresponding lymph node metastases? Are specific genetic aberration(s) associated with the metastatic phenotype? (Chapter 6).

Why do a significant proportion of early laryngeal tumours fail to respond to radiotherapy? Are specific genetic marker(s) able to predict resistance to radio-therapy? (Chapter 7).

Do any loci of DNA copy number aberration correlate with clinical outcome? Statistical analysis of clinical parameters and genetic aberrations detected by CGH (Chapter 8).

Chapter 3

Materials and Methods

The majority of this thesis was focused on the establishment and optimisation of Comparative genomic hybridization (CGH) and its application to HNSCC. Chapter 4 details the principles behind CGH and discusses the technical aspect of the method in more details as well as presenting data on the optimisation of the method. The following sections describe the final optimised protocol that was applied to all specimens studied using this method. Figure 3.1 depicts a schematic representation of the different stages within a successful CGH experiment.

All general laboratory chemicals were obtained from Sigma unless otherwise indicated. All CGH reagents were purchased from Vysis unless otherwise indicated. The full addresses of all other suppliers are listed in Appendix 1.

3.1 Specimen acquisition

Tissue samples were collected at time of surgical resection. A representative sample of tumour tissue was dissected from the resected tissue, in a manner agreed with the Department of Pathology (Hull and East Yorkshire Hospitals), and immediately snap frozen in liquid nitrogen in theatre. All tissue specimens were routinely transported to the laboratory where they were catalogued and stored at -80°C until required.

3.2 Haematoxylin and eosin (H&E) staining

Representative tissue, taken immediately adjacent to the specimen used for analysis, was analysed histologically to confirm diagnosis and to confirm the presence of epithelial cells. Specimens were fixed in 10% formal saline (0.15M NaCl; 10% v/v formaldehyde) for at least 24 hours. Fixed tissue was transferred to the Department of Pathology for standard paraffin embedding and sectioning and 4μm sections were obtained. For H&E staining, paraffin was first softened by warming slides over a Bunsen until the paraffin was seen to melt and then removed with three changes of Xylene for 5 minutes each. Sections were rehydrated through a series of alcohols (100%, 90%, 75%, 45%, and 25%) for two minutes each and then rinsed in distilled water for 2 minutes. Slides were stained in Gill's haematoxylin for 5 minutes and excess stain removed by placing slides in running tap water for 5 minutes. Sections were then dipped in 1% acid / alcohol (1% v/v HCl; 70% v/v ethanol) for 2 seconds followed by 5 minutes in 1% w/v eosin (Sigma). The slides were washed in running tap water for 2 minutes, dehydrated through a series of alcohols (45%, 75%, 95%, 100%) for 1 minute each and taken through 3 changes of xylene for 2 minutes each to clear the sections. Finally, cover slips were applied to the slides using Histomount (National Diagnostics).

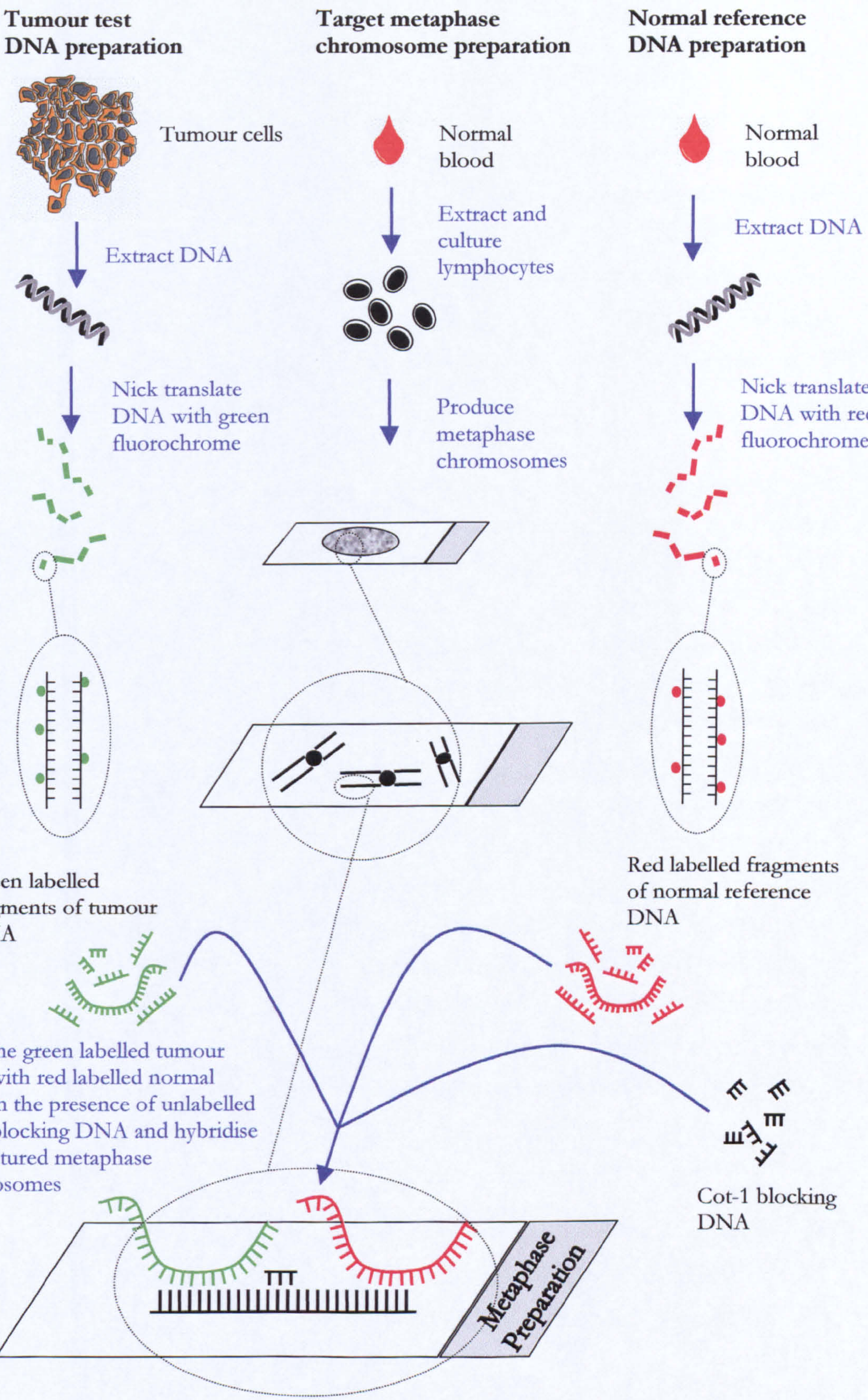

Figure 3.1 – Schematic representation of Comparative Genomic Hybridization

3.3 DNA extraction

DNA was extracted using standard proteinase K / phenol extraction protocols (Sambrook *et al*, 1989). A piece of tumour tissue, approximately 0.5cm^{3,} was placed in a mortar pre cooled in liquid nitrogen and ground to a fine powder. Liquid nitrogen was added to the mortar as required to keep the tissue frozen. The powdered tissue was re-suspended in 4.5ml of TEN (10mM Tris HCL; 40mM EDTA; 10mM NaCl. pH 7.5), 0.5ml 10% w/v sodium dodecyl sulphate (SDS) and 50µl of proteinase K (10mg/ml stock) added to a final concentration of 0.1mg/ml. Tissue was incubated overnight at 37°C until the suspension became clear, if necessary more proteinase K was added, up to a final concentration of 1mg/ml and the incubation time increased (up to 3 days).

Genomic DNA was purified from this solution using a phenol-chloroform extraction. An equal volume of Tris saturated phenol (pH 7.5, Rathburn) was added to the suspension and agitated for 5 minutes on a rotator. The aqueous and phenolic phase were then separated by centrifugation at 2500g for 5 minutes and the upper aqueous layer collected to a new 15ml polypropylene tube. An equal volume of phenol: chloroform: iso amyl alcohol (25:24:1) was added and separated as before. The upper aqueous layer was collected to a new 15ml tube and an equal volume of chloroform: iso amyl alcohol (24:1) added. This mixture was agitated and centrifuged as before to separate the aqueous layer containing the genomic DNA. The upper aqueous layer was collected to a new 15ml tube and the DNA precipitated out of solution by the addition of 2 volumes of 100% Ethanol and 0.1 volumes of 3M Sodium Acetate. The tube was then incubated at –20° for 15 minutes to maximise yield. DNA was pelleted by centrifugation at 4500g for 5 minutes and the supernatant discarded. Pellets of DNA were then washed with 5ml of 95% ethanol and re-pelleted as before. The supernatant was then discarded and the pellet dried at 37°C until the remaining ethanol had evaporated (approximately 5 minutes). Finally the pellet was re-suspended in an appropriate volume of TE buffer (approx 50µl; 10mM Tris; 1mM EDTA. pH 8.0).

3.4 DNA quantification

To ensure that the extracted DNA was of sufficient quality for Nick Translation, the quality (purity) was first assessed. In addition, the concentration of the DNA was also measured. Both these factors were determined by measuring the light absorbance of the DNA solution at defined wavelengths (260nm and 280nm).

An aliquot of DNA sample was diluted 1:50 in TE buffer prior to DNA quantification. This dilution was then quantified spectroscopically using a GeneQuant DNA calculator (Amersham Pharmacia Biotech). The GeneQuant calculator was calibrated using 100µl of TE buffer (the same batch of solution the DNA was re-suspended in). DNA concentration was calculated according to the following equation:

Concentration µg/ml = Optical Density at 260nm x 50^{Ψ} x (dilution factor)

$^{\Psi}$ (DNA constant – 1 A_{260nm} unit is equivalent to 50µg of DNA/ml)

and DNA purity was calculated as:

Optical density at 260nm / Optical density at 280nm

A DNA purity ratio of > 1.7 was desirable for a successful CGH.

3.5 Verification of genomic DNA Size

All genomic DNA samples were electrophoresed on an agarose gel to confirm the DNA was of suitable size for nick translation. For a successful nick translation, genomic DNA fragments of >10,000kb were desired.

A 1.2% w/v submarine agarose gel was prepared by adding 0.6g of Ultrapure Agarose (Gibco) to 50ml of tris-acetate EDTA (TAE) buffer (40mM Tris-acetate, pH7.5-7.8, 1mM EDTA) and 2.5µl of Ethidium Bromide (10mg/ml) added to visualise the DNA. 8µl of genomic DNA (at an approximate dilution of 0.2µg/µl) was mixed with 2µl of 6x Gel Loading Buffer (0.25% w/v bromophenol blue, 30% v/v glycerol in Tris HCl pH 8.0) and electrophoresed at 10V/cm for approximately 20 minutes, until the dye in the gel loading buffer was approximately 2-3 cm from the end of the gel.

3.6 Nick Translation

Nick Translation is the process by which fluorescently-labelled dUTP molecules are incorporated into double stranded genomic DNA (Balmain and Birnie, 1979). Limited treatment of the genomic DNA with DNase I introduces random nicks in the double stranded DNA. 3'- free hydroxyl groups are exposed by the DNase I and act as a substrate for the DNA polymerase (Figure 3.2 and Figure 3.3). The 5' to 3' exonucleolytic activity of DNA polymerase releases 5' mononucleotides whilst simultaneously incorporating nucleotides repeatedly in a 5' to 3' direction (thus translating the nick along the length of the DNA strand). The four deoxynucleoside triphosphates are included in the nick translation mix with the final concentration of the dTTP reduced by 50% and supplemented with dUTP labelled with a fluorescent molecule. dUTP is used as this molecule has a similar binding affinity for dATP but can accommodate the inclusion of a

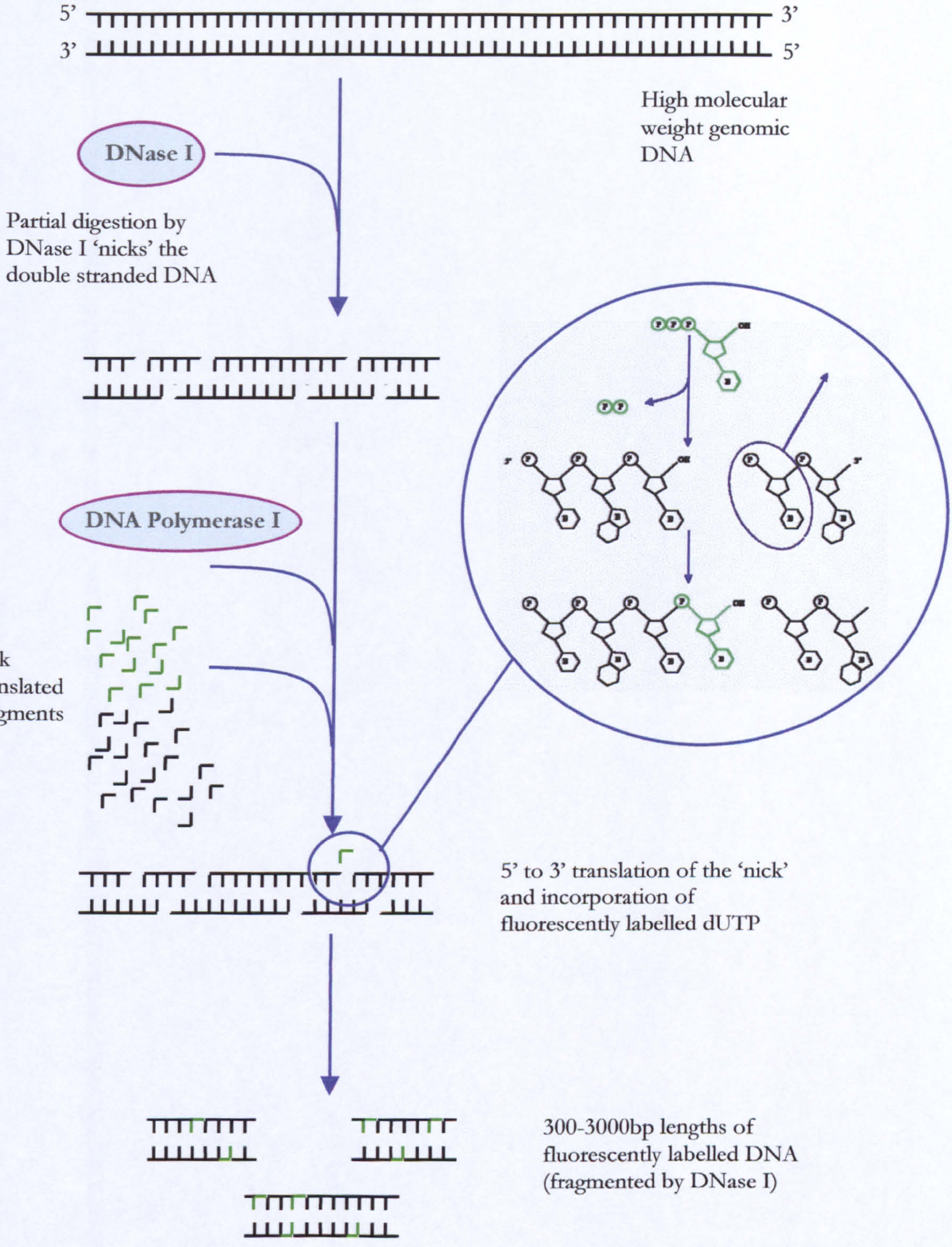

Figure 3.2 – Nick Translation. Treatment of high molecular weight genomic DNA with an optimised balance of DNase I and DNA polymerase I generates short double stranded lengths of fluorescently labelled DNA. The magnified region depicts nucleotide incorporation at the molecular level and is shown in Figure 3.3 (overleaf)

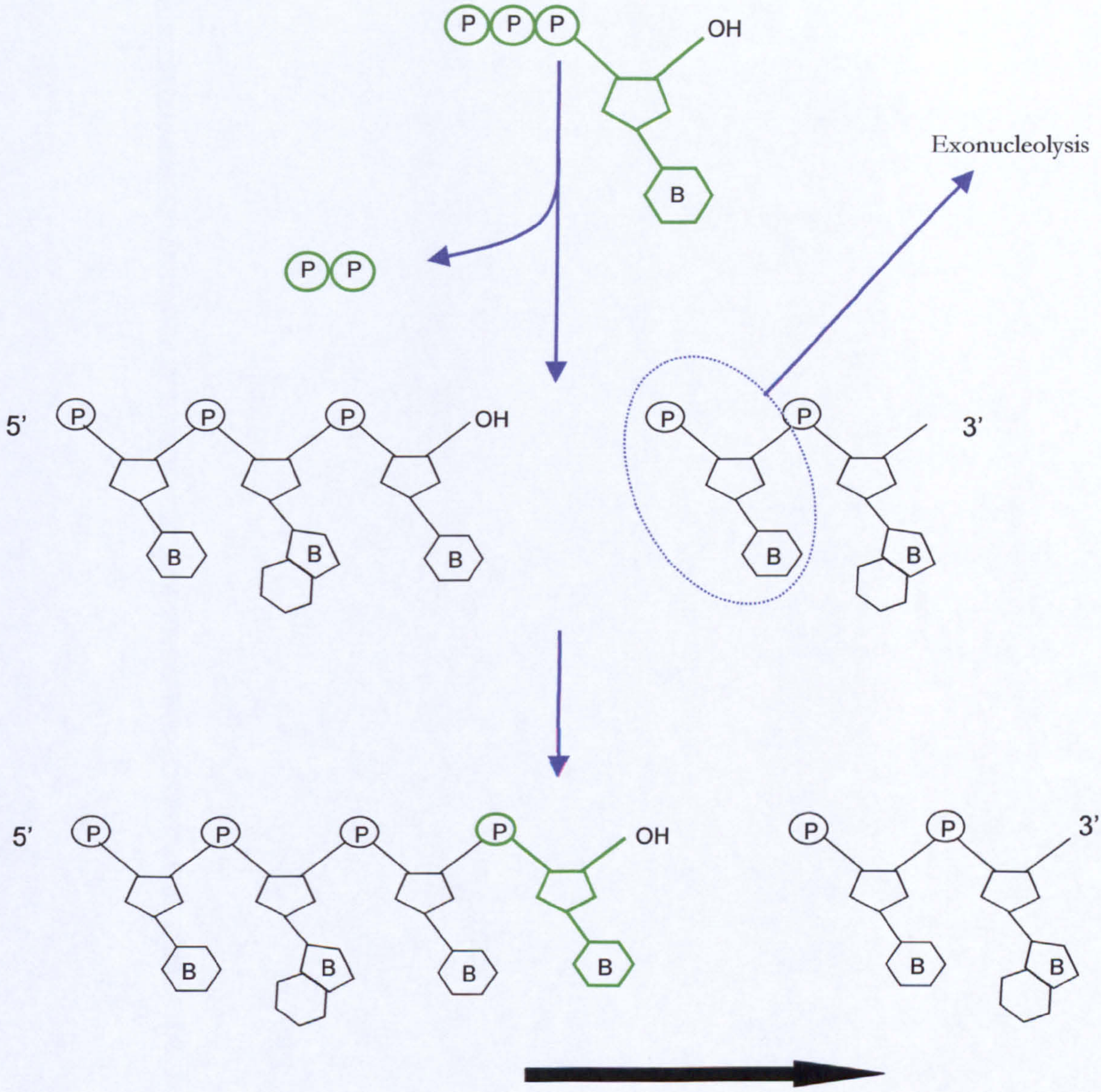

Figure 3.3 – Nucleotide incorporation during nick translation. Limited action of DNase I introduces random 'nicks' into the DNA (Single strand only shown) revealing a 3' free hydroxyl group. This forms the substrate for DNA polymerase I, which recruits and incorporates deoxy-nucleotide-triphosphates (including fluorescently labelled dUTP molecules) forming a covalent phosphodiester bond with the previous nucleotide of the same strand. The 5' to 3' exonucleolytic activity of DNA polymerase releases 5' mononucleotides resulting in propagation of the 'nick' in a 5' to 3' direction along the length of the molecule (arrow).

P – Phosphate group; B – DNA base; -OH – hydroxyl group

large fluorescent molecule better than dTTP. In standard CGH analysis, tumour DNA is typically labelled with a green fluorochrome and normal reference DNA labelled with red, although these can be reversed. Figure 3.2 depicts the incorporation of fluorescently labelled nucleotides into genomic DNA. 1µg of high quality genomic DNA was made up to a volume of 17.5µl with nuclease free distilled water in a 500µl microcentrifuge tube. To this was added: 2.5µl of 0.2mM Spectrum Green, 5µl of 0.1mM dTTP, 10µl of dNTP mix (0.1mM dATP, 0.1mM dCTP, 0.1mM dGTP), 5µl of 10 x nick translation buffer (500mM Tris-HCl, pH 7.2, 100mM $MgSO_4$, 1mM DTT) and vortexed briefly. 10µl of nick translation enzyme (DNA polymerase I, DNase I in 50% glycerol, 50mM Tris-HCl, pH 7.2, 10mM $MgSO_4$) was then added and pipetted several times to mix thoroughly. For all DNA specimens a duplicate nick translation mix was set up increasing the amount of enzyme used to 12µl and decreasing the volume of nuclease free water by 2µl to maintain a final volume of 50µl. Tubes were pulsed briefly in a microcentrifuge to collect the contents and incubated for 2 hours at 15°C in a Techne Genius thermal cycler (Scientific Laboratory Supplies). Enzyme activity was terminated by denaturation at 70°C for 10 minutes and samples stored at 4°C until required.

3.7 Verification of nick translation products

The size range of the fragments generated by enzymatic digestion was established by agarose gel electrophoresis. A 1.2% w/v agarose gel was prepared as described in Section 3.5 and 8µl of nick translation product electrophoresed. The sizes of the nick translation fragments were visualised under UV illumination and recorded on Polaroid film. The desired range of the DNA fragments was 300-3000 bp and only smears of DNA fragments containing a significant proportion of DNA within this range were processed further (See Section 4.2 for examples).

3.8 Comparative Genomic Hybridization

CGH generates a copy number profile for a DNA sample of interest identifying chromosomal loci that are relatively over- or under-represented in the genome. As the entire genome is screened in a single experiment CGH requires no prior knowledge of the genetic aberrations nor does it require an extensive series of loci-specific probes to evaluate the extent of genetic gains and losses in the genome. Differentially labelled DNA samples are simultaneously and competitively hybridized (Figure 3.1), in the presence of COT-1 DNA to block repetitive sequences, onto normal human metaphase chromosomes. COT-1 DNA is prepared from human genomic DNA enriched for the interspersed repetitive

sequences found throughout the genome. After hybridization the slides are stringently washed, counterstained and the test-to-normal fluorescence intensity is measured along the length of the metaphase chromosomes. As the kinetics of a CGH hybridization are independent, and competitive, any imbalance in the green to red staining intensity is proportional to the copy number of the sequences in the DNA sample of interest. DNA copy number changes (losses and gains of DNA) are therefore mapped directly onto normal chromosomes allowing simple identification of loci demonstrating imbalances in copy number in the test DNA.

3.8.1 Probe preparation

Differentially labelled tumour (test) DNA and normal (reference) DNA were combined as follows. 800ng of SpectrumGreen™ labelled test DNA, 200ng of SpectrumRed™ labelled reference DNA and 30µg of COT-1 DNA were combined in a 0.5ml microfuge tube and mixed well. 7.5µl (0.1 volumes) of 3M sodium acetate and 186µl (2.5 volumes) of 100% ethanol were added, to precipitate the DNA, and vortexed briefly. The probe mix was then incubated at –80°C for 15 minutes and the DNA pelleted by centrifugation at 10 000g for 15 minutes. The supernatant was removed and the pellet dried by carefully absorbing droplets from the inside of the tube with clean tissue paper followed by incubation at 37°C for 3-5 minutes. Re-suspension of the probe was a crucial step and was achieved by firstly adding 3µl of nuclease free water to the pellet and mixing with the tip of the pipette until the pellet was seen to go into solution, and secondly by pipetting repeatedly for several minutes until the solution of DNA was seen to pipette 'smoothly'. Finally, 7µl of hybridization buffer was added and pipetted repeatedly until the two solutions were mixed thoroughly. Due to the light sensitive nature of the fluorescent molecules all probe handling was performed in subdued lighting. Probes were then incubated at 4°C, protected from light, overnight to ensure the DNA was fully re-suspended.

3.8.2 Probe hybridization

The CGH probe and the target metaphase chromosome slides were denatured simultaneously. The probe was denatured by heating to 73°C in a Techne Genius PCR block for 10 minutes, followed by at least 2 minutes pre-annealing time at 37°C. Whilst the probe was denaturing normal male metaphase preparations were also denatured. 70ml of freshly made denaturation solution (70% v/v de-ionised ultra-pure formamide, 2xSSC pH 7.25) was pre-warmed to 73 ±1°C in a Coplin jar in a water bath. Metaphase slides were denatured 4 at a time (clean, plain glass slides were added if less than 4 slides were processed to maintain the desired temperature) for 5 minutes at 73 ±1°C. Slides were then

dehydrated through a series of ethanols: 70% for 1 minute, 85% for 1 minute and 100% for at least 1 minute. Slides were left in the final ethanol until the probe was ready and then excess liquid was blotted from the slide edge and the remaining ethanol allowed to evaporate. Hybridization areas were marked on the back of the slide and 10 µl of probe applied to two coverslips which were then applied to the slide by touching the inverted slide onto the droplet of probe mix. Any air bubbles present were carefully excluded by gentle pressure with a clean pipette tip and the coverslips sealed with rubber cement (Oncor). Slides were left to hybridize in a dry, lightproof box at 37°C for 72 hours.

All hybridizations were performed alongside control hybridizations of DNA extracted from the MPE600 breast cancer cell line which contains several known and well documented copy number changes (Kallioniemi *et al*, 1992). Any batches of slides for which the control experiment did not produce the expected result were discarded.

3.8.3 Slide washing

After hybridization, rubber cement was removed from the slides without disturbing the coverslips (in subdued lighting) and coverslips were removed by lifting vertically away from the slide avoiding scratching the chromosomes. Slides were then immediately placed in 70ml 0.4 x SSC/ 0.3% NP-40 pre-warmed to 74±1°C. 4 slides were processed simultaneously and were agitated for 2-3 seconds in this stringent wash solution and left for exactly 2 minutes. Washing was quenched by transferring the slides to 70ml 2 x SSC/0.1% NP-40, agitating for 2-3 seconds and leaving to stand for 40 seconds. Slides were then air dried in darkness and counterstained by applying 15µl of DAPI solution (180ng Diamidinophenylindole dissolved in antifade). Slides were stored at 4°C (protected from light) for at least 30 minutes and viewed under fluorescent illumination.

3.8.4 Image acquisition

Slides were examined using a Nikon Eclipse E800 epi-fluorescent microscope (Nikon) equipped with a Ludl six-position automated filter wheel and a SenSys cooled Charged Coupled Device (CCD) camera (Photometrics) connected to a Power Macintosh 7500/100 running the IP Lab Smart Capture Software. Slides were illuminated with a 100 Watt mercury lamp with three excitation filters specific for TRITC, FITC and DAPI and a triple band pass filter to allow simultaneous viewing of the Spectrum Green™, Spectrum Red™ and DAPI fluorescence. For visualisation purposes and metaphase location x10 and x40 objective lenses were used and all images were captured using a x100 objective lens. Hybridization was initially evaluated by eye for adequate and balanced red and green probe intensity and minimal background fluorescence. Slides were scanned using DAPI

fluorescence to limit photo-bleaching of the red and green fluorochromes and suitable metaphases were captured. Only metaphases that demonstrated optimal spreading and minimal overlapping of chromosomes were captured.

For each metaphase, black and white images of the three fluorochromes were captured using the SmartCapture™ software program (Digital Scientific). Images were ideally captured using exposure times calculated automatically by the software, however when fluorescent debris rendered auto-exposure inaccurate manual exposure times were employed as sescribed in Section 4.4.1.1. All images were captured using a standard 'binning' of 2x2. Binning reflects the resolution of the digital camera and indicates that a square of 4 pixels on the camera sensor was grouped as a single unit. Fluorescent light striking any one of the four pixels would be result in a pixel in the final image thereby increasing the sensitivity of the camera x4 (with a simultaneous x4 decrease in the resolution). The three images were then pseudocoloured, combined as a single three-colour image and exported in the image cytometry standard as .ics files. Images were transferred to a QuipsXL Genetics Workstation equipped with CGH analysis software (Vysis). For each hybridization at least 10 good quality metaphases were captured.

3.8.5 Image analysis

Image analysis consisted of several automated stages by the Quips CGH software. Initially images were segmented, separating chromosomes from the background. Red and green fluorescence intensities were normalised and corrected for background colour and the chromosomes karyotyped through visualisation of the banding pattern of an inverted contrast image of the DAPI image. Chromosomes were karyotyped automatically using the CGH software, checked manually and corrected as required. Chromosome axes were then identified and the intensity of the two fluorochromes was measured by integration of the normalised pixel values along lines perpendicular to the chromosome axis. Finally, ratio profiles were calculated by dividing the green intensity by the red intensity down the axis of each chromosome and averaged to produce a mean ratio profile for each metaphase spread. Average ratio profiles were generated from 5-10 good quality metaphases and presented as a mean ratio profile with 95% confidence limits. A ratio of 1 was used to indicate no imbalance in the copy number, i.e. equal binding of the test and reference DNA indicating the locus was represented with the same relative frequency in the test and reference DNA samples. Copy number imbalances were scored whenever the mean ratio profile deviated outside threshold values pre-determined in normal / normal CGH hybridization's (See Chapter 4). Repeated normal / normal hybridizations indicated that in

these experiments the mean ratio profiles never exceed 1±0.15 and for this thesis gains and losses of DNA were identified when the ratio profile was outside the 1.15 to 0.85 range respectively.

3.9 Immunohistochemistry

Immunohistochemistry is a detection method for the *in situ* localisation of antigens within a tissue section of interest (See Figure 3.4). Monoclonal antibodies raised against an antigen of interest are used to detect cell surface, cytoplasmic or nuclear antigens. A secondary antibody (specific for the species in which the primary antibody was raised) conjugated to biotin molecules is then applied to bind the first antibody. The secondary antibody is usually polyclonal and recognises multiple binding sites on the primary antibody. An amplification step is then applied exploiting the high affinity of avidin for biotin (over 1 million times higher than antibody for most antigens; Hsu *et al*, 1981a; 1981b). Conjugation of the enzyme horseradish peroxidase (HRP) to several biotin molecules allows the formation of an avidin biotin complex (ABC) with avidin acting as a bridge between biotin-labelled peroxidase molecules. This amplification reaction incorporates many enzyme molecules (in this case horseradish peroxidase) at the histological site of the primary antibody reaction and can be visualised by the subsequent enzymatic conversion of a substrate (in this case 3,3 Diamino benzidine tetrahydrochloride – DAB) to an insoluble brown precipitate. The secondary detection kit employed during the work of this thesis was the StreptABC Complex/HRP Duet kit (DAKO). Negative controls were included in all batches of slides. Irrelevant mouse antibodies (Becton Dickinson) of the same subclass as the test antibody were applied to the sections in place of the primary antibody. Before commencing staining a titration of the primary antibody concentration was performed for each antibody. This was used to determine the optimum concentration of antibody and to establish a level which minimised background staining whilst maintaining a specific and sensitive positive stain. Titration also determined the minimum amount of antibody that produced satisfactory results, minimising costs and maximising the number of experiments that could be done. All incubations were performed at room temperature unless otherwise indicated.

3.9.1 Rehydration of paraffin embedded tissue sections

4μm tissue sections, cut onto SuperFrost Plus slides (Menzel-Glaser), were obtained from the Department of Histology, Hull and East Yorkshire Hospitals. All sections were de-paraffinised and rehydrated as described in Section 3.2. Slides were then rinsed in distilled

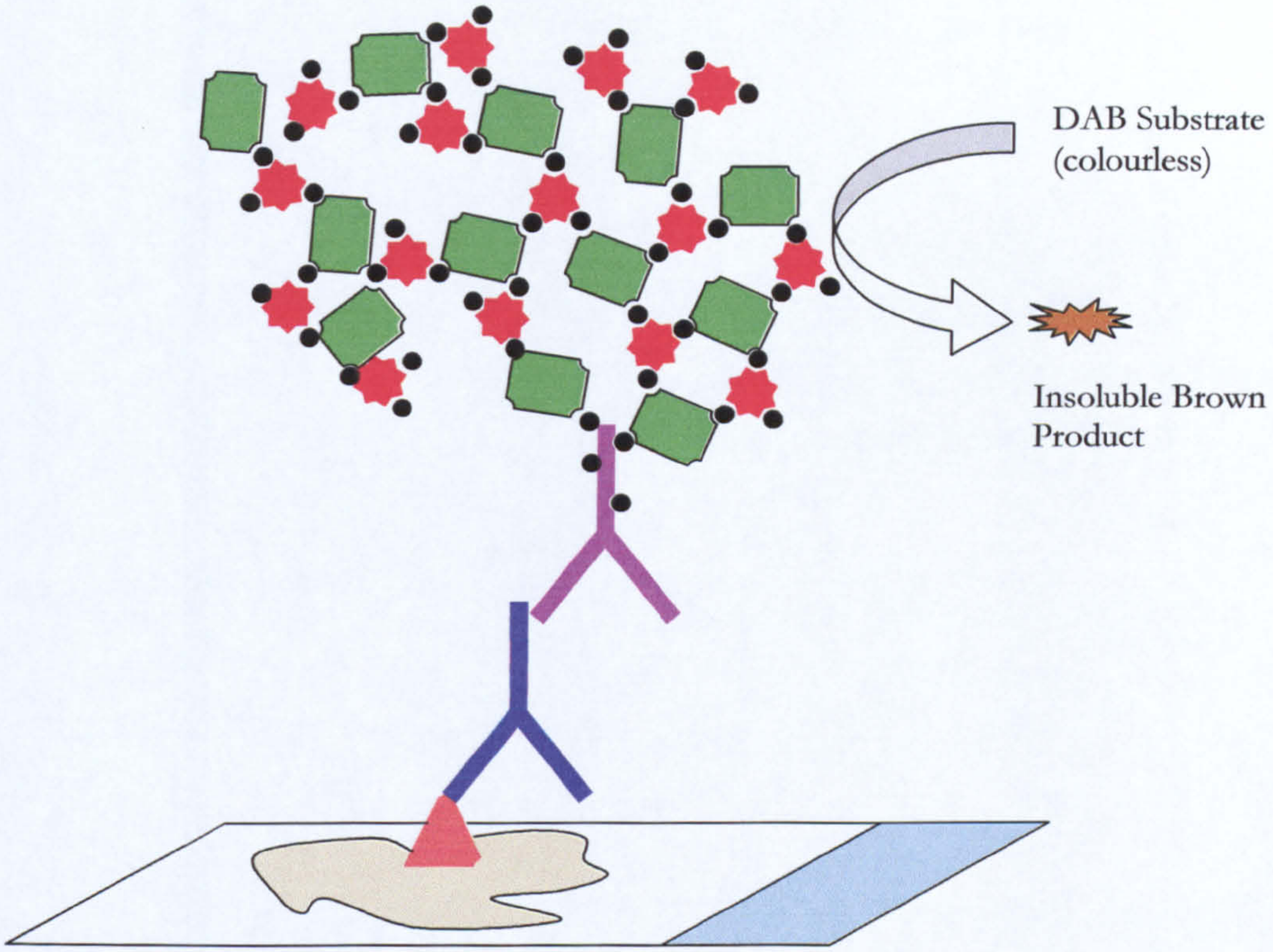

Figure 3.4 – Schematic representation of Immunohistochemistry. Localisation of an antigen of interest was accomplished by the use of the Avidin: Biotinylated enzyme Complex (ABC) immunohistochemistry system. Sections were incubated with a monoclonal antibody raised against the antigen of interest (blue). A biotinylated secondary antibody specific for the species in which the primary was raised was then added (purple) introducing many biotin molecules at the site of the antigen. Biotinylated enzyme was then introduced as part of an avidin: biotinylated enzyme complex localising many units of horseradish peroxidase (HRP) enzyme at the site of the antigen. Incubation of the section in DAB, a substrate for HRP, resulted in an insoluble brown deposit identifying the location of the antigen of interest.

water for 5 minutes and endogenous peroxidase activity was quenched by incubating sections for 20 minutes in 3% v/v hydrogen peroxide in distilled water.

3.9.2 Epitope retrieval

Slides were rinsed in distilled water for 5 minutes before proceeding to the epitope retrieval step. The process of tissue fixation and embedding alters the conformation of certain antigens and thus an additional epitope retrieval step is required in order to uncover certain antigen of interest. Different methods of retrieval were applied depending on the antigen under investigation. The PCNA antigen required no epitope retrieval method.

Heat Induced Epitope Retrieval

Two different methods for heat induced epitope retrieval were used depending on the recommendations of the supplier of each antibody. Both methods involved boiling the sections in a buffer optimised for the unmasking of cellular antigens.

Microwave method (p53, p16, p21, Mib1)

Slides were immersed in a beaker of freshly prepared 10mM Citrate buffer (pH 6.0) and microwaved on full power (600W) for 4 x 5 minutes with replacement of buffer as it evaporated. Slides were left to cool for 20 minutes in the Citrate buffer and then rinsed in TBS (Tris Buffered Saline pH7.5: 15mM NaCl; 40mM Tris(HCl)) for 3 minutes.

Pressure cooker method (bcl-2, Cyclin D1)

Retrieval buffer was prepared by diluting Antigen Unmasking Solution (Vector) in distilled water (1.5 litre final volume of 1:100 dilution) and bringing to the boil in a conventional pressure cooker heated by a halogen hotplate. Slides were placed into boiling solution and timed for 3 minutes (timing commenced when the pressure had reached 15 psi). The pressure cooker was then removed from the heat, de-pressurised and the slides removed to TBS for 5 minutes.

Trypsin digestion (her2)

Slides were incubated in Trypsin (0.1% w/v in PBS, Sigma) for 12 minutes at room temperature. Enzyme digestion was terminated by transferring the slides into soybean trypsin inhibitor (0.1μg/ml in PBS – Sigma) for 5 minutes followed by a 3 minute rinse in TBS.

3.9.3 Immunostaining

After epitope retrieval, slides were rinsed for 5 minutes in TBS and the tissue sections were circled with an ImmEdge™ Pen (Vector Laboratories Ltd) to generate a hydrophobic boundary. This provides a heat-stable, water-repellent barrier that keeps staining reagents localised on the tissue sections and prevents mixing of reagents. 50-200µl (depending on the size of the tissue section) of 1x casein (Diluted 1:10 according to manufacturer's instructions – Vector Laboratories Ltd) was applied to the section. Sections were incubated for 20 minutes after which the slides were rinsed in TBS for 5minutes before endogenous biotin and avidin were blocked to limit background staining (Wood and Warnke, 1981). Some tissues may bind avidin, biotinylated HRP or other biotin/avidin system components due to endogenous biotin, lectins, or other biotin binding substances in the section and therefore require blocking (with free avidin and biotin) to prevent non-specific staining. 50-200µl of Avidin D solution (Diluted 1:50 according to manufacturer's instructions – Vector Laboratories Ltd) were applied to the tissue sections and incubated for 15 minutes followed by rinsing in TBS for 5 minutes. Biotin solution (Diluted 1:50 according to manufacturer's instructions – Vector Laboratories Ltd) was then applied for 15 minutes and the sections rinsed in TBS as before. During this incubation the primary antibody working solution was diluted in 0.2x casein in TBS. The dilutions used for each antibody are detailed in Table 7.2. 50-200µl of diluted primary antibody were applied to the section and incubated for 2 hours (0.2x casein in TBS alone was applied to the negative control). Sections were then rinsed twice in TBS for 5 minutes each and 50-200µl of freshly prepared secondary antibody (Biotinylated goat anti mouse/rabbit antibody in 0.05M Tris/HCl; 0.15M NaCl pH 7.6 – Dako) was applied and the sections incubated for 30 minutes. Slides were rinsed in TBS for 5 minutes and incubated for 30 minutes in StreptABC Complex/HRP working solution (Streptavidin and biotinylated horseradish peroxidase in 0.05 mol/L Tris/HCl; 0.15M NaCl pH 7.6 – Dako).

Slides were then rinsed in TBS for 5 minutes and visualised using DAB (Vector Laboratories Ltd). Immunoreactivity was visualised with 0.05% w/v DAB as the chromogen and 0.01% v/v hydrogen as the enzyme substrate. Sections were incubated for exactly 5 minutes, then rinsed in distilled water for a further 5 minutes before proceeding to counterstaining.

3.9.4 Counterstaining

Sections were counterstained to allow visualisation of the cell nuclei. As the Becton Dickinson Cell Analysis System 200 was used to analyse the staining of some of the antibodies (see Table 7.2 for details) it was important to utilise the methyl green counterstain for these. The green/brown colour difference between the primary antibody and the counterstain is optimal for the dual wavelength CAS 200 optical coupler See Section 3.9.5).

Methyl green counterstain

Slides were first incubated in 0.1M Sodium acetate buffer (0.1M Sodium acetate, 0.12% v/v Acetic acid, pH 5.2) for 8 minutes. Slides were then laid on a staining rack and flooded with 2-3ml of 0.01g/ml methyl green (Sigma) made up in sodium acetate buffer for exactly 16 minutes, for sections which had undergone heat induced epitope retrieval, or exactly 8 minutes for all other sections. Excess counterstain was removed by 3 quick dips into ice cold distilled water (0-2°C) followed by immediate dehydration in butanol. Three changes of butanol were employed with slides undergoing 20 quick dips into the first and second changes followed by 2 minutes in the third. Slides were then cleared in 3 changes of xylene for 2 minutes each and mounted using Histomount (National Diagnostics).

Haematoxylin counterstain

Slides were rinsed in running tap water for 2 minutes and the DAB staining enhanced by incubation in copper sulphate (0.5% w/v copper sulphate in 0.9% w/v saline) for 5 minutes. Slides were then rinsed again in running tap water and counterstained in freshly filtered Harris haematoxylin (BDH) for 20 seconds. Slides were rinsed in running tap water for 30 seconds and differentiated by 10 dips in acid-alcohol (1% v/v HCl in 70% v/v ethanol) followed by a further rinse in rinse in running tap water for 30 seconds. Slides were then 'blued' in Scott's tap water solution (0.2% w/v potassium bicarbonate, 2% w/v magnesium sulphate) to enhance the contrast between the DAB and the counterstain before finally rinsing in running tap water for 10 seconds. Slides were finally dehydrated through a series of alcohols as described in Section 3.2. Slides were incubated in 100% ethanol for 3 changes of 10 seconds each before clearing in Xylene and mounting as for the methyl green counterstain.

3.9.5 Image cytometry using the CAS 200

Slides were analysed using the Becton Dickinson Cell Analysis System (CAS) 200 running the Quantitative Nuclear Antigen (QNA) software. A strong correlation between visual

scoring of immuno-localised antigens and conventional histochemical analysis has previously been reported (Potten *et al*, 1993), however the CAS system allows the process of analysis to be speeded up and is designed to minimise inter-observer variability. Lambert Beer's Law allows optical density measurements to be converted to concentration providing the stain used is stoichiometrically taken up, and that optical density is measured through a narrow bandpass using a linearly calibrated instrument. The CAS 200 employs two sensors operating through narrow bandpass filters at two different wavelengths which have minimal spectral overlap (500nm and 620nm – These wavelengths determined the choice of immunochemical reagents). These sensors are integrated into a black and white camera (to make up the 'optical coupler') and allow measurements at both wavelengths to be taken with minimal interference. This optical coupler was attached to a custom made Nikon microscope and connected to a PC running the CAS200 software suite. All optical density measurements were made as pixel intensities on the computer monitor and it was important to perform analysis with the image focussed on screen and as visualised down the microscope. As the quantitation of immunohistochemical staining relies on measuring the optical density of stained tissue sections it was essential that the microscope was maintained in optimal condition and was regularly serviced by a qualified engineer.

Microscope optics were cleaned and set-up before each analysis to ensure optimal performance. The light was calibrated by focussing on the section and setting the light intensity on a blank area of the slide. Using the 500nm filter the image was segmented and a mask drawn around either the nuclei (in the case of nuclear antigens) or the entire cell (for analysis of non-nuclear antigens) using the methyl green counterstain. Positive staining was measured using a 620nm filter specific for the light emitted by illumination of the brown stain generated by the DAB deposition. A threshold was determined for positive DAB staining by first analysing 5 fields on the negative control slide to determine the level of background, or non-specific DAB stain. All the test cases from each batch of staining were then analysed sequentially. The threshold was represented as a computer generated mask and was checked for each slide to ensure that this mask accurately mirrored the DAB stain. 20 fields of tumour cells were captured and the absorbtion at 620nm was measured as an integrated optical density (IOD). The slide was scanned randomly in a outward spiralling pattern and malignant epithelium only was graded, avoiding areas of non-tumour cells such as stromal cells and tumour blood vessels. Using the measurements from the two different sensors, results were reported as percentage of positive area stained, generated by dividing the area of positive stain by the area of nuclear (or cellular)

counterstain. The total area of stained cells/nuclei was also determined in μm^2 using the CAS system.

3.10 DNA ploidy staining

DNA ploidy was quantified by image cytometry using the Feulgens staining reaction (Deitch, 1966). Hydrolysis of ribose-purine bonds in DNA by hydrochloric acid generates aldehyde residues to which a dye is then coupled stoichiometrically via the Schiff reaction to generate a blue colour. Calibration slides containing cells with known DNA content were included in every batch of slides to provide a reference for assessment of DNA content. Measuring the intensity of the blue stain in the nuclei of test cells on a system calibrated with control cells allows the amount of DNA in the test cases to be quantified.

5µm tissue sections were obtained from the Department of Histology, Hull and East Yorkshire Hospitals and processed as follows. Sections were deparaffinised and dehydrated as described in Section 3.2. Slides were then incubated in 5N HCl for 60 minutes to hydrolyse the DNA. Whilst slides were incubating, fresh Feulgens stain was prepared by dissolving the stain reagent (Becton Dickinson) in 100ml of 0.1N HCl and mixing for 60 minutes. Flasks were sealed tightly to prevent the loss of SO_2 from the stain solution. The stain was filtered through No.1 Whatman filter paper, keeping the funnel covered to prevent SO_2 loss, and then used immediately. Slides were incubated in the stain solution for 60 minutes with constant shaking and agitation of the solution. During staining, fresh rinse solution was prepared by dissolving the Rinse reagent (Becton Dickinson) in 300 ml of 0.5N HCl and mixing well. Slides were rinsed in three changes of rinse solution for 30 seconds, 5 minutes, and 10 minutes respectively and then rinsed in 3-5 changes of deionised water for 5 minutes. Slides were then incubated in 1% acid alcohol for exactly 5 minutes and dehydrated with two changes of 100% ethanol for 3 minutes each. Finally slides were cleared in two 3 minute changes of xylene and mounted using Histomount.

3.10.1 Quantitative DNA analysis using the CAS 200

Slide analysis requires accurate quantitation of the optical density of the blue Feulgens stain. All slides were analysed on the CAS200 using the Quantatative DNA Analysis software (QDA). Analysis of Feulgens stained slides mirrored the analysis of standard immunohistochemistry (Section 3.10.2) in that light intensity was first calibrated whilst focussing on a blank area of the slide and a threshold mask was implemented to segment the Feulgens stained nuclei. Calibration slides prepared from rat hepatocytes containing a

known amount of DNA (6.68pg of DNA per cell) were first scanned to measure the OD of at least 25 nuclei. The CAS system had a linear response over a wide optical density allowing Lambert's Law to be implemented to correlate OD with concentration of DNA. Test cases were then measured sequentially. Firstly the illumination of the specimen slide was checked using the software to ensure it was equivalent to that used to measure the calibration cells. The slide was then scanned to capture fields of nuclei within the tissue and individual nuclei segmented using the cut tool. Overlapping nuclei were discarded and the automated filter system performed a preliminary assignment of the measured nuclei to one of several classes depending on the measured charateristics (size, shape, granularity, DNA concentration). This was repeated for many fields until the total nuclei count was ≥300. All analysed nuclei were then reviewed and fragments and overlapping nuclei removed. Finally a tissue correction algorithm was applied to the data set to compensate for the thickness of the tissue section. Feulgens analysis of tumour imprints does not require such a correction as all nuclei are left on the slide intact, however within a tissue section many nuclei will be truncated resulting in many partial nuclei being included in the data set. A population of lymphocytes was captured during analysis and were used as an internal control and checked to ensure they generated the expected DNA mass of a normal human diploid cell of 7.18 pg. Results were presented as a histogram with cell count plotted against DNA index (Calculated as mass of DNA / 7.18pg).

Chapter 4

Establishment, Optimisation and Quality Control of Comparative Genomic Hybridization

4.1 Introduction

Non-random chromosomal abnormalities in the genome of cancer cells underlie the phenotypic characteristics of human tumours. A wide range of genetic aberrations has been detected in HNSCC through a variety of methods, however the multi-step process of tumour development still remains to be elucidated. Molecular cytogenetic studies have identified several genes important in the development of HNSCC however most of these studies have been limited to small, previously defined genetic loci. The technical difficulties involved in performing conventional cytogenetics on solid tumours such as HNSCC, described in Section 2.2.2, have limited the acquisition of genomic wide analysis of HNSCC cells. The expectation that identification of regions of copy number change would provide further markers of prognosis and diagnosis led to the development of Comparative Genomic Hybridization (CGH). This Chapter reports the results of the establishing and optimization of CGH in a clinical laboratory setting and details the criteria identified to ensure the data generated was of a high quality.

4.1.1 Establishment, optimisation and quality control of CGH

At the time of initiation of the work for this thesis CGH was a newly described technique and much of the initial work was involved in establishing and optimising the technique within the laboratory. Prior to this, limited experience had been gained using multicolour fluorescent *in situ* hybridization on interphase nuclei to identify the copy number of a small number of chromosomes in colorectal cancer (Greenman *et al*, 1998). The techniques developed during this work were the basis for attempting CGH. CGH is recognised to be technically difficult and suffers from a lack of standardisation, validation, and quality control. Each stage of the CGH protocol was optimized in turn including:

- Nick translation
- Probe preparation
- Target metaphase denaturation
- Digital image acquisition

The results of optimisation and control experiments are presented and the data generated through analysis of images generated during CGH experiments are used to identify key criteria for assessing the quality of a CGH hybridization. These include:

- The influence of probe size on CGH hybridizations
- The measurement of background fluorescence
- The assessment of fluorescent staining of metaphase chromosomes

- The assessment of confidence limits

As the results of this chapter relate to optimisation of the technical aspects of CGH, the data generated at each stage of optimisation is presented and discussed in turn.

4.1.2 Resolution of CGH

The resolution of CGH is significantly affected by the quality of the hybridization and by the length of the metaphase chromosomes analysed. Initial theoretical estimations of the resolution of CGH (Piper *et al*, 1995) postulated the identification of deletions within the range of 2-4 megabases. Experimental data indicates that single copy number changes (i.e. deletion or single copy gain) in the order of 10 megabases can be detected by CGH (Kallioniemi *et* al, 1994; du Manoir *et al*, 1995; Bentz *et al*, 1998) although advances in the analysis of CGH data using standard reference intervals (Kirchhoff *et al*, 1999) have repeatedly detected deletions of as little as 3 megabases. For amplifications, the size of the amplicon unit (size of the amplification x number of copies) determines resolution and has been estimated at 2 Megabases (Joos *et al*, 1993). When the CGH method is modified by replacing the target metaphase chromosomes with other sources of DNA such as combed DNA fibres (Kraus *et al*, 1997) or DNA micro arrays (Solinas-Toldo *et al*, 1997) the resolution increases substantially to the range of 40 – 170 kb.

4.2 Nick Translation

The first stage of a CGH experiment is the differential labelling of high quality DNA samples from two sources. By convention, the tumour DNA (or test DNA) is labelled by the incorporation of a green fluorochrome into probe length fragments of DNA (Kallioniemi *et al*, 1992). Similarly, a source of normal reference DNA is obtained from a karyotypically normal donor and labelled differentially with a red fluorochrome. High molecular weight DNA of a high purity were found to be essential for successful nick translation, although an equally important factor was ensuring that the DNA was completely re-suspended in the nick translation mixture. The most common reason for labelling failure was that the DNA polymerase and DNase enzymes in the mix were unable to act on the genomic DNA due to inadequate re-suspension of the DNA mix. The optimum size range of labelled DNA fragments is between 300-3000 base pairs. Enzyme concentration and duration of the reaction were controlled to ensure the fragments generated were within this range. More importantly this was the size range of the pre-labelled reference DNA obtained commercially (Vysis) against which the fragments of differentially labelled test DNA were competitively hybridized. Other authors have noted the importance of matching the average length of the test and reference DNA fragments

(James, 1999). The exact conditions for nick translation had to be re-assessed for each new batch of the nick translation enzyme and often required a number of repeats.

4.2.1 Multiple simultaneous Nick Translations

Initial attempts at generating labelled DNA fragments suitable for CGH were often hampered by having to repeat the nick translation reaction due to the fragments generated falling outside of the optimal range of 300-3000 base pairs required for a successful CGH. If the first attempt at labelling produced fragments that were too large, the reaction was repeated with an increased concentration of enzyme (or allowed to proceed for an empirically determined extended period of time). Conversely, if the fragments generated were too small, the reaction was repeated using a lower concentration of enzyme in the reaction mix or for a shorter period of time. Experimental variations between reactions set up at different times were found to be the main reason for multiple attempts being required. Firstly, the nick translation reaction begins immediately the enzyme mix is added (the optimal temperature for the reaction was 15°C, within the range of laboratory ambient temperatures). Depending on the number of nick translation reactions set up, mixtures completed first would have a several minute increase in incubation time. Secondly, the enzyme mix was stored in glycerol to prevent freezing during storage at –20°C (and therefore multiple freeze thawing cycles). This made the enzyme solution difficult to handle and care was taken to avoid coating the outside of the pipette tip with viscous enzyme liquid as this could increase significantly the amount of enzyme added to the reaction by several microlitres. Other experimental conditions which could potentially vary between experiments included, pipette calibration, use of different pipettes, fluctuations in laboratory ambient temperature and the period of time spent mixing the reaction mixture.

Simultaneously duplicating translation reactions on the same DNA sample using two different enzyme concentrations (see Figure 4.1) was found to be the most efficient method for ensuring optimal fragments were generated within a single batch of translation reactions. Figure 4.1 shows the result of performing two nick translation reactions on 7 DNA samples. The pairs of DNA smears demonstrate a shift in size range for each of the 7 DNA samples but for each sample at least one of the smears was optimal for CGH. 10µl and 12 µl were established to be the optimal enzyme volumes, although these values occasionally varied between different batches of enzyme and test reactions were performed for each new batch. Initial attempts using 10µl and 15µl of enzyme were found to generate too large a difference between the two attempts and did not always ensure that at least one of the reactions generated optimal smears. The application of simultaneous nick

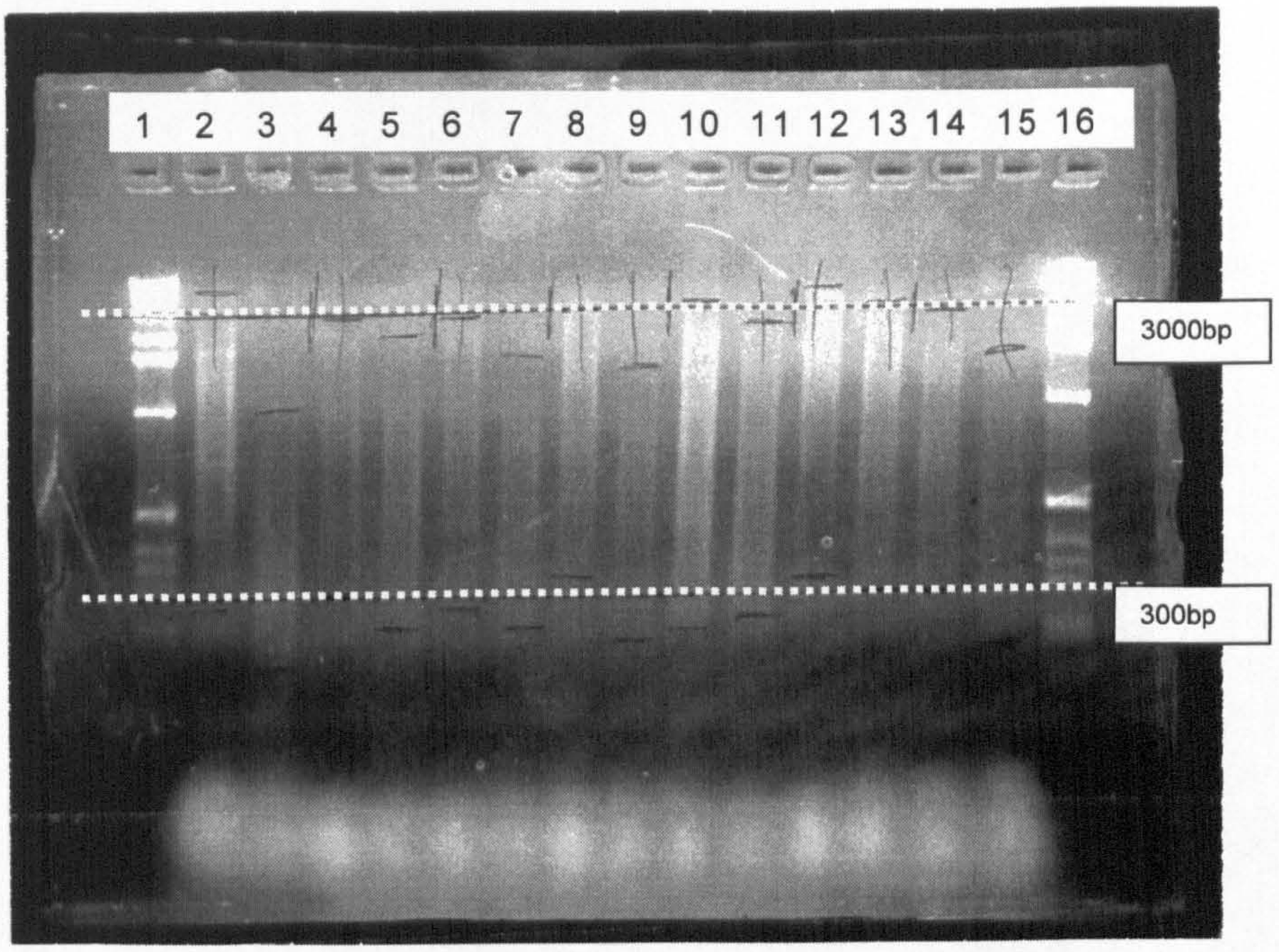

Figure 4.1 – Duplicated nick translation reactions using two different enzyme concentrations. Lanes 1 and 16 contain DNA standards allowing estimation of the size range of the DNA fragment smears contained in lanes 2-15. Duplicate nick translation reactions of 7 DNA samples labelled with 10 and 12µl of enzyme are shown. Lanes 2 and 3 contain the fragments generated from sample A using 10 and 12µl of enzyme respectively, lanes 4 and 5 contain sample B etc. The standard reaction mixture for nick translation is detailed in Section 3.6. This gel demonstrates how using two different nick translation conditions simultaneously ensured that at least one reaction generated fragments suitable for CGH in each case. The standard 2 hour incubation was used for all samples. The dotted lines indicate the optimal range for nick translation products, 300-3000bp, calculated by reference to the size standards. Size standard used – 10µl of 1kb DNA ladder (Life Technologies). Fragment sizes: 201bp, 220bp, 298bp, 344bp, 399bp, 506bp, 1018bp (lowest bright band), 1636bp, 2036bp, 3054 bp (+larger fragments not separated at this resolution). A band of unincorporated excess SpectrumGreen™ labelled dUTP is visible at the bottom of the gel.

translation reactions with different enzyme content was the most effective method for generating optimal labelled DNA fragments within the shortest period of time and the most cost effective method in the long run.

4.2.2 DNA concentration and Nick Translation

The routine quantity of genomic DNA included in a nick translation reaction was 1µg of high molecular weight DNA. After removal of a representative aliquot for verification of DNA fragment size, approximately 800ng of labelled DNA fragments were available for CGH hybridization. Despite quantification of DNA concentrations using the GeneQuant spectroflurometer (Amersham Pharmacia Biotech) before nick translation the intensity of smears generated by nick translation was seen to vary (see Figure 4.1), indicating differing quantities of DNA in the final nick translated product. This may be explained by one of several reasons including, measurement of an initial genomic DNA solution incompletely re-suspended, measurement of an unrepresentative aliquot of DNA solution, the presence of impurities in the DNA solution and known inaccuracies in quantifying DNA spectrofluorometrically. Because of this, it was occasionally necessary to empirically estimate the volume of DNA solution to include in the nick translation mix to generate a smear of DNA that was visually assessed to be suitable for hybridization. To evaluate whether increasing the DNA concentration effected the kinetics of the nick translation reaction the standard quantity of DNA (1µg) was nick translated using several concentrations of enzyme alongside double the normal DNA concentration. Figure 4.2 shows the results of 6 nick translation experiments using 2 DNA samples of different concentrations and applying 3 different enzyme concentrations to each (8µl, 10µl and 12µl of enzyme mix in the reaction).

All 6 lanes show smears of DNA with lanes 5-7 staining brighter than lanes 2-4, reflecting the increased DNA content. For both quantities of DNA there is a gradual decrease in the range of fragment size with increasing enzyme concentration. There is little difference in the size range of smears for the different DNA concentrations when identical enzyme concentrations are compared (lanes 2 and 5 - 8µl of enzyme; lanes 3 and 6 - 10µl of enzyme; lanes 4 and 7 - 12µl of enzyme). This indicates that increasing the quantity of DNA within the nick translation mix (and therefore increasing the substrate available to the nick translation enzymes) does not significantly alter the amount of DNA digestion performed by the DNase enzyme. More significantly, all 6 lanes of the gel demonstrate a visible band of unincorporated Spectrum green labelled dUTP nucleotide indicating the

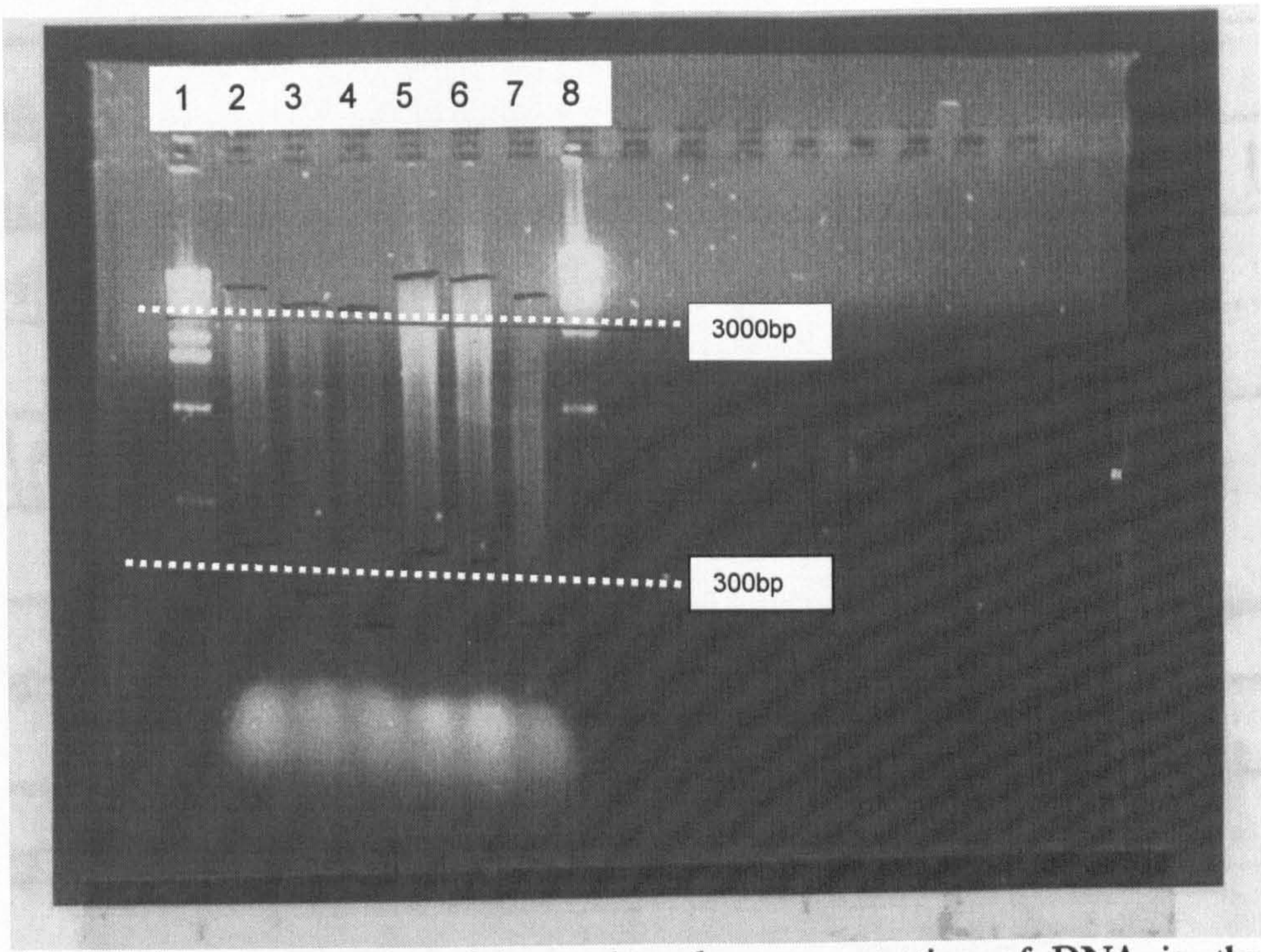

Figure 4.2 – The effect of increasing the concentration of DNA in the nick translation mix on the size range and fluorochrome incorporation of the DNA fragments generated. Lanes 2-4 represent the result of labelling 1µg of genomic DNA using different volumes of nick translation enzyme (8µl, 10µl and 12µl of enzyme respectively), incubated at 15°C for 2 hours. Llanes 5-7 represent the labelling of 2µg of DNA (8µl, 10µl and 12µl of enzyme respectively). Two different DNA ladders were run on the gel, 10µl of 1Kb Standards in lane 1 (Life Technologies; see Legend to Figure 4.1 for fragment sizes) and 10µl of High Molecular Weight Standards (Life Technologies) in lane 8 (Fragment sizes: 1000bp, 2000bp, 3000bp, 4000bp, 6000bp, 10000bp – not all separated at this resolution). The dotted lines indicate the optimal size range for nick translated products. A band of unincorporated excess SpectrumGreen™ labelled dUTP is visible at the bottom of the gel.

supply of labelled nucleotide available to the DNA polymerase has not been exhausted. The increased quantity of DNA therefore did not significantly reduce the incorporation of fluorescent label into the DNA fragments generated during nick translation. In summary this experiment showed that doubling the DNA concentration, to increase the amount of available labelled DNA, did not significantly affect the size of nick translated DNA fragments generated (compared with enzyme concentration which did). Therefore, for difficult to label DNA samples, the quantity of DNA included within the nick translation experiment could be determined empirically by a combination of GeneQuant measurement and visual examination of genomic DNA on an agarose gel. DNA samples which initially generated faint smears of DNA using the recommended concentration of 1µg of DNA in 50µl reaction mix were repeated using increased amounts, to generate brighter smears of DNA fragments. Altering the amount of enzyme mix within a nick translation is the most effective way of producing DNA fragments of a suitable size range for hybridization.

4.3 Hybridization

4.3.1 Probe preparation

Preparation of the DNA probe mix prior to hybridization was found to be the single most important factor in the success of hybridization. Many of the initial attempts at hybridizing successfully labelled CGH probes failed due to incomplete re-suspension of the probe mix. This was found to be due to several reasons. Firstly, prior to re-suspension the DNA fragments are precipitated out of solution using excess ethanol and subsequently are re-suspended in a mix of nuclease free water and pre-prepared hybridization solution. It was determined that failure to ensure the pellet of precipitated DNA was completely dry of residual ethanol could significantly hamper re-suspension in the aqueous hybridization solution. In addition it was important to ensure the DNA fragments were completely re-suspended in the nuclease free water before adding the hybridization buffer. Finally, prolonged mixing of the probe solution (>3 minutes) was found to be necessary to ensure complete suspension of the DNA probe fragments. This is due to the complexity of the probe mix and the high concentrations, most notably the excess COT-1 (30µg/µl), of DNA present. This important point is not emphasised in many CGH protocols, presumably as most CGH protocols are modifications of standard FISH protocols, which utilise far less DNA in the probe mixture.

4.3.2 Denaturation of target and probe DNA

The temperature and duration of the metaphase denaturation, as well as the quality of spreads used were important in ensuring an adequate amount of single stranded DNA was generated to act as a target for the labelled DNA probes. The aim of metaphase denaturation is to treat the preparations as harshly as possible to generate the maximum amount of single stranded DNA (allowing probe access to the target sequence), whilst still maintaining the morphology of the chromosomes; essential for accurate metaphase chromosome identification. The conditions detailed in the Methods section were considered optimal. It was found to be important that all experiments were done using 4 slides denatured simultaneously with 'blank' slides being included if less than 4 metaphase spreads were required. This was to maintain the denaturation conditions as the addition of each slide to the coplin jar reduced the temperature of the solution by 1-2°C.

4.3.3 Influence of metaphase preparations on CGH experiments

The next factor requiring optimization was the quality of metaphase preparations used as hybridization targets. Several authors have commented on the optimal characteristics of metaphase spreads (Kallioniemi *et al*, 1994; de Meulmeester *et al*, 1996; Karhu *et al*, 1997; James *et al*, 1999). Metaphase preparations are made from phytohemagglutinin stimulated, methotrexate synchronised, peripheral blood lymphocytes from a karyotypically normal donor. Cells are cultured and arrested in metaphase by colcemid application. Following hypotonic treatment and fixation with Carnoy's fixative the cell suspension was dropped onto good quality, clean, microscope slides. Typically, large-scale batches of metaphases are prepared from several sources of cells and the highest quality preparations then selected for CGH. Metaphase preparation is still considered to be somewhat of a 'black art' and many batches of cells prepared in a standard manner have to be discarded as unsuitable for CGH (James *et al*, 1999). Acceptable quality CGH slides must fulfil the following criteria: high mitotic index, minimal numbers of overlapping chromosomes, adequate chromosome length for accurate fluorescent ratio (FR) determination and minimal residual cytoplasm (Kallioniemi *et al*, 1994). Excessive amounts of residual cytoplasm can generate background fluorescence and result in faint chromosomal staining due to poor probe penetration and hybridization of probe to residual RNA molecules contained within. Preparations must also be able to withstand the harsh denaturation conditions detailed in Section 4.3.2. Karhu *et al* assessed the denaturation characteristics of several batches of metaphase preparations and demonstrated the requirement for denaturation conditions to be optimised for each batch of slides (Karhu *et al*, 1997). The balance between denaturation and retention of morphology is very important and is reflected in the hybridization

characteristics of different preparations and/or denaturation conditions. Slides that are over-denatured will demonstrate brighter staining due to greater probe penetration, however morphology (visualised as DAPI banding) will be lost preventing accurate karyotyping of the chromosomes. Conversely, under-denatured chromosomes will retain excellent banding patterns but faint hybridization signals. During the course of this thesis, initial attempts at metaphase preparations proved to have some degree of success, however it was not thought to be feasible to generate large enough batches of slides to ensure consistency throughout the work. For this reason it was decided to use commercially prepared metaphase spreads (Vysis, UK) which were optimised for acceptable and consistent chromosome characteristics and minimal residual cytoplasm.

4.4 Data analysis of CGH images

4.4.1 Capturing of images

DAPI counterstaining was optimised by overnight incubation at 4°C, enhancing DAPI penetration of the chromosomes and strengthening DAPI bands. Images were captured using the system described in Section 3.84. Images of the individual colour planes were captured separately (Figure 4.3a (A-C)) and combined as a composite image (Figure 4.3a (D)). All images were saved to disk and then exported in the .ics format (image cytometry standard) for later analysis.

4.4.1.1 Manual exposure compensation

Ideally, all CGH images were captured using automatic exposure times calculated by the Photometrics CCD digital camera under the control of the SmartCapture software package. This ensured optimum fluorescent images for the three colour planes which is essential for the normalization of red and green fluorescence levels and the accurate calculation of the colour ratio along the axis of the chromosomes. However, for some hybridizations, automatic exposure was not always possible due to areas of intense fluorescence within a chosen metaphase. Exposure times varied between experiments due to factors such as the amount of DNA used to make up the probe, the degree of hybridization and intrinsic differences between the brightness of the red and green fluorochromes. Figure 4.4 demonstrates two common reasons for over-riding the automatic exposure times determined by the system. Figure 4.4(A) depicts the original exposure of a metaphase from a successful hybridization captured using automatically determined exposure times. The presence of a small, brightly staining interphase nucleus within the metaphase resulted in very short exposure times for the red and green colour planes (0.7 seconds and 0.6 seconds

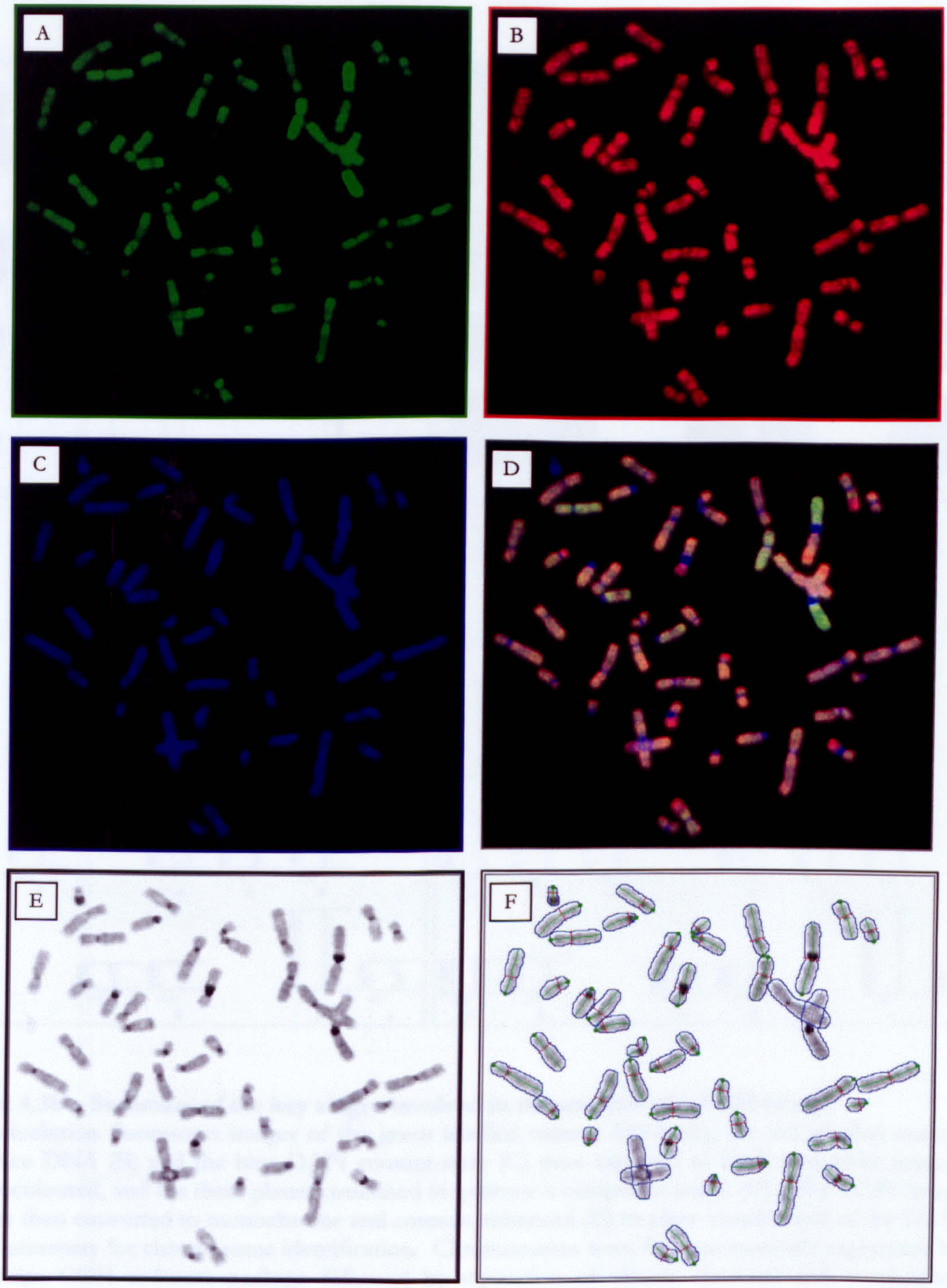

Figure 4.3a – Summary of the key stages involved in the analysis of a CGH image.

For figure Legend see Figure 4.3b.

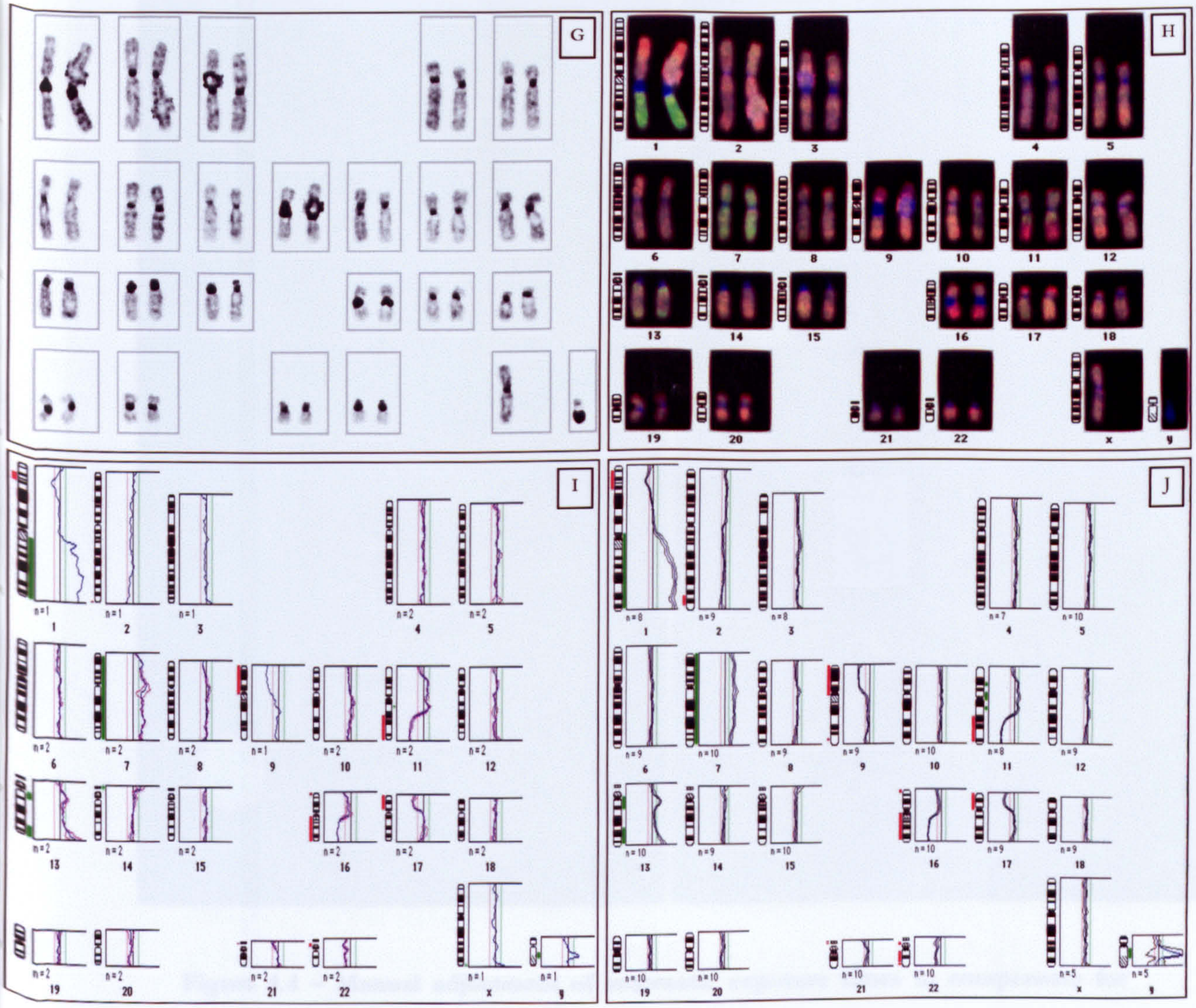

Figure 4.3b – Summary of the key stages involved in the analysis of a CGH image.
High resolution fluorescent images of the green labelled tumour DNA (A), the red labelled normal reference DNA (B) and the blue DAPI counter-stain (C) were captured as black and white images, pseudocoloured, and the three planes combined to generate a composite image (D). The DAPI image (C) was then converted to monochrome and contrast enhanced (E) to allow visualisation of the DAPI bands necessary for chromosome identification. Chromosomes were first automatically segmented by the Quips CGH software package followed by separation of closely clustered and overlapping chromosomes by the operator and the axis of each chromosomes displayed and checked (F). Images were then kayotyped based on the DAPI bands visible in the enhanced DAPI image and chromosome homologues paired up (G, H). The green to red fluorescent ratio was calculated by measuring the normalised pixel intensity down the axis of each chromosome and displayed as a ratio profile for each metaphase analysed (I) (Shown in detail in Figure 4.5). Finally the ratio profile of several metaphase images (typically 5-10) from a single experiment were combined together to generate an average ratio profile (J) from which copy number changes in the test specimen were calculated.

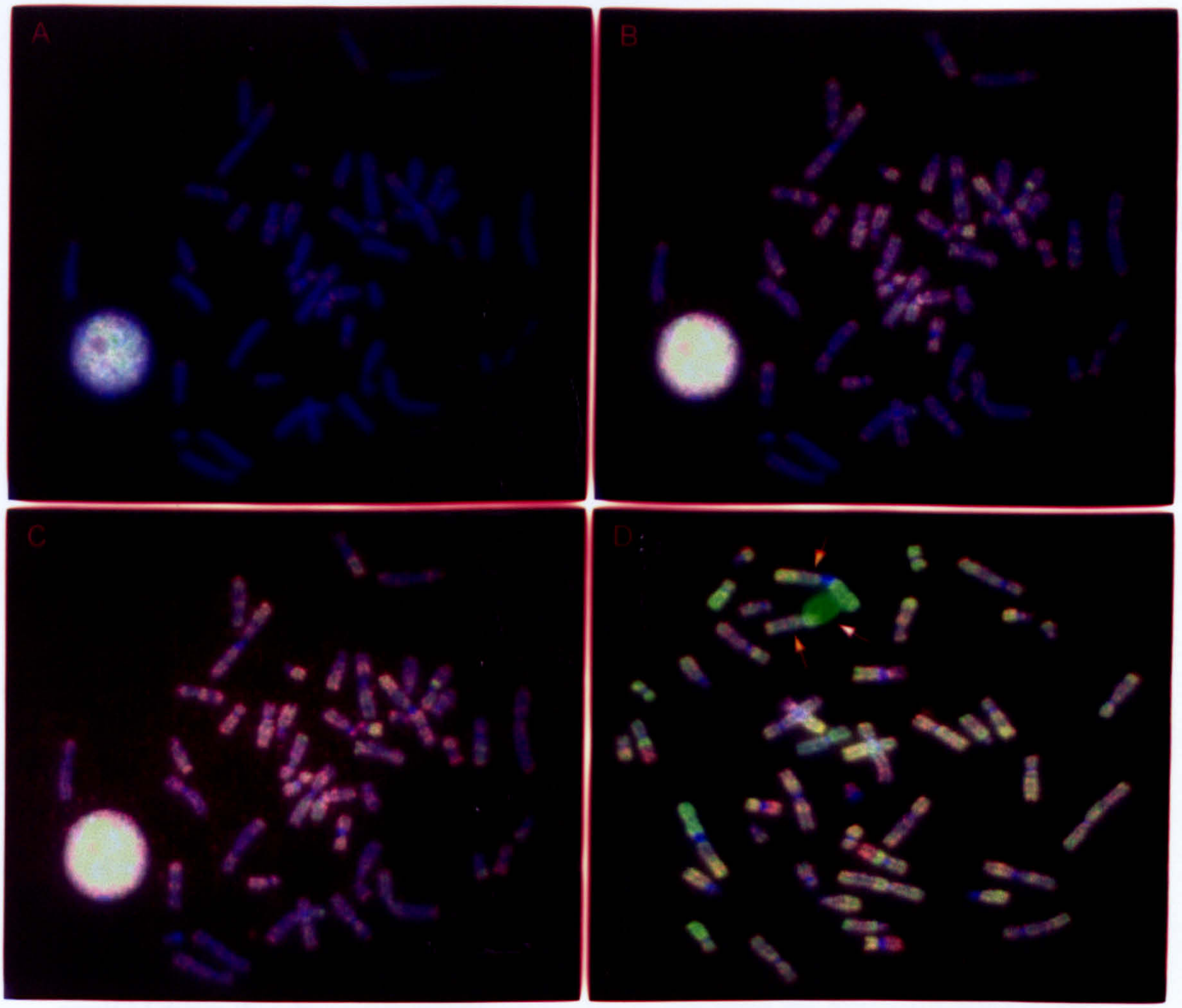

Figure 4.4 – Manual adjustment of automatic exposure times to compensate for areas of intense fluorescence. Images A, B and C represent three sequential exposures of the same metaphase with increasing exposure times. Image A depicts the original image captured using automatic exposure times of 0.6 seconds and 0.7 seconds for the green and red fluorescence respectively. Image B was subsequently captured using empirically determined exposure times of 1.2 seconds (green) and 1.4 seconds (red). A further image C, was finally captured with exposure times of 1.6 seconds (green) and 1.9 seconds (red). Image D depicts a manual exposure of a high quality metaphase for which automatic exposure was unsuccessful due to the presence of intensely fluorescent debris (arrow).

respectively). As a result of this bright region within the image the rest of the chromosomes show very faint red and green colour levels. Figure 4.4(B) shows the result of manually altering the exposure times (1.4 seconds for the red; 1.2 seconds for the green). This produced brighter, more satisfactory colour levels for the red and green fluorescence and a useable CGH image. These times were either determined empirically based on experience or, more usually, by repeating the exposure times from a previously captured adjacent metaphase. Exposure times within a single experiment were relatively constant, however due to occasional variations in hybridization intensity within different areas of the slide, it was found to be important to use similar exposure times from a metaphase immediately adjacent to the problematic metaphase. Figure 4.4(C) demonstrates a third attempt at capturing the same metaphase using slightly longer exposure times of 1.9 seconds for the red and 1.6 seconds for the green. Although the chromosomes appear slightly brighter, an increase in the red background fluorescence is visible as red 'speckles' in the space within the metaphase. This is due to a combination of excessively long exposure and the effect of multiple exposures of the same area of the slide (i.e. photobleaching of the fluorochromes). Figure 4.4(A-C) also demonstrates the effect of overexposure on the interphase nuclei within the spread. In the first image the interphase nucleus appears bright but still retains some granularity (resolution). Images B and C demonstrate reaching maximal exposure, exceeding the spectral range of the camera. Each pixel in a CGH image has a brightness value of between 0 (black) and 255 (maximum intensity). In images B and C large areas of the interphase nuclei demonstrate the same level of maximum fluorescence (i.e. many of the pixels have an intensity value of 255). The result of this is that the system would not be able to determine the difference between any of these pixels as they are at the maximal resolution range for a CGH image (whereas in image A, differences in brightness of the pixels constituting the interphase nuclei are visible). This is of no consequence for this particular image, as the interphase nuclei would be removed from the image during analysis leaving behind the metaphase chromosomes for which the compensation in exposure times was required. It is important to note that manual exposure times must be carefully determined to prevent maximal exposure occurring on chromosomes from which quantitative measurements are to be made.

Figure 4.4(D) represents the more commonly occurring scenario requiring manual compensation of exposure times. This image of a successful hybridization was captured using exposure times determined as described above to compensate for the intensely green fluorescent piece of debris lying within the metaphase spread (white arrow). Visualisation of the DAPI image confirmed that this was indeed debris and not chromosomal DNA and

so the image was re-exposed manually. The image can be seen to be a high quality metaphase worthy of inclusion in the analysis for this experiment. However, due to the overlying debris and its surrounding glow, neighbouring chromosomes were excluded from the analysis (yellow arrows) as the green fluorescence on these chromosomes was partly due to the debris. Fluorescent debris such as is pictured in Figure 4.4(D) was an occasional finding (affecting both or either of the colour planes). The source of this debris was believed to be dust, which had either accumulated on the slide during setting up of the CGH or had escaped filtration in the wash solutions. However, batches of the Spectrum Red pre-labelled reference DNA (Vysis) were occasionally found to generate noticeable levels of red fluorescent particles of debris when the images were viewed. This complicated the capturing of images for analysis and required more images to be collected before proceeding to image analysis as several chromosomes had to be discarded due to debris. This did not affect the data collected from such experiments as the CGH analysis software was able to select and exclude small particles from the image and therefore did not affect the normalization and colour ratio analysis of the image.

4.4.2 Image analysis and interpretation

Suitable images were analysed on a Power Macintosh 6400/200 running the Vysis CGH Analysis software. Image processing consisted of several stages depicted in Figures 4.3a and 4.3b. Chromosomes were initially segmented from the background and overlapping or closely aligned chromosomes separated using the software (Figure 4.3(F)). The axis of each chromosome was displayed and checked for accuracy. Particles of debris were then removed from the image along with any interphase nuclei. The remaining chromosomes were karyotyped using the automated function of the software based on the chromosome bands visible in the enhanced DAPI image. The accuracy of the automated karyotyping varied depending on the quality of the image and was generally within the range of 65-85% so all karyotypes had to be manually checked and adjusted. Chromosome karyotyping is recognised as a difficult technique and training was generously provided by Dr Mark Sales and Dr Norman Pratt of the University of Dundee. A representative sample of 15 early CGH experiments were validated by Dr Mark Sales to ensure karotyping had been performed accurately. The green to red fluorescent ratio (FR) was then measured perpendicular to the axis of each of the chromosomes and displayed as a CGH ratio profile (Figure 4.3b(I)). This process was repeated for between 5 and 10 metaphase images and the results compiled and presented as an average CGH ratio profile (Figure 4.3b(J)). Figure 4.5 depicts a CGH interpretation for a representative chromosome (chromosome 11) in more detail. The enhanced DAPI image is depicted next to a chromosome ideogram

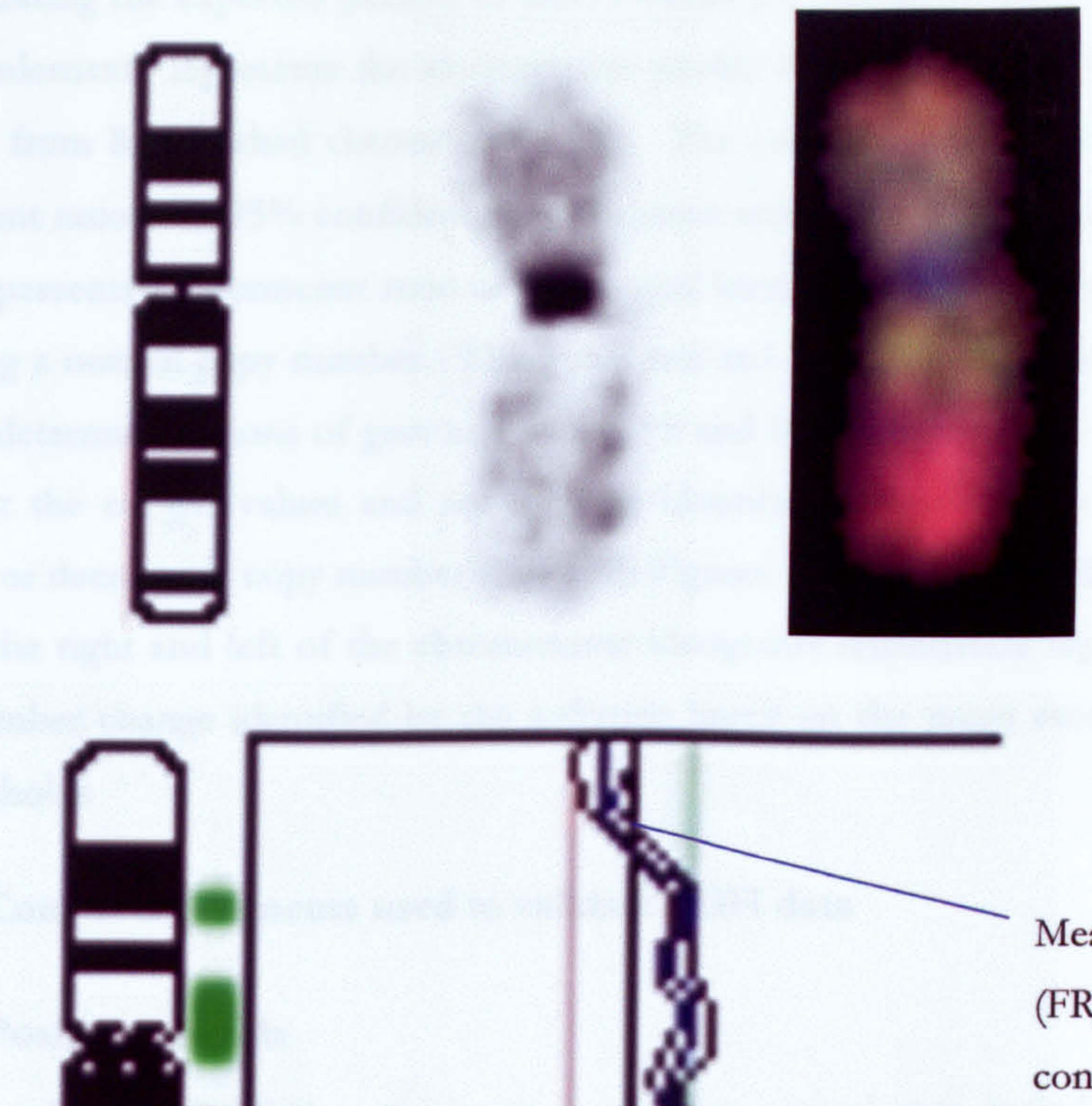

Figure 4.5 – Green to Red Fluorescent Ratio (FR) measurement. The enhanced DAPI image of a typical chromosome is shown along with the composite colour image. The graph below demonstrates an example of the ratio profiles generated for each chromosome in a CGH experiment. The blue line represents an average ratio profile generated from the measurement of 8 chromosomes from a stained metaphase preparation. 95% confidence limits are depicted either side of the mean. The graph demonstrates the thresholds (green and red line) used to determine regions of copy number change (gain >1.15; loss <0.85). The thick black line down the centre represents a FR of 1 i.e. indicates the position representing no change in copy number. The thick green and red bars either side of the chromosome ideogram indicate regions of DNA copy number gain and loss respectively, identified when the FR crosses the thresholds described.

demonstrating the expected pattern of DAPI bands for that particular chromosome. The graph underneath represents the average ratio profile for chromosome 11 generated from the data from 8 individual chromosome 11's. The central blue line represents the mean fluorescent ratio with 95% confidence limits shown either side. The solid black line on the graph represents a fluorescent ratio of 1 i.e. equal binding of red and green labelled DNA indicating a normal copy number. The green and red lines represent the threshold values used to determine regions of gain and loss (1.15 and 0.85 respectively). These thresholds represent the cut-off values and are used to identify gains and losses of DNA (as an increase or decrease in copy number). In both Figures 4.3b and 4.5 the thick green and red bars to the right and left of the chromosome ideograms respectively represent regions of copy number change identified by the software based on the mean ratio profile crossing the thresholds

4.5 Control experiments used to validate CGH data

4.5.1 Positive controls

For every batch of CGH experiments a positive control was included. These were performed using DNA extracted from the MPE600 breast cancer cell line (Vysis). This cell line has been extensively studied and contains several known and well-characterised genetic abnormalities allowing the success of hybridization conditions to be determined. Any batches of CGH experiments for which the control did not generate the expected pattern of copy number alterations were discarded and repeated. Figure 4.6(A) shows an example MPE600 CGH result. It is interesting to note that during the course of this thesis the aberrations detected in the MPE600 DNA did change and a gain of the entire chromosome 7 appeared and was subsequently consistently detected. After discussions with other laboratories using the MPE600 control DNA from the same source (Vysis) it became clear that this change represented clonal evolution in the line of MPE600 used to generate the source of DNA, and did not represent an artefact of CGH hybridizations.

4.5.2 Normal : Normal controls

Normal : normal hybridizations were performed regularly to determine appropriate threshold levels for identifying copy number alterations (Figure 4.6(B)). These thresholds are important and greatly influence the sensitivity and accuracy of a CGH experiment. Two different normal DNA controls were performed. Firstly, normal genomic DNA (Sigma, Promega) was nick translated with SpectrumGreen™ as described in Section 3.6

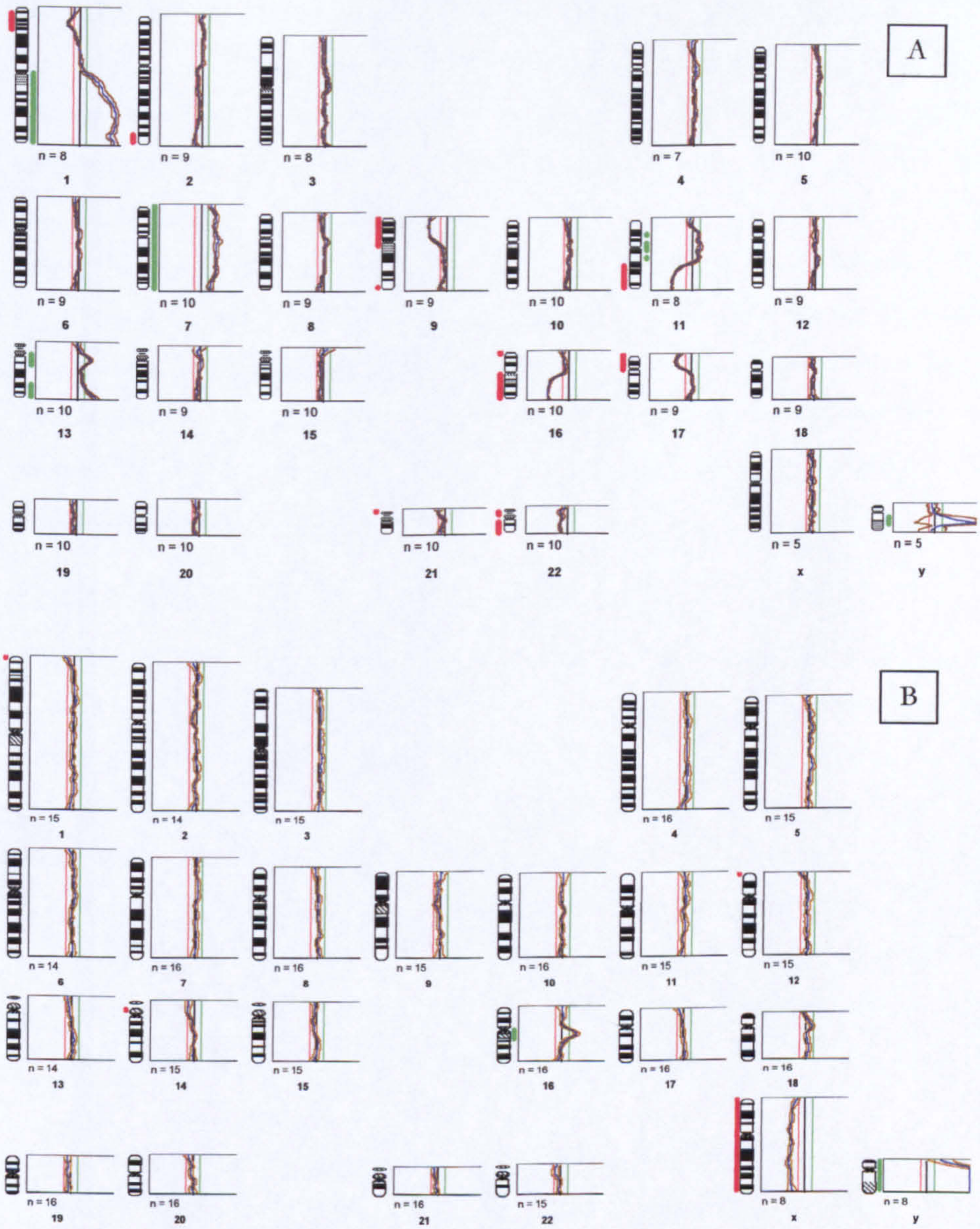

Figure 4.6 – Control experiments used to evaluate CGH. Both positive (A) and negative (B) control experiments were routinely incorporated into batches of CGH experiments in order to evaluate the data generated from test experiments. The well characterised breast cell line MPE600 (A) was used as a positive control and only batches of hybridizations in which the known aberrations were identified were included. Hybridization of normal : normal DNA samples (B) was used as a negative control in order to establish suitable thresholds for the evaluation of copy number change. The apparent loss of chromosome X and gain of Y reflects the mismatching of red labelled normal female DNA hybridized against green labelled normal male DNA.

and hybridized against pre-labelled SpectrumRed™ reference DNA obtained from Vysis. Secondly, normal genomic DNA was nick translated with both Spectrum Green and Spectrum Red DNA and hybridized directly against each other. The CGH profile from a normal control experiment depicted in Figure 4.6(B) demonstrates that the FR did not exceed the thresholds, apart from at chromosomal regions of known unreliability due to Cot-1 suppression such as telomeric regions, acrocentric chromosome arms and heterochromatic regions at the centromers of certain chromosomes (such as chromosome 16 in Figure 4.6(B)). Both controls allowed the evaluation of the normal fluctuations in the FR, and only differences in the FR in test cases that exceeded those of the normal controls were scored as gains and losses. Repeated normal control experiments determined that gains of DNA were detected when the FR exceeded 1.15 and losses when the FR was less than 0.85. These limits were applied to all hybridizations.

4.5.2.1 Evaluation of normal genomic DNA

Throughout this thesis several batches of normal reference DNA were used both for normal : normal control hybridizations and as a source of reference DNA in experimental hybridizations. The majority of red labelled reference DNA used was obtained pre-labelled from Vysis (UK) as this eliminated the need for nick translation. Other batches of normal genomic DNA were obtained from both Promega and Sigma and nick translated as described in Section 3.6 using the SpectrumRed™ fluorochrome (Vysis). This was found to be an equally effective alternative to using pre-labelled normal genomic DNA and at a significant cost saving. Large-scale nick translations could be performed generating a batch of reference DNA enough for numerous CGH experiments (approximately 20).

However problems were encountered highlighting the need to evaluate every batch of normal DNA obtained before using it in a CGH experiment. One batch of DNA obtained from a previously tested source of DNA (Sigma) originating from human placental material was nick translated and used in a batch of 6 successful hybridizations. When analysed it was noted that all the experiments from the batch contained several identical aberrations (which had not previously been seen at a high frequency in other HNSCC CGH experiments, most notable was a consistent gain of chromosome 19. The batch of normal DNA obtained from Sigma was subsequently tested against pre-labelled reference DNA (Vysis, UK) (Sigma 'normal' genomic DNA nick translated with green against Vysis pre-labelled red genomic DNA). Figure 4.7a depicts the results of a typical experiment from the batch of six test experiments for which the Sigma genomic DNA was used as reference DNA, Figure 4.7b shows the results of a repeat hybridization of the same test sample

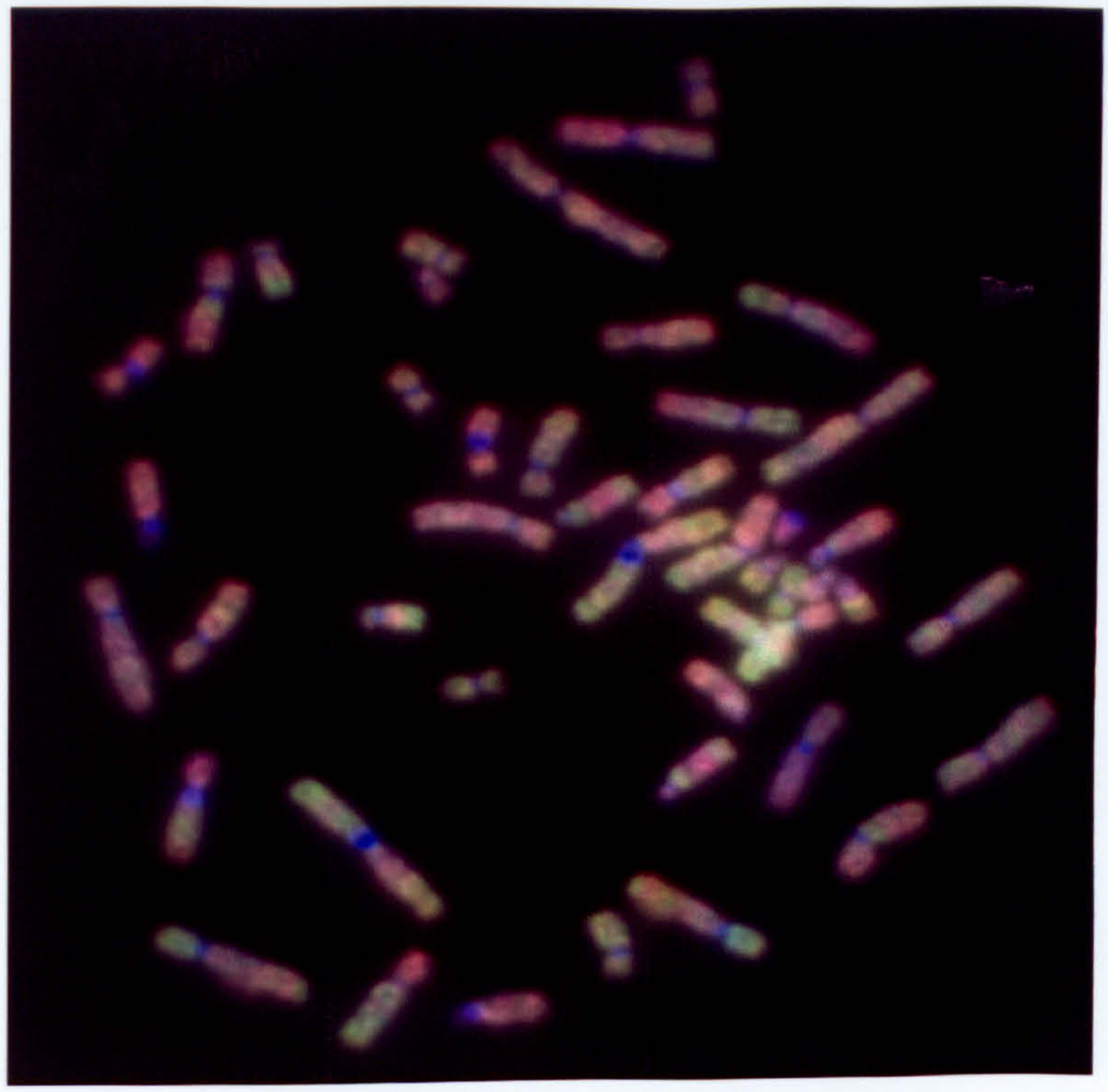

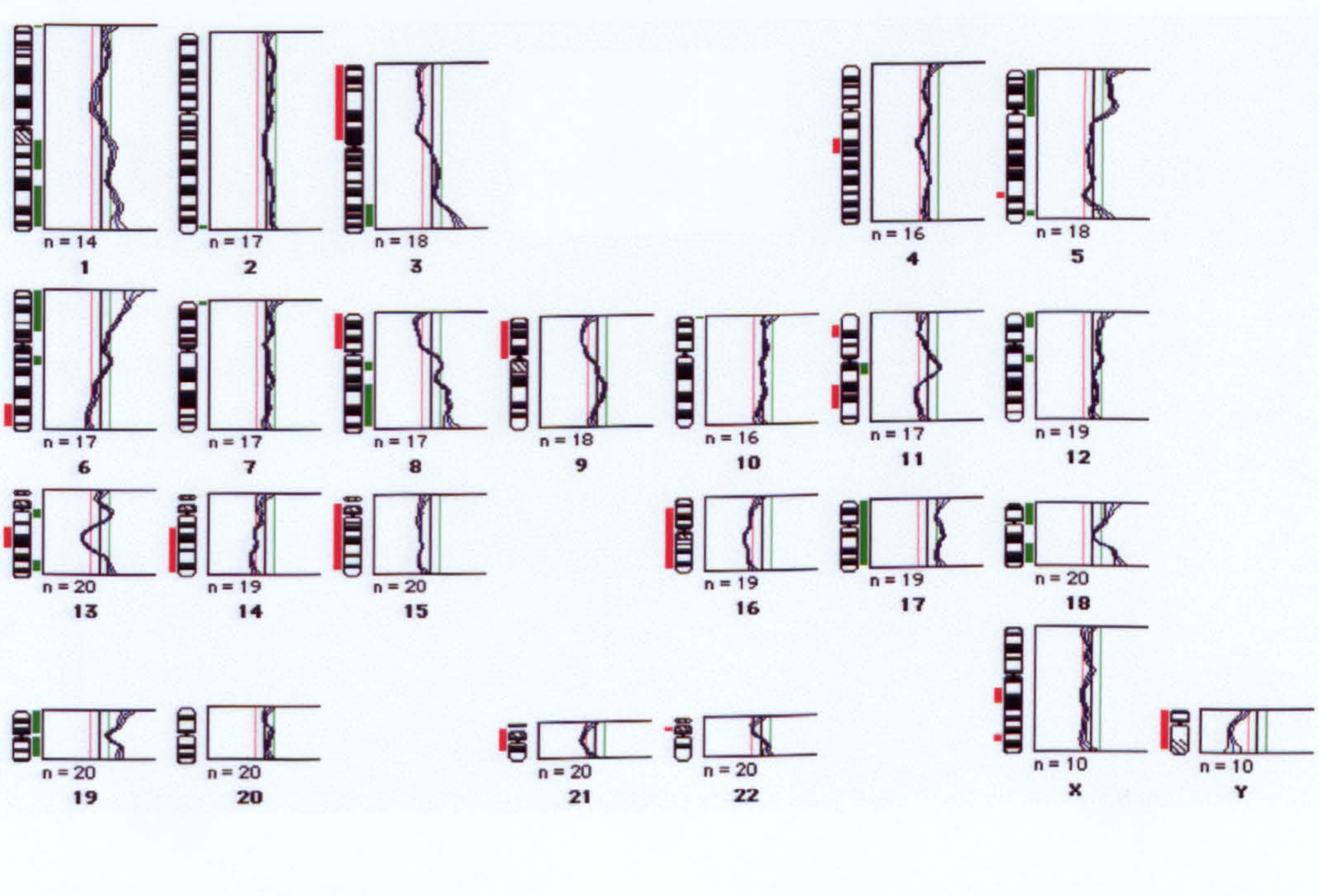

Figure 4.7a – Representative image and CGH ratio profile from a tumour hybridized against 'normal' genomic DNA obtained from Sigma. Several identical novel aberrations were seen in a batch of 6 test cases hybridized against a new batch of 'normal' DNA obtained from Sigma. Note the apparent 'gain' of chromosome 19.

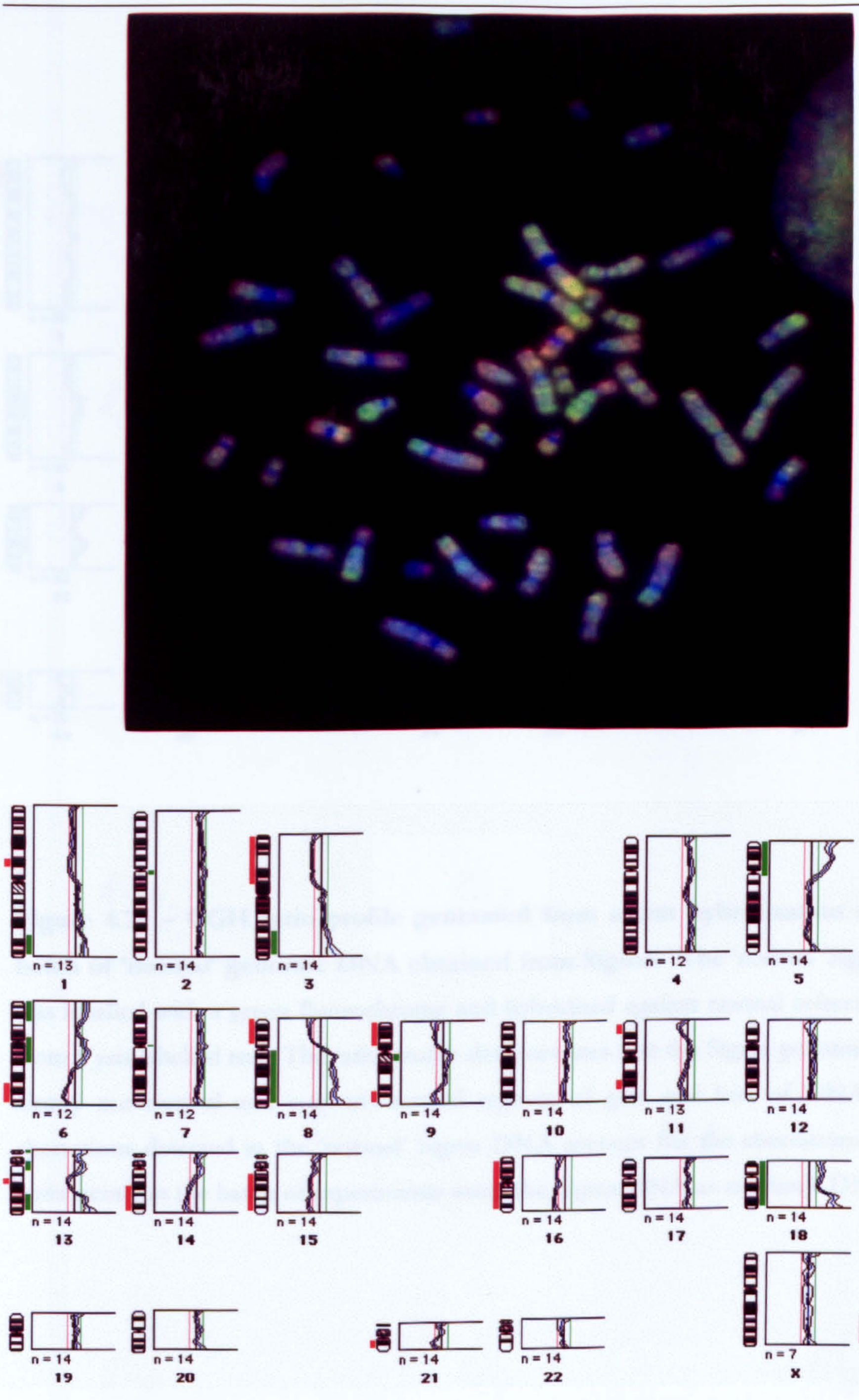

Figure 4.7b – Representative image and CGH ratio profile from a repeat hybridization of the tumour DNA depicted in Figure 4.7b. In this experiment Vysis pre-labelled normal DNA was used as the reference DNA. Overall the profiles are similar, however several important discrepancies can be seen. Note the normal copy number for chromosome 19.

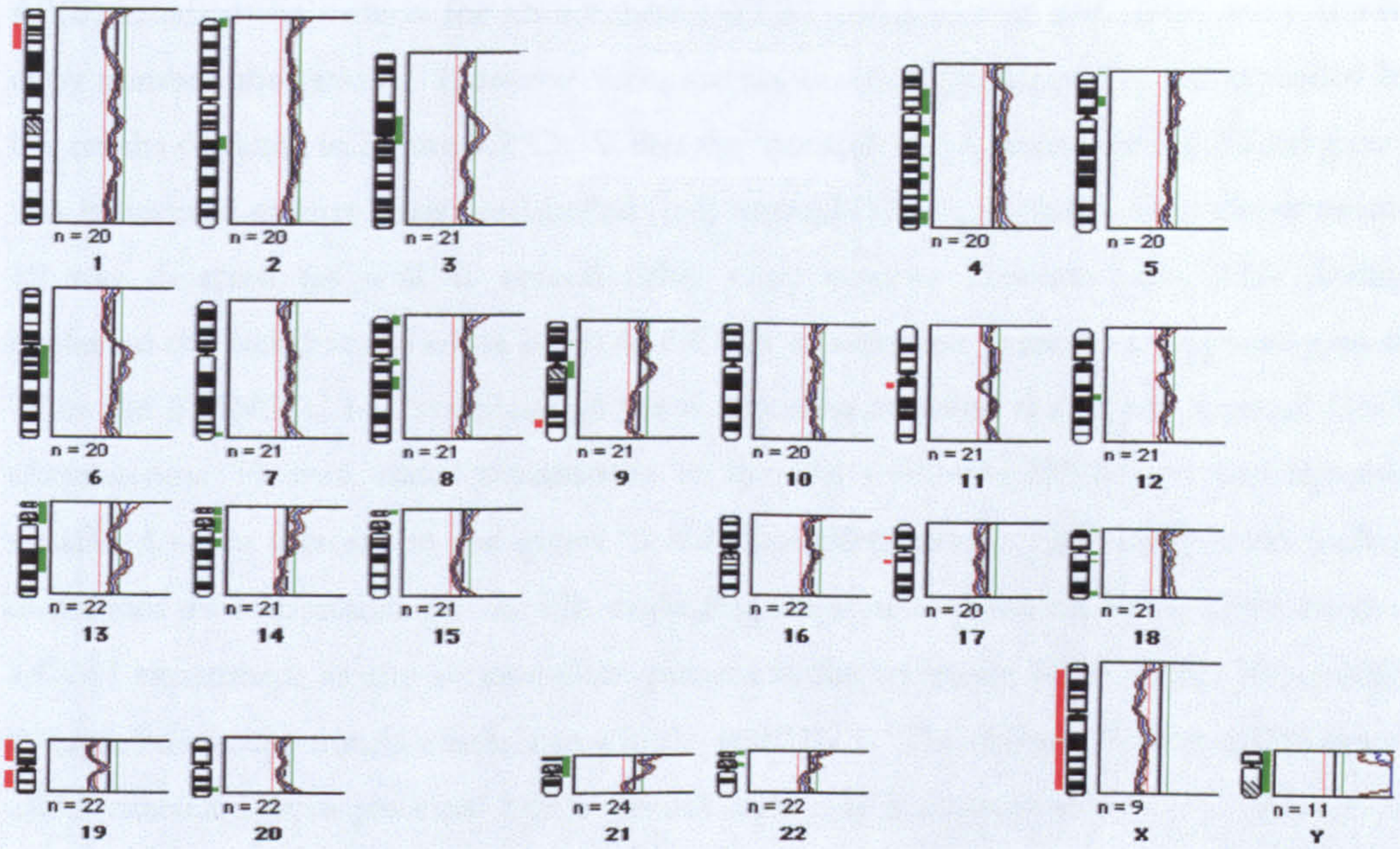

Figure 4.7c – CGH ratio profile generated from a test hybridization of a new batch of 'normal' genomic DNA obtained from Sigma. The 'normal' Sigma DNA was labelled with a green fluorochrome and hybridised against normal reference DNA from Vysis labelled red. The ratio profile demonstrates that the Sigma genomic DNA is clearly not normal and contains several regions of gain and loss of DNA. These aberrations detected in the 'normal' Sigma DNA account for the aberrations detected consistently in the batch of experiments using the Sigma DNA as reference DNA.

against Vysis pre-labelled normal reference genomic DNA and Figure 4.7c demonstrates the aberrations identified when the 'normal' genomic DNA from Sigma was subsequently tested against Vysis reference DNA. Both the experiments shown in Figures 4.7(A) and 4.7(B) satisfied the criteria for an acceptable CGH hybridization and share many similar copy number aberrations. However there are important differences that are explained by the results depicted in Figure 4.7(C). When the 'normal' DNA from Sigma (labelled green) was hybridized against Vysis pre-labelled (red) normal DNA complete loss of chromosome 19 was detected (as well as several other copy number abnormalities). This finding explained the fact that the entire batch of 6 CGH experiments detected a supposed gain of 19 in the 6 HNSCC test samples. In the 6 experiments using the Sigma 'normal' DNA chromosome 19 was under represented in the red reference DNA and subsequently visualised as an increase in the green to red fluorescent ratio. This unexpected finding underlines the importance of carefully evaluating the source of the reference DNA used in a CGH experiment as any abnormalities present in the reference DNA would be wrongly interpreted as copy number imbalances in the test DNA. The origins of gains and losses in DNA extracted from placental DNA are not clear. As a consequence of this, the use of normal DNA from Sigma was discontinued and remaining experiments were performed using Vysis pre-labelled normal DNA.

4.6 Quality control of CGH

4.6.1 Influence of probe size on CGH hybridizations

The minimal size of a DNA probe required in order for a fragment of DNA to be unique (i.e. to prevent binding to unrelated sequences) for the human genome has been estimated at 17 base pairs (Anderson, 1999). The longer fragments of DNA utilized in the CGH probe mix are therefore highly likely only to bind to their appropriate target sequences. The longer length of fragments used was designed to reduce granularity of the hybridization and maximises the intensity of fluorescence as these longer fragments can withstand the high stringency washes employed to remove non-specifically bound fragments. However, excessively large DNA fragments would fail to penetrate the target metaphase chromosomes adequately and would be prevented from finding their target loci (Anderson Ed., 1999). To investigate the influence probe size had on the success of a CGH hybridization control experiments were performed.

DNA was extracted from the breast cell line MCF7 and two nick translations were performed using 10µl and 12µl of enzyme mix to generate smears of fragments of differing

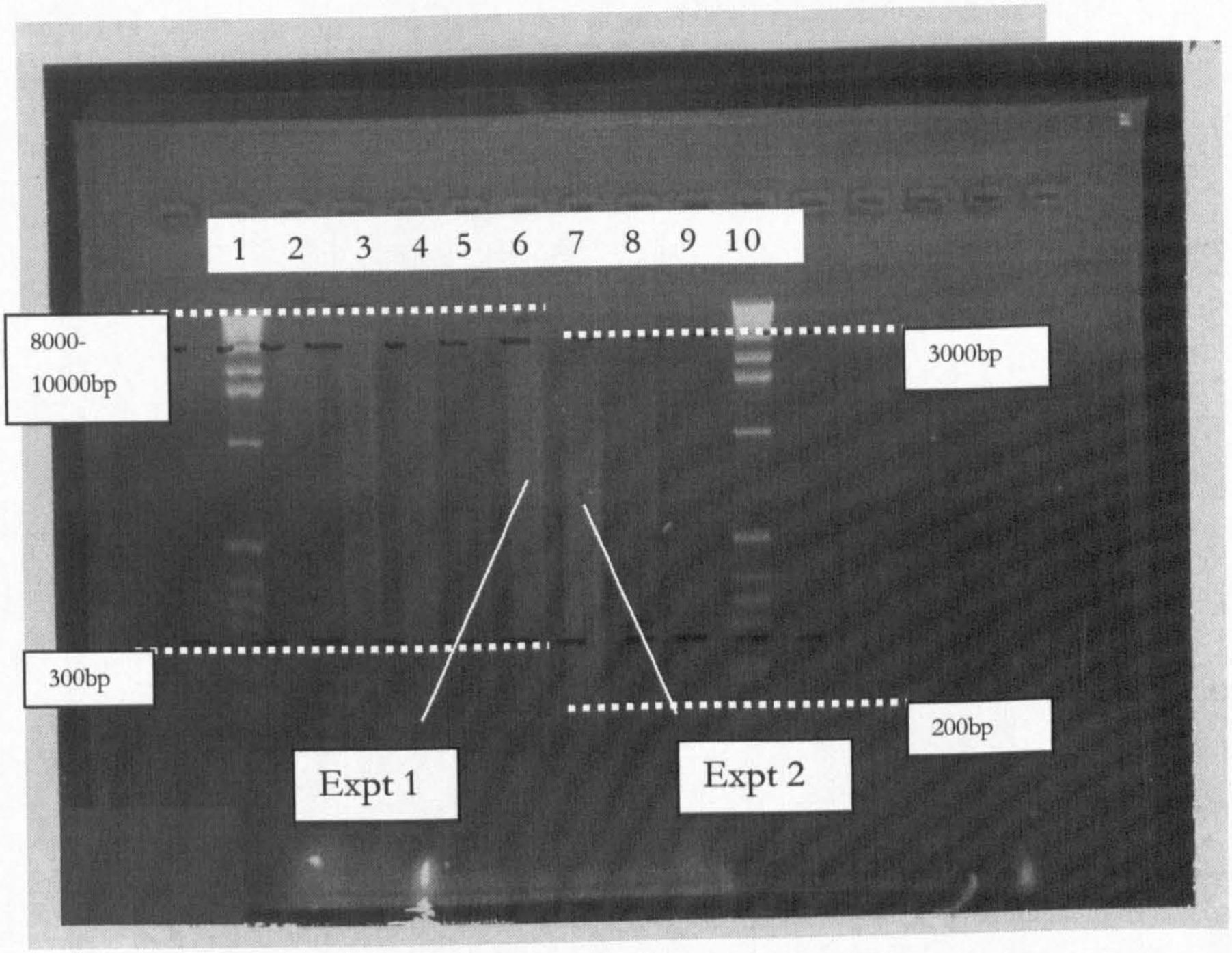

Figure 4.8 – Influence of probe size on CGH hybridization. The two experiments used in evaluating the influence that nick translation products had on the success of a CGH hybridization are labelled experiments 1 and 2. Experiment 1 (lane 6 on the gel) contains DNA fragments within the range 8 000/10 000 to 300 base pairs in length. Experiment 2 (lane 7 on the gel) contains a smear of DNA fragments of optimal size for CGH, 3000 to 200 base pairs in length. Both smears of DNA fragments were obtained by nick translating 2µg of DNA extracted from the MCF7 breast cell line. 10µl of enzyme mix were used to generate the smear of fragments for experiment 1 and 12µl of enzyme mix for the smear of fragments for experiment 2. Size standard used (lanes 1 and 10) – 10µl of 1kb DNA ladder (Life Technologies). Fragment sizes: 201bp, 220bp, 298bp, 344bp, 399bp, 506bp, 1018bp, 1636bp, 2036bp, 3054 bp (+larger fragments not separated at this resolution). Lanes 2-5 and 8-9 contain additional, unrelated, nick translation experiments.

lengths. Figure 4.8 depicts the two sets of smears obtained. Experiment 1 was performed using large nick translation fragments ranging from approximately 8 000/10 000 to 300 base pairs in length and experiment 2 used DNA fragments within the optimal range for CGH of approximately 3 000 to 200 base pairs in length. Both hybridizations were performed simultaneously utilising the same batch of Spectrum Red labelled male reference DNA. The only difference between the two CGH experiments was the size of the Spectrum Green labelled DNA fragments used.

Figure 4.9a depicts representative metaphase images obtained from the two experiments. The difference between the two images is immediately obvious. The image from experiment 1 Figure 4.9a(A) demonstrates even hybridization over the length of all the chromosomes and several areas of gain and loss are clearly visible. When the chromosomes from the spreads are karyotyped (Figure 4.9b) the difference between the two experiments is again clearly evident. Experiment 2 (Figure 4.9b(B)) demonstrates a significantly different pattern of hybridization to experiment 1 (Figure 4.9b(A)). Hybridization is seen to be less even with a characteristic 'banding pattern'. These bright bands of hybridization correspond to the light regions of the metaphase chromosomes generated by DAPI banding (see Figure 4.9c). Relatively little hybridization of the larger DNA fragments was seen within the dark DAPI bands. Both experiments were performed on metaphase preparations from the same batch of slides and processed simultaneously within the same denaturing solution eliminating the possibility that uneven denaturation resulted in this pattern of hybridization. Figure 4.9c shows the similar DAPI banding patterns and quality of chromosomes between the two experiments.

Despite the difference in the visual quality of the images obtained from the two experiments, measurement of the red to green colour ratio generated remarkably similar results. The CGH profiles generated from the two experiments are shown in Figure 4.9e and indicate that the two hybridizations generate essentially similar results. The visual difference between the hybridizations is represented in the CGH profiles as a difference in noise 'levels' and experiment 1 demonstrates smoother profiles with closer correlation between the ratios generated from the 2 chromosome homologues. However when data from several images for each experiment are combined in an average CGH ratio profile (Figure 4.9e) the results are even more similar. Experiment 2 does demonstrate wider 95% confidence limits due to the increased noise from the individual metaphases included within the analysis. The majority of DNA copy number imbalances are detected within both hybridizations however some important differences can be seen between the two sets

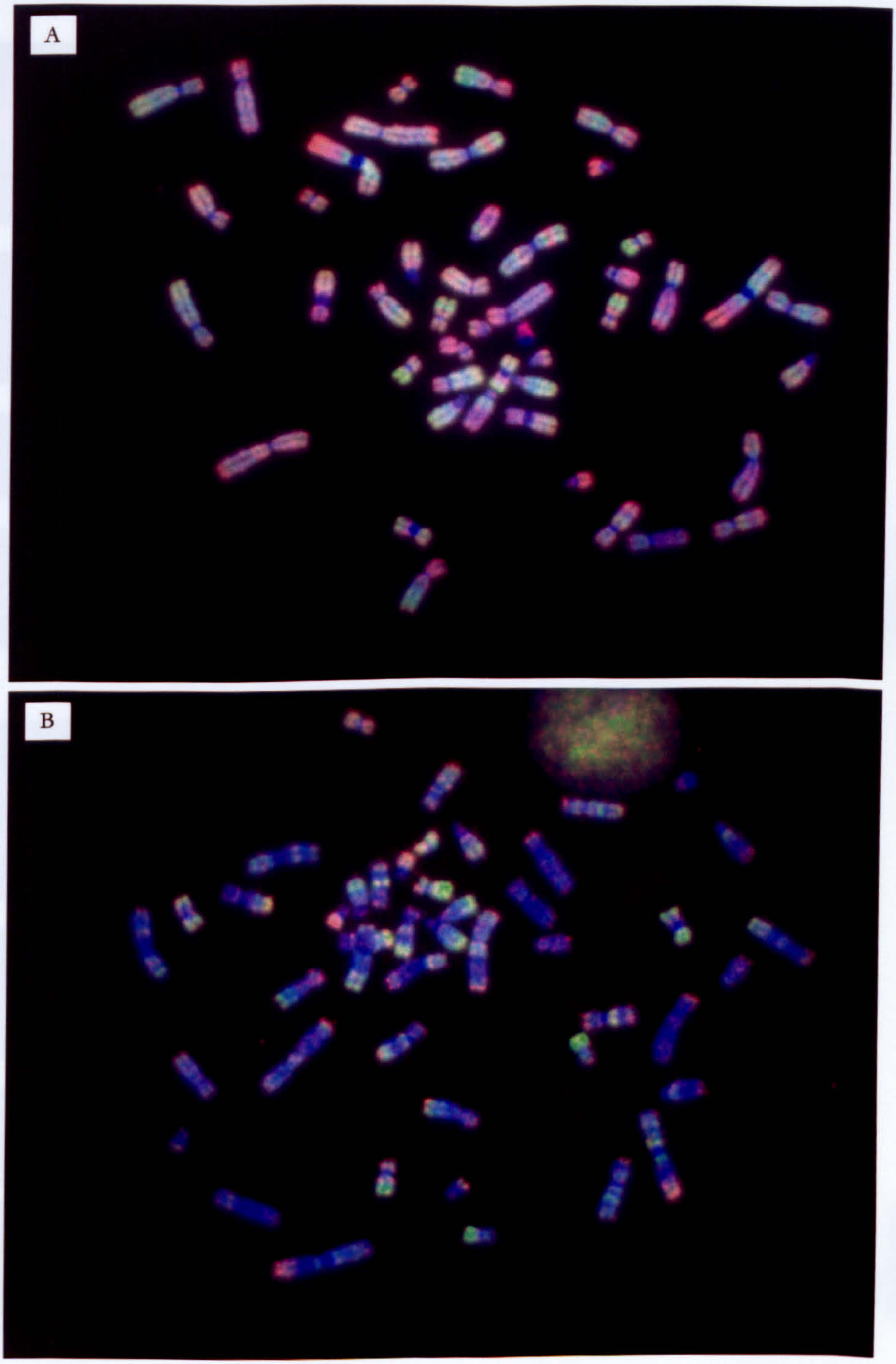

Figure 4.9a – Representative metaphase images from two CGH experiments utilising different sized probe fragments of the same DNA sample. Image A depicts the hybridization of optimally sized fragments and B depicts hybridization of excessively large fragments.

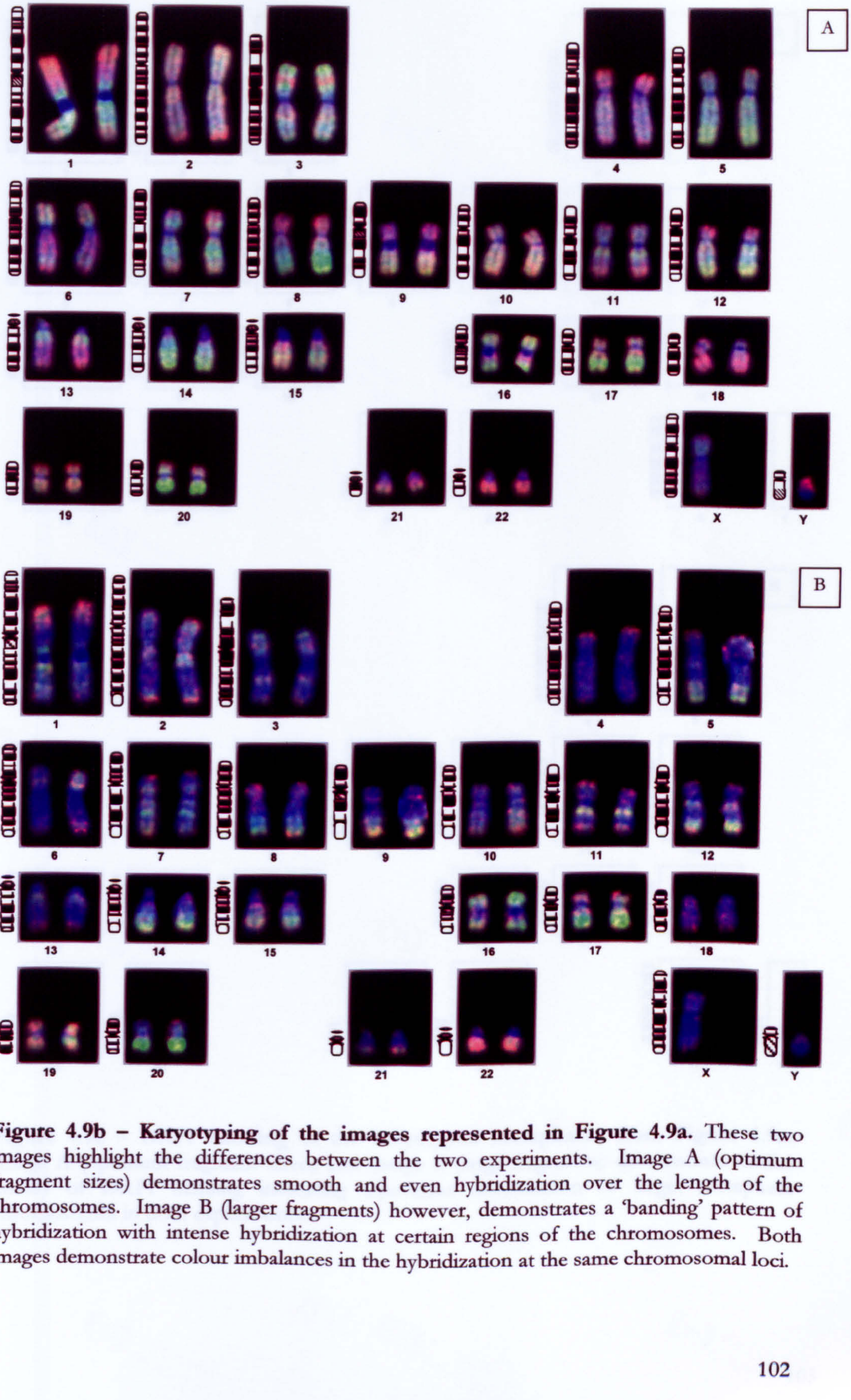

Figure 4.9b – Karyotyping of the images represented in Figure 4.9a. These two images highlight the differences between the two experiments. Image A (optimum fragment sizes) demonstrates smooth and even hybridization over the length of the chromosomes. Image B (larger fragments) however, demonstrates a 'banding' pattern of hybridization with intense hybridization at certain regions of the chromosomes. Both images demonstrate colour imbalances in the hybridization at the same chromosomal loci.

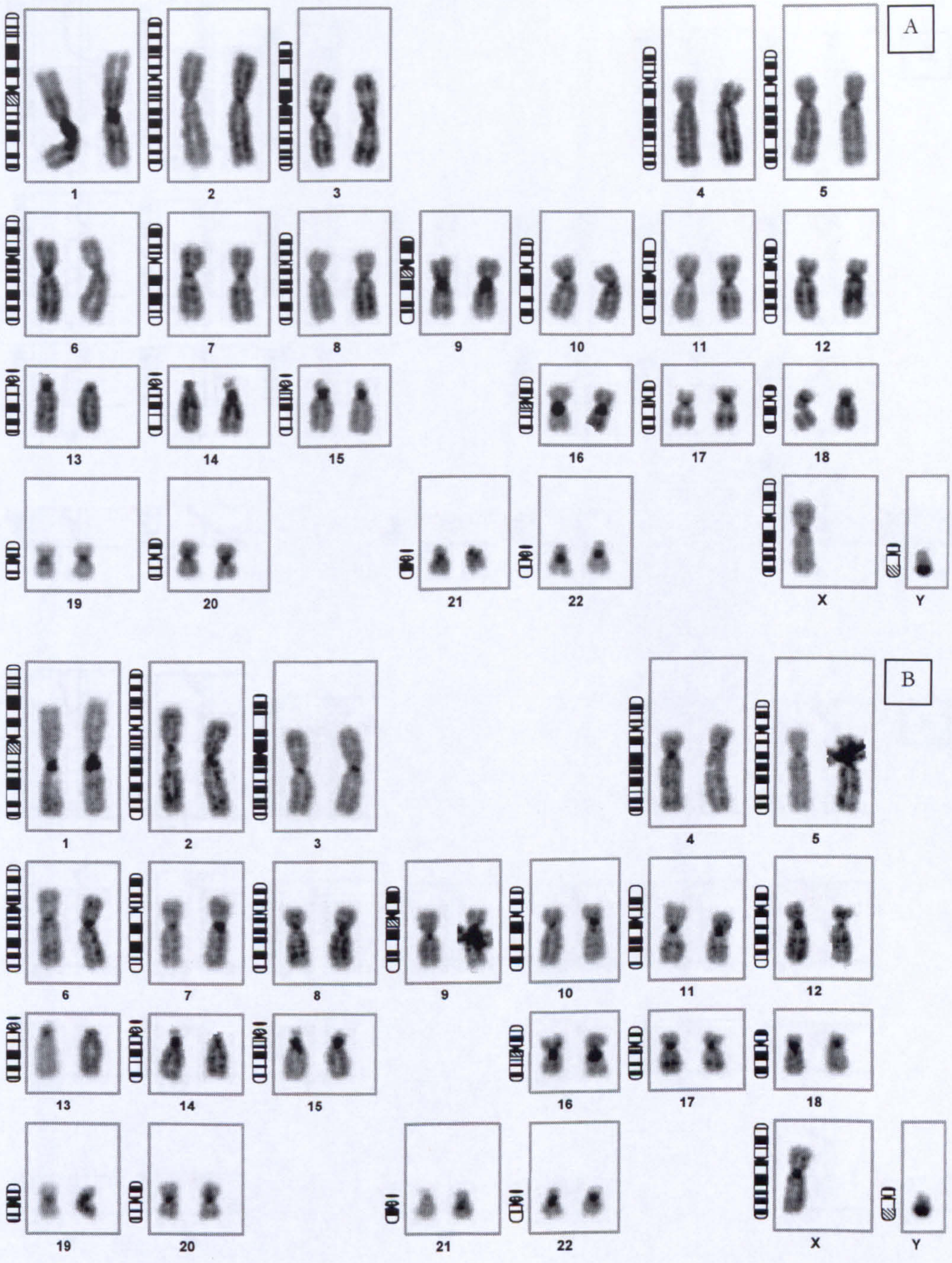

Figure 4.9c – DAPI banding of the karyotyped metaphases from Figure 4.9a. Image A (optimum fragment sized) and Image B (large fragments) demonstrate similar quality of DAPI banding indicating equivalent denaturation of target metaphase chromosomes in both experiments.

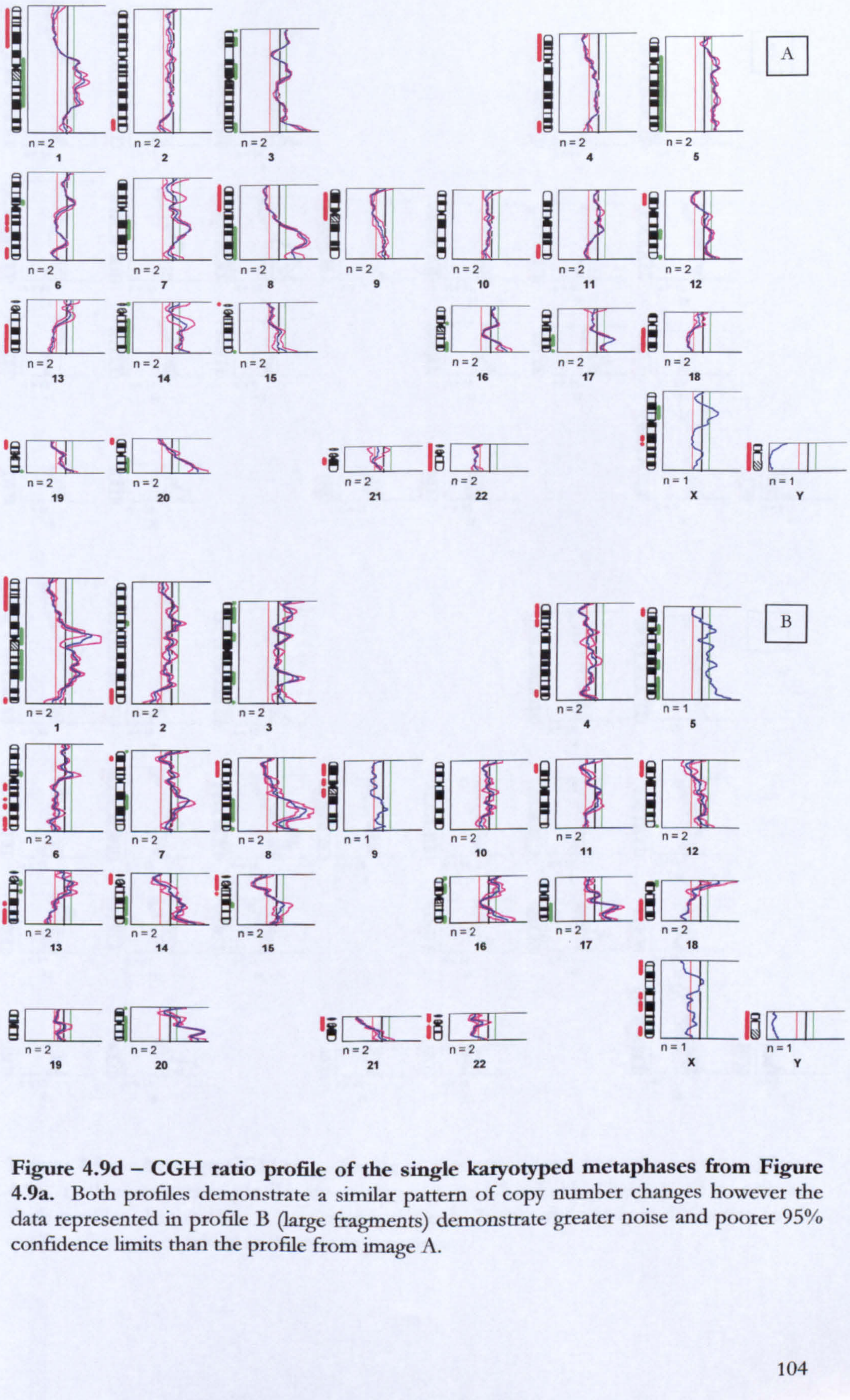

Figure 4.9d – CGH ratio profile of the single karyotyped metaphases from Figure 4.9a. Both profiles demonstrate a similar pattern of copy number changes however the data represented in profile B (large fragments) demonstrate greater noise and poorer 95% confidence limits than the profile from image A.

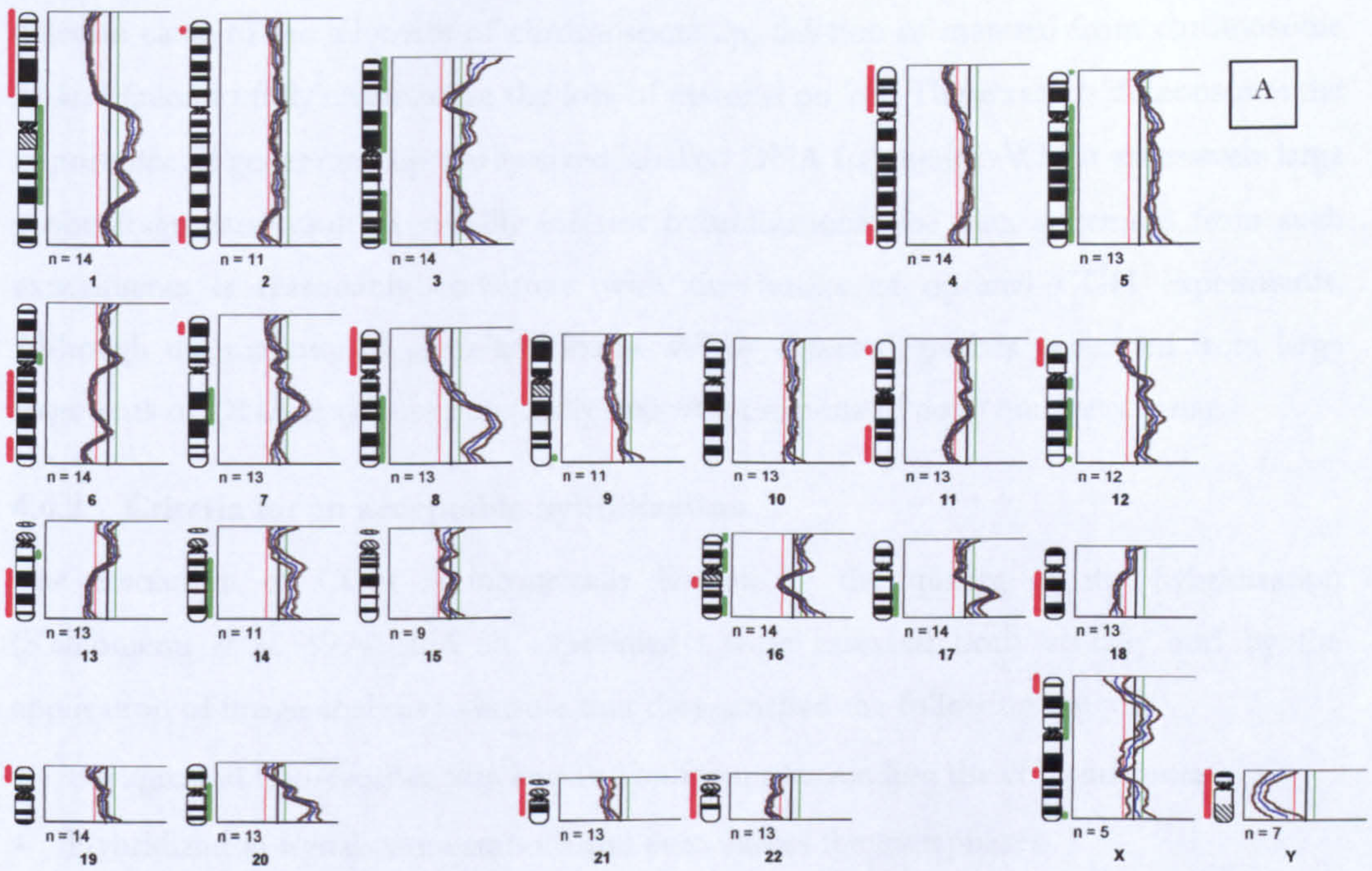

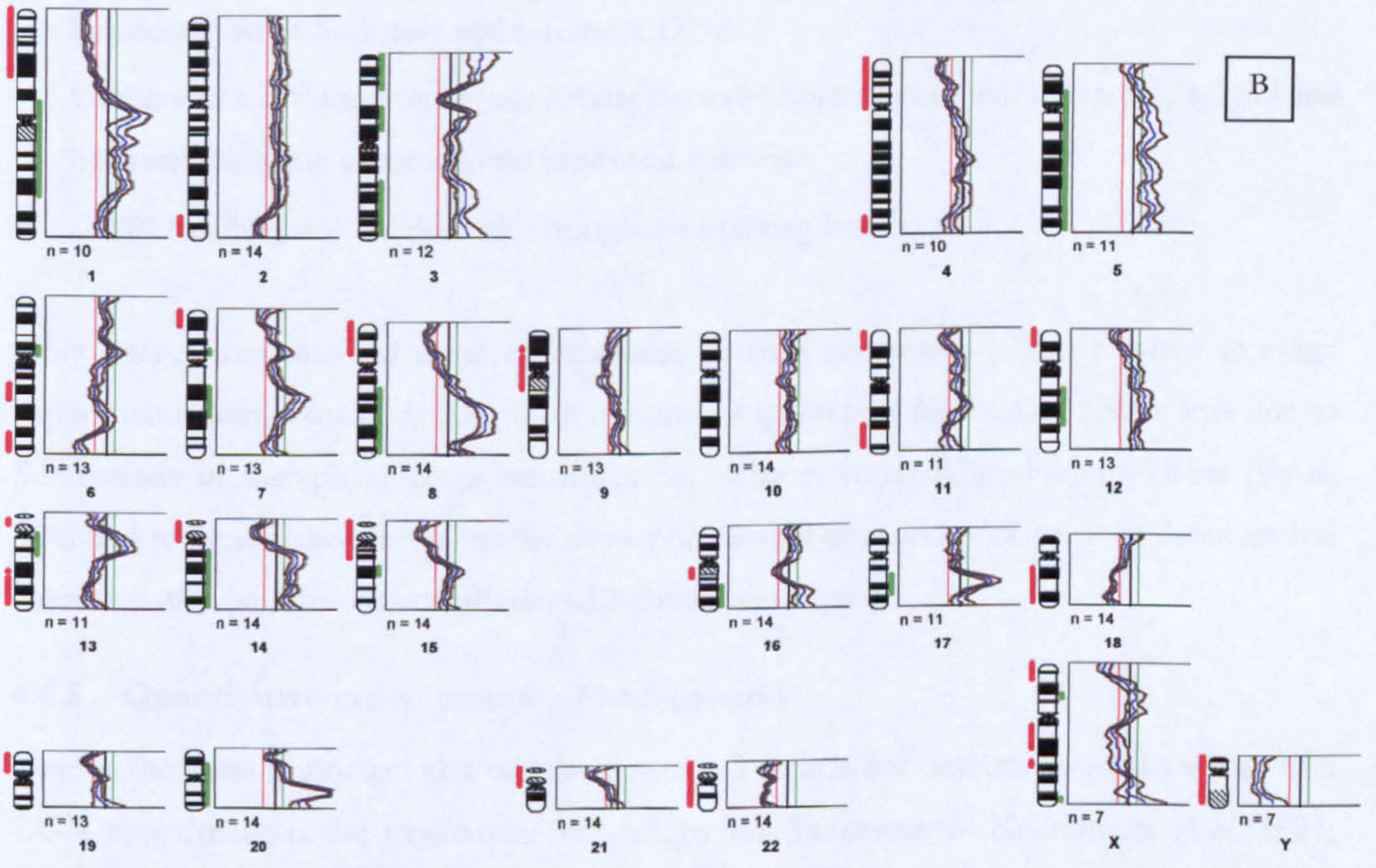

Figure 4.9e – Average CGH ratio profile of the karyotyped metaphases from Figure 4.9a. Both average ratio profiles are constructed from 7 individual karyotyped metaphases. Both profiles demonstrate a near identical result despite the obvious difference in the quality of images obtained in the two experiments.

of results. The larger DNA fragments failed to detect a gain of 16p as well as a small deletion close to the telomere of chromosome 2p, deletion of material from chromosome 21 and failed to fully characterise the loss of material on 9p. These results demonstrate the importance of generating optimally-sized labelled DNA fragments. Whilst excessively large probe fragments result in visually inferior hybridizations, the data generated from such experiments is reasonably consistent with the results of optimal CGH experiments. Although the majority of gains and losses will be detected, probes generated from large fragments of DNA may miss potentially important regions of copy number change.

4.6.2 Criteria for an acceptable hybridization

The resolution of CGH is intrinsically limited by the quality of the hybridization (Kallioniemi *et al*, 1994) and all experiments were assessed both visually and by the application of image analysis to ensure that they satisfied the following criteria:

- Background fluorescence was low and uniform surrounding the chromosomes.
- Hybridization signals were smooth and even across the metaphases.
- Centromeric and heterochromatic regions of the chromosomes demonstrated minimal hybridization of both test and reference DNA.
- Green and red fluorescence was similar between homologues within a single spread and between the same chromosome in several spreads.
- DAPI banding was bright with strongly contrasting bands.

Only images that satisfied these criteria were deemed acceptable. This resulted in many experiments being repeated. The most common explanation for a CGH failure was due to fluctuations in metaphase preparation quality. The commercially obtained slides (Vysis, UK) had to be returned to the manufacturer on several occasions due to poor denaturation characteristics (an observation shared with other customers).

4.6.3 Quantitative measurement of background

One of the most important and widely recognised criteria for determining the success of a CGH experiment is the evaluation of background fluorescence (Kallioniemi *et al*, 1994; Karhu *et al*, 1997). Background fluorescence arises due to two main factors, the presence of residual cytoplasm overlying the metaphase spread and prolonged exposure times due to faint fluorescent staining of the chromosomes. Residual cytoplasm occurs during the preparation of metaphase spreads as discussed earlier.

Representative CGH images from each experiment were evaluated initially by eye, and then by quantitative image analysis, to determine the signal to background fluorescent ratio for both fluorochromes (SB ratio). The SB ratio was defined as the fluorescence intensity measured on the metaphase chromosomes (signal) divided by the fluorescence intensity in the areas between the chromosomes (background). For this thesis a SB ratio of >3.0 was determined to be required for acceptable results in accordance with other laboratories performing CGH (Kallioniemi *et al*, 1994; Karhu *et al*, 1997). Figures 4.10 to 4.12 demonstrate the quantification of the SB ratio for both acceptable and unacceptable CGH images using the IP Lab image analysis software package. For all images a line was drawn randomly across the image crossing both metaphase chromosomes and the areas in between. A graph was then drawn representing the fluorescent intensity at each pixel along the length of the line for each colour plane, using a range of 0-255 to represent the range of no fluorescence to maximum fluorescence. Figure 4.10 demonstrates the quantification of the SB ratio using an unacceptable CGH image. The graph depicts the fluorescent intensities along the length of the line for all three-colour planes. For the red fluorochrome fluorescence levels measured on the metaphase chromosomes (Signal) are within the range of 100 to 200 whilst the areas in between the chromosomes (Background - blank areas of the glass slide) contain very little fluorescence with an intensity of approximately 20. This generates a SB ratio of between 5.0-10.0. However, the green SB ratio can be seen to be much lower due to unacceptably high levels of green background fluorescence. For the green fluorochrome the signal intensity is between 140-200 and the background much higher at approximately 90 generating a low SB ratio of between 1.55 and 2.22. The red SB ratio indicates that hybridization conditions were successful, however the green probe either failed to hybridise or that the test probe did not incorporate enough green fluorochromes during nick translation.

Figure 4.11 and 4.12 depict acceptable, high quality CGH images that demonstrate high SB ratios for both fluorochromes. For both these images the SB ratio exceeded 3.0 for both fluorochromes.

4.6.4 Assessment of fluorescent intensities at the centromeric and heterochromatic regions

The suppression of interspersed repetitive sequences (IRS) is necessary in CGH as failure to do so can lead to unreliable FR measurements, both at the centromeres and throughout the genome (Kallioniemi *et al*, 1994; Kirchoff *et al*, 1997; James *et al*, 1999). If these sequences are not blocked sufficiently, labelled fragments originating from IRS elements

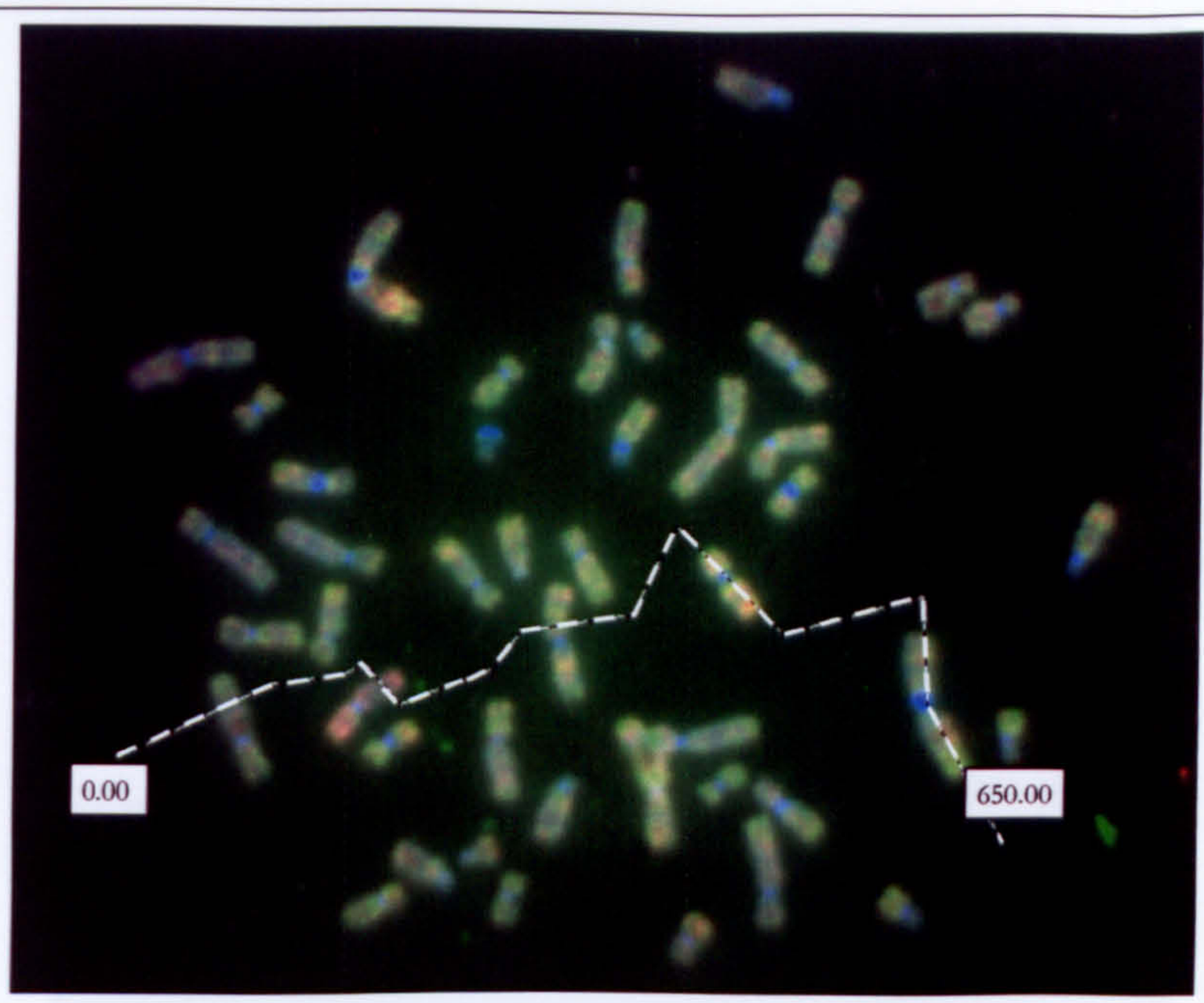

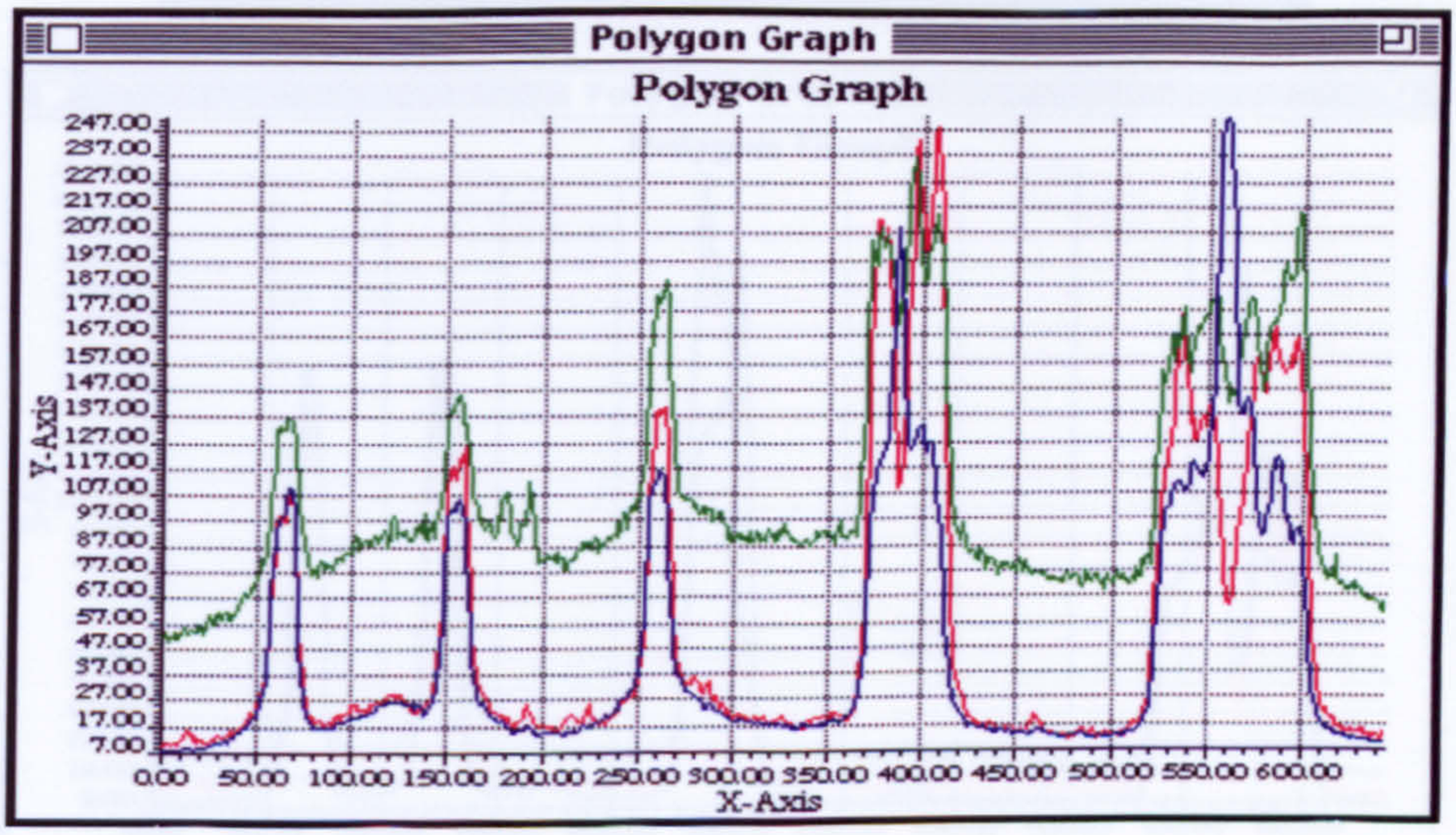

Figure 4.10 – Determination of background fluorescence by image analysis. The image above represents a typical metaphase from a failed CGH hybridization. The image demonstrates a high level of background staining due to poor hybridization of the green probe and subsequent lengthy automatic exposure for the green plane. Using the IP Lab image analysis package a line was drawn on the image randomly crossing both chromosomes and spaces in between. The graph below presents fluorescence intensities (Y axis) for the three fluorochromes along the length of the line (X axis) (Green – Test DNA; Red – Reference DNA; Blue – DAPI counterstain). Note the high level of fluorescence for the green plane in the spaces between chromosomes.

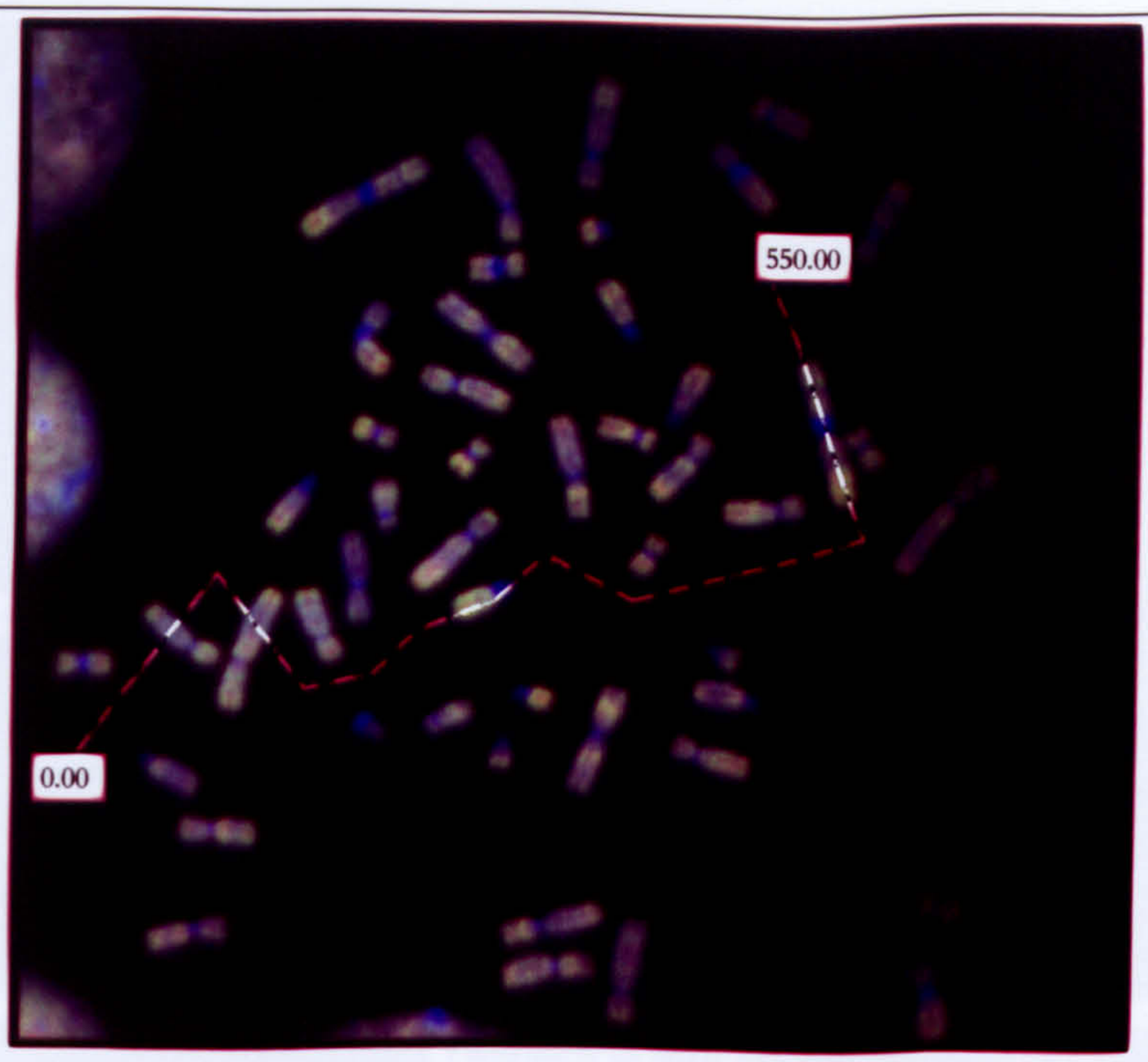

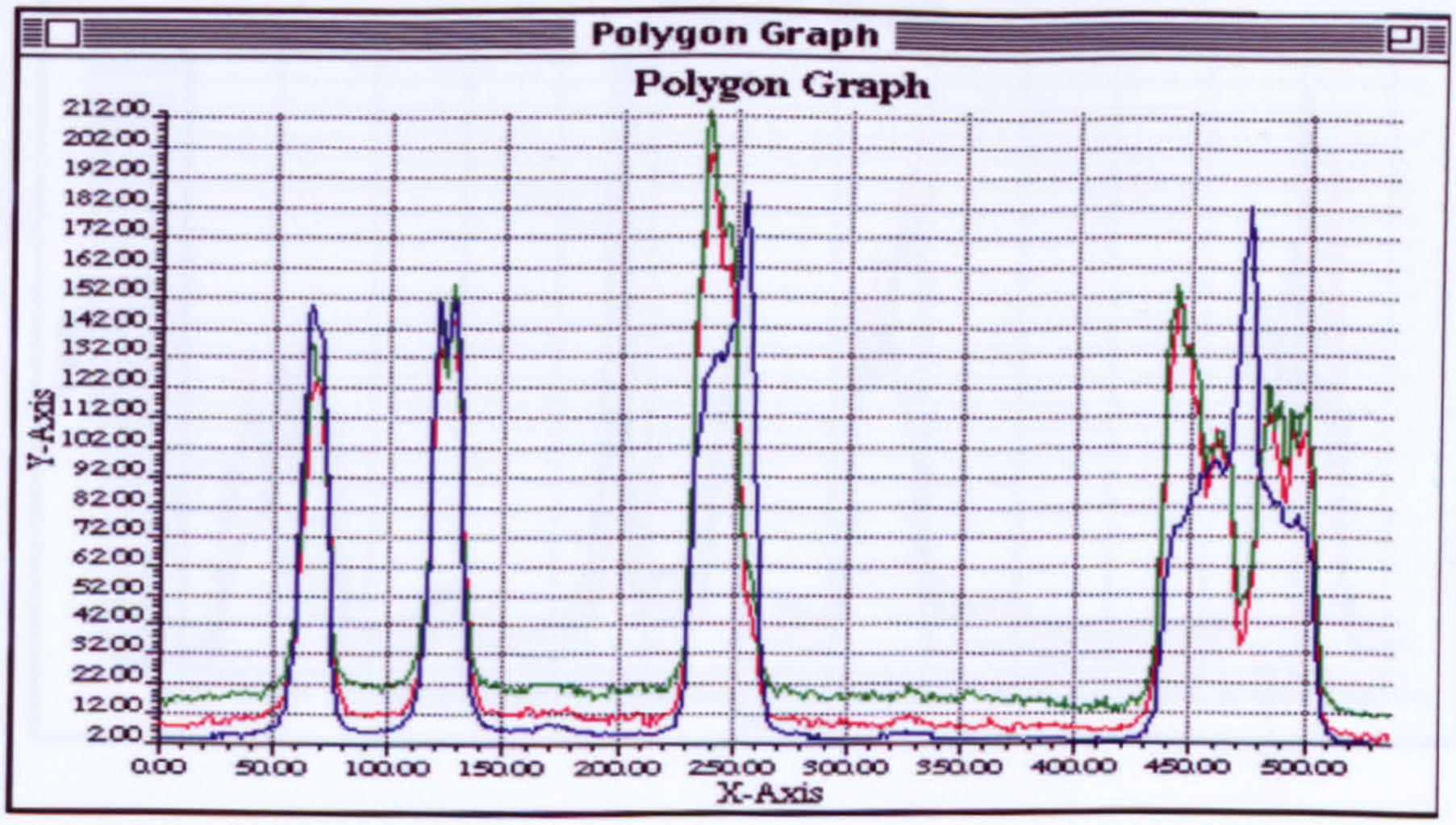

Figure 4.11 – Determination of background fluorescence using image analysis. The image above represents a typical metaphase from a successful CGH hybridization. The image was processed using the IP Lab image analysis package in the same way as Figure 4.10 (Green – Test DNA; Red – Reference DNA; Blue – DAPI counterstain). Note the low levels of fluorescence for all three planes in the space between the chromosomes.

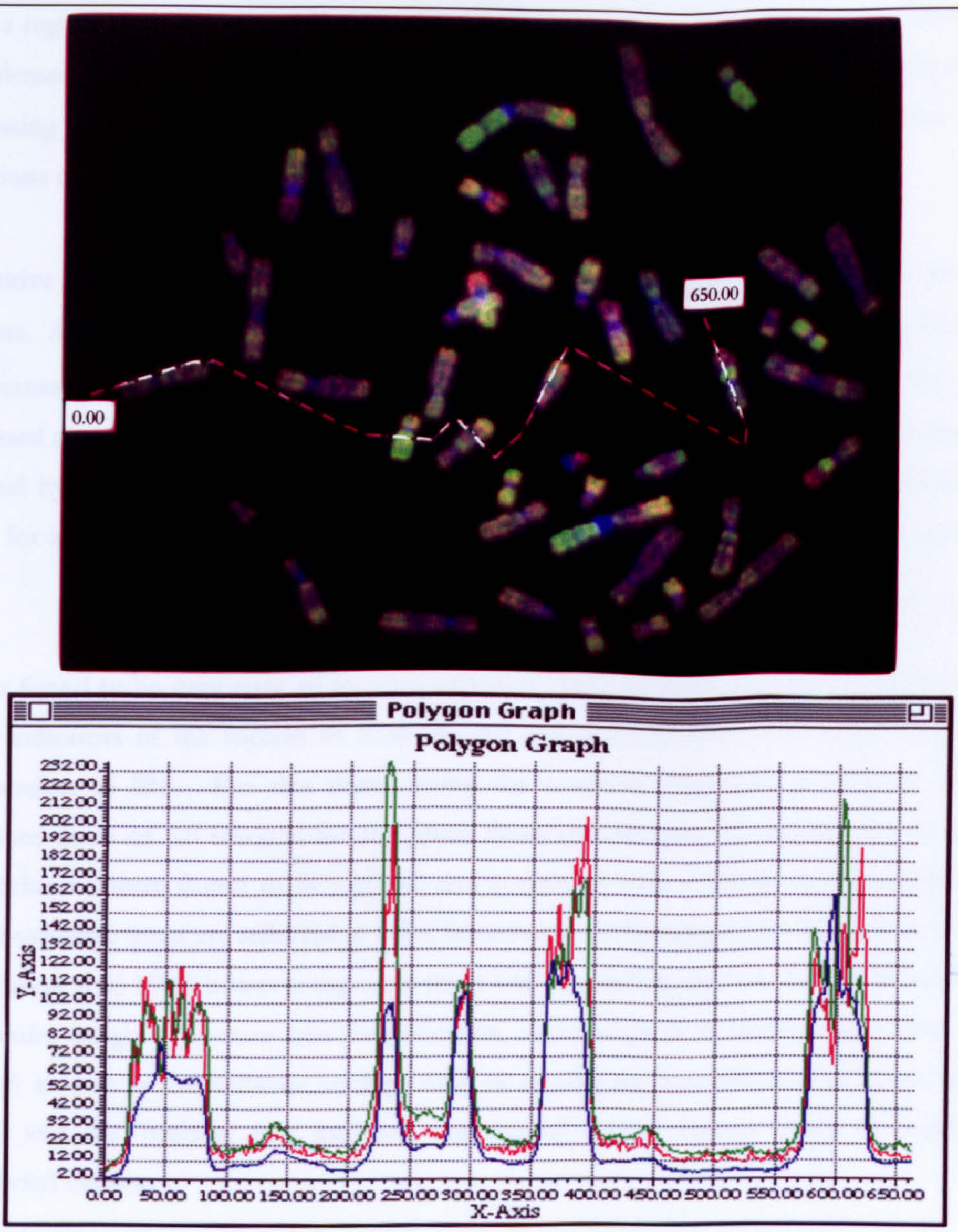

Figure 4.12 – Determination of background fluorescence using image analysis. The image above depicts a typical image obtained from a control CGH experiment using the MPE600 control DNA. The image was processed using the IP Lab image analysis software in the same way as for Figures 4.10 and 4.11 (Green – Test DNA; Red – Reference DNA; Blue – DAPI counterstain). The image demonstrates low background staining and fluorescent intensity variations corresponding to copy number changes in the DNA sample.

from a region of chromosome amplified in a particular tumour will be available to bind to IRS elements throughout the metaphase chromosomes adding 'noise' to the system and decreasing sensitivity. By removing these repeated (i.e. non-unique) sequences, true FR variations in the regions of interest can be assessed.

Repetitive sequences were blocked by adding 30μg of unlabelled COT-1 to the probe mixture. Although the COT-1 is always in vast excess, it was found that the amount had to be increased from that recommended in the protocol (10μg) to compensate for the increased amounts of labelled test and reference probes used in the probe mix to generate optimal hybridizations. After denaturation of the probe, the mixture was incubated at 37°C for at least 5 minutes to allow the COT-1 to bind and suppress the IRS in the probe mix.

It was found to be important to monitor exposure times as these were also shown to be good indicators of the success of both the red and green probe hybridization and the suppression of IRS. For this thesis (using the hardware described in Section 3.8.4) exposure times of <8 seconds for the green fluorochrome and <5 seconds for the red fluorochrome were found to be optimal and correlated with a successful hybridization. These exposure times are reflected in other laboratories performing CGH (Piper *et al*, 1995; Du Manoir *et al*, 1995) however exposure times vary depending on both the hardware used to acquire images (objective lens magnification, microscope bulb intensity and filter set quality) as well as the software settings such as signal gain (amplification of actual light levels) and the 'binning' (the grouping together of several camera pixels to enhance sensitivity) chosen.

One of the criteria for accepting a CGH image is low fluorescence at the centromeric and heterochromatic regions of the chromosomes, indicating satisfactory blocking of these regions meaning that such sequences of DNA throughout the genome are also sufficiently blocked. Two different situations were encountered resulting in high levels of fluorescence at the centromeric and heterochromatic regions. One commonly occurring scenario was the observation of unacceptably low red and green SB ratios. This was indicative of a failure in the hybridization conditions resulting in little or no staining of both red and green probes resulting in long automatic exposure times. The actual fluorescence captured by the system (and subsequently pseudo-coloured) was thought to be non-specific and due to the bleed-through of DAPI fluorescence during long exposure times (due to the spectral limitations of the triple band-pass filter block employed). This situation is important to

distinguish from hybridizations with insufficient blocking of IRS elements. The important difference between the two scenarios is that experiments in which IRS suppression failed were characterised by low background fluorescence (as the actual hybridization was successful), whereas experiments in which centromeric fluorescence was an artefact of long exposure times were characterised by very high levels of background fluorescence (as there was little if any hybridization on the metaphase chromosomes). Inadequate suppression was rectified by increasing the length of time the probe was incubated at 37°C to improve binding to the IRS elements or by increasing the amount of Cot-1 included in the probe mix. Both scenarios resulted in experiments that had to be discarded and repeated, but the technical reason for the failure was different.

4.6.5 Assessment of 95% confidence limits

The final criterion used to assess the success/quality of the hybridization was the 'tightness' of the 95% confidence limits of the mean ratio profile. Inconsistencies in the range of 95% confidence limits were indicative of both noise in the experiment and misclassification of karyotyped chromosomes.

4.6.6 Repeated CGH hybridizations

Figures 4.13 to 4.16 depict CGH experiments of two DNA samples that were repeated due to the initial failure of each sample. The first attempts (Figures 4.13 and 4.15) resulted in images that failed to satisfy the criteria mentioned above of a high SB ratio and low levels of fluorescence at the centromeric and heterochromatic regions of the chromosomes. The final ratio profiles of the two failed experiments demonstrate wide 95% confidence intervals and several false gains on the longer chromosomes (e.g. chromosomes 1-5). In addition, the profiles demonstrate a characteristic 'bow' shape with low FR at the telomeres and higher FR at the middle of the chromosomes. These two experiments highlight the importance of rigorously assessing the quality of each hybridization using the criteria detailed in Sections 4.6.4-4.6.5. Importantly, two failed experiments are depicted to highlight the similarity of the failed experiments. Both depict a common pattern of false gain and loss consistently seen in failed CGH hybridizations. This characteristic pattern is thought to reflect the DAPI banding of the chromosomes bleeding through into the red and green colour planes due to reasons mentioned above. If CGH experiments are not performed to a high degree of accuracy, and each step is not monitored for quality, such a pattern could incorrectly be interpreted as a consistent pattern of genetic abnormalities in the cells under analysis.

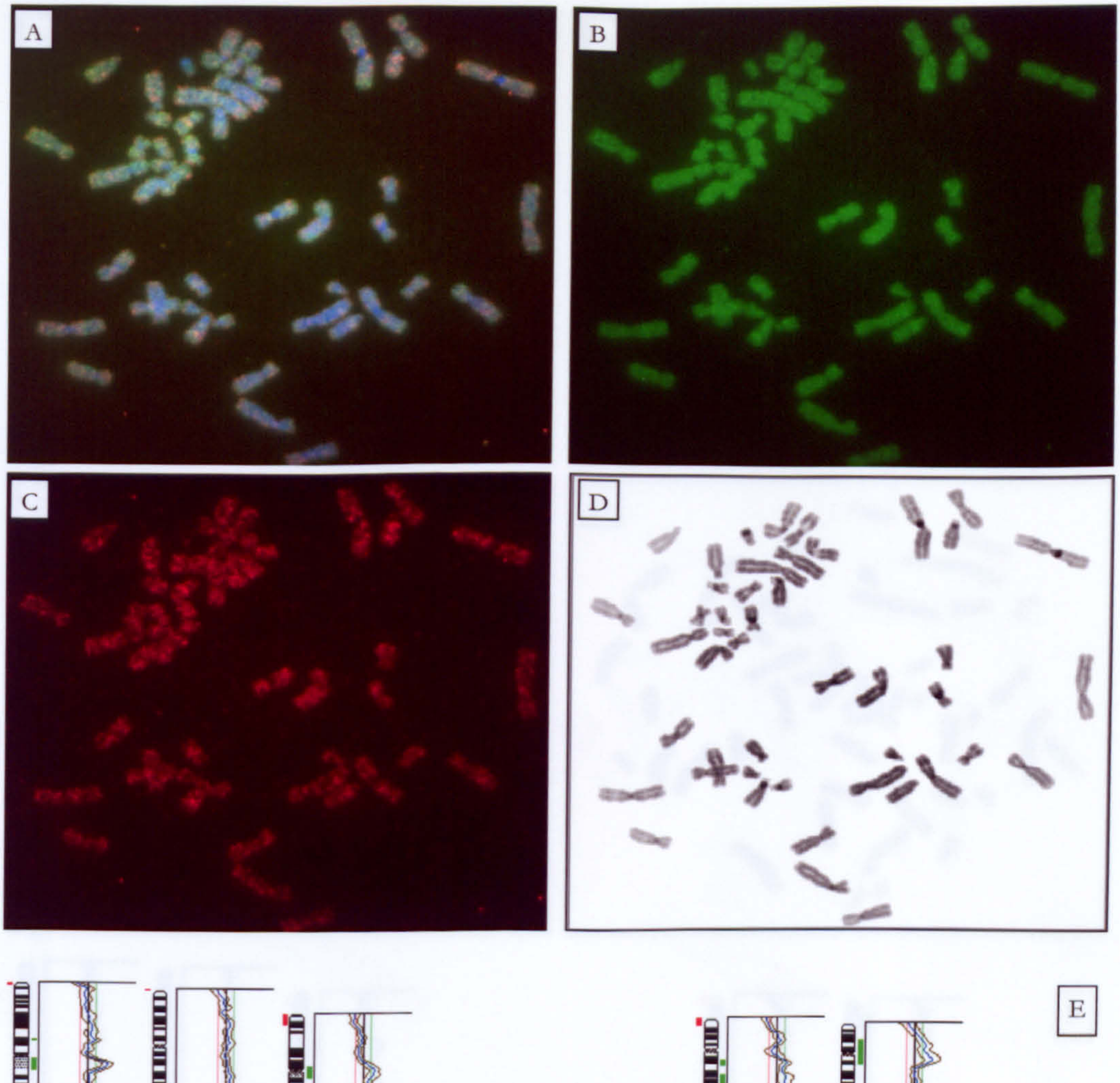

Figure 4.13 – Repeated CGH experiments – initial failed CGH. The composite image (A) is depicted along with individual green (B) and red (C) fluorescent images. The counterstained chromosomes are also shown (D). The fluorescence in the individual colour planes is faint, with a 'washed out' appearance characteristic of non-specific fluorescence generated during automatic exposure of poorly stained specimens. The ratio profile for this experiment (E) (n=8 metaphases) demonstrates wide 95% confidence limits and regions of false copy number change (most notable along 4q). This experiment failed to satisfy the criteria for a successful CGH described in Section 4.6.

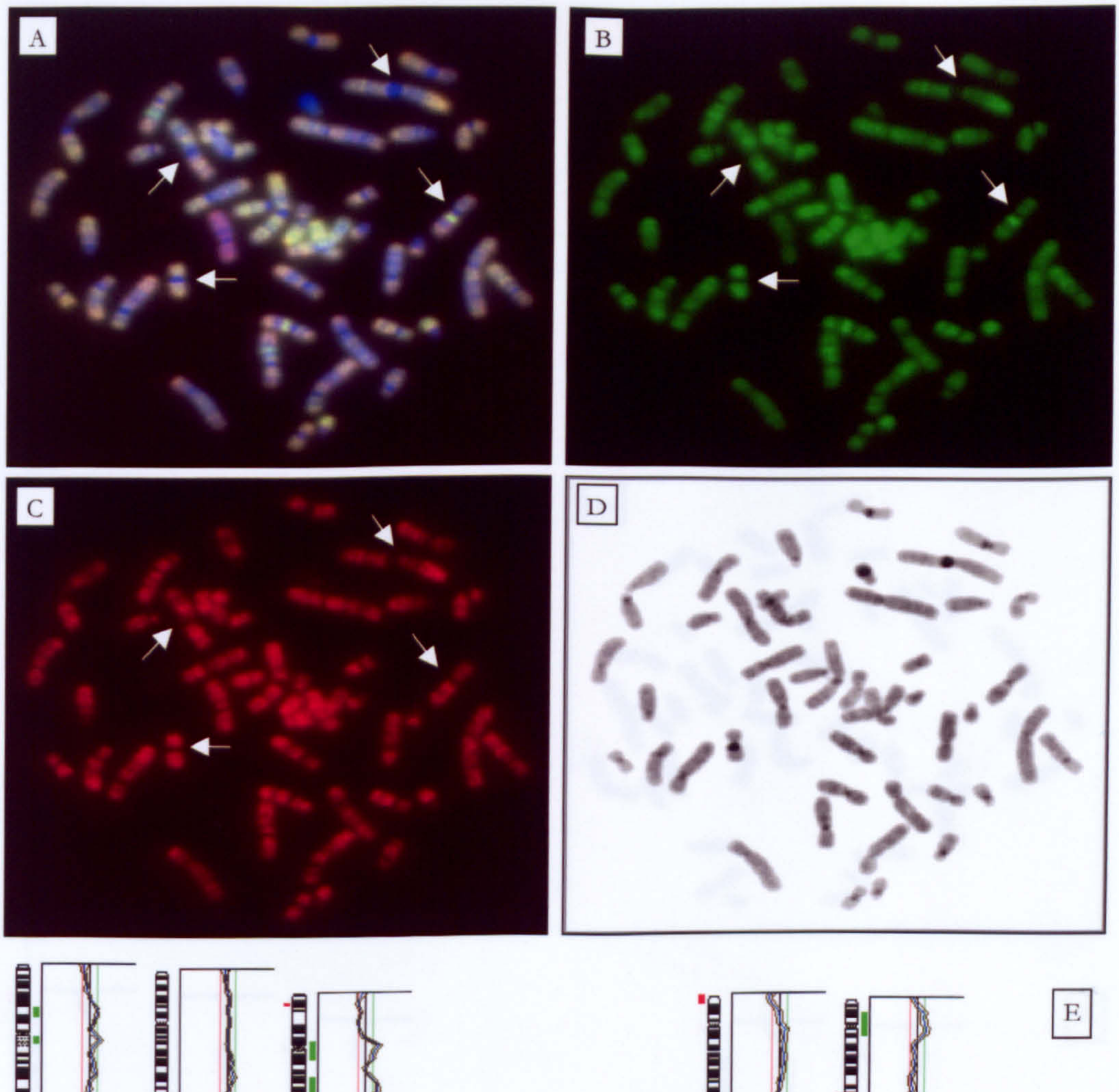

Figure 4.14 – Repeated CGH experiments – repeated successful CGH. These images depict a repeat of the failed hybridization shown in Figure 4.13. This experiment satisfied the criteria for an acceptable CGH experiment. Individual fluorescent images (B and C) can be seen to be brighter than those of Figure 4.13 and demonstrate a specific staining pattern, indicated by the absence of fluorescence at the chromosome centromeres (white arrows). The ratio profile generated from this experiment (E) (n=8 metaphases) demonstrates much tighter 95% confidence limits and the false gain on 4q is absent.

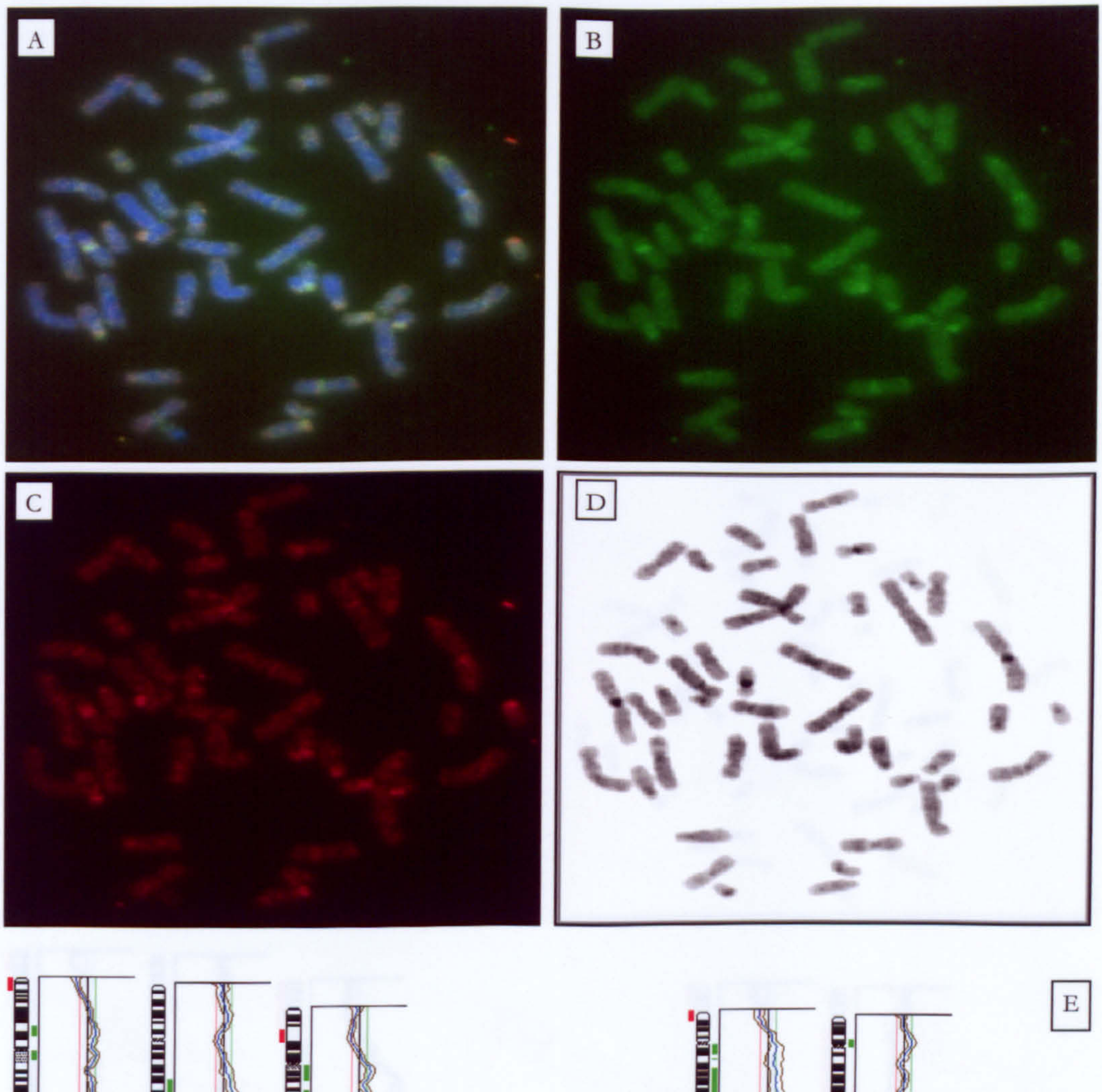

Figure 4.15 – Repeated CGH experiments – initial failed CGH. This Figure represents another CGH experiment for which the initial hybridization failed to satisfy the criteria for an acceptable hybridization. Staining is again seen to be faint with the composite image (A) demonstrating 'washed out' blue chromosomes indicative of faint non-specific fluorescence due to prolonged automatic exposure of a faintly staining metaphase. The average ratio profile (E) (n=8 metaphases) appears similar to that of Figure 4.13 with wide 95% confidence limits and false gains (most notable on 4q).

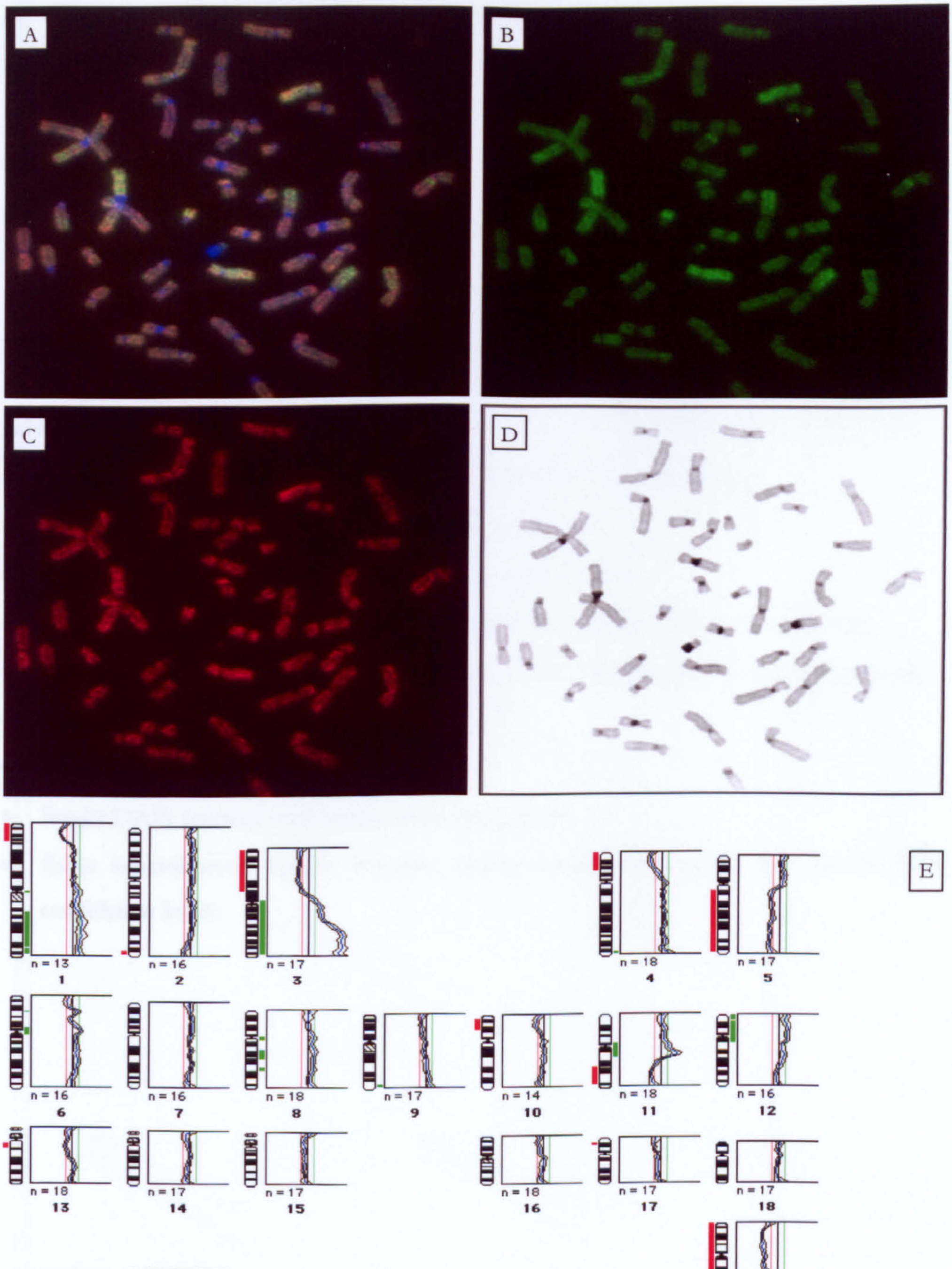

Figure 4.16 – Repeated CGH experiments – repeated successful CGH. These images depict a repeat of the failed hybridization shown in Figure 4.15. This experiment satisfied the criteria for an acceptable CGH experiment. Individual fluorescent images (B and C) can be seen to be brighter than those of Figure 4.15 and regions of colour imbalance are clearly visible. The ratio profile generated from this experiment (E) (n=9 metaphases) demonstrates much tighter 95% confidence limits and the false gain on 4q is absent. In addition, regions of copy number loss (such as 5q and 10p) are present which are absent in Figure 4.13.

4.7 Summary

Overall, CGH proved to be a challenging technique to establish and optimise. Many experiments had to be repeated in order to ensure that the data generated were of optimal quality. The demanding nature of CGH and the lack of standardisation of data analysis have been recognised by many other authors (Karhu *et al*, 1997; James *et al*, 1999, Barth *et al*, 2000). The aim of this chapter was to optimise the CGH experimental procedure and to generate a set of objective criteria for the evaluation and analysis of CGH images. These criteria were applied to all CGH experiments included in this thesis, and are summarised below.

- Generation of labelled fragments of DNA 300-3000 base pairs in size.
- Matching of test and reference labelled fragment sizes.
- Complete resuspension of probe mix before hybridization
- Adequate denaturation of metaphase chromosomes without loss of morphology.
- Satisfactory blocking of regions of repetitive DNA (centromeric, heterochromatin etc).
- Low background fluorescence.
- Smooth and even hybridization signals.
- Bright DAPI staining with strong contrasting bands.
- Even hybridization signals between chromosome homologues and narrow 95% confidence limits.

Chapter 5

Genetic Analysis of Head and Neck Squamous Cell Carcinoma and Surrounding Mucosa

5.1 Introduction

The identification of early events in the multistep tumourigenesis sequence of HNSCC would be invaluable both for predicting and assessing the success of surgical resections and monitoring patients for recurrence at an early stage of the disease. Identification of a genetic aberration using targeted and sensitive molecular technologies e.g. FISH and PCR-based techniques, have major methodological limitations in that they require prior knowledge of the candidate genetic loci or gene product to be examined. Utilizing the 'global screening' facet of comparative genomic hybridization, samples of tissue from primary HNSCC patients were examined for the presence of chromosomal abnormalities. Simultaneous analysis of the entire genome for chromosomal gains and losses both in samples of tumour tissue as well as samples of histologically normal epithelia was performed to address the question of 'field change' and to investigate whether or not chromosomal abnormalities can be detected.

5.2 Materials and Methods

5.2.1 Patient details

19 sequentially presenting patients undergoing composite resections for tumours of the oral cavity and oropharynx, or total laryngectomy with or without partial pharyngectomy were included in this study. Hull and East Yorkshire local ethical committee approval was granted for the study and informed consent was obtained from all patients. A sample of the primary tumour was removed directly adjacent to the tumour sent for histological assessment and 5mm biopsy sized specimens of macroscopically normal epithelia were collected from 1 cm and 5cm away from the superior macroscopic margin, running superiorly from the tumour mass. Care was taken when taking the 1cm and 5cm distant biopsies to ensure that minimal underlying submucosal tissue was included. All specimens were snap-frozen in theatre and stored at -80°C until analysis. Representative sections of the distant samples were stained with haematoxylin and eosin (H&E) to confirm the presence of epithelial tissue, as well as to look for signs of dysplasia or tumour. Figure 5.1 demonstrates the histological appearance of representative sections of distant mucosa stained by H&E.

5.2.2 CGH

DNA was extracted from all samples of tissue as described in Section 3.3 and CGH experiments performed as described in Sections 3.6-3.8. Table 5.1 details the clinical characteristics of the 19 patients included in the study. Approximately 30% of all CGH experiments were repeated to confirm the data generated (five primary tumour specimens, seven 1cm mucosa specimens and six 5cm mucosa specimens).

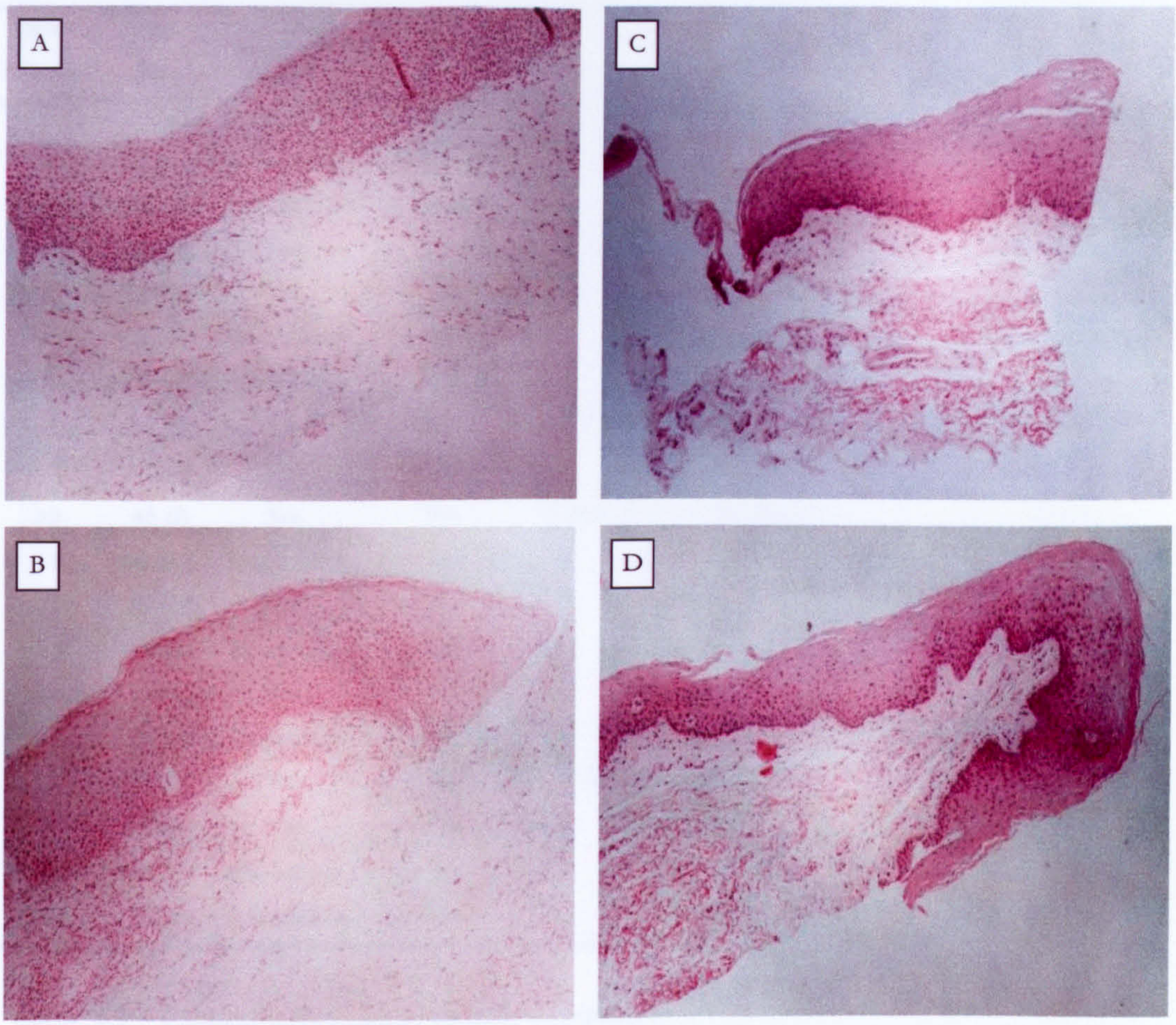

Figure 5.1 – Haematoxylin and Eosin stained sections of mucosal specimens

H&E stained sections of mucosal tissue taken from 1cm (A and C) and 5cm (B and D) distant from the site of the primary tumour. Specimens from two representative patients (A & B; C & D) are shown. When specimens were removed, care was taken to include as little of the underlying connective tissue as possible. Magnification x400.

Patient Number	Age (Sex)	Smoking status	Radiotherapy	Primary Site	Staging	Pathology (Differentiation)
1	78 (m)	Ex-smoker	No	Larynx	T_3N_1	Moderate
2	74 (m)	Ex-smoker	No	Larynx	T_2N_0	Moderate
3	57 (f)	Yes	Yes	Tongue	T_3N_1	Well
4	56 (m)	Yes	No	Pyriform fossa	T_4N_{2a}	Poor
5	51 (m)	Yes	No	Larynx	T_4N_{2a}	Poor
6	72 (f)	Ex-smoker	No	Larynx	T_2N_0	Well
7	59 (m)	Ex-smoker	No	Tonsil	T_3N_{2b}	Poor
8	56 (f)	Yes	No	Tonsil/tongue base	T_3N_1	Undifferentiated
9	64 (m)	Yes	Yes	Larynx	T_4N_0	Moderate
10	45 (f)	Yes	Yes	Tonsil/Retromolar trigone	T_2N_1	Poor
11	64 (m)	Ex-smoker	Yes	Larynx	T_2N_1	Moderate
12	81 (m)	Yes	Yes	Larynx	$T_{1a}N_0$	Well
13	68 (m)	Ex-smoker	No	Larynx	T_4N_0	Poor
14	72 (m)	Yes	Yes	Larynx	T_3N_{2c}	Moderate
15	73 (m)	Ex-smoker	No	Larynx	T_2N_0	Well
16	75 (m)	Yes	No	Retromolar trigone	T_3N_{2b}	Poor
17	67 (m)	Yes	Yes	Post Cricoid	T_4N_0	Moderate
18	66 (m)	Ex-smoker	No	Oral Cavity	T_4N_{2b}	Moderate
19	78 (m)	Ex-smoker	Yes	Larynx	T_2N_0	Good/Moderate

Table 5.1 – Clinicopathological details of patients

5.3 Results

5.3.1 Histological assessment.

All but 1 of the distant epithelial specimens were confirmed as being histologically normal. An area of carcinoma *in situ* was seen in the one exception, however this accounted for only a minority of the mucosal tissue (~5%). All histological examinations were performed by Dr A MacDonald, Consultant Pathologist, Department of Pathology, Hull & East Yorkshire Hospital. Examination of the pathological specimen taken directly adjacent to the tumour biopsies indicated no significant non-tumour cell infiltration (<30% non tumour cells) indicating the DNA extracted from the tumour biopsy was suitable for CGH analysis. Inflammation was detected in 9 of the distant biopsies although the infiltrating lymphocytes did not constitute a substantial portion (>30%) of the tissue indicating that the contaminating 'normal' cells would be unlikely to affect the final CGH result (James, 1999).

5.3.1 CGH analysis of surrounding mucosa

CGH failed to detect genetic aberrations in any of the specimens taken from 1cm and 5cm away from the primary site. Figures 5.2 to 5.4 depict example CGH profiles from both the tumour and mucosal samples distant from the tumour for three patients included in this study. All experiments were high quality CGH hybridizations and satisfied the criteria detailed in Chapter 4. The CGH copy number profile did exceed the thresholds for gain and loss of DNA at several chromosomal loci, however, these were all small regions confined to telomeric, centromeric and heterochromatic regions of the genome from which little reliable information can be gained due to the reasons described in Chapter 4. The 11 CGH experiments that were repeated confirmed the absence of genetic abnormalities in the distant mucosa.

5.3.2 CGH analysis of primary tumours

This study successfully identified DNA copy number changes in the biopsies of tumour tissue including several regions of frequent chromosomal gain and loss. Figure 5.5 summarises the genetic aberrations detected in the 19 tumour specimens. The mean number of gains and deletions did not differ significantly (mean gains and standard deviation per tumour = 5.2 [4.6] and mean and standard deviation deletions per tumour = 5.4 [4.3]). Analysis of the 19 primary tumours revealed a characteristic pattern of genetic aberrations detectable in HNSCC. Deletions on chromosome 3p were the most common abnormality detected occurring in 13/19 cases, with the entire chromosome arm being

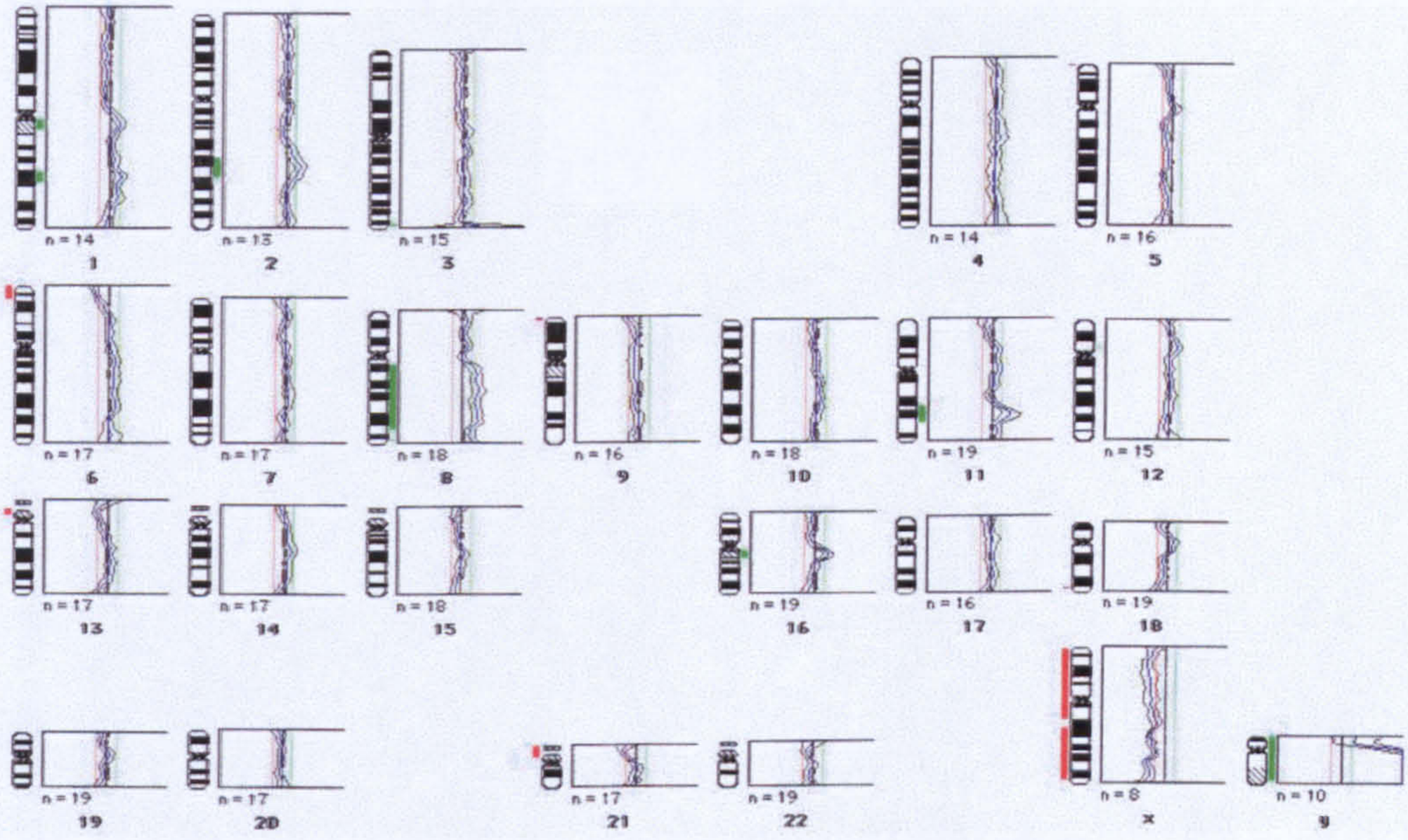

Figure 5.2a – Comparative genomic hybridization profile of a representative tumour biopsy taken from a patient with HNSCC. The mean CGH ratio profile is depicted in blue with 95% confidence limits displayed in brown. Vertical green bars to the right of the chromosome ideograms indicate gain of genetic material and vertical red bars to the left of the chromosome ideogram indicate loss of material. n = the number of chromosomes analysed. This tumour demonstrated few regions of copy number aberration.

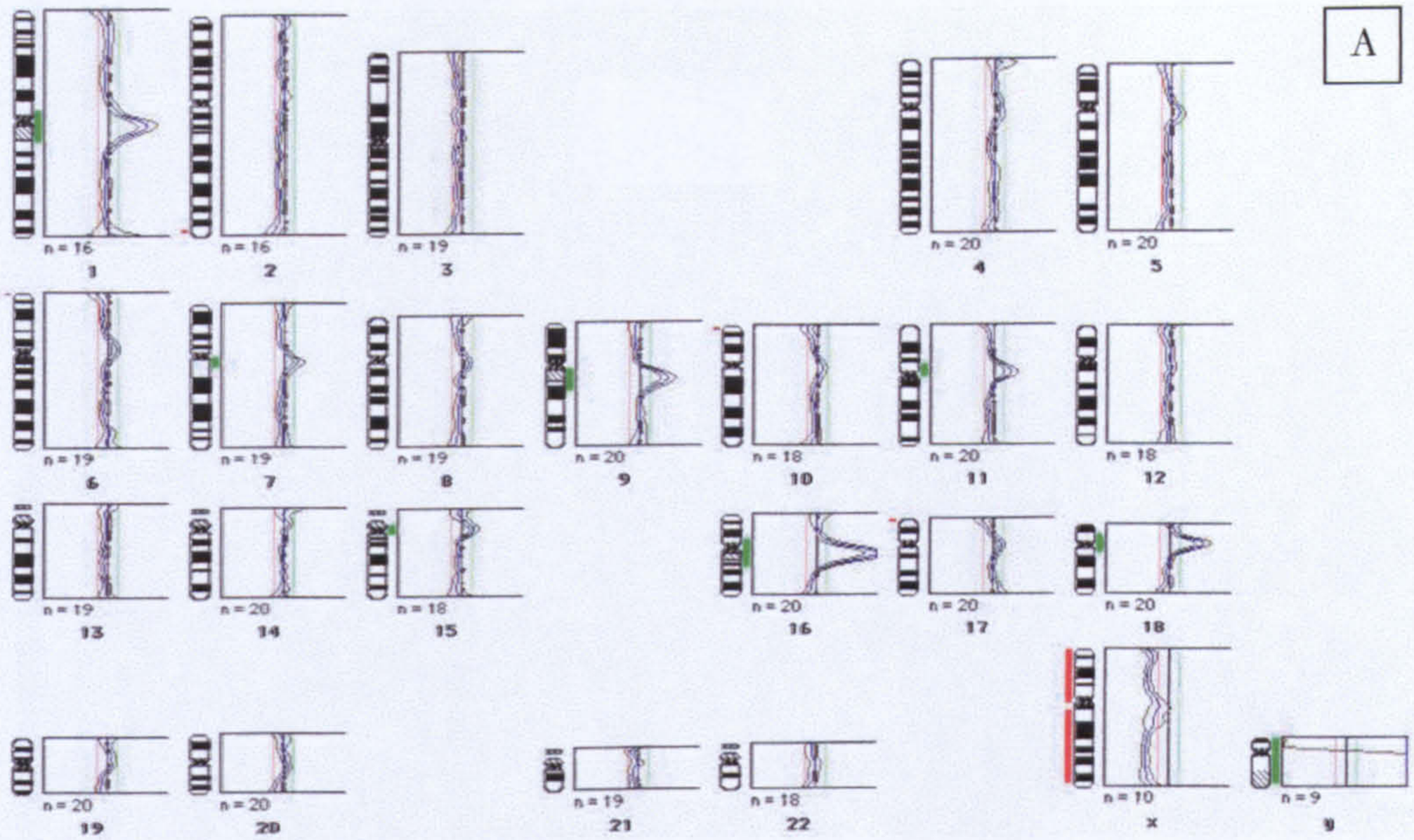

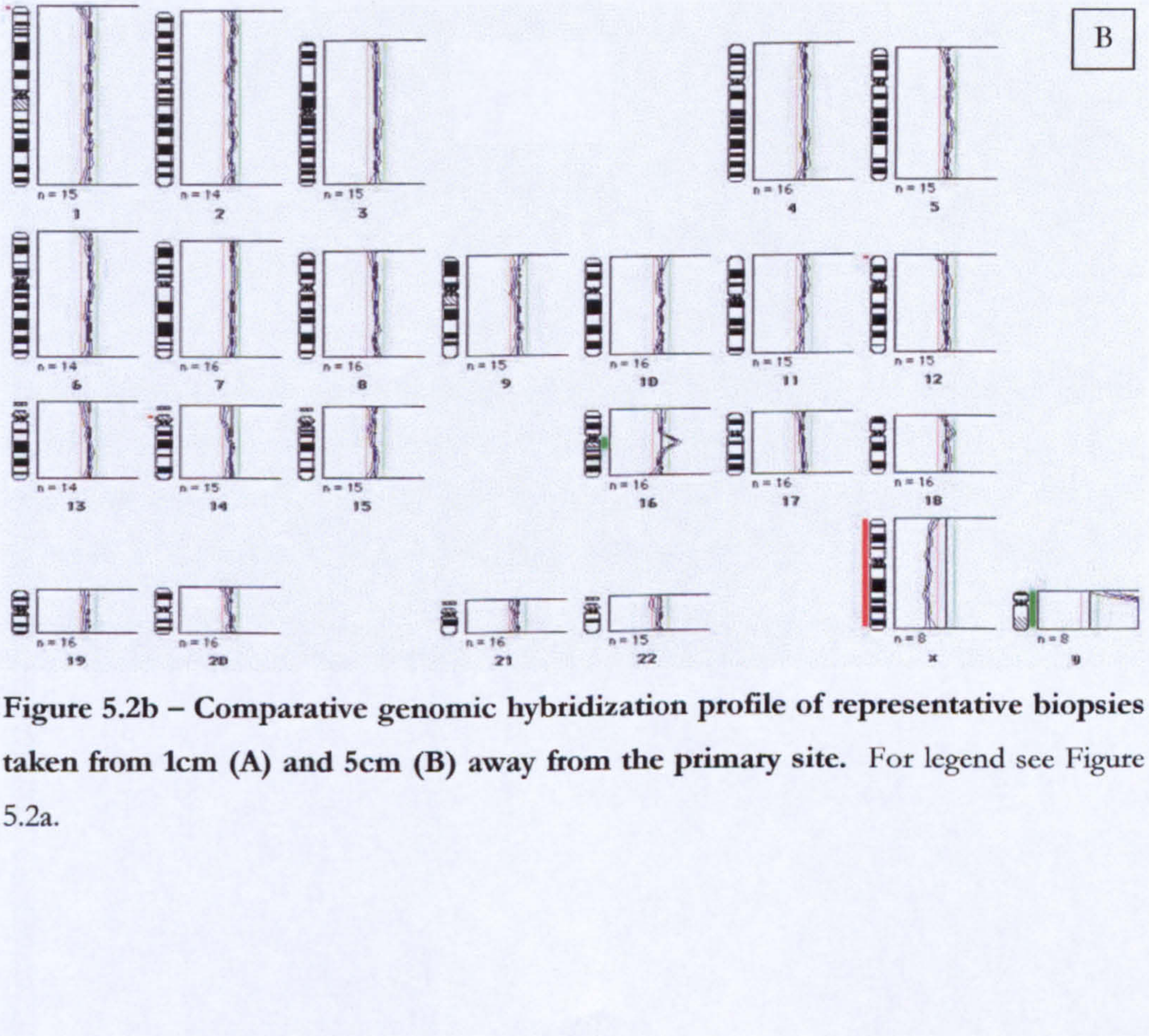

Figure 5.2b – Comparative genomic hybridization profile of representative biopsies taken from 1cm (A) and 5cm (B) away from the primary site. For legend see Figure 5.2a.

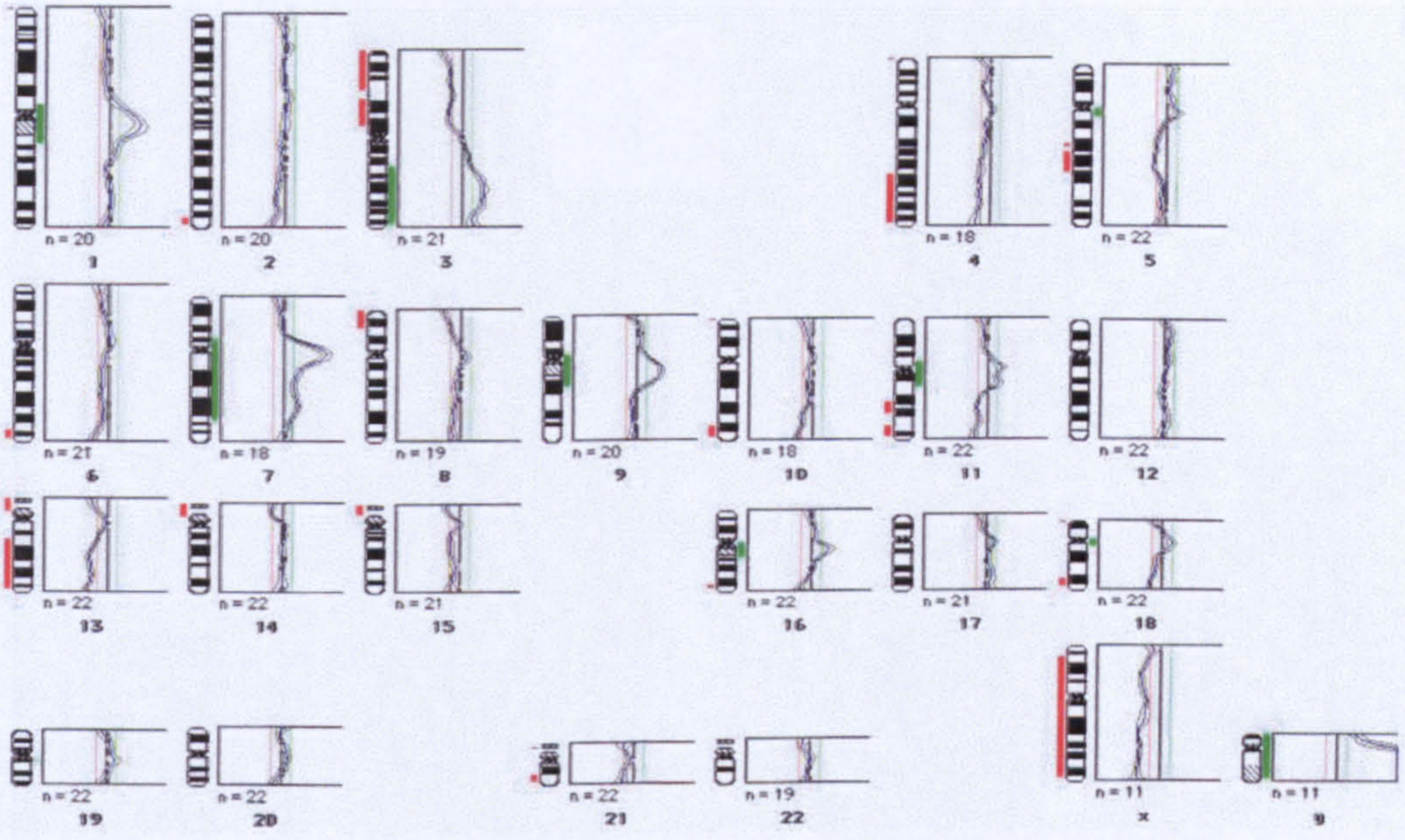

Figure 5.3a – Comparative genomic hybridization profile of a representative tumour biopsy taken from a patient with HNSCC. For legend see Figure 5.2a. This profile depicts an example of a tumour containing multiple loci of copy number aberration, none of which are detectable in the mucosa distant to the primary tumour (Figure 5.3b and 5.3c).

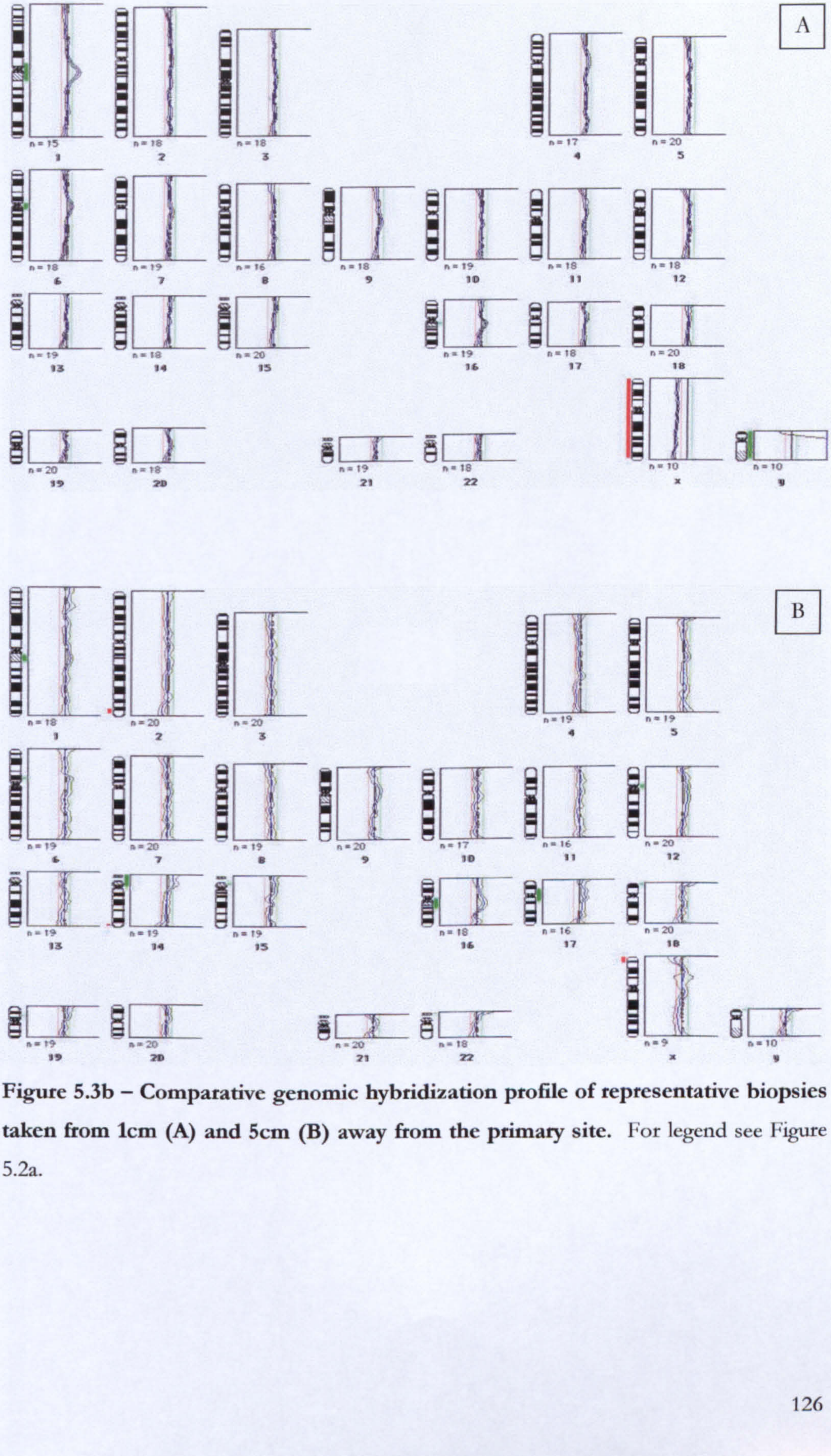

Figure 5.3b – Comparative genomic hybridization profile of representative biopsies taken from 1cm (A) and 5cm (B) away from the primary site. For legend see Figure 5.2a.

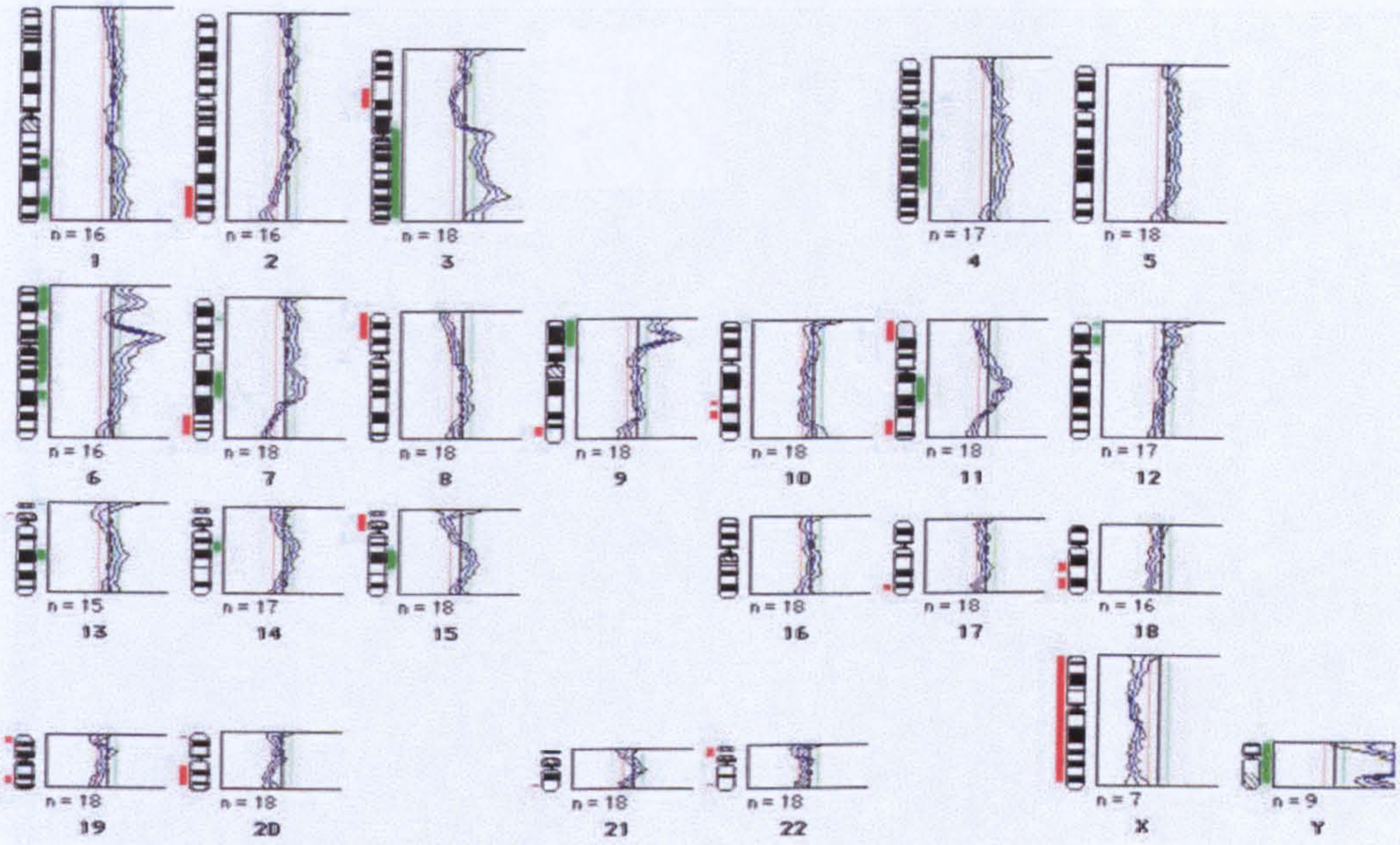

Figure 5.4a – Comparative genomic hybridization profile of a representative tumour biopsy taken from a patient with HNSCC. For legend see Figure 5.2a. Again this tumour contains multiple regions of copy number change which are absent in the distant samples of mucosa (Figure 5.4b and 5.4c).

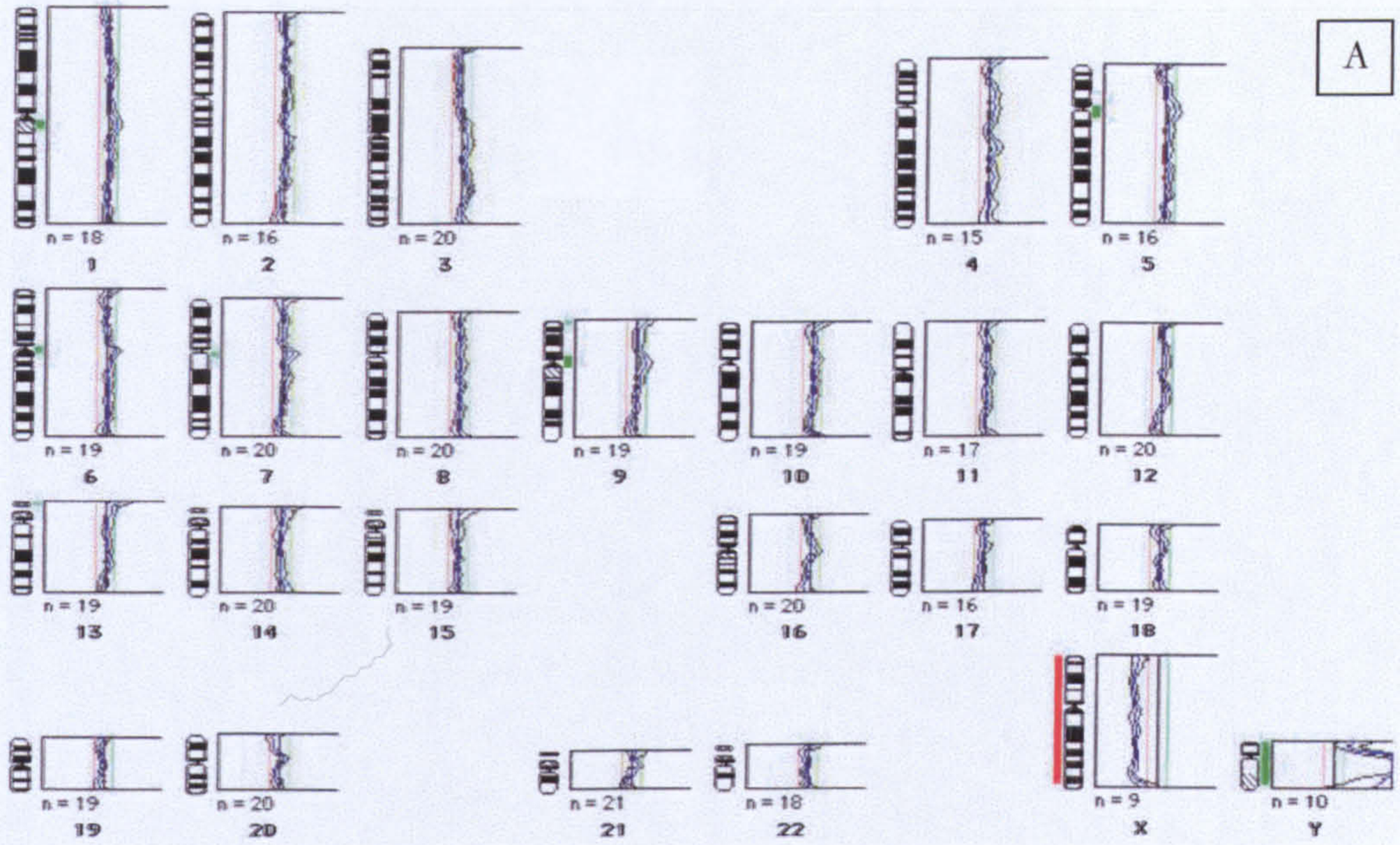

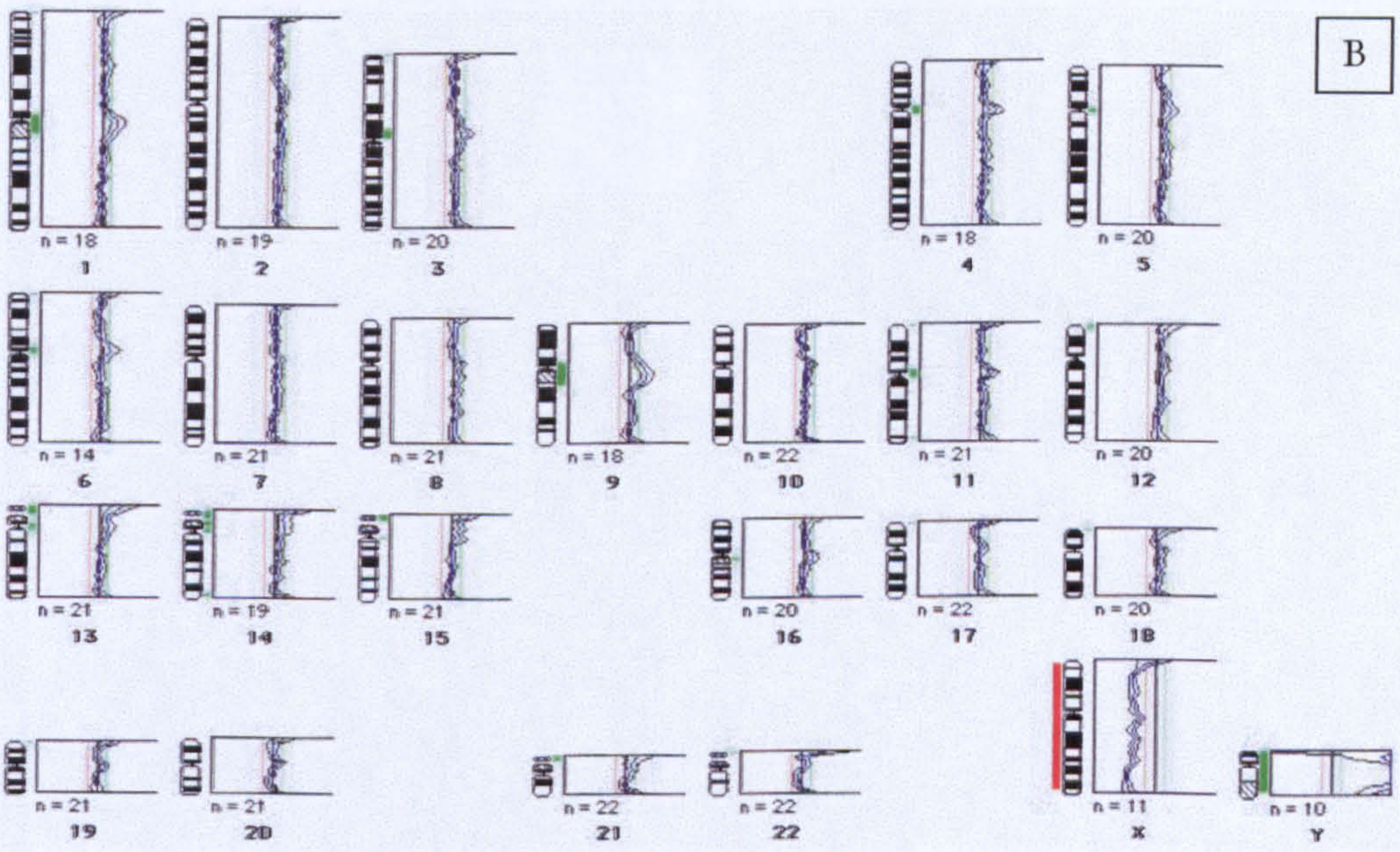

Figure 5.4b – Comparative genomic hybridization profile of representative biopsies taken from 1cm (A) and 5cm (B) away from the primary site. For legend see Figure 5.2a.

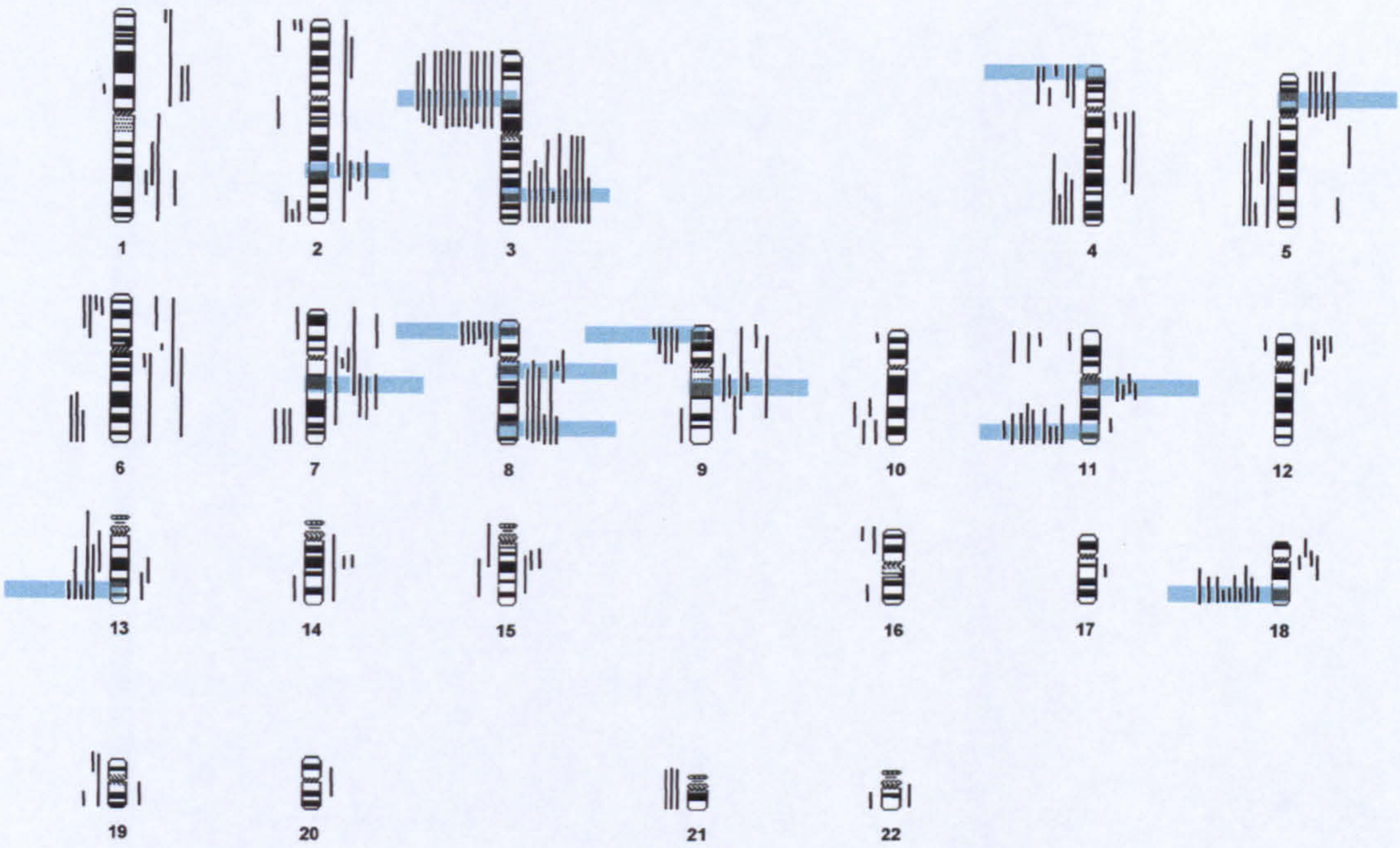

Figure 5.5 – Summary of the DNA copy number changes identified in all 19 primary tumours. Vertical bars to the right of the chromosome ideograms represent gain of genetic material and bars to the left indicate loss. Shaded regions highlight aberrations identified in at least 25% of tumours.

deleted in 10 cases. Similarly, gains on 3q were detected at a high frequency in 11/19 cases with simultaneous loss of material from the p arm occurring in tandem with gains on the q arm in 10/19 cases. Four such cases demonstrated loss of the entire p arm in tandem with gain of the entire q arm suggesting the formation of a 3q isochromosome as a mechanism for this imbalance. 11q was the next most frequently involved chromosome with deletions encompassing 11q23-qter occurring in 9/19 cases including 5/19 cases with simultaneous gain of material at the 11q13 locus, the location of the cell cycle stimulatory gene *prad1*. Other regions of loss included 9p2-pter (5/15), 18q21.2-qter (10/19), 8p21.1-qter (6/19), 13q32-qter (5/19), 4q31.3-qter (4/19) and 5q14-q23 (4/19). Regions frequently found to be gained included 8q23-q24.2 (6/19), 8q12-13 (5/19), 9q13-q23 (5/19), 5p11-p13(5/19) and 2q31-q32 (5/19).

5.4 Discussion

Numerous and diverse molecular studies have investigated the concept of field cancerization in patients with tumours of the UADT. Multiple tumours within an individual HNSCC patient have been demonstrated to share many genetic aberrations. However it is still unclear as to whether these shared aberrations represent early genetic events shared by many histologically normal cells within a field of cancerization or represent clonal markers indicating the migration of fully malignant clones from the original primary site. The majority of the literature concurs that molecular and genetic abnormalities can be detected in the mucosa surrounding primary tumours supporting the concept of a 'field of cancerization' in HNSCC. Several studies have demonstrated an increase in the frequency and spectrum of genetic aberrations in tandem with the degree of histological abnormality from normal mucosa; hyperplasia; mild, moderate and severe dysplasia through to squamous cell cancer. These include the progressive increase in LOH at several chromosomal loci (Califano *et al*, 1996; Lydiatt *et al*, 1997; Tabor *et al*, 2001), the increase in chromosomal polysomies (Hittelman *et al*, 1993; Voravud *et al*, 1993; Charuruks *et al*, 1996; Choi and Chung, 1996; Ai *et al*, 1999; Lenz *et al*, 2000; Kim *et al*, 2001; Shin *et al*, 2001), the increase in telomerase activity (Soria *et al*, 2000), the increase in p53 mutation (Shin *et al*, 2001), the increase in *EGFR* expression (Grandis and Tweardy, 1993; Shin *et al*, 1994), the increase in cellular proliferation (determined by PCNA measurement) (Shin *et al*, 1993) and the increase in *CyclinD1* gene amplification and protein over-expression (Rousseau *et al*, 2001). In order to evaluate CGH as a potential screening tool this study was designed to see whether abnormal cells could be identified by CGH within histologically normal mucosa.

CGH successfully identified common regions of chromosomal abnormality within the population of tumour specimens. Several regions of chromosomal gain and loss were detected at high frequencies, highlighting the non-random nature of these abnormalities. The regions identified in this study are in general agreement with other CGH studies on HNSCC (Bockmühl et al, 1998; Gebhart et al, 1998; Wolff et al, 1998; Bergamo et al, 2000; Bockmühl et al, 2000; Hermesen et al, 2001). CGH identified many genetic loci to which several known or putative oncogenes and tumour suppressor genes have been mapped confirming the importance of such regions in HNSCC tumourigenesis. This study indicated an important role for chromosome 3 in the tumourigenesis of HNSCC being the site for both the most frequent gain and loss identified. Potential candidate genes on 3p include the FHIT gene at 3p14 and the Von-Hippel Lindau (*VHL*) tumour suppressor gene 3p25-26. Allelic loss studies on chromosome 3p suggest that the *VHL* gene may not be the target gene at this region in HNSCC (Waber *et al*, 1996). However, the observation of frequent abnormalities in the *FHIT* gene in other studies does strongly suggest a role for this gene in HNSCC (Mao *et al*, 1996; Virgilio *et al*, 1996). Gain of material on 3q was the most frequently detected aberration and this region appears to harbour at least one oncogene important to HNSCC, as well as other cancers. Gains on 3q have been demonstrated at high frequency in other studies of HNSCC, oesophagus, lung, ovary, pancreas and uterus with the common region of gain 3q26-qter in all studies (Gebhart and Liehr, 2000). Despite the obvious importance of this region the crucial oncogene residing here still remains to be elucidated and definitive gene probe strategies will be required to identify the genes involved in HNSCC. The strongest candidate for the amplification on 3q is the *PIK3CA* gene, located at 3q26.3, which encodes the 110 KDa alpha catalytic sub-unit of phosphatidylinositol 3'-kinase (PI3-kinase; Volinia *et al*, 1994). The role of *PIK3CA* and gain of material on 3q in HNSCC is discussed in detail in Chapter 8.

CGH has also confirmed the importance of genes located at 11q13 to HNSCC. This region is frequently found to be amplified in HNSCC specimens and has been associated with poor prognosis (Callender *et al*, 1994; Akervall *et al*, 1995). Several potential oncogenes reside at this locus *(PRAD-1, HST1, INT2, EMS1* and *glutathione-S-tranferase-pi-1* (*GST-π-1*)). Several studies have attempted to elucidate which genes are the target of amplification of this region in HNSCC with amplification of *PRAD-1* and *EMS1* the most likely candidates (Rodrigo *et al*, 2000; Davidson *et al*, 1996).

The failure of CGH to detect any chromosomal abnormalities, assuming that abnormalities are present, has two non-exclusive explanations. Firstly, any genetic aberrations underlying

the field cancerization phenomenon may be below the resolution of CGH (10-20 Mb). For example point mutations and small deletions will not be detected by CGH. Secondly, abnormal cells that make up the field of cancerization may only constitute a minority of the mucosa. A recent FISH study (Ai *et al*, 1999) using a panel of DNA probes for 14 chromosomes identified chromosomal aneuploidy in clinically normal mucosa distant to oral cancer in 7/10 patients tested. This polysomy was detected in 5-20% of normal mucosal cells with copy number changes of chromosomes 3, 12, 15 and X being the most common. Choi and Chung (1996) similarly identified polysomies of chromosomes 7 and 17 in normal mucosa adjacent to a variety of HNSCC tumours using *in situ* hybridisation at a frequency of 6.61% (range 2.5-15%) and 7.13% (range 2.0-22%) respectively. These two studies suggest that a field of abnormal cells is present in the UADT of HNSCC patients, however the low frequency of polysomies detected indicate such a field comprises a minority of abnormal cells. The majority of normal cells when analysed by CGH would mask altered genomes present at a low frequency within the mucosa. Tissue micro-dissection by laser capture micro-dissection is one approach, which would allow sampling of individual cells. Wells *et al* (1999) have recently shown that high quality CGH is possible from a single cell by the application of degenerate oligonucleotide primed PCR, a method for the unbiased amplification of genomic DNA, generating sufficient DNA for a CGH hybridization. Such an approach would require multiple sampling and CGH experiments to ensure that abnormal cells, from the field of histologically normal mucosa, were analysed. Whilst the technical complexity and laborious nature of this approach would render it impractical for use as a screening method, it may identify genetic abnormalities that could then be assessed using simpler, more automated methods.

Based on the assumption that the most frequently detected abnormalities in pre-invasive HNSCC are likely to be amongst the earliest genetic changes, several groups have examined chromosomes 3p and 9p in normal mucosa. Lydiatt *et al* (1997) failed to identified LOH of 3p in 17 informative specimens of normal mucosa but did identify a high level (46%; n=13) of LOH at 9p21 (the site of *p16*). A similar finding was reported by Tabor *et al* (2001) with 36% (n=28) of patients demonstrating a field of histologically normal mucosa containing LOH at 9p. These studies provide further support for the presence of genetically altered fields of histologically normal mucosa.

As stated previously, the majority of the literature concurs that the UADT of HNSCC patients is characterised by areas of genetically altered cells occurring in the absence of histological change and that these cells presumably have a greater propensity for the

formation of second primary tumours. This highlights the limitations of conventional histopathological assessment of both tissue biopsies and more importantly, of tumour margins, after resection and indicates the need for the further characterisation of these early genetic abnormalities in order to develop novel and more sensitive diagnostic techniques. The second challenge, of significant clinical relevance, remains to establish whether these multiple primary tumours are of polyclonal or monoclonal origin. If tumours are polyclonal then the emphasis should be on prevention with immediate removal of the carcinogenic stimuli. A monoclonal origin would indicate the need for better markers for histological evaluation of tumour margins, of metastasis, and for the monitoring of patients with previously treated HNSCC.

A recent technological development in the methodology of CGH first described in 1998 by Kirchhoff *et al* (1998) may allow the higher level of resolution necessary in order to apply standard CGH to histologically normal mucosa. This modification in the analysis of CGH ratio profiles takes into account deviations from a ratio profile of 1.0 seen to occur at some chromosomal regions during normal : normal CGH experiments (e.g. the distal half of chromosome 1p). Kirchhoff performed a large scale series of normal : normal CGH experiments (n-33) to establish 99.5% confidence limits and determined a standard reference interval based on 17 of these normal CGH experiments. This standard reference interval was seen to be especially wide at profile areas where CGH measurements are known to be unreliable. By measuring mean ratio profiles and corresponding 99.5% confidence intervals for each test case and comparing with the standard reference intervals generated in normal experiments Kirchhoff was able to demonstrate deletions as small as 3 Mb. This is much lower than the often-quoted figure of 10-20Mb for conventional CGH using fixed reference thresholds (Kirchhoff *et al*, 1999). Interestingly, CGH using standard reference intervals claims to be able to detect aberrations present in as few as 20-30% of cells compared with standard CGH using fixed thresholds which requires ~70% abnormal cells. However the accuracy of this technique remains to be confirmed by multi-laboratory studies. A comparison of the analysis of CGH data using both Kirchhoff's data driven procedure and the conventional fixed reference thresholds was performed by Barth *et al.* This study evaluated the 2 methods by comparing the accuracy of detection of chromosomal imbalances characterised by the higher resolution technique of FISH analysis at selected chromosomal loci (Barth *et al*, 2000). The higher sensitivity of the data driven procedure was confirmed, however they identified a significantly higher fraction of false positive results concluding that the alternative procedure generates an unacceptably high portion of incorrectly scored chromosomal imbalances.

In conclusion, this study has shown that CGH is not suitable for screening histologically normal mucosa to detect genetic aberrations underlying the phenomenon of field cancerization. However, application of recent developments in the methodology of CGH combined with tissue microdissection may prove to yield informative information on genetic alterations present in histological mucosa surrounding HNSCC tumours, although analysis of these aberrations will need to be technically simple if they are to become a routine part of histological analysis.

Chapter 6

Genetic Comparison of Primary and Metastatic Head and Neck Squamous Cell Carcinoma

6.1 Introduction

The presence of nodal metastases is the single most important prognostic factor for HNSCC patients with survival rates decreasing by approximately 50% in node positive patients (O'Brien *et al*, 1986). Understanding the genetic events responsible for the process of metastasis is likely to have a major clinical impact. The lack of accurate criteria available to predict nodal metastasis causes many clinicians to treat the neck electively, allowing accurate staging and improved local control (Cachin *et al*, 1983). However, this results in many node negative patients undergoing unnecessary surgery. Therefore genetic markers predicting nodal involvement would be of benefit both in the management of patients at risk of local metastases and in reducing unnecessary surgery in pathologically node negative patients.

The progression of HNSCC from benign hyperplasia through to invasive cancer is associated with the accumulation of genetic aberrations (Califarno *et al*, 1996). Limited data are available on the relationship between the expression of tumour markers in primary and metastatic disease and little is known about the genetic aberrations associated with the metastatic event. Small-scale immunohistochemistry studies have demonstrated similar expression of p53, CyclinD1, myc, bcl-2, EGFR and Rb between primary and metastatic disease whilst decreased expression of cell adhesion molecules nm23 and Ep-cam has been demonstrated in lymph node metastases (Takes *et al*, 2001; Sauter *et al*, 1995). Discordance in p53 status between primary and metastatic HNSCC has also been demonstrated by mutation analysis (Kropveld *et al*, 1996).

HNSCC, like other solid tumours, is believed to demonstrate heterogeneity within the primary tumour mass, with multiple clones of differing phenotypic characteristics being present (Veltman *et al*, 1998). Therefore, in order to identify genetic aberrations associated with metastasis, CGH was performed directly on nodal metastases along with matched samples of primary tumour. Several studies have been published comparing chromosomal aberrations between primary breast, colon, lung and bladder tumours and their metastases however there have been no published data evaluating genetic aberrations in primary HNSCC and their regional metastases. The purpose of this study was firstly to asses whether lymph node metastases exhibit genetic aberrations at the same loci as their matched primary tumours and secondly, to try to identify genetic aberrations preferentially associated with the metastatic tumours.

6.2 Materials and Methods

6.2.1 Patient details

Tissue specimens taken from both the primary tumour and lymph node metastases (LNM) were obtained from 18 patients and snap frozen in theatre as described in Section 3.1. Diagnosis of the primary tumours was confirmed pathologically on specimens taken directly adjacent to the tissue used in this study. Lymph node specimens were obtained by removing a portion of lymph node, in a manner agreed with the Department of Pathology and nodal involvement was confirmed definitively by pathological assessment of the remainder of the node. All matched pairs of primary tumour and metastatic node were obtained during the same surgical procedure to prevent further genetic evolution. Table 6.1 details the clinicopathological details of the 18 patients included in this study. DNA was extracted from all specimens as described in Section 3.3 and CGH performed as described in Section 3.6-3.8.

6.2.2 Modified CGH: Direct hybridization of tumour DNA against nodal DNA

In order to confirm the aberrations detected in the individual CGH experiments a modified CGH protocol was performed on a small subset of 5 pairs of tumour and node specimens. Tumour DNA was labelled with SpectrumGreen™ fluorochrome and nodal DNA, from the same patient, was labelled with SpectrumRed™ fluorochrome (Section 3.3). For these confirmatory experiments the two DNA concentrations were equal. The two abnormal DNA samples were then directly hybridised under standard CGH conditions and analysed as normal. CGH performed in such a manner was designed to directly analyse the clonal relationship between primary tumours and LNM.

6.3 Results

6.3.1 Overview of copy number aberrations

CGH analysis successfully identified regions of copy number change in primary tumours and matched nodal metastases. Aberrations were identified in all samples with the exception of one patient for whom no gross chromosomal aberrations were detected in either the specimen of primary tumour or the metastatic lymph node. Overall a similar pattern of aberrations was seen in the two groups of tumour with frequent (>25% in both tumour sites) regions of DNA gain mapping to chromosomes 3q, 5p, 6q, 8q, 11q, and 12q. Losses of DNA were identified frequently on chromosomes 1p, 3p, 5q, 8p, 13q, and 17p. The regions of copy number change are consistent with those reported in Chapter 5.

Patient Number	Age at Operation (Sex)	Tumour Site	Stage	Differentiation
1	59 (m)	Left Pyriform Fossa	T_4N_{2b}	Poor
2	54 (m)	Right Pyriform Fossa	T_4N_3	Poor
3	55 (f)	Larynx	T_4N_{2c}	Poor
4	56 (m)	Right Pyriform Fossa	T_1N_2	Poor
5	55 (m)	Right Tonsil	T_4N_1	Moderate
6	66 (f)	Larynx	T_3N_1	Moderate
7	71 (m)	Larynx	T_2N_1	Well
8	51 (f)	Posterior Hypopharyngeal Wall	T_4N_{2b}	Poor
9	67 (m)	Right Pyriform Fossa	T_4N_1	Poor
10	52 (f)	Larynx	T_4N_{2c}	Poor
11	72 (m)	Larynx	T_4N_1	Moderate
13	57 (m)	Larynx	T_4N_1	Moderate
14	58 (m)	Left Tonsil	T_4N_2	Poor
33	66 (m)	Floor of Mouth	T_4N_{2b}	Moderate
41	68 (m)	Left Pyriform Fossa	T_3N_{2a}	Poor
48	55 (m)	Left Pyriform Fossa	T_3N_{2a}	Moderate
49	61 (m)	Larynx	T_3N_{2b}	Poor
50	48 (m)	Left Pyriform Fossa	T_3N_1	Moderate

Table 6.1 – Clinicopathological details of the 18 patients for which specimens of tumour and nodal metastases were available.

Figure 6.1 depicts the chromosomal loci of copy number changes in both the primary tumour and lymph node metastases (LNM).

Table 6.2 summarises the mean number of copy number aberrations (CNAs) detected in the primary and metastatic tumours. On average, there were 15.3 aberrations/primary tumour: 8.7 deletions (range 0-20) and 6.6 gains (range 0-13). Similar values were detected in the metastatic lymph nodes with a mean of 14.6 aberrations/metastatic tumour: 7.8 deletions (range 0-17) and 7.2 gains (range 0–12). Deletions were detected at a slightly higher frequency in both sets of samples however this was not statistically significant. Deletions were more common than gains in 12/18 primary tumours (66.7%) and 9/18 lymph node metastases (50%).

6.3.2 Modified CGH experiments

Modified CGH successfully confirmed the presence of different loci of copy number change in the sub-set of 5 samples chosen for confirmatory analysis. Interpretation of modified CGH experiments is more complex than standard CGH due to the competitive hybridization of two abnormal DNA samples. With primary tumour labelled in green, and nodal DNA labelled in red, an excess of green binding (colour ratio > 1.15) represents two possible scenarios:- a gain present in the primary tumour but absent in the nodal specimen or a deletion present in the node but not in the tumour. Alternatively, loss of genetic material within the primary tumour alone or gain of material in the node alone would both result in an excess of red binding (colour ratio <0.85). Hybridizing both samples against normal DNA definitively identified which of the possible scenarios the aberrations in the modified CGH experiments represented. This method proved to be powerful for confirming the presence of different aberrations within the matched samples of primary tumour and metastatic lymph node. Aberrations detected in both tumour and node CGH experiments were confirmed as no imbalance in the CGH colour ratio, whilst aberrations only detected in one tissue sample were confirmed as ratio imbalances.

The complete set of three CGH experiments (Tumour DNA vs. Normal DNA; LNM DNA vs. Normal DNA; Tumour DNA vs. LNM DNA) for two of the 5 tumour pairs are depicted in Figures 6.2 and 6.3. Figure 6.2 represents the data from patient 3 – a patient for whom the genetic aberrations in the primary tumour and LNM were remarkably consistent. Figure 6.2 (A) and (B) demonstrate that many aberrations were shared between the primary tumour and the LNM (deletions on 1p, 2p, 3p, 4q, 6p, 8p, 10p, 10q, 11q, 13q, 17p, 18q, 19p; gains on 1q, 3q, 5p, 8q, 11p, 11q). Additional regions of copy number

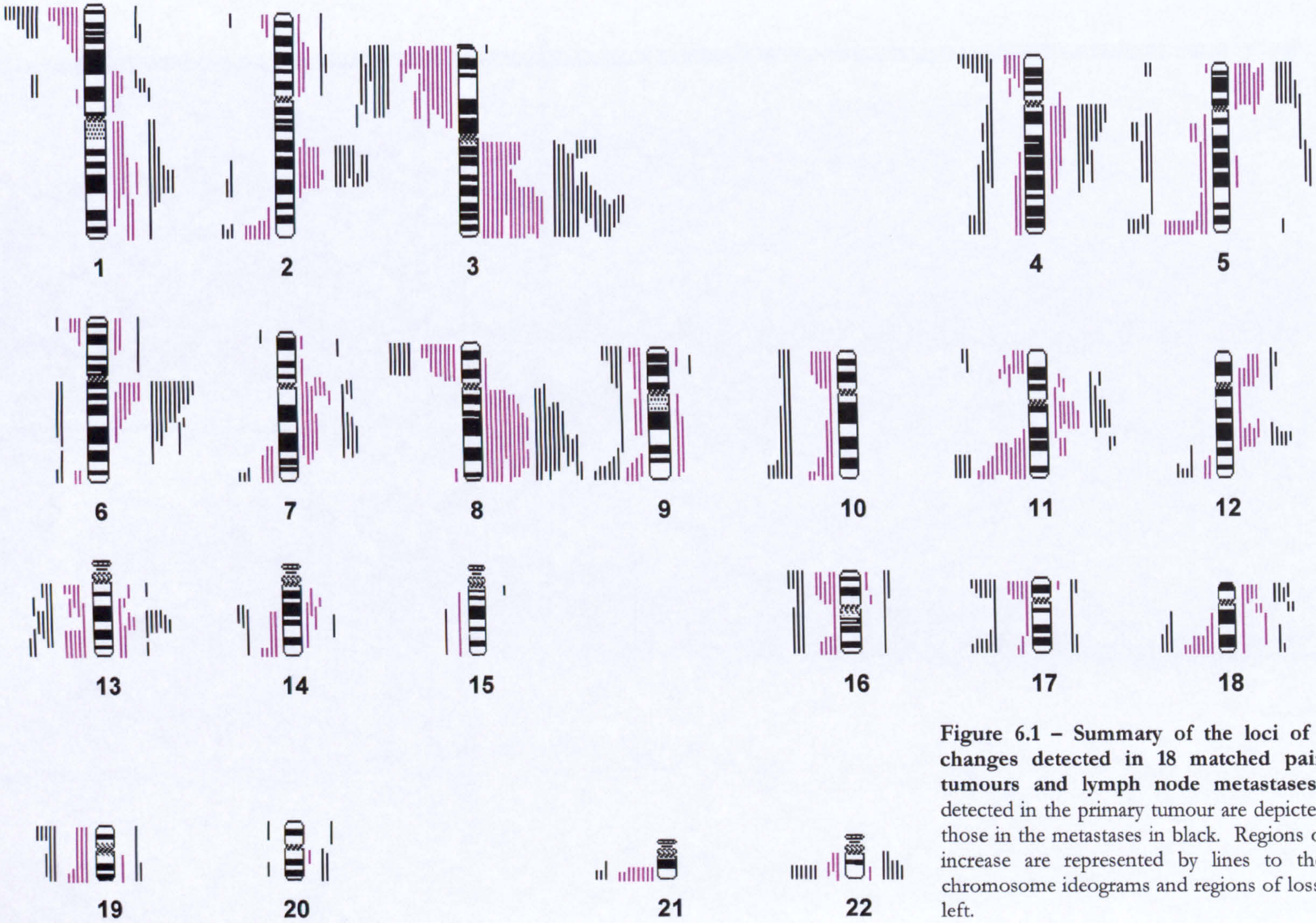

Figure 6.1 – Summary of the loci of copy number changes detected in 18 matched pairs of primary tumours and lymph node metastases. Aberrations detected in the primary tumour are depicted in purple and those in the metastases in black. Regions of copy number increase are represented by lines to the right of the chromosome ideograms and regions of loss by lines to the left.

Patient Number	Tumour CNA		LNM CNA		Total No. of CNA	
	Deletions	Gains	Deletions	Gains	Tumour	Node
1	9	6	13	9	15	21
2	11	4	3	3	15	7
3	18	5	17	7	23	22
4	4	1	2	5	5	3
5	2	5	7	7	7	12
6	11	9	8	12	20	17
7	10	2	6	8	12	8
8	9	8	5	6	17	13
9	8	4	6	5	12	10
10	8	13	8	6	21	21
11	5	9	3	11	14	12
13	0	0	0	0	0	0
14	6	2	10	7	8	12
33	9	10	12	8	19	22
41	13	8	12	10	21	20
48	1	13	0	7	14	13
49	20	12	19	11	32	31
50	13	8	10	8	21	18
Mean	8.7	6.6	7.8	7.2	15.3	14.6
Standard Deviation	5.2	3.9	5.3	2.9	7.3	7.5
Range	0-20	0-13	0-17	0-12	0-32	0-31

Table 6.2 – Number of deletions and gains detected in the primary tumours and the matched lymph node metastases. The mean number of copy number aberrations (CNA) was similar in both the primary tumours and the LNM, with a mean of 15.3 (range 0-32) CNAs in the primaries and 14.3 (range 0-31) in the metastases. The mean number of deletions was slightly higher in both primary tumours (8.7 vs. 6.6) and LNM (7.7 vs. 7.3) however the large standard deviations rendered this statistically non-significant.

A Patient 3 - Tumour

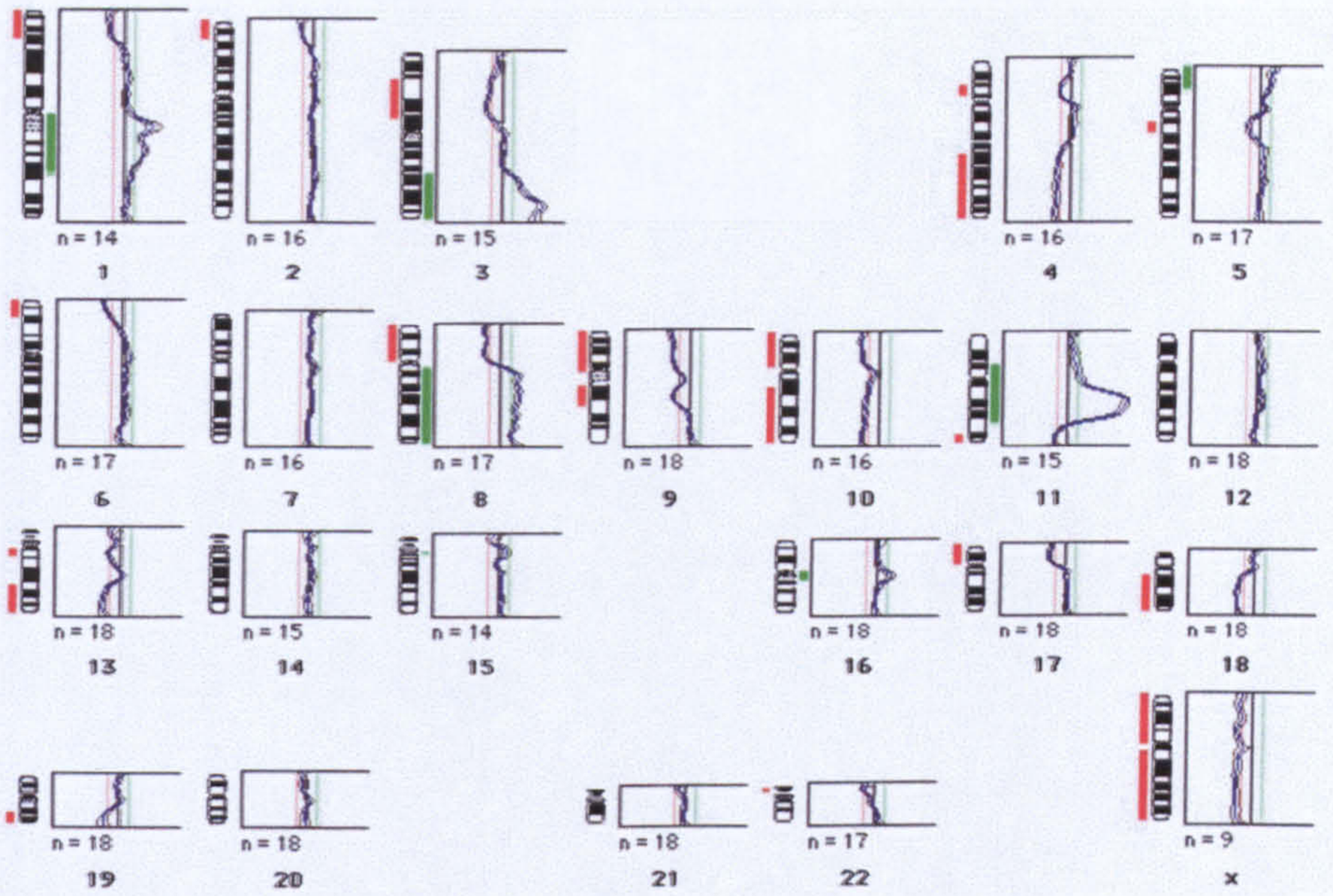

B Patient 3 - LNM

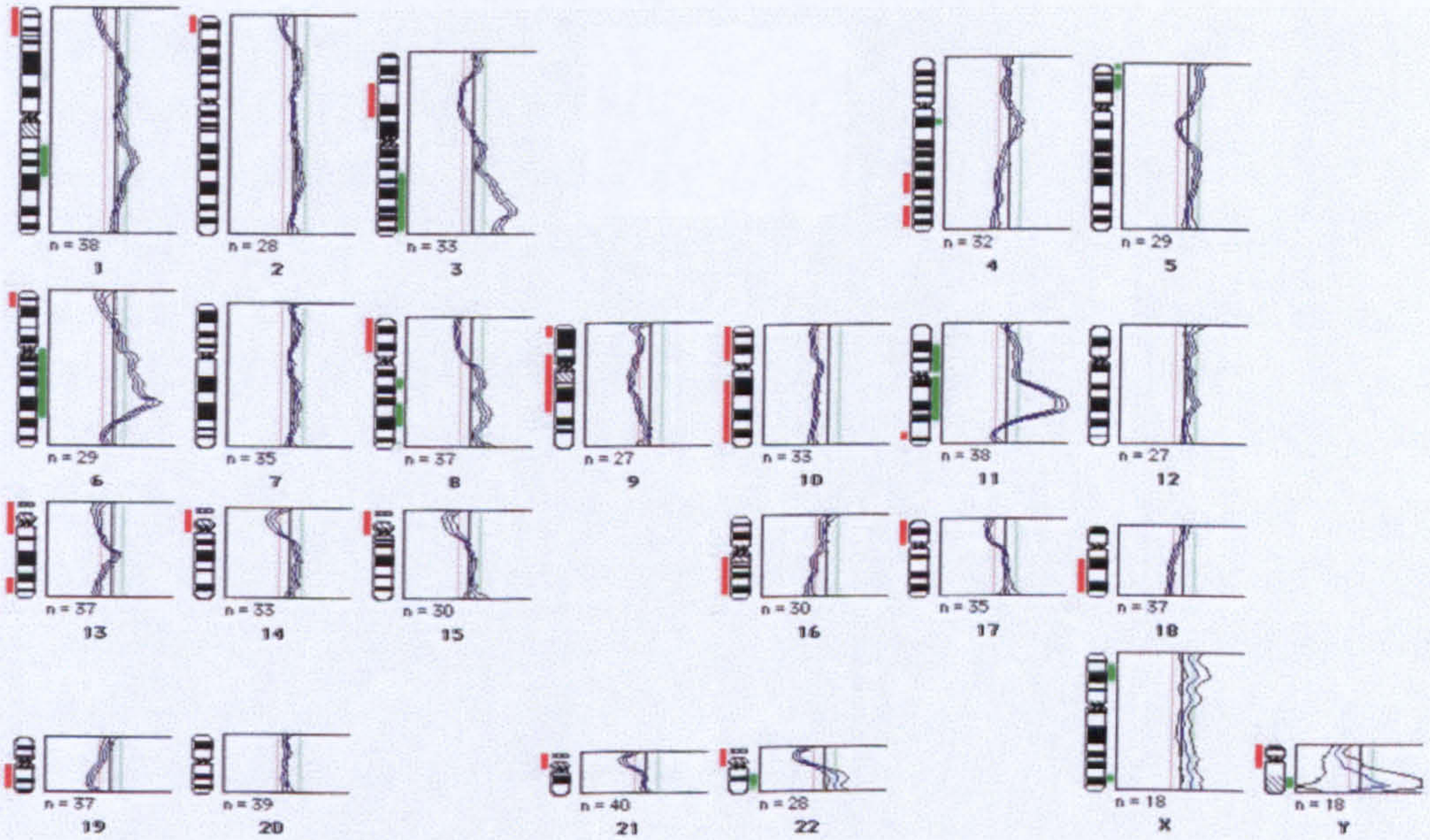

Figure 6.2 – CGH ratio profiles depicting the regions of copy number change in the primary tumour (A) and LNM (B) for patient No. 3. Regions of DNA gain are represented by green bars to the right of the chromosome ideograms and regions of loss by red bars to the left. Overall the two CGH profiles demonstrate similar patterns of aberrations with additional regions of copy number change detected in the metastatic tumour. Additional gains were detected on 6q and 22q and deletion on 16q in the LNM.

C Patient 3 – Tumour vs. LNM

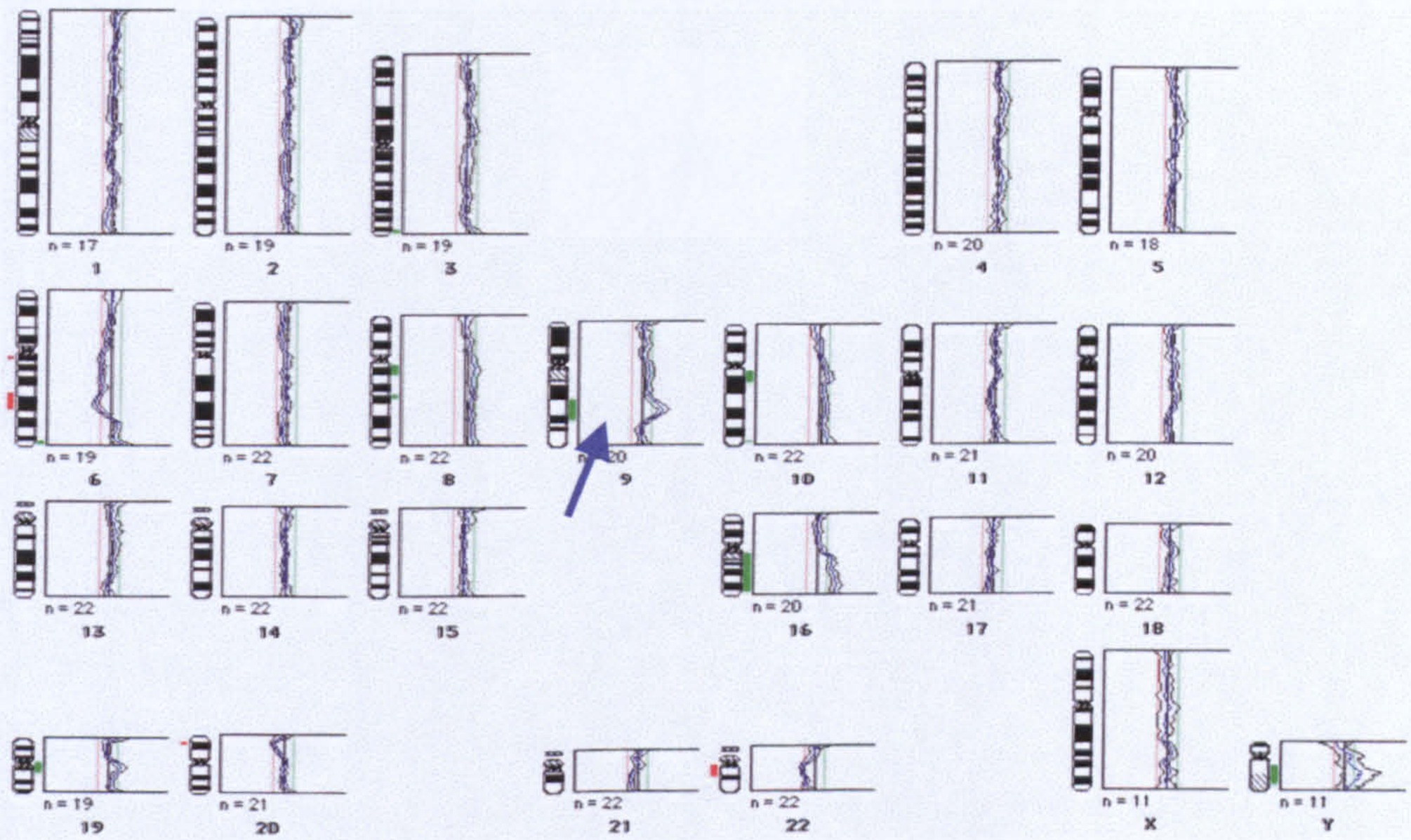

Figure 6.2 (C) – Modified CGH experiment confirming the aberrations detected in the standard CGH experiments depicted in Figure 6.2 (A) and (B). To confirm the aberrations detected in the two standard CGH experiments (Figure 6.2 A and B), a modified form of CGH was performed in which DNA from primary and metastatic tumours were differentially labelled and directly hybridized onto normal metaphase chromosomes under standard CGH conditions (Primary tumour labelled green, LNM labelled red). Regions of copy number change that differed between the primary and metastatic disease were confirmed as imbalances in the colour ratio. The gains of 6q and 22q detected only in the LNM were confirmed by modified CGH as a preponderance of red labelled DNA hybridizing at these regions and the loss of 16q in the LNM alone as an excess of green DNA. Interestingly, deletion of material on chromosome 9q was detected in both the tumour and the LNM by standard CGH, however modified CGH proved that the deletion extended further in the nodal specimen (an excess of green tumour DNA at 9q22 – see arrow).

change were identified in the LNM including gains on 6q and 22q and deletion of 16q. These differences were confirmed by modified CGH as an excess of SpectrumRed™ (LNM DNA) on 6q and 22q (i.e. a gain in the node that was not present in the primary tumour) and an excess of SpectrumGreen™ (primary tumour DNA) on 16q (i.e. a deletion in the node that was not present in the primary tumour) Figure 6.2 (C).

Figure 6.2 (C) also highlights the power of modified CGH in identifying subtle differences between the primary tumour and LNM which were not immediately obvious from the two individual CGH experiments. Most notable was the deletion on 9q detected in both primary and metastatic tumour. In Figure 6.2 (A) and (B) the deletion appeared to extend a similar distance down the chromosome to approximately 9q22.1. The LNM CGH data suggests that the deletion encompassed a larger region of the chromosome, however the resolution of the CGH ideograms prevented accurate confirmation of this. Modified CGH identified an excess of SpectrumGreen™ labelled DNA in the chromosome band 9q22.3 indicating the relative under-representation of this region in the LNM compared with the primary. Therefore modified CGH, combined with the two standard CGH profiles, identified the deletion of 9qcen-q22.1 in the primary tumour and 9qcen-q22.3 in the LNM.

Figure 6.3 depicts another tumour for which modified CGH was performed. CGH analysis of primary tumour, Figure 6.3 (A), and LNM, Figure 6.3 (B), identified aberrations common to both the primary and metastatic tumour including loss of 3p, 9p, 14, 15 and 16 and gains on 3q, 5p, 8q, 13 and 18q. However significant differences were also seen between the two specimens. Additional gains were detected on 19p and 20p in the nodal specimen along with loss of all of chromosome 10. In addition, some copy number changes detected in the primary tumour were not maintained within the nodal metastasis including gains on 1q and 6q and losses on 8p, 11q and 21. All of these differences were confirmed by the modified CGH experiment shown in Figure 6.3 (C).

6.3.3 Influence of signal dilution on copy number changes detected in tumours and LNM

In one LNM (patient 8), regions of deletion were suggested in which the CGH ratio approached, but did not exceed, the threshold for detection of a copy number decrease. Figure 6.4 depicts CGH profiles of several chromosomes from this case selected to demonstrate the effect of dilution of the signal from malignant cells within the lymph node metastasis. Using the strict CGH analysis criteria employed throughout this thesis, 3p loss was detected in the tumour but not in the LNM. The CGH profile for the LNM did

A Patient 41 - Tumour

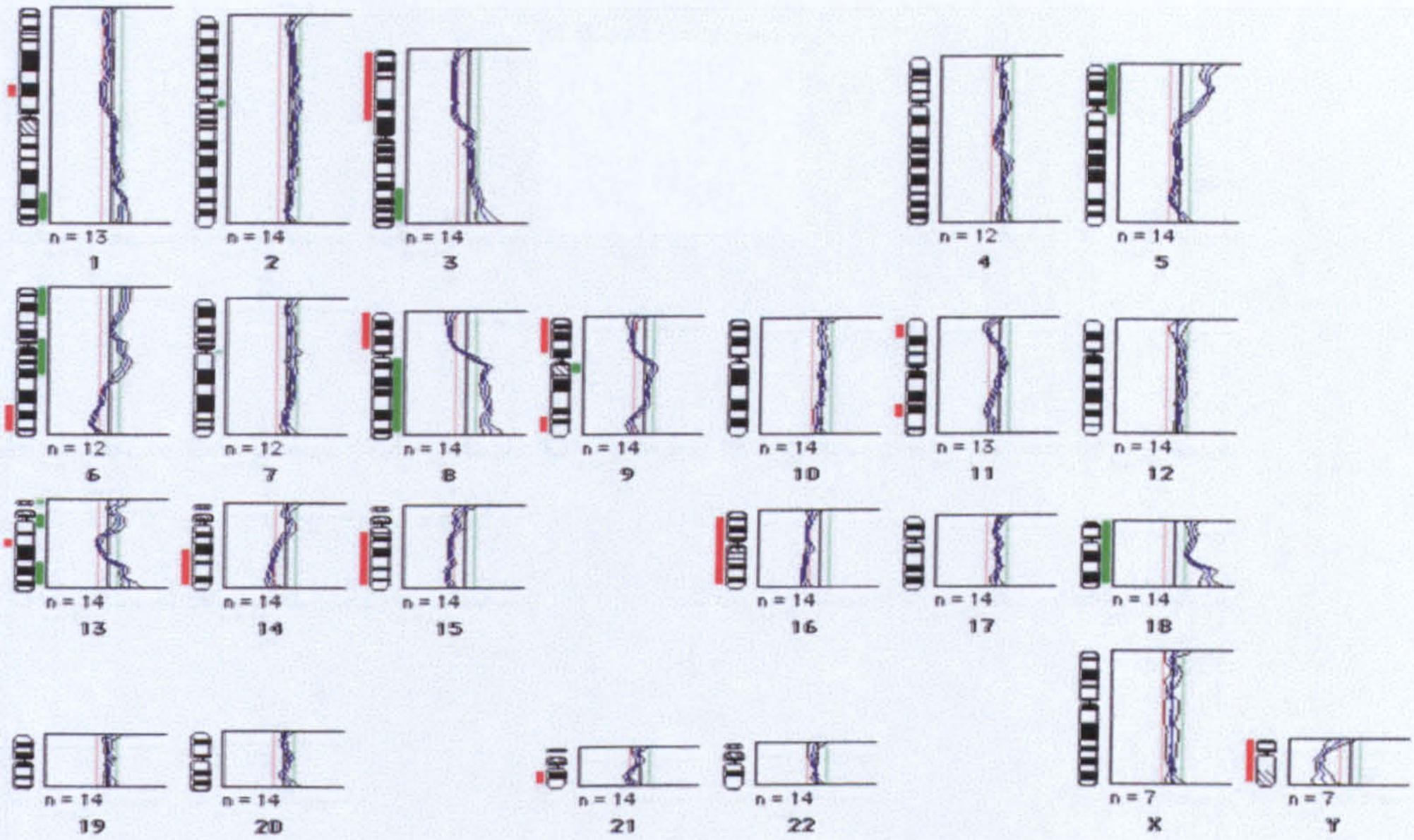

B Patient 41 - LNM

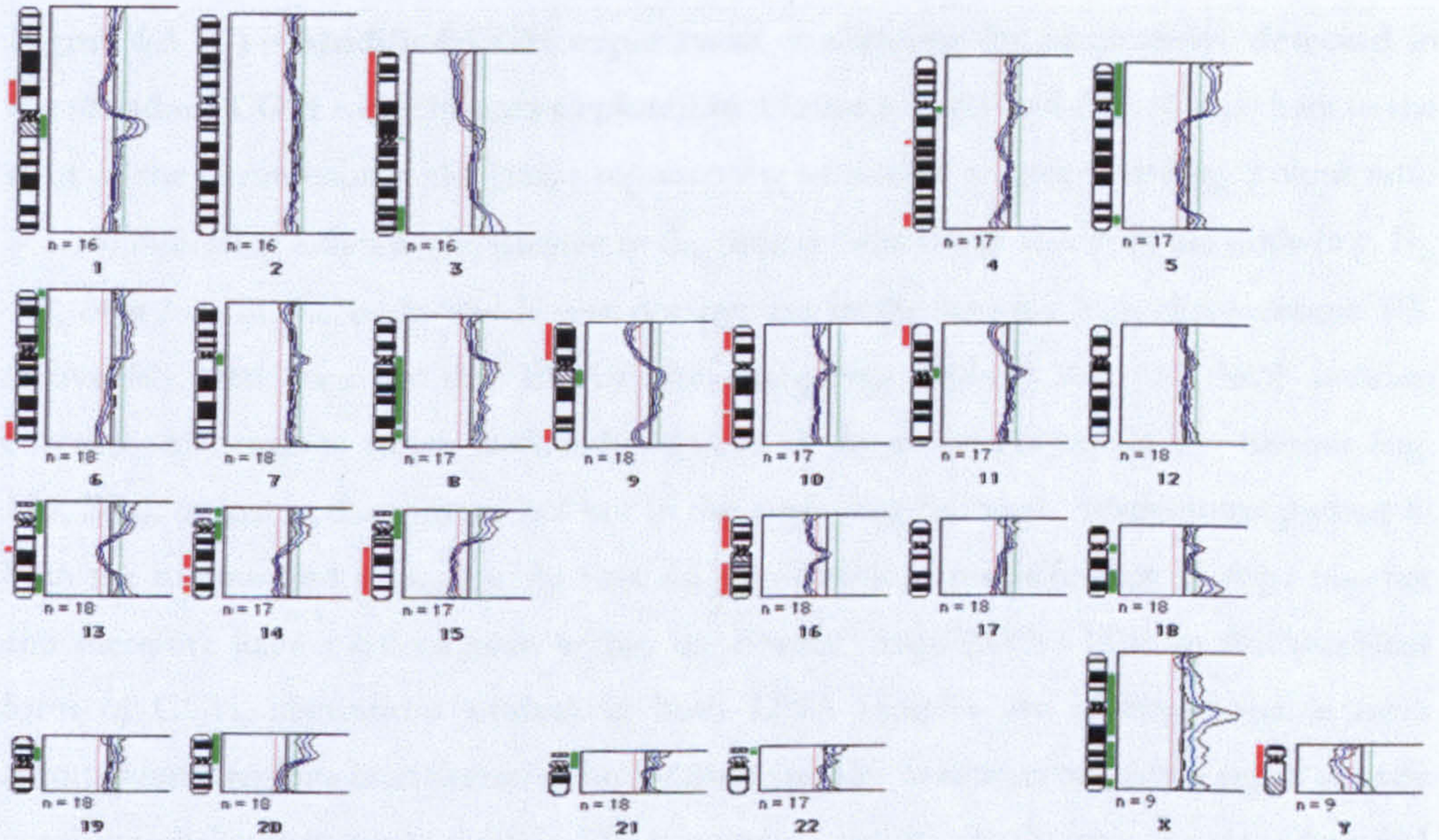

Figure 6.3 (A) and (B) – CGH ratio profiles depicting the regions of copy number change in the primary tumour (A) and LNM (B) for Patient No. 41. Regions of DNA gain are represented by green bars to the right of the chromosome ideograms and regions of loss by red bars to the left. Many of the chromosomal aberrations were shared between the primary tumour and the nodal metastases however significant differences were noted also.

C Patient 41 – Tumour vs. LNM

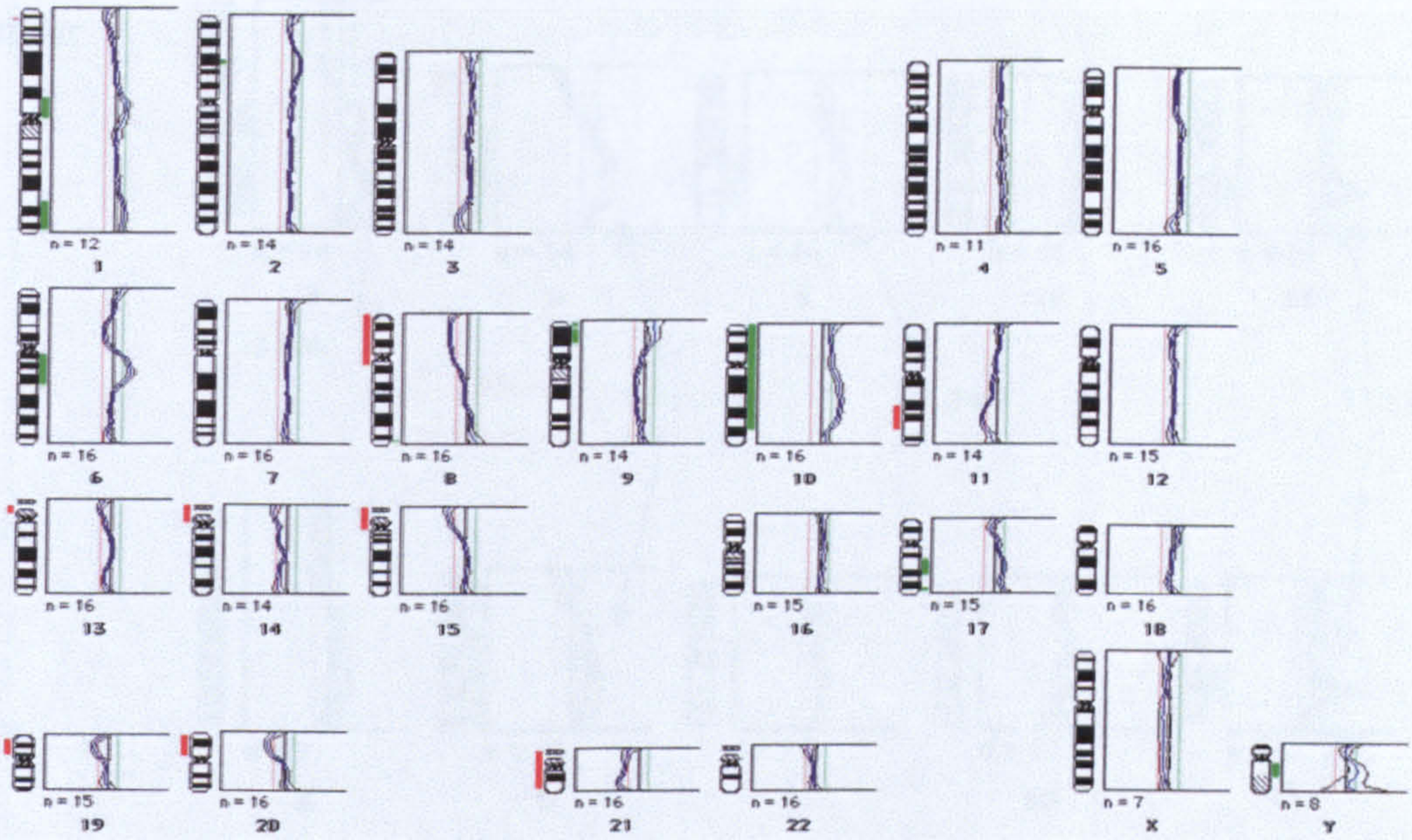

Figure 6.3 (C) – Modified CGH experiment confirming the aberrations detected in the standard CGH experiments depicted in Figure 6.3 (A) and (B). Green bars to the right of the chromosome ideograms representing an excess of green binding (colour ratio > 1.15) indicating either a gain present in the tumour which was absent in the node (e.g. 1q, 6q), or a loss in the node which was not present in the tumour (e.g. chromosome 10). Conversely, red bars to the left of the ideograms (colour ratio < 0.85) indicate chromosomal regions which were either gained in the node and not in the tumour (e.g. 19p, 20p), or lost in the tumour but not in the node (e.g. 8p, 11q). Aberrations present in both the tumour and node (e.g. 3p loss, 8q gain) result in no difference in copy number and therefore have a colour ratio within the normal range (0.85-1.15). In this modified form of CGH, aberrations present in both DNA samples are indistinguishable from chromosomal regions unafffected in both DNA samples as neither scenarios result in copy number imbalance between the two DNA samples. Significant discordance was identified between the primary tumour and LNM (Figure 6.3 A and B) for this patient and all aberrations were confirmed by modified CGH.

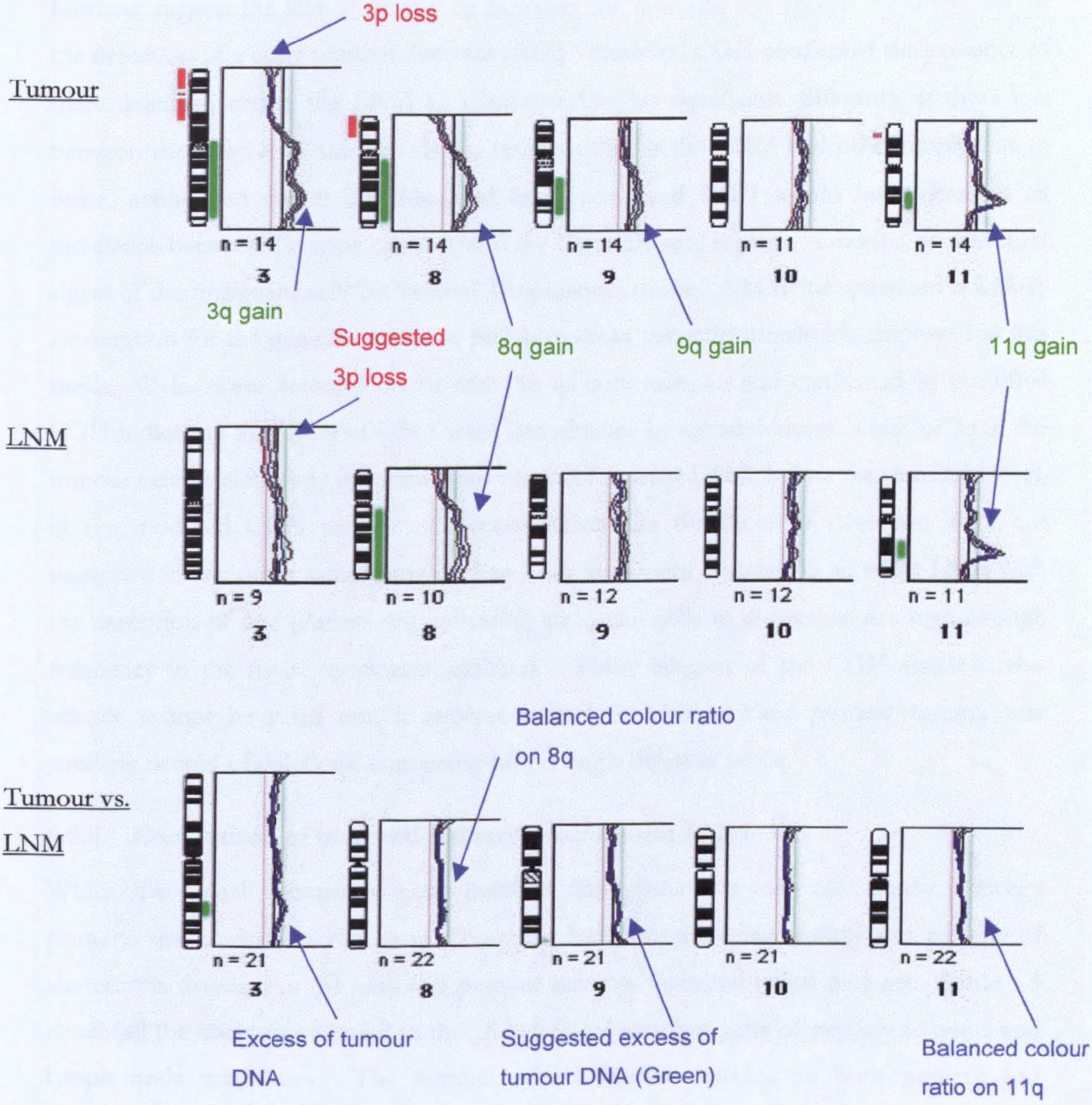

Figure 6.4 – Discrepencies between Tumours and LNM: Influence of signal dilution. CGH profiles of selected involved chromosomes from patient 8 are depicted with regions of copy number change highlighted. Loss of 3p was identified within the primary tumour but not in the LNM - using the strict CGH analysis criteria employed throughout this thesis. The LNM CGH profile for chromsome 3 suggested the loss of 3p, however the ratio did not exceed the 0.85 deletion threshold. Modified CGH failed to identify a significant difference in copy number on 3p confirming the similar status of 3p in both samples. Gains detected on 8q and 11q in both samples were confirmed by modified CGH (balanced between tumour and LNM). Gain of 9q in the tumour specimen was not detected (or suggested) in the LNM and this was reflected in the modified CGH profile where an excess of CGH, below the threshold level, was seen.

however suggest the loss of 3p and 8p however the ratio did not exceed the threshold for the detection of a copy number decrease (0.85). Modified CGH confirmed the presence of these deletions within the LNM by demonstrating no significant difference at these loci between the two DNA samples. If the ratio profiles in the LNM had been simply due to noise, maintained within the threshold limits, modified CGH would have detected an imbalance between the copy number at these chromosomal regions. Dilution of the CGH signal of the malignant cells by 'normal' lymphocytes in the LNM tissue specimen is a likely explanation for the genuine deletions failing to cross the ratio thresholds employed in this thesis. Gains were detected on 8q and 11q in both samples and confirmed by modified CGH indicating that gains of DNA were less affected by signal dilution. Gain of 9q in the tumour sample alone was reflected as an excess of tumour DNA, below the threshold level, in the modified CGH profile. Deletions below the threshold of detection were not suggested in any other sample analysed and deletions were detected in all other LNM with the exception of one (Patient 48) indicating malignant cells were present at a high enough frequency in the tissue specimens analysed. Whilst dilution of the CGH signal in this sample cannot be ruled out, it appears unlikely as the matched primary tumour was similarly devoid of deletions, containing only a single deletion on 6q.

6.3.4 Comparison of matched primary tumours and LNM

Whilst the overall pattern of copy number aberrations was relatively similar between primary and metastatic tumours, a marked variation was seen within the pattern of aberrations detected in the matched pairs of samples from individual patients. Table 6.3 details all the aberrations found in the 18 individual matched pairs of primary tumours and lymph node metastases. The number of aberrations detected in both primary and metastatic tumour (common aberrations) is listed, as well as the number of unique aberrations detected in either the primary alone or the LNM alone. These data are presented graphically in Figure 6.5. Of the 17 matched pairs of specimens with detectable aberrations, 9/17 (53%) LNM contained more aberrations shared with the primary tumour than unique aberrations. A slightly higher value was found for the primary tumours with 11/17 (65%) containing more shared aberrations than aberrations unique to the primary. The aberrations detected uniquely in the LNM for each matched pair are shown in Table 6.4.

The percentage of tumour copy number changes maintained in the nodal metastases demonstrated a range of values from 100%, i.e. all tumour CNAs detected in the nodal metastasis, to only 8.3%, with a mean value of 55.9% (Table 6.5). No correlation was

Patient / Site	Gains	Losses	Common Aberrations	Unique to Tumour	Unique to Node
49 Tumour	1q, 2p16-p21, 2q24-q32, 3q, 6qcen-q22, 7cen-q33, 8q, 11q13, 14q, 17cen-q21, 18p, 20cen-q12	1p32-pter, 2q35-qter, 4p15.3-pter, 5q34-qter, 8p, 9p23-pter, 9q34-qter, 10p14, 10q25-qter, 11p15-qter, 11q23-qter, 13q31-qter, 16p12-pter, 16q22-qter, 17p, 17q24-qter, 18q21-qter, 19p, 21, 22	27	6	4
49 LNM	1q, 2p13-pter, 2q24-q32, 3q, 6q15-q24, 7cen-q32, 8q, 9q31, 11q13, 14q23-24, 18p	1p35-pter, 2q36-qter, 4p15-pter, 4q33-qter, 5p15 1-pter, 7p21-pter, 8p, 9p23-pter, 9q34-qter, 10q25-qter, 11p15-pter, 13q33-qter, 16p13-pter, 17p, 17q24-qter, 18q22-qter, 19p, 21, 22			
3 Tumour	1q21-31, 3q22-qter, 5p, 8q, 11qcen-q22	1p33-pter, 2p23-pter, 3p, 4p14-15, 4q26-qter, 5q13, 6p22-pter, 8p, 9pter-q22.1,10p,10q22-qter, 11q23-qter, 13q12-13, 13q22-qter, 17p, 18q, 19q	22	0	3
3 LNM	1q21-31, 3q22-qter, 5p, 8q, 11qcen-q22, 6qcen-23, 22q	1p33-pter, 2p23-pter, 3p, 4p14-15, 4q26-qter, 5q13, 6p22-pter, 8p, 9pter-q22.3, 10, 11q23-qter, 13q12-13, 13q22-qter, 16q, 17p, 18q, 19q			
41 Tumour	1q32-qter, 3q24-qter, 5p, 6p22-pter, 6qcen-q16, 8q, 13q31-qter, 18	1p31.1-31.2, 3p,6q24-qter, 8p, 9p, 9q32-qter, 11p14-pter, 11q21-23, 13q14, 14q21-qter, 15q, 16, 21	16	5	6
41 LNM	3q24-qter, 5p, 5q34-qter, 6p22-pter, 7q11 2, 8q, 13q31-qter, 15cen-q14, 18q, 20p	1p31.1-31 2, 3p, 4q33-qter, 6q24-qter, 9p, 9q32-qter, 10, 11p, 13q14, 14q21-qter, 15q, 16			
10 Tumour	1p31-22, 2q22-32, 3q24-26, 4p13-q31, 5p, 5q15-23, 6qcen-q23, 8q, 11p14, 11q21-22, 12q21, 13q, 18q12	1p35-pter, 5q34-qter, 9q32-qter, 16p, 17p, 17q21-qter, 19,22	11	10	3
10 LNM	2q22-31, 3q24-26, 4qcen-q31, 6qcen-23, 8q, 12q21	1p35-pter, 4p15 3-pter, 9q32-qter, 12q24 2-qter, 17q23-qter, 19p, 21q, 22q			
33 Tumour	1pcen-p22, 2q22-32, 3q24-qter, 4p14-q31, 6qcen-q22, 8q21-23, 9q, 11p13, 12q15-21, 14q13	3p14-p25, 5q33-qter, 7q31.3-qter, 8p, 11q22-qter, 18q12-qter, 19, 21, 22	11	8	9
33 LNM	1pcen-p22, 2q22-32, 3q24-27, 4cen-q25, 6cen-q15, 12q21, 13q21, 17q23-qter	1p33-35, 4p16, 5q34-qter, 6q25-qter, 8p, 11q23-qter, 16p, 16q22-qter, 17p, 19p, 20q12-13.1, 22			
50 Tumour	2q24-q32, 3cen-q21, 4cen-q31, 5p, 8q21, 11q13, 12p13-pter, 19q	3p24, 5q13, 5q34-qter, 7q32-qter, 10p, 10q25-qter, 11q23-qter, 12q24-qter, 13cen-q14, 13q31-qter, 16p, 16q22-qter, 21	12	9	8
50 LNM	1q31, 2q22-q32, 3q, 4q22-23, 6q22-q24, 8q, 11p14-q13, 18p	1p36-pter, 3p, 4p15, 5q13, 10, 11q23, 13, 17q24-qter, 20p, 22			
8 Tumour	1qcen-q32, 3q, 5p, 8q, 9q, 11q22, 12q21.3, 14q22-23	2q37, 3p, 5q31-qter, 6p23-pter, 7q32-qter, 8p, 11p14-pter, 18q22-qter, 21	9	8	2
8 LNM	1q31, 3q, 5p, 8q, 11q22, 13q21	3p, 4p16, 5q32-qter, 7q32-qter, 8p			
48 Tumour	2p, 3q24-qter, 4cen-q21, 5p, 7p21-pter, 7q11 2, 8q23, 12p, 13q21, 16p13.1-pter, 17p13, 18p, 22	6q26-qter	7	7	0
48 LNM	3q24-qter, 4cen-q13, 5p, 8q23, 13q21, 18p, 22	-			
6 Tumour	3q, 5p, 7p15-q32, 8, 12p11.2-q 23, 13q14, 14qcen-q22, 16p11.2-12, 18p	1p32-pter, 3p2-pter, 4p15.3-pter, 5q34-qter, 9q34, 10, 11p15-pter, 14q31-qter, 16q, 17p, 21	7	14	13
6 LNM	1p22, 2q22-32, 3qcen-13, 3q24-27, 4cen-q31, 5qcen-23, 6qcen-23, 8q22-32, 9p21, 11p13, 12q21, 13q21-31	1p32-pter, 9q34, 12q24-qter, 16p, 17p, 17q24-qter, 19, 22			
5 Tumour	1p22, 3q24-qter, 6p22-pter, 7q21-31.2, 11q13	3p2-pter, 11q21-qter	6	1	8
5 LNM	1p22, 3q24-qter, 5p, 6qcen-15, 7q21-31.2, 11q13, 13q21-22	2q37, 3p, 4p15.3-qter, 5q34-qter, 7q31.3-qter, 11q23-qter, 12q22-qter			
11 Tumour	2p13-p16, 2q22-q32, 3cen-q13, 3q24-q27, 7q11.2, 8q, 12p, 12q21, 13q21	5q35, 6p24-pter, 11p15, 18q22-qter, 21	6	8	8
11 LNM	1q22, 2q32,3qcen-q13, 3q24-25, 4q, 5q21-22, 6qcen-q21, 8q21.3-22, 9p21, 12q21, 13q21-22	1p35-pter, 9q34, 17p13,			
1 Tumour	1q25-qter, 3q, 6p22, 8q21-23, 11q13, 12p	1p34-pter, 2q37-qter, 3p, 4p, 5q, 10p, 11q14-qter, 13q12-13, 17p	6	9	16
1 LNM	1p33-35, 3q, 11q13, 16, 17, 18p, 19, 20q, 22	1p2, 2q24-32, 3p, 4pter-q28, 5q, 6qcen-q23, 9p, 13cen-q33, 14q21-23, 18q, 21			
14 Tumour	3q, 6qcen-q21	3p, 8p22-pter, 11q14-qter, 13q, 14q22-qter, 16p12-cen	5	4	12
14 LNM	3q, 12p13, 16p, 17q12, 19q, 20q, 22	2p32, 3p12-13, 3p22-pter, 4qcen-q28, 5q13, 5q21-23, 6q12-q22, 9p23, 13q21-31, 14q22			
9 Tumour	3q25-26, 5p, 7q11.2, 12p	1p36-pter, 2q37, 5q34-qter, 10p12-pter, 12q24-qter, 14q32-qter, 17q24-qter, 19q	5	7	6
9 LNM	2q32, 6q21-23, 7q11.2, 11q22, 12p	2q37, 4p15 3-pter, 7q36, 10q25-qter, 12q24-qter, 17q24-qter			
2 Tumour	3q22-qter, 7qcen-q32, 11q13, 18q11.2	2q37, 3p, 4q26-qter, 5q14-23, 6q26-qter, 8p, 10q25-qter, 11q21-qter, 13q2-qter, 18q22-qter, 21	4	11	2
2 LNM	1q21-32, 3q, 22q	4q26-qter, 5q14-23, 13q2-qter			
4 Tumour	1q25	3p24-pter, 8p22-pter, 10q26, 11q24-qter	3	2	4
4 LNM	1q25-31, 3q, 6q21, 8q22-24, 18q	8p21-pter, 10q26			
7 Tumour	7q11.2, 18q11.2	1p36, 2p25, 2q37, 3p23-pter, 4p15-pter, 5p15.1-pter, 5q35, 10q25-qter, 11q23-qter,18q22-qter	1	11	13
7 LNM	2p16, 2q22-q32, 3q25-26, 4p14-q31, 5q21-23, 6qcen-q23, 12q21, 13q2-31	1p34-pter, 9q34, 17, 19, 20q13-qter, 22			
13 Tumour	-	-	0	0	0
13 LNM	-	-			

Table 6.3 – Detailed list of all aberrations detected in the 18 matched pairs of primary tumours and lymph node metastases. The cytogenetic location of all regions of gain and loss is listed along with the number of aberrations which were common to both samples and the number of aberration which were unique to either the primary tumour or LNM. A range of the number of common aberrations was seen from 27 down to only 1. A single patient had no aberrations detectable in either specimen.

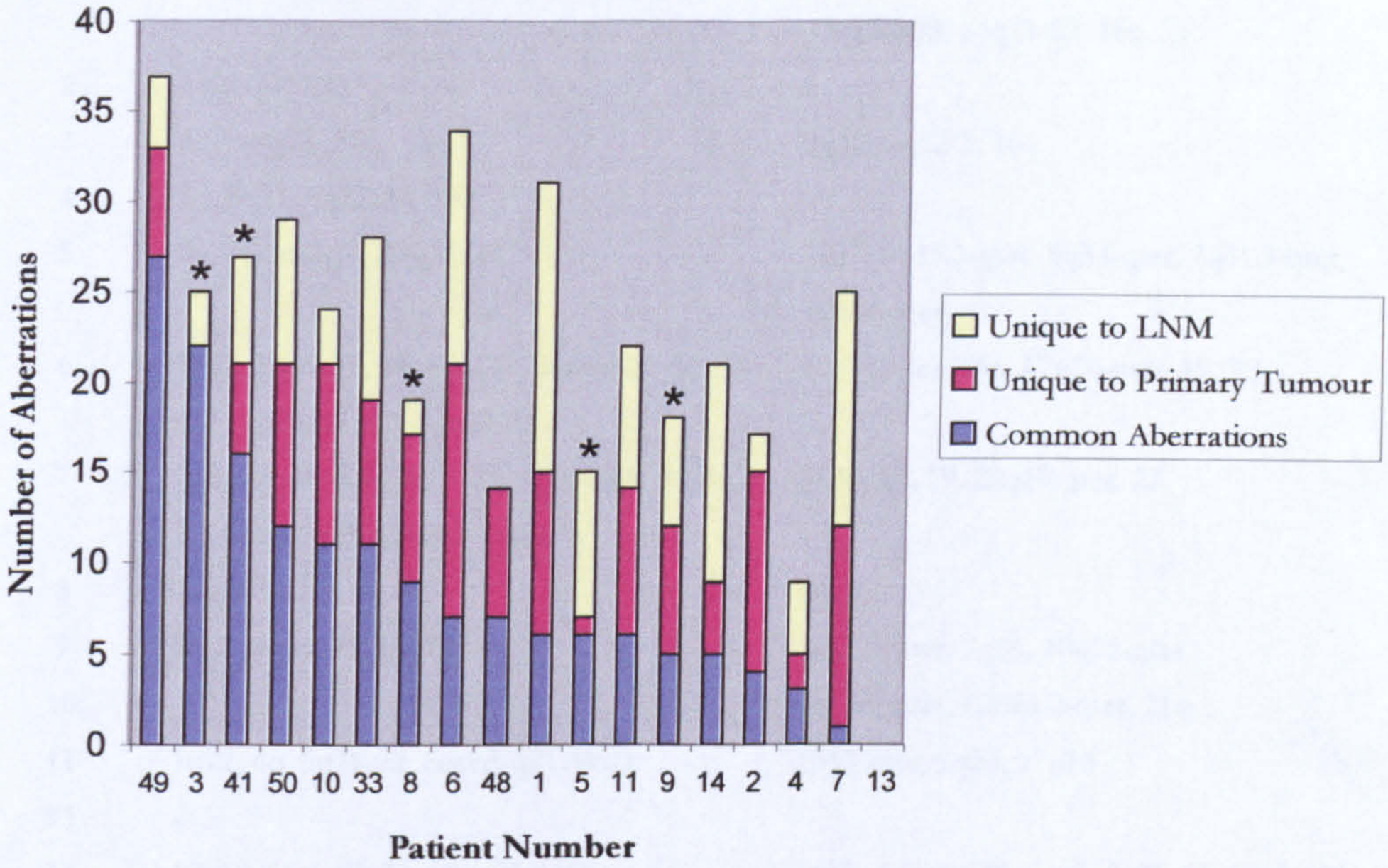

Figure 6.5 – Estimation of the degree of clonal relationship between primary tumours and lymph node metastases. The number of genetic aberrations that were found to be shared between the primary tumour and metastasis is depicted for each patient, as well as the number detected uniquely at either tumour site. Asterisks indicate the pairs of specimens that were validated by direct hybridization of tumour DNA against LNM DNA.

Patient	Gains	Losses
1	1p33-35, 16, 17, 18p, 19, 20q, 22	1p22, 2q24-q37, 4qcen-q28, 6qcen-q23, 9p, 13q13-q33, 14q21-23, 18q, 21
2	1q21-32, 22q	-
3	6qcen-q23, 22q	9q22.1-q22-3, 16q
4	3q, 6q21, 8q22-24, 18q	-
5	5p, 6qcen-q15, 13q21-22	2q37, 4p15.3-qter, 5q34-qter, 7q31.3-qter, 12q22-qter
6	1p22, 2q22-32, 4qcen-q31, 5qcen-23, 6qcen-q23, 9p21, 11p13, 13q21-31	12q24-qter, 16p, 17q24-qter, 19, 22
7	2p16, 2q22-q23, 3q25-25, 4p14-q31, 5q21-23, 6qcen-q23, 12q21, 13q2-31	9q34, 17, 19, 20q13-qter, 22
8	13q21	4p16
9	2q23, 6q21-23, 11q22	4p15.3-pter, 7q36, 10q25-qter
10	-	4p15.3-pter, 12q24.2-qter, 21q
11	1q22, 4q, 5q21-22, 6qcen-q21, 9p21	1p35-pter, 9q34, 17p13
13	-	-
14	12p12, 16p, 17q12, 19q, 20q, 22	2p32, 4qcen-q28, 5q13, 5q21-23, 6q12-q22, 9p23
33	13q21, 17q23-qter	1p33-35, 4p16, 6q25-qter, 16p, 16q22-qter, 17p, 20q12-13
41	5q34-qter, 7q11.2, 15qcen-q14, 20p	4q33-qter, 10
48	-	-
49	9q13	4q33-qter, 5p15.1-pter, 7p21-pter
50	1q31, 6q22-q24, 18p,	1p33-35, 4p15, 17q24-qter, 20p, 22,

Table 6.4 (a) – Aberrations unique to the LNM. The chromosomal loci of gains and losses detected exclusively in the LNM in the 18 pairs of samples studied.

Gains	Frequency	Losses	Frequency
6q	8/18	4p	6/18
22, 13q, 5q	4/18	1p, 4q	4/18
1q, 2q, 4q	3/18	6q, 12q, 17p, 22	3/18
1p, 16, 20q	2/18	7q, 9p, 9q, 16q	2/18

Table 6.4(b) – Frequent aberrations detected exclusively in the LNM.

These loci may contain the sites of tumour genes associated with the metastatic event.

Patient Number	Total tumour CNA's	Tumour CNA's also detected in the LNM	Percent common to LNM
3	22	22	100.0
5	7	6	85.7
41	19	16	84.2
49	33	27	81.8
4	5	3	60.0
33	19	11	57.9
50	21	12	57.1
14	9	5	55.6
8	17	9	52.9
10	21	11	52.4
48	14	7	50.0
11	14	6	42.9
9	12	5	41.7
1	15	6	40.0
6	21	7	33.3
2	15	4	26.7
7	12	1	8.3
13	0	0	-

Table 6.5 – The percentage of copy number aberrations present in the primary tumour that were also detected in the LNM. The number of CNAs shared between the LNM and primary tumour was calculated for each patient and expressed as a percentage of the total number of aberrations detected in the primary tumour. This value indicates the clonal similarity between the tumour and its corresponding metastasis, representing the proportion of genomic aberrations present in the primary tumour that were maintained at the metastatic site.

identified between the anatomical location of the primary tumour and the degree of clonality with the LNM. Based on the CGH results presented in Table 6.3, hypothetical progenitor cell clones could be constructed based on the assumption that chromosomal aberrations shared between the primary and metastatic tumour occurred early in tumour progression. Three examples of hypothetical progression pathways for individual tumours are depicted in Figures 6.6-6.8. Figure 6.6 depicts the aberrations detected in patient 3, the tumour demonstrating the clearest example of genetic progression between primary and metastatic disease. All aberrations detected in the primary tumour were maintained in the metastatic cells. However, the cells which formed the LNM demonstrated clear genetic progression with additional aberrations: gain of DNA at 6qcen-q23 and 22q; deletion of 9q22.1-q22.3 and16q. Figure 6.7 depicts an example of a patient for which the majority of aberrations were common to both sites. In this case the primary tumour has undergone further karyotypic evolution after the genetic divergence of the metastatic cells. Again, several aberrations were detected uniquely in the LNM. Figure 6.8 depicts a patient whose primary and metastatic tumour demonstrated a more limited clonal relationship. In this case the common aberrations constituted the minority of aberrations detected at either site suggesting that metastatic cells genetically diverged from the primary tumour at a relatively early stage.

The overall frequency of chromosomal alterations for all loci found to be gained or lost in at least 25% of either primary tumours or nodal metastases is listed in Table 6.6. Many chromosomal regions were found to be altered at similar frequencies in both the primary and metastatic tumours including losses on 1p35-pter, 3p14, 10q25-qter, 13q21-q22, 13q31-qter, 16p and 17p and gains on 1q25-31, 2q22-32, 3q, 5p, 8q, 11qcen-q13 and 12q15-q21. CNA detected at higher frequencies in the primary tumours were exclusively losses, including deletion of 2q37, 3p21-pter, 5q34-qter, 8p, 10p12-pter, 11p15-pter, 11q22-qter, 12p, 18q21-qter and 21. Regions more frequently affected in the LNM included deletion of 4p15.3-pter and 17q22-qter and gain of 6qcen-q15 and 13q21-22. Interestingly, both gain and loss of genetic material on chromosome 22 was detected at much higher frequencies in the LNM.

6.4 Discussion

CGH analysis of paired primary tumours and their regional lymph node metastases (LNM) has generated a novel molecular genetic view of the relationship between primary and metastatic HNSCC. The present study has demonstrated that HNSCC are characterised by deletions on chromosomes 3p, 5q, 8p, 11q, 13q 17p and 18q and gains on 3q, 8q, 5p and

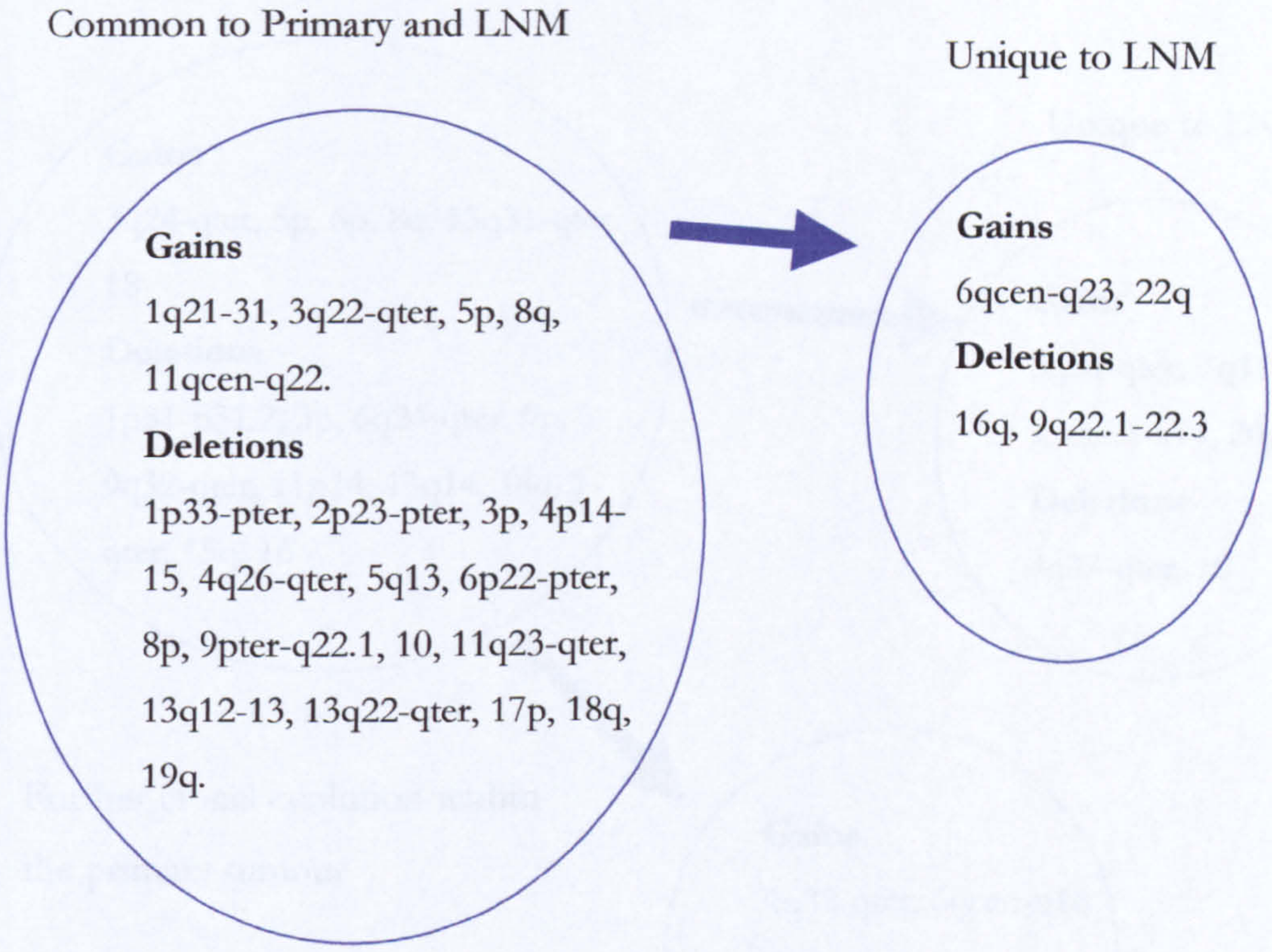

Figure 6.6 – Aberrations detected in primary tumour and matched nodal metastasis (Patient No.3). All the chromosomal aberrations identified in the primary tumour were also identified in the nodal metastases. However, additional genetic aberrations were detected exclusively in the metastatic tumour.

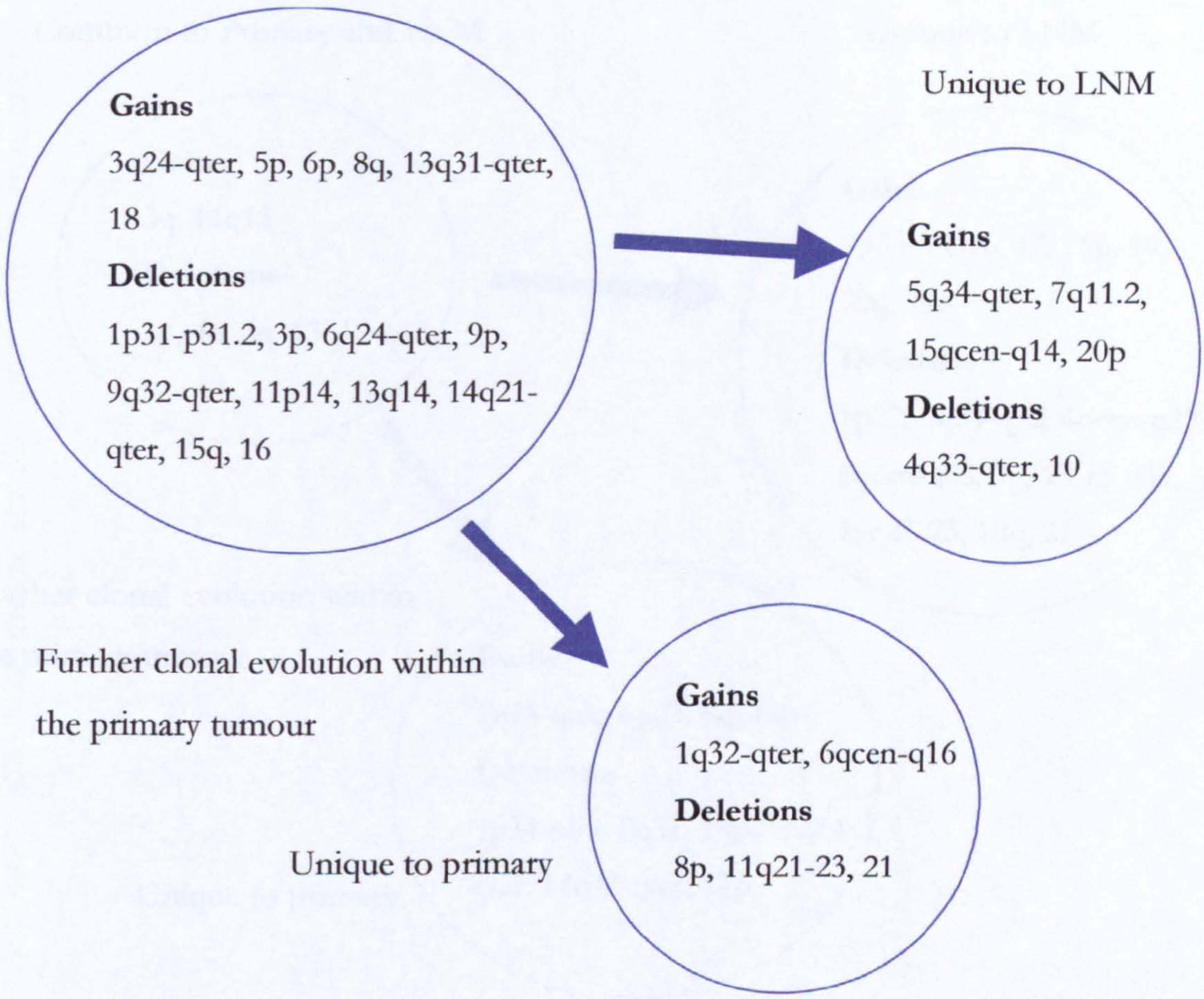

Figure 6.7 – Aberrations detected in primary tumour and matched nodal metastasis (Patient No.41). The majority of chromosomal aberrations detected were common to both the primary tumour and the lymph node metastasis. Again, additional aberrations were detected exclusively in the LNM. In this patient the primary tumour appeared to have undergone karyotypic evolution after the genetic divergence of the cells which seeded the lymph node.

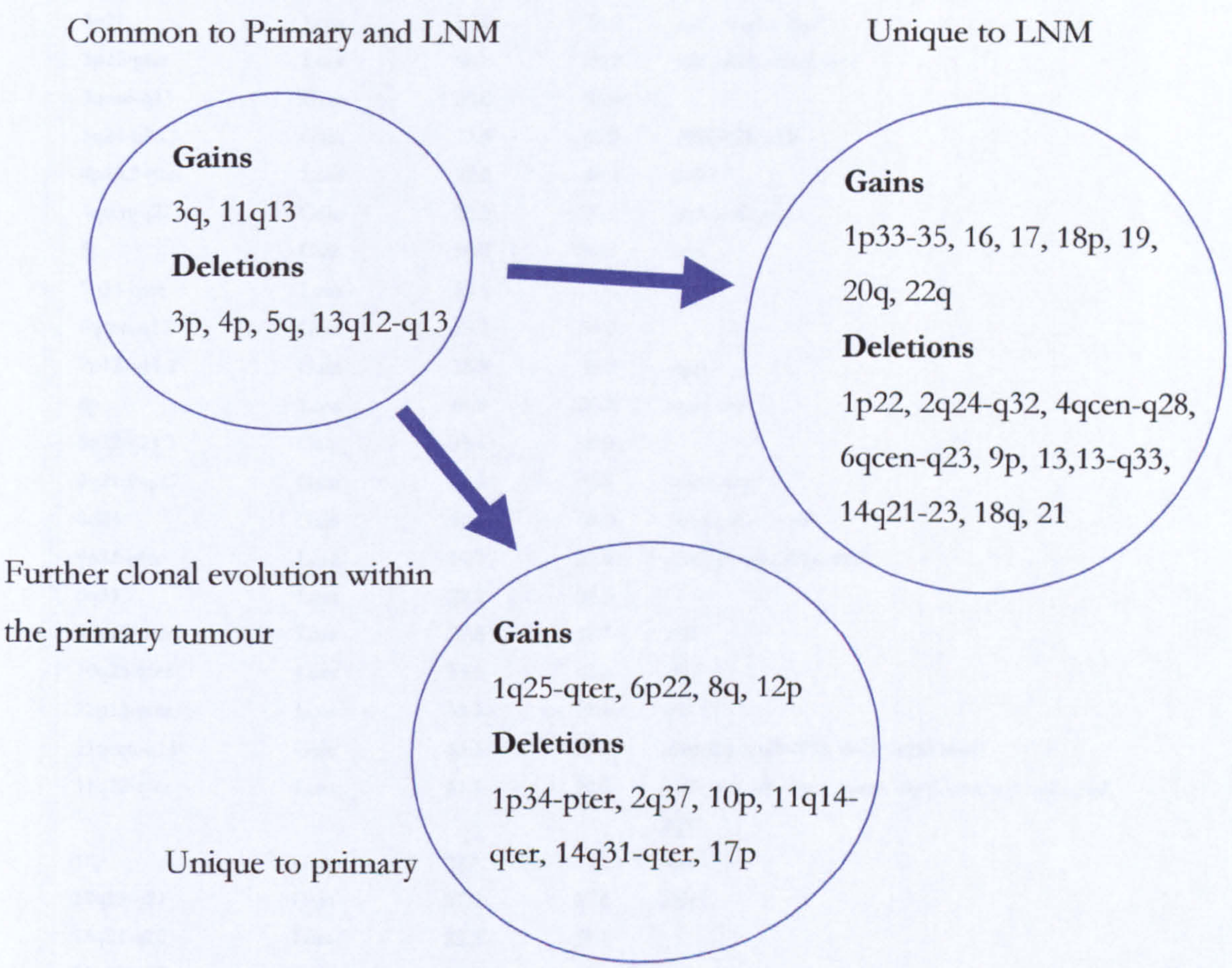

Figure 6.8 – Aberrations detected in primary tumour and matched nodal metastasis (Patient No.1). For this patient, the aberrations common to both sites represented the minority of the aberrations detected in either sample. Additional aberrations, unique to both the primary and metastatic tumour, were also identified.

Locus	Gain/Loss	Tumours	LNM	Genes
1p35-pter	Loss	38.9	44.4	
1q25-q31	Gain	22.2	27.8	*tpr, abl2*
2q22-32	Gain	33.3	44.4	
2q37	Loss	33.3	16.7	
3p14	Loss	44.4	38.9	***fhit,***
3p21	Loss	50.0	38.9	*sclc1, rassf1a, itga9*
3p22-pter	Loss	66.7	38.9	***vhl, dlc1,*** *ctnnb1, ogg1*
3qcen-q13	Gain	50.0	55.6	
3q24-q26.3	Gain	77.8	88.9	***PIK3CA,*** *hTR*
4p15.3-pter	Loss	22.2	44.4	*pcdh7*
4qcen-q21	Gain	22.2	38.9	*gro1, gro2, gro3*
5p	Gain	38.9	33.3	***tert***
5q34-qter	Loss	55.6	27.8	
6qcen-q15	Gain	33.3	55.6	
7p12-q11.2	Gain	38.9	16.7	***egfr***
8p	Loss	44.4	27.8	***nat1,*** *dr5*
8q12-q21.3	Gain	55.6	38.9	
8q21.3-q23	Gain	55.6	55.6	*rad54, int6*
8q24	Gain	50.0	50.0	*hhla1, pvt-1,* ***myc***
9p21-pter	Loss	16.7	27.8	*ifna1,* ***mts1 (p16),*** *mts2*
9q34	Loss	22.2	33.3	
10p12-pter	Loss	27.8	16.7	*st12*
10q25-qter	Loss	33.3	33.3	*dec*
11p15-pter	Loss	33.3	11.1	***wt1***
11qcen-q13	Gain	33.3	27.8	***ccnd1 (cyclinD1),*** *int2,* ***gstp1,*** *ems-1*
11q22-qter	Loss	61.1	22.2	*api1, api2, anc, casp1, casp4, casp5, atm, lob11cr2a, pig8, tsg11*
12p	Gain	27.8	11.1	***kras***
12q15-q21	Gain	27.8	27.8	*mdm2*
13q21-q22	Loss	22.2	33.3	
13q21-q22	Gain	16.7	27.8	
13q31-qter	Loss	27.8	27.8	***ing1,*** *tnf5fi3b*
16p	Loss	27.8	22.2	
17p	Loss	27.8	33.3	*bcpr,* ***p53***
17q22-qter	Loss	11.1	33.3	*nme1*
18q21-qter	Loss	38.9	16.7	***dcc***
19q13.2-qter	Loss	27.8	16.7	*bax*
21	Loss	44.4	16.7	
22	Gain	5.6	27.8	*stmy3, timp3*
22	Loss	16.7	33.3	*stmy3, timp3*

Table 6.6 – Summary of the frequency of chromosomal aberrations detected in the 18 matched pairs of primary tumour and LNM (%age). Aberrations detected at >25% in either of the tumour sites are listed. Tumour associated genes mapping to these chromosomal loci are also listed (bold text indicates genes specifically implicated in the formation of HNSCC).

11q. The results are consistent with data presented in Chapter 5, as well as the findings of other groups who have used CGH to investigate HNSCC. In general, the pattern and number of frequently affected chromosomal regions was similar for primary tumours and nodal metastases. There was, however, discordance between individual patient's primaries and matched LNM, in all cases where genetic alterations were detectable. A clear clonal relationship was identified between many of the tumour pairs investigated, however other pairs demonstrated heterogeneity, with extensive differences in their genetic make-up suggesting clonal divergence of populations of malignant cells.

The frequency of deletions was detected at a lower level in the LNM compared with the primary tumours, 7.7 (range 0-17) vs. 8.7 (range 0-20) respectively. Histological assessment of tissue sections taken adjacent to the specimens included in this study was made to estimate tumour cell content. Only specimens (both primary and LNM) for which H&E stained sections demonstrated >70% tumour cells were included in this study to ensure the CGH signal from malignant cells would not be 'diluted' by DNA from normal cells. This would result in a reduction in the sensitivity of CGH in detecting deletions (gains of DNA are less prone to this effect as they can involve multiple copy gains). However, histological assessment was limited to one facet of the specimen and the potential for the tumour cell content of the specimen to decrease through the tissue specimen used for DNA extraction remained a problem. Nodal specimens were believed to be more prone to such signal dilution due to the densely packed lymphocytes present within the LNM. However since the inconsistencies in several pairs of primary / metastasis are deletions as well as gains, the discordance between tumours and metastases cannot be attributed solely to differences in the percentage of tumour cells within the lymph node and hence sensitivity of detection.

Several chromosomal loci were identified which differed considerably in the frequency of copy number change between the primary and metastatic tumour (Table 6.6). These included aberrations found more frequently (> 2 fold) in the primary tumour (gain of 7p12-q11.2 and 12p and loss of 11q22-qter, 18q21-qter and 21) and those found more frequently in the LNM (gain of 22q and loss of 4p15.3-pter, 17q22-qter and 22). Overall copy number changes on chromosome 22q demonstrated the greatest difference between primary and metastatic tumours with copy number changes (both gains and losses) detected in 61.2% of LNM and 22.2% of primary tumours, suggesting a key role for genes on this chromosome to be involved in the formation of metastases. Previously, Bockmühl and colleagues reported gain of 22q at a similar frequency in HNSCC as reported here in the metastases (Bockmühl *et al*, 1995 and 1996), but their work included no data on

metastases. However, these studies reported a higher frequency of copy number changes for all aberrations than most other studies (Speicher *et al*, 1995; Brzoska *et al*, 1995; Stafford *et al*, 1999). Chromosome 22q11.2 is the site of the metalloproteinase stromelysin III (*STMY3* also termed *MMP11*; Levy *et al*, 1992). Stromelysins have the widest substrate specificities of all the matrix metalloproteinases identified to date, and have been shown to be important in tissue repair and tumour progression. Lying telomeric to *STMY3* at 22q12.1-13.2 is an inhibitor of the matrix metalloproteinases, *TIMP3* (Apte *et al*, 1994). The apparently conflicting finding of both gain and loss on 22q may possibly reflect the formation of a derivative 22q isochromosome, with deletion of the telomeric portion and duplication of the remainder. The deletions identified in the LNM on chromosome 22q were all within the band 22q13, however the gains were detected along the length of the chromosome. The short length of the chromosome hinders CGH analysis of chromosome 22. The resolution of CGH (Approx. 10Mb) is approximately a quarter of the entire length of the chromosome (Approx. 44Mb) therefore simultaneous subcentromeric gains and telomeric losses on such a short chromosome (as in the formation of a derivative 22q iso) may result in only one of the copy number changes being detected by CGH. Further, higher resolution characterisation of 22q is required to evaluate its role in HNSCC tumourigenesis and to resolve the apparent discrepancy given by CGH.

Deletion of material on 17q was found three times more frequently in the metastatic tumours. This region contains the putative metastasis suppressor gene *NME1* (*nm23*) for which reduced expression and/or LOH has previously been associated with a high metastatic potential in HNSCC and other types of human cancers such as breast and colorectal (Freije *et al*, 1998; Song *et al*, 2000; Takes *et al*, 2001). In an immunohistochemical study of 8 tumour markers, Takes *et al* demonstrated reduced expression of *NME1* in metastases compared with matched pairs of HNSCC primary tumours. More interestingly, Song *et al* demonstrated a significant reduction in *NME1* expression in primary tumours with lymph node metastases compared with tumours with negative nodal status (P=0.0006 – Chi squared test) suggesting that *NME1* status may have prognostic potential in predicting metastases from primary biopsy material. This finding is supported by the results presented here.

Loss of material on chromosome 4p15-pter was found twice as frequently in metastatic tumours (44.4%) compared with primary tumours (22.2%). Few genes at this loci have been implicated in tumour formation, however one potential candidate is the recently characterised *pcdh7* gene encoding a proto-cadherin (Yoshida *et al*, 1998). Cadherin

molecules have been implicated in cell adhesion, amongst other functions, and an increased frequency of loss at this locus may indicate a potential role for deletion of *pcdh7* in the loss of adhesion of metastatically-competent cells from the primary tumour mass. The relevance of the *pcdh7* gene to human cancer remains to be elucidated.

Heterogeneity within the primary tumour mass is now recognised to be a characteristic feature in many, if not all, HNSCC (Lleonart *et al*, 2000). Several small-scale studies have identified multiple and genetically distinct clones within primary tumours using FISH (Veltman *et al*, 1998), microsatellite markers (El-Naggar *et al*, 1997b), as well as immunohistochemical analysis of proliferation markers (Jacob *et al*, 1996) and cell adhesion molecules (Andrews *et al*, 1997). Whilst it is believed that clones with the potential to metastasise will eventually become the dominant clone within the primary tumour (Kerbel *et al*, 1988), at the time of treatment, many of the aberrations associated with the metastatic event may be masked by other clones, when analysed with a technique such as CGH.

Tumour heterogeneity has also been demonstrated in a mouse melanoma model with individual clones exhibiting differing abilities to produce metastatic colonies (Fidler and Kripke, 1977). This work led Fidler to conclude that highly metastatic tumour cell variants pre-exist in the heterogeneous primary tumour. Such an explanation is supported by this work which suggest a linear progression model may not satisfactorily explain the progression to metastases in all HNSCC. A similar conclusion was drawn by Kuukasjärvi who identified a similar variation in clonal relationship between primary and metastatic breast tumours by CGH analysis of matched specimens (Kuukasjärvi *et al*, 1997). This work also supports the idea that metastatic clones are present at a very low frequency in the primary tumour as they reported that metastatic cells can rarely be detected in the primary breast tumours using FISH, with probes specific for the metastatic clones. However it is clear that the early detection and treatment of primary HNSCC leads to a significantly reduced risk of metastatic recurrence therefore any pre-existing, metastatically competent cells must be initially constrained within the primary tumour mass. The mechanisms required for a cell to metastasise are gradually being unravelled and are known to include loss of adhesion to surrounding cells, degradation of the basement membrane, invasion into the subjacent connective tissue and entry to the lymphatic circulation (Petruzzelli *et al*, 1998). Once in the circulation a clone must evade the host's immuno-surveillance, attach to the cells in the lymph node and establish a source of nutrients (angiogenesis). However, it is not yet clear as to whether tumour cells which successfully establish a metastasis possess all the biological capabilities for each step of the metastatic process or whether a

mass of multiple clones competing and co-operating at the primary site is responsible for the breaching the basement membrane and subsequent invasion into the underlying connective tissue. Pre-existing cells with metastatic potential, lacking some of the biological characteristics required for metastasis, may be able to metastasise only *after* other clones, with differing genetic and biological characteristics, have progressed to an aggressive, invasive phenotype. Such an explanation would explain the discordance identified and be in keeping with the apparent non-linear progression to the metastatic phenotype suggested by the CGH analysis of the LNM.

In conclusion CGH analysis of primary and metastatic HNSCC successfully identified many chromosomal loci of copy number change shared between the two groups. Discordance was noted between matched pairs of tumour specimens suggesting that metastatic cells did not constitute the majority of the primary tumour mass in a significant proportion of the specimens analysed. Finally several chromosomal loci were identified which may harbour genes important in the metastases of the disease.

6.5 Future Directions

The data presented in this chapter was the basis for a successful grant from the Royal College of Surgeons of England. The fellowship obtained is currently undertaking high resolution mapping of chromosome 22 in HNSCC archival tissue specimens with emphasis on metastatic tumours, in order to characterise the role of 22q in HNSCC tumourigenesis. A major challenge remains to determine whether the status of markers in the LNM can be applied prognostically to biopsies of the primary tumour specimen. Whilst aberrations of chromosome 22 were frequently detected in the LNM, fewer primary tumours demonstrated copy number changes. For any marker to be of clinical use in reducing elective nodal dissections it must be able to predict metastatic potential based solely on the primary tumour mass. Further investigation into the timing of the genetic divergence of metastatically-competent cells and evaluation of the proportion of these cells within the primary tumour will aid in the development of suitable clinical markers of metastasis. Higher resolution analysis of chromosome 22 aberrations in HNSCC LNM will aid in the design of suitable genetic probes for *in situ* analysis of primary specimens. Such markers are now urgently needed to evaluate the primary tumour mass for cells with the potential to metastasise.

Chapter 7

Immunohistochemical Analysis of Radio-Resistant Laryngeal Carcinoma

7.1 Introduction

The lack of clinically available markers to predict response to radiotherapy in HNSCC patients remains a major problem. Radio-resistance in HNSCC is believed to be due to defects within the cancer cells' apoptotic (or 'cell suicide') mechanisms discussed in Section 1.5.2. In 10-30% of patients with T1 and T2 stage laryngeal tumours, DNA damage (initiated by radiotherapy) fails to induce tumour regression. The aim of this chapter was to identify molecular markers that could differentiate between radio-resistant and radio-sensitive tumours. Markers were selected for their role in cellular proliferation, DNA synthesis or repair, and apoptosis. For this study a homogenous population of laryngeal glottic tumours was selected to circumvent the problem of sub-site variation in marker expression encountered in many studies of HNSCC tumours.

7.2 Material and Methods

7.2.1 Patient details

For the purpose of this study, radio-resistance was defined as recurrence within the original field of radiotherapy within 12 months of treatment. This strict criterion was chosen to minimise the likelihood of including second primaries arising in patients who have continued exposure to carcinogens after their original radiotherapy. Laryngeal tumours of the glottis, a group of tumours in which radio-resistance is a known complication, were chosen for analysis. Pathology records were searched for all patients treated for laryngeal HNSCC with external beam radiotherapy at Princess Royal Hospital between 1989 and 1998. Eight pathological specimens were obtained which fulfilled the criteria for radio-resistance and a further 13 radio-sensitive tumours were selected for comparison. All specimens obtained were tissue biopsies taken prior to receiving radiotherapy. A therapeutic regime of radical external beam radiotherapy of 60+/- 2 Gy given in 25 fractions over a course of 5 weeks was common to all patients. The small number of radio-resistant tumours obtained is due to the strict inclusion criteria. Table 7.1 shows the clinicopathological details of the patients included in this study.

7.2.2 Selection of immunohistochemical markers

p53 is known to play a key role in the maintenance of the human genome and abnormal p53 has been correlated with poor prognosis and implicated in resistance to both chemo- and radiotherapy. p53 recognises radiotherapy-induced genotoxic damage, arrests growth in G1 and 'decides' whether the cell undergoes DNA repair or apoptosis (Nylander *et al*, 2000). Normally p53 is present at undetectable levels in the cell, when mutations occur

Patient Number (sex)	RR or RS	Date of Biopsy	T stage	Time to Recurrence (m)	Original Grade	Follow Up (yrs)(2000)	Current Status (2000)
1 (m)	RR	1996	1a	3	well	4	AW
2 (m)	RR	1991	1a	7	moderate	9	AW
3 (m)	RR	1995	1a	4	moderate	5	AW
4 (m)	RR	1995	2	2	poor	3	LTFU
5 (m)	RR	1989	1a	10	well	11	AW
6 (m)	RR	1989	1a	8	moderate	11	AW
7 (m)	RR	1989	1b	10	poor	11	AW
8 (m)	RR	1997	2	12	well	3	DOD '98
9 (f)	RS	1998	2	N/A	moderate	2	AW
10 (m)	RS	1998	1	N/A	poor	2	AW
11 (m)	RS	1998	1	N/A	moderate	2	AW
12 (m)	RS	1995	1a	N/A	moderate	5	AW
13 (m)	RS	1994	1	N/A	moderate	6	AW
14 (m)	RS	1990	1b	N/A	*in situ*/well	10	AW
15 (m)	RS	1991	1a	N/A	well	9	AW
16 (m)	RS	1996	2	N/A	moderate	4	AW
17 (m)	RS	1990	1	N/A	moderate	10	AW
18 (m)	RS	1992	2	N/A	moderate	8	AW
19 (m)	RS	1996	1a	N/A	poor	4	AW
20 (m)	RS	1994	2	N/A	moderate	6	AW
21 (m)	RS	1994	1b	N/A	moderate	6	AW

Table 7.1 – Clinicopathological details of the HNSCC patients with radio-sensitive and radio-resistant glottic tumours from which pre-treatment biopsies were obtained. RR- Radio-resistant, RS- Radio-sensitive, AW- Alive and Well, LTFU- Lost to Follow Up, DOD- Died of Disease

abnormal p53 protein can accumulate allowing immunohistochemical detection. Mutant p53 protein has been found in approximately half of HNSCCs analysed by immunohistochemistry (Nylander *et al*, 1995). A major component of the growth arrest signal is p21 (CIP1/WAF1). p53-induced p21 inhibits the cyclin/cdk dependant phosphorylation of the Rb protein. This prevents the subsequent release of the E2F transcription factor and silences genes required for transition into S phase. p16 is another factor that specifically inhibits the Cyclin D1/cdk 4/6 complex. Loss of p16 function has been detected at frequencies of up to 83% in HNSCC (Reed *et al*, 1996). p21 also interacts with PCNA, a subunit of DNA polymerases δ and ε (Luo *et al*, 1995) inhibiting the replication function of the polymerase complex whilst maintaining its DNA repair function (Li *et al*, 1994). Loss of p16 and p21 function would therefore weaken the G1 brake, with p21 loss also favouring DNA replication as opposed to repair. The role of p21 in HNSCC remains to be clarified. Protein over-expression has been correlated with both chemotherapy responders and increased overall survival in stage III patients (n=93, p=0.02 and p=0.02 respectively, Kapranos *et al*, 2001). Conversely, over-expression of p21 has also been linked to increased incidence of recurrent disease and shortened disease-free survival and (n=43, p=0.03 and p=0.0071 respectively, Erber *et al*, 1999).

Mitogen induced expression of Cyclin D1 is a critical step in the initiation of S phase. The formation of an activated Cyclin D1/cdk 4 or 6 complex leads to phosphorylation of the Rb protein. Several immunohistochemistry studies have demonstrated Cyclin D1 over-expression in approximately half of all HNSCCs and revealed a correlation with tumour recurrence, advanced stage, the presence of occult metastases and a general poor prognosis (Michalides *et* al, 1997; Cappacio *et al*, 2000). Over-expression of Cyclin D1 has been postulated as one mechanism by which tumour cells may overcome the inhibitory effects of normal cellular levels of p21 (van Oijen *et al*, 1998).

The Mib-1 antibody recognises another marker of proliferation: Ki-67, a large, 358 kd nuclear protein. The Ki-67 antigen is expressed in cells throughout cell division but is undetectable during the G0 resting phase (Scholzen *et al*, 2000) making it a useful indicator of overall cellular proliferation. The proliferating cell nuclear antigen (PCNA) is only expressed during S phase and is another regularly used proliferation marker.

Her-2/neu (also known as c-erb-B2) is an epidermal growth factor receptor (EGFR) responsible for transducing the growth stimulatory signal of the extracellular mitogen, epidermal growth factor (EGF). Over-expression of Her-2/neu has been demonstrated in

roughly half of all HNSCCs and is associated with shortened overall survival (Xia *et al*, 1999).

bcl-2 is a member of a family of apoptotic proteins including bclx, bax, bid, bak and bik. Over 35 apoptotic proteins have been described to date, some are pro-apoptotic, such as bax, whilst others, such as bcl-2, inhibit the apoptotic response. The bcl-2 gene is located on chromosome 18 and encodes for a 26 kDa pore forming protein found within mitochondrial membranes. Interaction of bcl-2 with Apaf-1 (Apoptosis activation factor 1) prevents the release of cytochrome c from mitochondria, inhibiting the apoptotic process (Rosen *et al*, 1999).

MSH2 and MLH1 are members of a family of proteins involved in the repair of DNA mismatches. Absence of the protein product is indicative of the loss of mismatch repair (MMR) function and is characterised by genetic instability in short, repeat sequences termed micro-satellites. Deficiencies in the MMR pathway have been shown to result in elevated resistance to specific inducers of DNA damage, possibly via the disregulation of apoptosis (Hardman *et* al, 2001). Several studies have correlated MMR deficiency with resistance to chemotherapy drugs in breast, colon and ovarian cell line studies (Taverna *et al*, 2000) however little is known about the role of MMR in HNSCC.

7.2.3 Immunohistochemistry

5μm tissue sections mounted on SuperFrost Plus slides (Menzel-Glaser) were prepared from formalin-fixed paraffin-embedded pre-treatment biopsies by the Department of Pathology, Hull and East Yorkshire Hospitals. H&E staining was performed as described in Section 3.2 and immunohistochemistry was performed as described in Section 3.9. Optimal antibody concentrations and other methodological variations are detailed in Table 7.2. Approximately 30% of all immunohistochemistry experiments were repeated to ensure reproducibility and to monitor for inter-batch variability.

7.2.4 Grading of immunohistochemistry

Antibody staining was analysed according to two different methods, digital image analysis and visual grading by two independent blinded observers. The Becton Dickinson CAS200 Cell Analysis System was used to digitally measure antigen expression within tumour biopsies (Section 3.9.2) for several of the antibodies used (Table 7.2). This previously validated system (Potten *et al*, 1993) was found to be highly effective at measuring nuclear antigen expression and was highly correlated with visual grading (Tables 7.3 and 7.4). All

Target	Antibody Clone	Isotype	Supplier	Dilution	Epitope Retrieval	Counterstain	Analysis Method
p53	DO1	Mouse IgG_{2a}	BD	1/100	Microwave	Methyl green	CAS/IBO
p16	G175-405	Mouse IgG_1	Pharmingen	1/50	Pressure Cooker	Haemotoxylin	IBO
p21	6B6	Mouse IgG_1	BD	1/50	Microwave	Methyl green	IBO
bcl 2	100	Mouse IgG_1	Serotec	1/50	Pressure Cooker	Haemotoxylin	IBO
MLH1	G168-728	Mouse IgG_{2a}	Serotec	1/50	Pressure Cooker	Haemotoxylin	IBO
MSH2	FE11	Mouse IgG_1	Serotec	1/100	Pressure Cooker	Haemotoxylin	IBO
PCNA	PC10	Mouse IgG_{2a}	BD	1/100	None	Methyl green	CAS/IBO
Ki-67	MIB-1	Mouse IgG_1	BD	1/100	Microwave	Methyl green	CAS/IBO
Her 2	3B5	Mouse IgG_1	BD	1/50	Trypsin	Methyl green	IBO
Cyclin D1	CD1.1	Mouse IgG_1	Serotec	1/100	Pressure Cooker	Haemotoxylin	IBO

Table 7.2 – Details of antibodies employed in this study. CAS – Cell Analysis System; IBO – Independent blinded observers.

Antibody	Staining Pattern	Grading (see text for details)	
p53	Nuclear	Presence/Absence	+/-
p16	Nuclear/Cytoplasmic	Presence/Absence	+/-
p21	Nuclear/Cytoplasmic	Presence/Absence	+/-
bcl 2	Cytoplasmic	Presence/Absence	+/-
MLH1	Nuclear	Presence/Absence	+/-
MSH2	Nuclear	Presence/Absence	+/-
PCNA	Nuclear	High/Low expression	>20% - High; <20% - Low
Ki-67	Nuclear	High/Low expression	>20% - High; <20% - Low
Her 2	Cytoplasmic/Membranous	High/Low expression	>10% - High; <10% - Low
cyclin D1	Nuclear	High/Low expression	>50% - High; <50% - Low

Table 7.3 – Details of the grading system employed by independent, blinded observers.

visual grading was performed under intermediate power light microscopy (x200) and only malignant epithelium was graded. If consensus was not obtained after initial grading the entire batch of slides, alongside H&E slides, was reviewed and independent grading repeated.

Table 7.3 lists the criteria used for the measurement of each antigen. As a consequence of the small numbers in the two groups, a two tier grading system was employed for all antibodies: either presence or absence of staining (p53, p16, p21/Waf1, bcl2, MLH1, MSH2), or grading into high and low expression categories (PCNA, Ki-67, her2, Cyclin D1).

7.2.5 Statistical analysis

Data were analysed using Fisher's exact test on the SPSS 10 statistical package.

7.3 Results

Clinical data obtained from patient records is shown in Table 7.1. All tumours were staged according to the TNM classification and graded histologically. The mean age of the patients at time of diagnosis was 61 years, ranging between 39 and 93 years. The length of follow-up for patients ranged from 2 to 10 years with a median of 6.1. The mean age at diagnosis in the resistant group was 64.8 compared with 57.8 in the sensitive group. The average time to clinically evident recurrence of the radio-resistant tumours was 7 months (range 2-12). No correlation of clinicopathological details and radiotherapy response was found.

7.3.1 Immunohistochemical staining

Duplicated experiments successfully confirmed the reproducibility of the technique and complete concordance was demonstrated between different batches of the same antibody performed on different days. The results of all tumour markers analysed in this study are depicted graphically in Figures 7.1 (markers graded as positive or negative) and 7.2 (markers graded into high and low expression categories). Table 7.5 summarises the results of all immunostaining performed for each individual patient.

7.3.2 p53 staining

p53 staining was universally nuclear with a constitutive pattern of expression (Figure 7.3). The percentage of positively staining nuclei was measured both by image analysis and by estimation by 2 blinded observers. Table 7.4 compares the two methods of analysis. Visual estimation of staining identified two distinct groups. 48% of tumours demonstrated

Patient Number	Visual Scoring	CAS	
		CAS Result (% positive cells)	Group
1	-	24	-
2	-	0	-
3	-	23	-
4	+	80	+
5	-	6	-
6	-	0	-
7	+	50	+
8	+	73	+
9	+	83	+
10	+	76	+
11	+	78	+
12	-	0	-
13	+	76	+
14	-	22	-
15	-	25	-
16	+	87	+
17	-	3	-
18	+	63	+
19	-	2	-
20	-	6	-
21	+	76	+

Table 7.4 – Comparison of visual scoring of p53 staining by blinded independent observers and image analysis using the CAS. For classification using the CAS analysis system cells were grouped as positive if >30% of cells demonstrated prominent nuclear p53 staining.

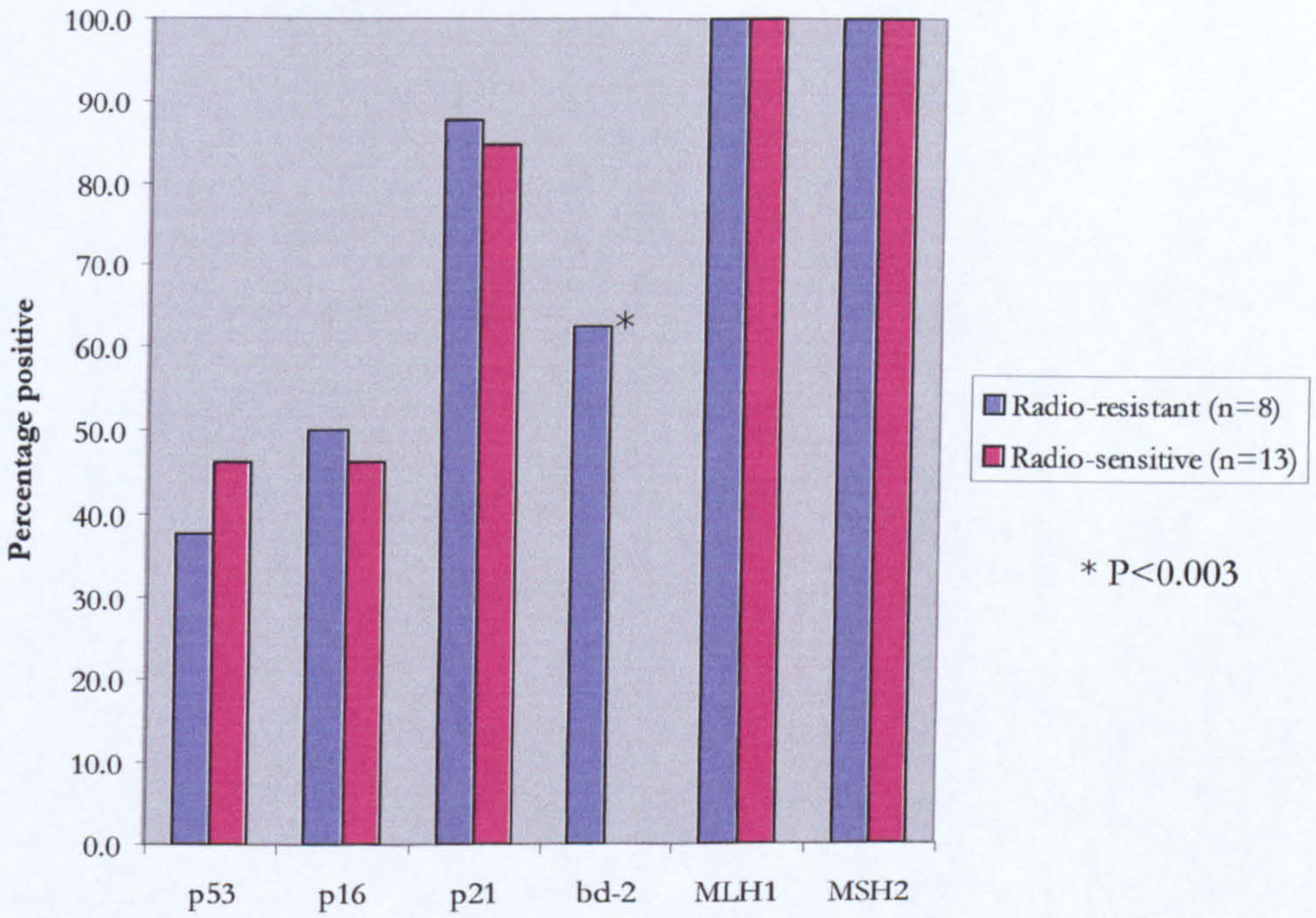

Figure 7.1 – Percentage of tumours positive for selected markers. Expression of the above tumour markers were graded as either positive or negative. Of the above markers, only bcl-2 demonstrated a significant difference between the radio-resistant (n=8) and radio-sensitive (n=13) tumours (P<0.003 – Fishers Exact test).

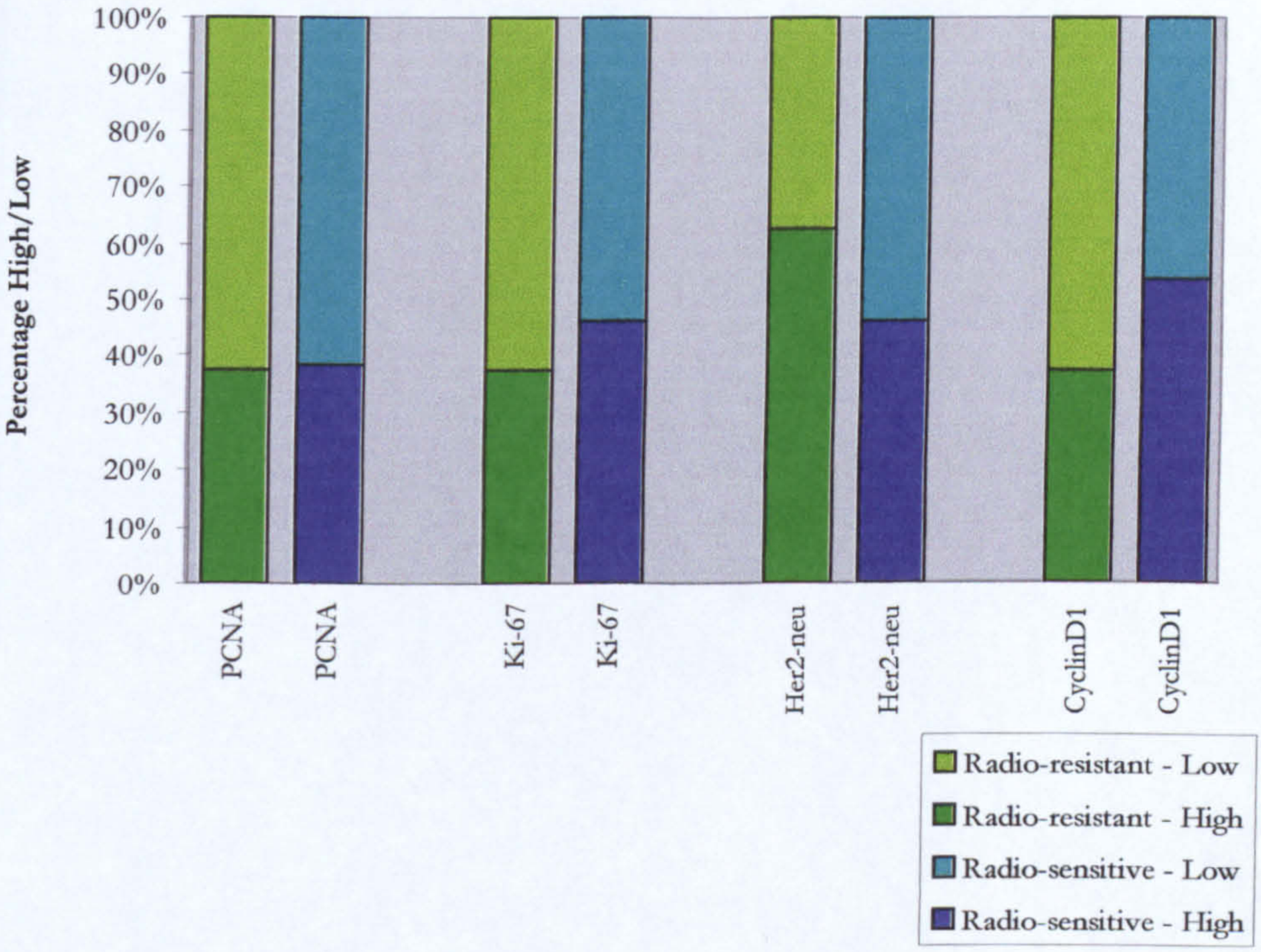

Figure 7.2 – Expression of tumour markers graded into high and low expression categories. No significant difference was identified between the frequency of high and low expression of the above markers between radio-resistant (n=8) and radio sensitive tumours (n=13).

Patient	RS/RR	p53	p16	p21	bcl2	MLH1	MSH2	PCNA	Ki-67	Her-2/neu	CyclinD1
1	RR	-	+	+	+	+	+	L	H	H	L
2	RR	-	+	+	-	+	+	L	L	L	L
3	RR	-	-	+	-	+	+	H	H	H	H
4	RR	+	+	-	+	+	+	L	H	L	H
5	RR	-	-	+	+	+	+	L	L	H	L
6	RR	-	-	+	-	+	+	H	L	H	L
7	RR	+	-	+	+	+	+	H	L	L	L
8	RR	+	+	+	+	+	+	L	L	H	H
9	RS	+	+	+	-	+	+	L	L	L	L
10	RS	+	-	+	-	+	+	L	H	L	H
11	RS	+	+	+	-	+	+	L	H	L	L
12	RS	-	+	+	-	+	+	L	L	H	H
13	RS	-	-	-	-	+	+	L	L	L	H
14	RS	-	-	+	-	+	+	H	H	H	H
15	RS	-	+	+	-	+	+	L	H	L	H
16	RS	+	-	+	-	+	+	H	L	H	L
17	RS	-	+	+	-	+	+	H	H	H	H
18	RS	+	-	+	-	+	+	H	H	H	L
19	RS	-	+	+	-	+	+	L	L	L	H
20	RS	-	-	+	-	+	+	L	L	H	L
21	RS	+	-	-	-	+	+	H	L	L	L

Table 7.5 – Summary of all immunohistochemical stains performed. Staining patterns were graded as either presence (+) or absence (-) of antigen or into high (H) and low (L) expression categories. RR – Radio-resistant; RS – Radio-sensitive.

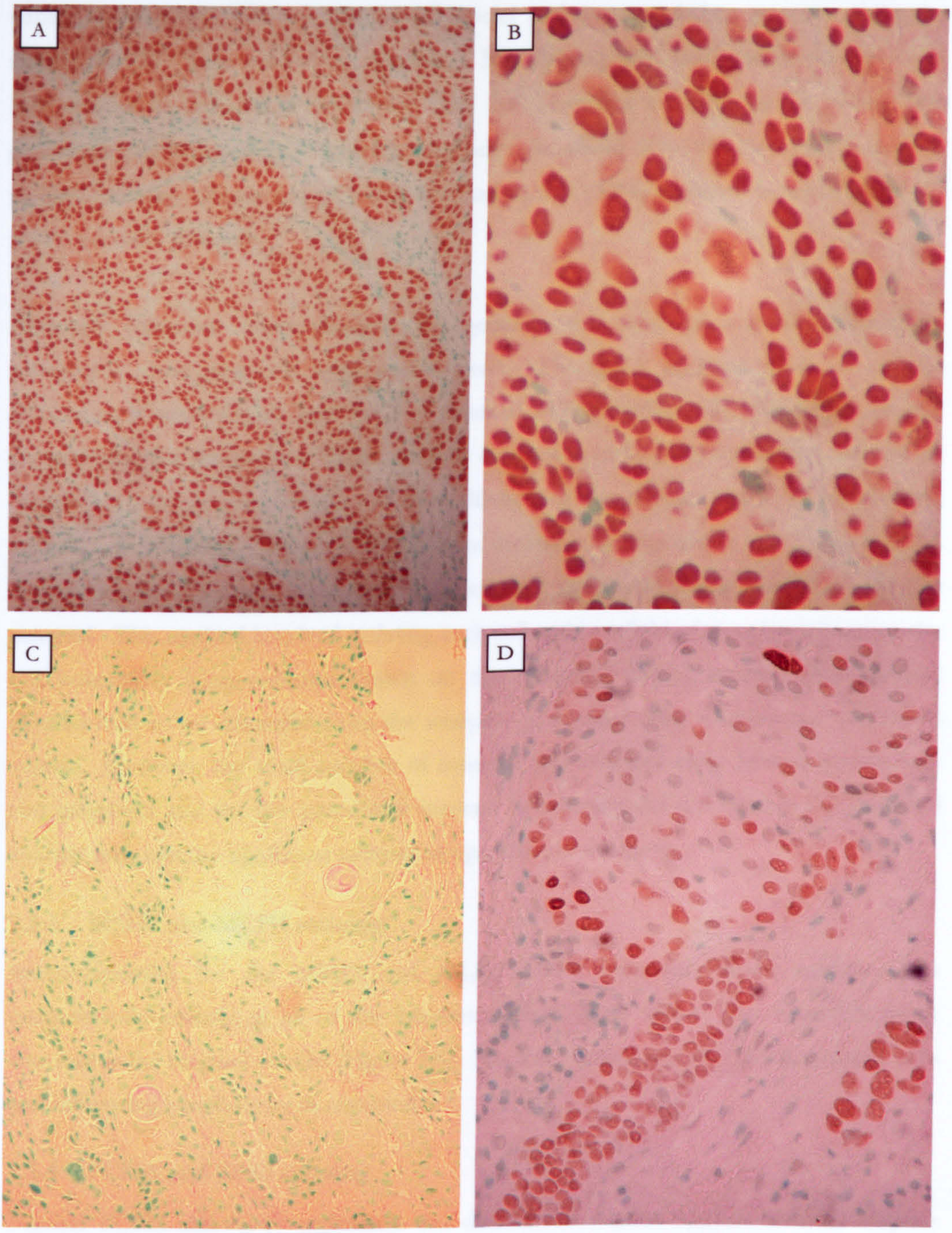

Figure 7.3 – p53 immunostaining. A - A representative image of a tumour demonstrating positive immunostaining for abnormal p53 (x100 magnification). **B** - Higher power magnification identifies abnormal p53 accumulated in the nuclei of all tumour cells (x400). **C** – A representative image of a tumour negative for p53, indicating the absence of accumulated abnormal p53 (x100). **D** – A further image of a tumour positive for p53 (x200). This image shows 'islands' and 'fingers' of p53 positive tumour cells growing into the surrounding stromal cells that are negative for p53 staining. Counterstain – Methyl Green.

strong staining in >30% of tumour cell nuclei and were graded as positive whilst the remaining 52% were graded as negative. No staining was seen within stromal cells. Independent image analysis using the CAS 200 identified a highly similar pattern and generated identical grading. For both methods a threshold of >50% was used to indicate positive staining. Abnormal p53 was detected in 3/8 (38%) resistant tumours and 6/13 (46%) sensitive tumours.

Although computer image analysis did generate the same grading as independent assessment some problems were encountered. The QNA program used for analysis allowed rapid screening of large fields of tissue at x400 magnification. Whilst this created no problems for the larger biopsies, marker expression in biopsies containing 'islands' or 'fingers' of tumour growth suffered from dilution of the tumour signal by surrounding stromal cells and small biopsies suffered from inclusion of edge effect (see Figure 7.3(D)). A more sophisticated program, allowing isolation of expression within individual cells was assessed. This method involved isolating each cell within a field of view by delineating the cell boundaries using contours drawn on the computer display screen. This method allowed cells to be discarded from the analysis, eg stromal cells, lymphocytes and blood vessels. However, the small number of resistant and sensitive cases limited grading into two categories and the few percentage increase in accuracy did not warrant the extended analysis time and the significant increase in operator involvement.

7.3.3 MSH2 and MLH1 staining

Immunostaining for the MSH2 and MLH1 DNA mismatch repair enzymes was unequivocally positive in all of the biopsies, indicating no loss of the mismatch repair enzymes in the biopsies studied (Figure 7.4). Nuclear staining was also seen in stromal cells and infiltrating lymphocytes as expected.

7.3.4 PCNA and Ki-67 staining

Nuclear PCNA and Ki-67 expression was detected in tumour epithelium in all biopsies (Figure 7.5 and 7.6). Tumours expressing PCNA in >30 % of cells were graded high and the remaining tumours graded low based on thresholds employed in previous studies (Storkel *et al*, 1993). High levels of PCNA positivity were detected at the same frequency in resistant (3/8 – 38%) and sensitive (5/13 – 38%) tumour biopsies. Ki-67 staining was graded as high if expression in >20 % of tumour cells, a threshold employed in other studies (Raybaud *et al*, 1997). Nuclear Ki-67 expression was detected at similar frequencies to PCNA in 3/8 (38%) resistant tumours and 6/13 (46%) sensitive tumours. Seven

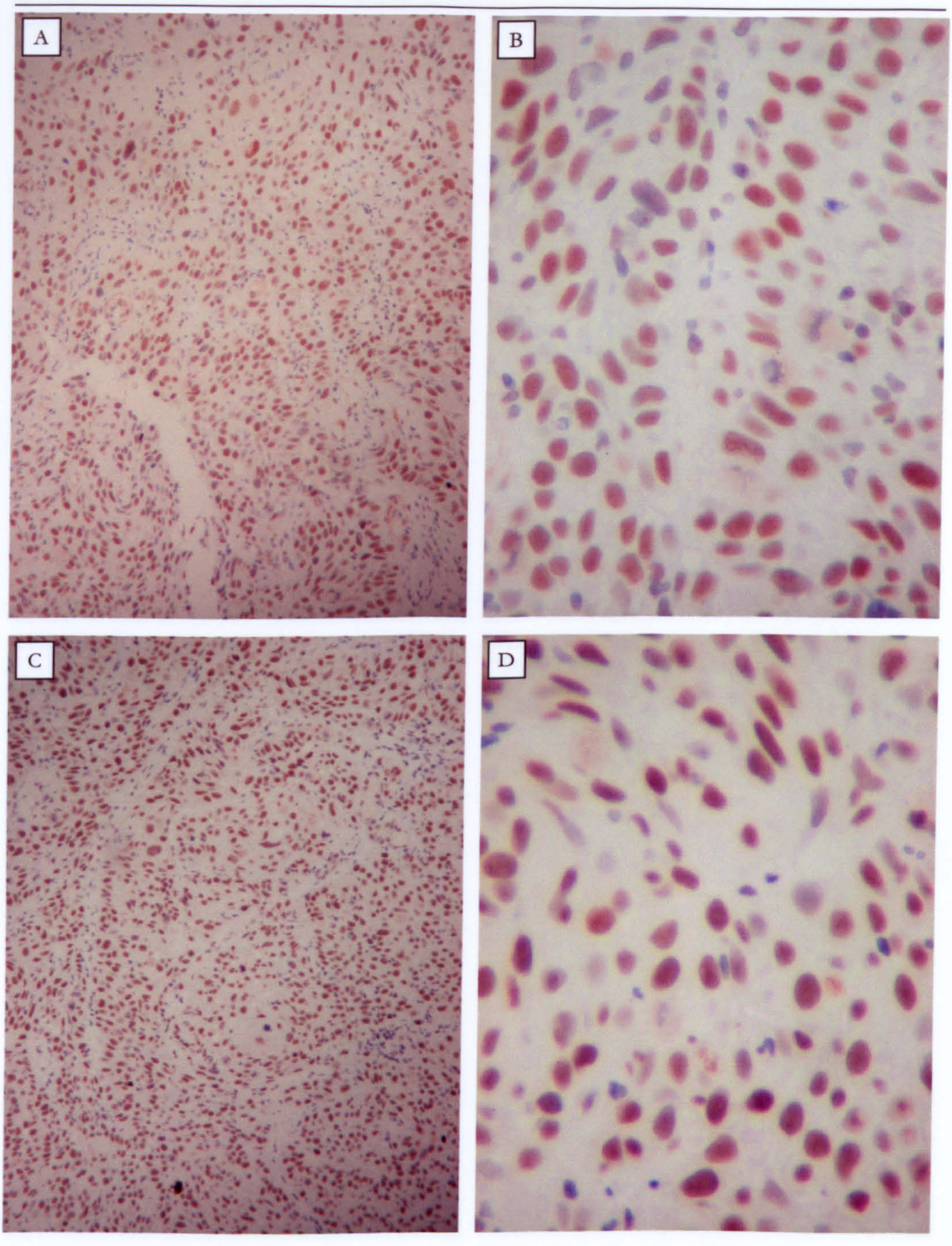

Figure 7.4 – MLH1 and MSH2 immunostaining. **A** and **B** – Low (x100) and high (x400) power magnification of MLH1 immunostaining respectively. **C** and **D** – Low (x100) and high (x400) power magnification of MSH2 immunostaining respectively. Staining for both MLH1 and MSH2 was localised to the nucleus and was positive for all tumours analysed. Counterstain – Haematoxylin.

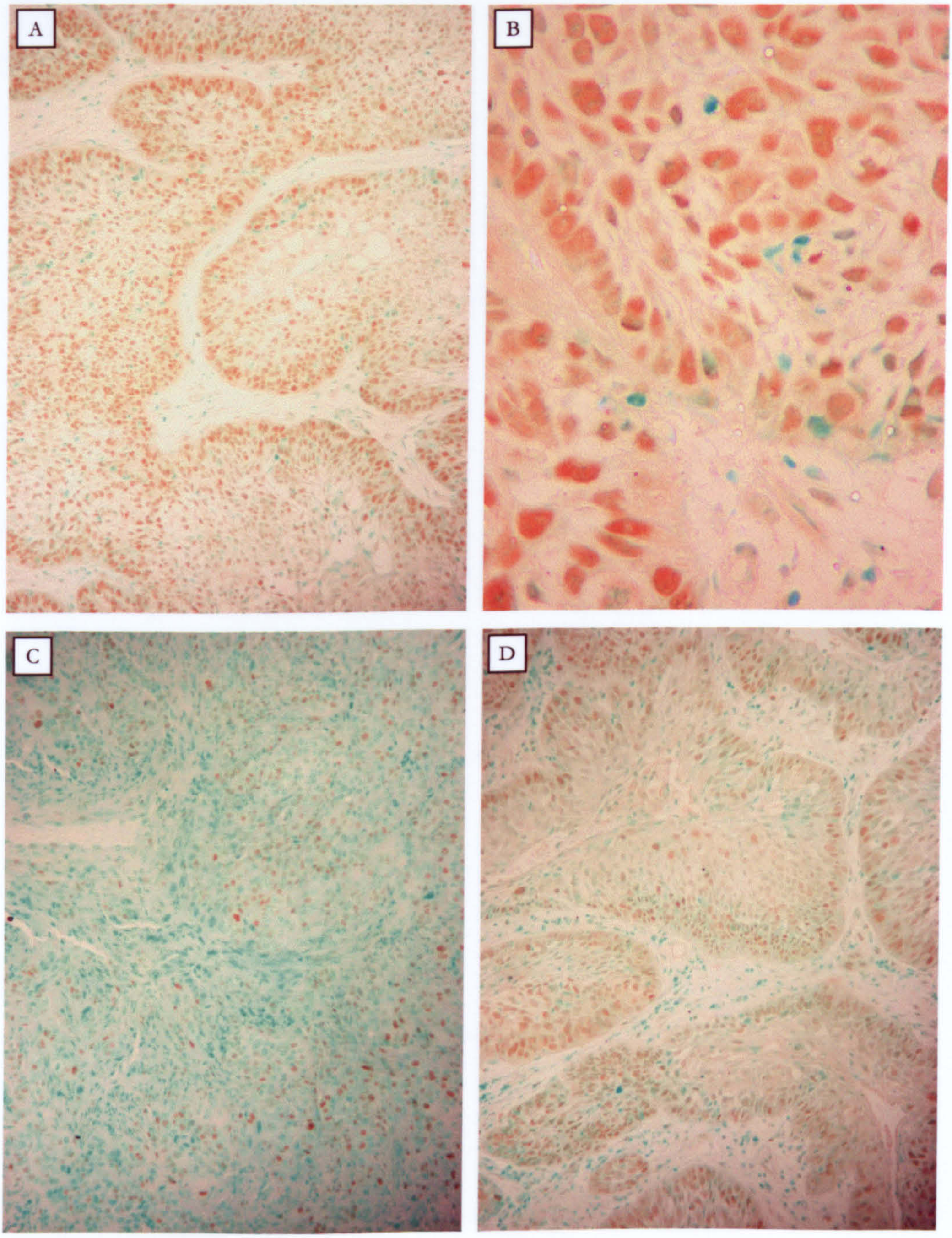

Figure 7.5 – PCNA immunostaining. **A** – Low magnification (x100) image of a tumour demonstrating high level of PCNA expression. **B** – High magnification (x400) image of the same tumour shows PCNA immunoreactivity in the majority of tumour cell nuclei. **C** – Low magnification (x100) image of a tumour demonstrating a low level of proliferation with PCNA staining a minority of tumour cell nuclei. **D** – Low magnification (x100) image depicting PCNA immunoreactivity within the nuclei of tumour cells at the periphery of islands of tumour cells. Counterstain – Methyl Green.

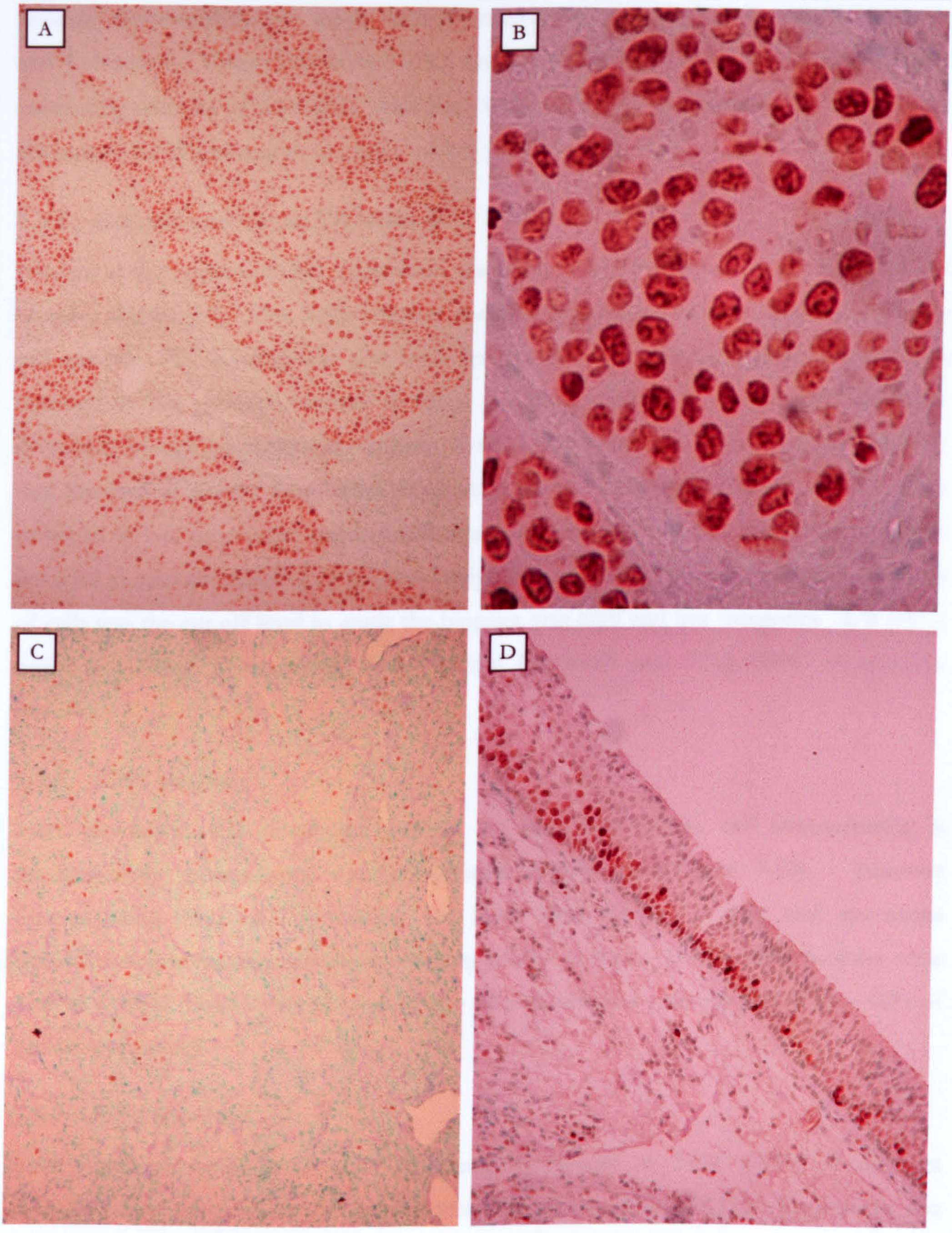

Figure 7.6 – Ki-67 immunostaining. **A** – Low magnification (x100) image of a highly proliferating tumour. **B** – High power magnification (x400) image of the same tumour demonstrating Ki-67 immunoreactivity in the majority of tumour cell nuclei. **C** – Low power magnification (x100) image of a tumour demonstrating low immunoreactivity for Ki-67. **D** – An example image of Ki-67 immunoreactivity within the basal epithelial layer (characteristic of some tumour biopsies). Counterstain – Methyl Green.

tumours demonstrated low levels for both markers of proliferation (3 resistant tumours and 4 sensitive). When comparing PCNA and Ki-67, 4 tumours demonstrated apparently conflicting patterns of expression with high levels of PCNA (a marker of S phase) in the absence of Ki-67 expression (a marker of cell proliferation).

7.3.5 p21, p16 and Cyclin D1 staining

Nuclear and cytoplasmic p21 expression was detected at low levels in all but 3 of the biopsies (Figure 7.7). One radio-resistant and 2 radio-sensitive tumours had no detectable p21 protein. P16 staining was also both nuclear and cytoplasmic (Figure 7.8) and was detected in two distinct patterns at either the leading edge of tumour cell islands or dispersed throughout tumour epithelium. Loss of p16 expression (<10% of cells positive) was detected at similar frequencies in resistant (4/8 - 50%) and sensitive (7/13 - 54%) tumours. A less prominent staining difference was seen with Cyclin D1, with expression detected in tumour nuclei of all biopsies analysed (Figure 7.9). Strong expression in >50% of cells was the cut off level to grade the biopsies into high and low categories. 3/8 (38%) resistant tumours demonstrated raised Cyclin D1 levels and 7/13 (54%) of sensitive tumours.

7.3.6 Her2 staining

Her2 expression was distributed around the periphery of the cell demonstrating a predominantly membranous and cytoplasmic distribution (Figure 7.10). Tumours demonstrating faint or no staining for Her2 were graded as low and specimens demonstrating prominent peripheral staining graded as high. 11/21 (52%) biopsies were seen to express raised levels of Her2 (5/8 – 63% of resistant tumours and 6/13 – 46% of sensitive tumours).

7.3.7 bcl-2 staining

bcl-2 expression was detected in the basal epithelium in 5/21 (24%) of tumours demonstrating a predominantly nuclear staining pattern (Figure 7.11). Expression was detected in stromal cells of all specimens but was completely absent from malignant epithelium of the remaining 16/21 (76%) specimens. Expression was exclusively detected in the resistant biopsies (5/8 – 63%) and not in the sensitive specimens (0/13).

7.3.8 Correlation of antigen expression with radio-resistance.

No relationship was identified between any of the antigens investigated and clinicopathological features. A statistically significant relationship was observed between bcl-2 expression and radio-resistant tumours ($p<0.003$ – Fisher's Exact test). With bcl-2

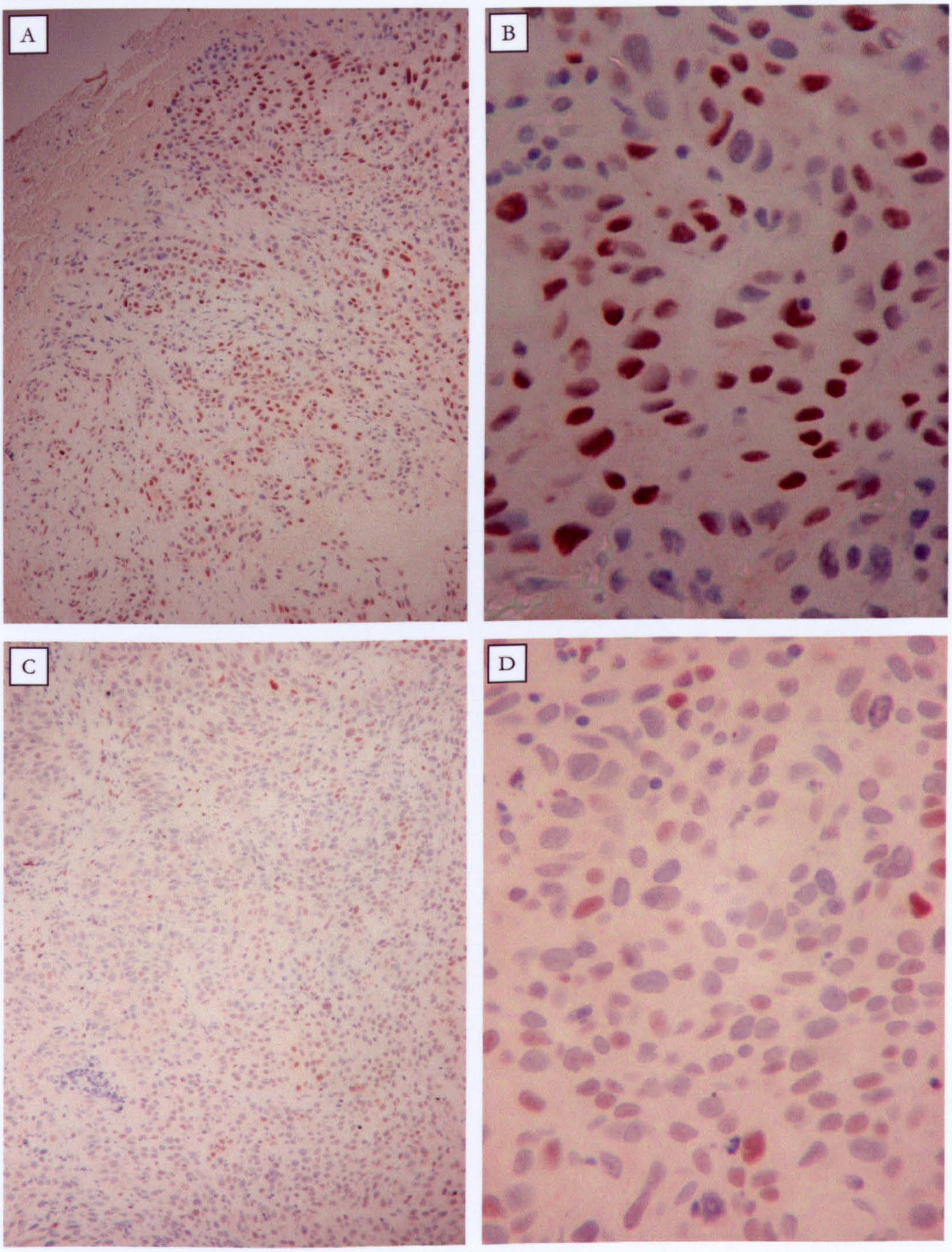

Figure 7.7 – p21 immunostaining. **A** – Low magnification (x100) image of a tumour demonstrating high levels of p21 immunoreactivity. **B** – High magnification (x400) identifies predominantly nuclear p21 staining. **C** – Low magnification (x100) image of a tumour demonstrating low levels of p21. **D** – High magnification (x400) demonstrates fewer nuclei positive for p21. Counterstain – Haematoxylin.

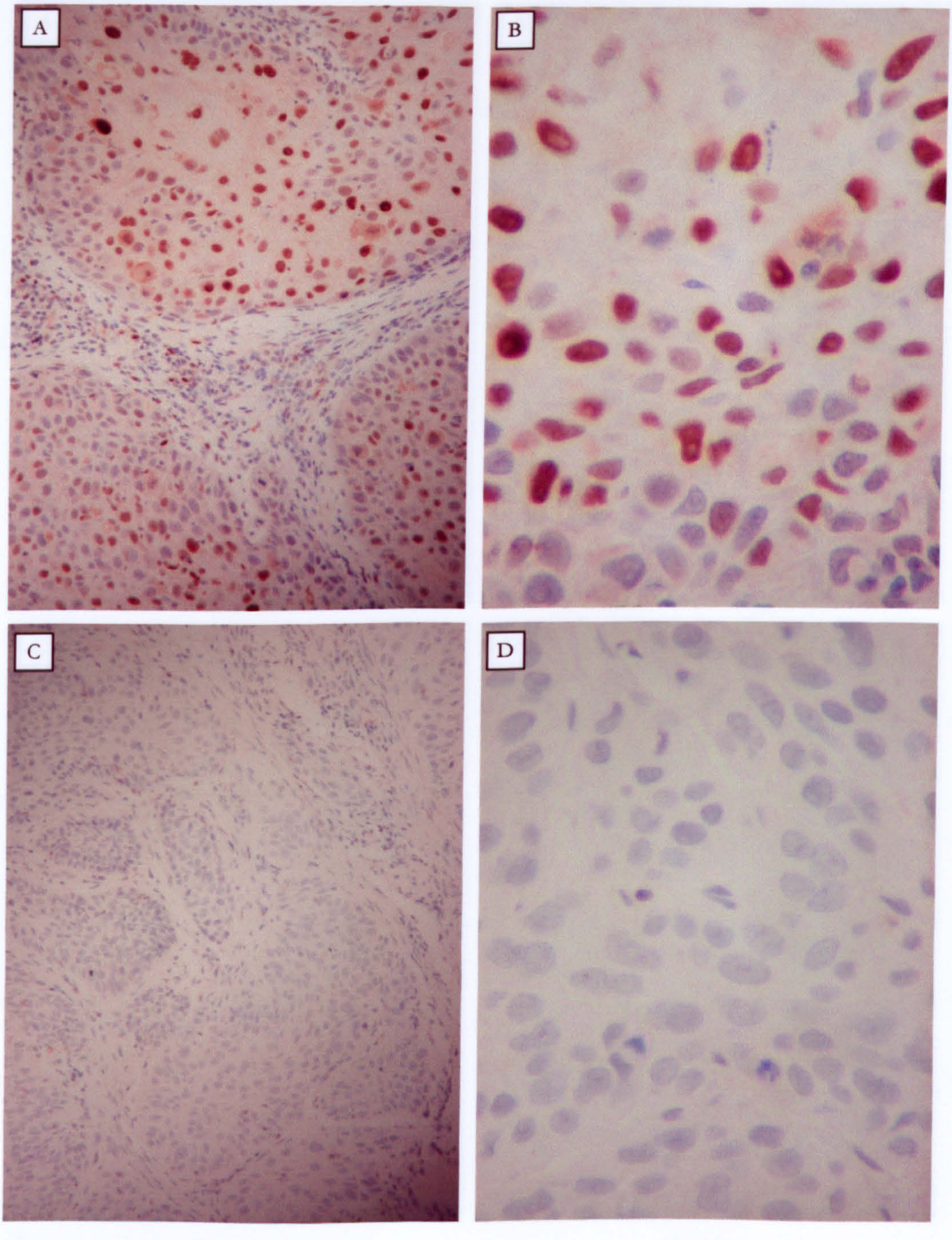

Figure 7.8 – p16 immunostaining. **A** – Low magnification (x100) image of a tumour demonstrating p16 immunoreactivity. **B** – High magnification (x400) image identifies p16 expression within the nuclei and cytoplasm of the majority of tumour cells. **C** – Low magnification (x100) image of a tumour demonstrating loss of p16 immunoreactivity. **D** – High magnification (x400) image of the same tumour. Counterstain – Haematoxylin.

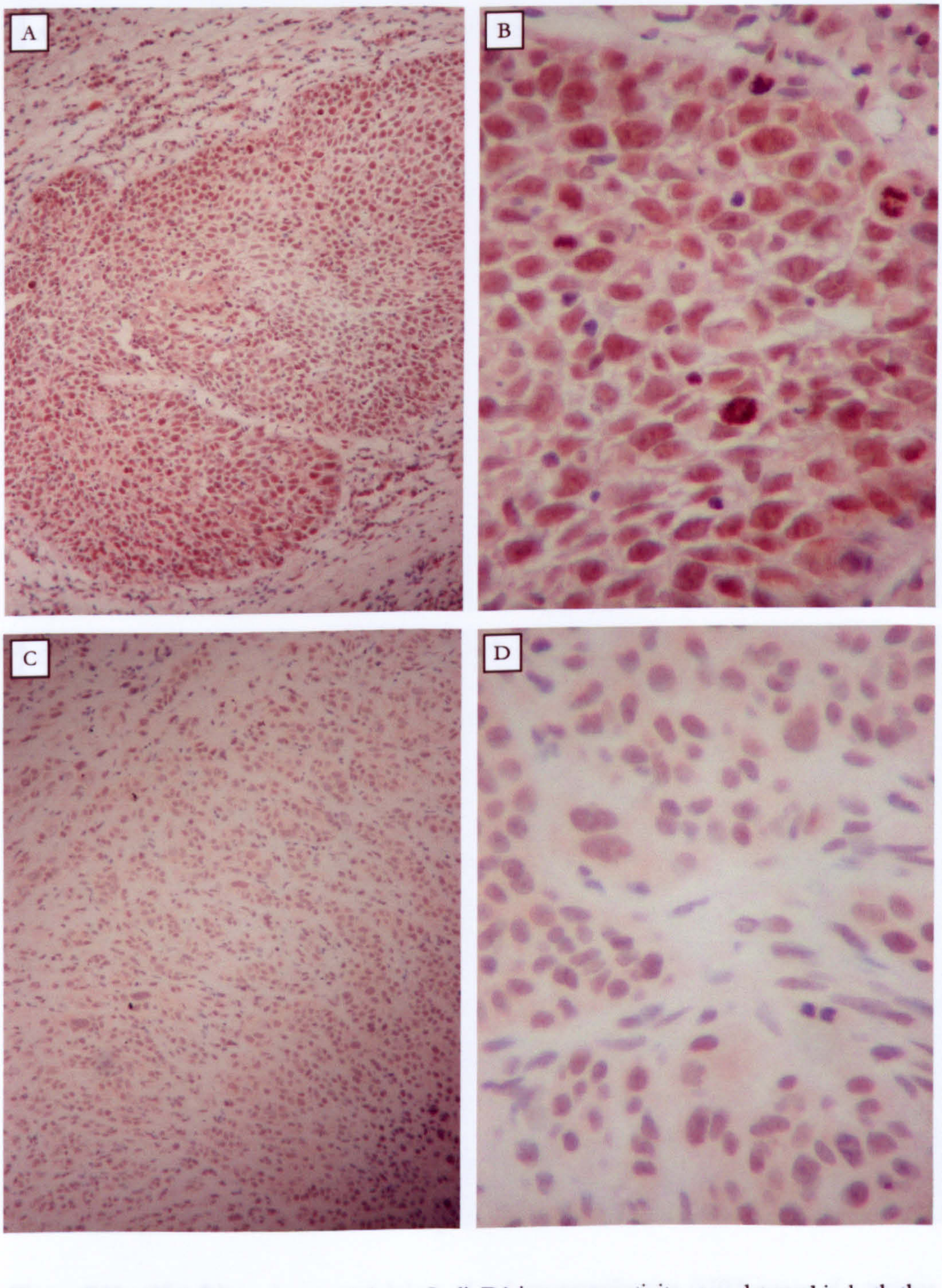

Figure 7.9 – CyclinD1 immunostaining. CyclinD1 immunoreactivity was detected in both the nuclus and cytoplasm. Immunoreactivity was detected in all biopsies and sections were graded as either high or low. **A** – Low magnification (x100) image of a tumour demonstrating high levels of immunoreactivity. **B** – High magnification (x400) identifies CyclinD1 predominantly in the nuclei with weaker cytoplasmic staining. **C** – Low magnification (x100) of a tumour demonstrating low levels of CyclinD1. **D** – High magnification (x400) demonstrates weaker nuclear and cytoplsmic staining. Counterstain – Haematoxylin.

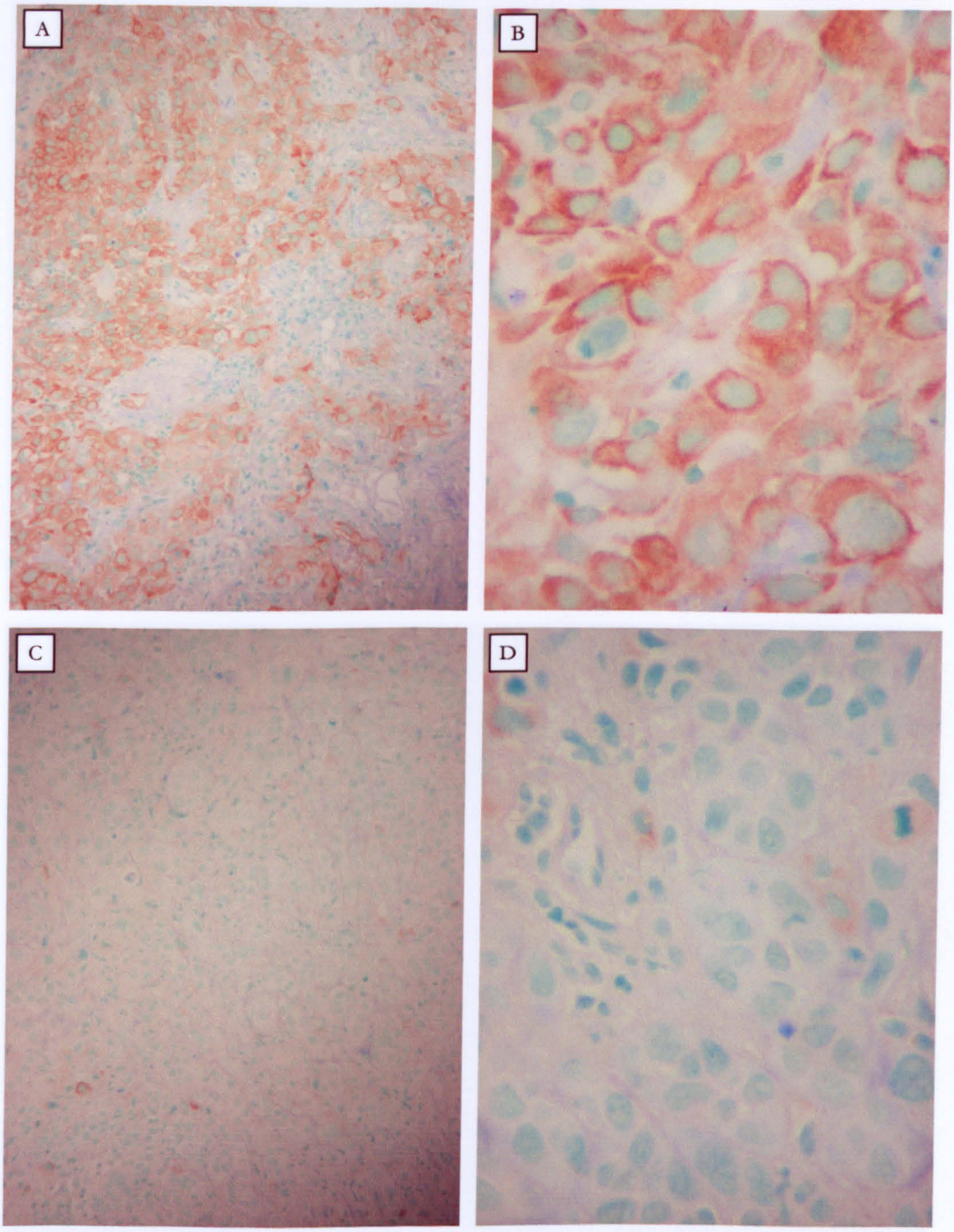

Figure 7.10 – Her-2/neu immunostaining._ A – Low magnification (x100) image of a tumour demonstrating high levels of Her-2/neu expression. **B** – High magnification (x400) image of the same tumour identifies Her-2/neu expression within the membrane and cytoplasm of tumour cells. **C** – Low magnification (x100) image of a tumour demonstrating low levels of Her-2/neu expression. **D** – High magnification (x400) image of the same tumour. Counterstain – Methyl Green.

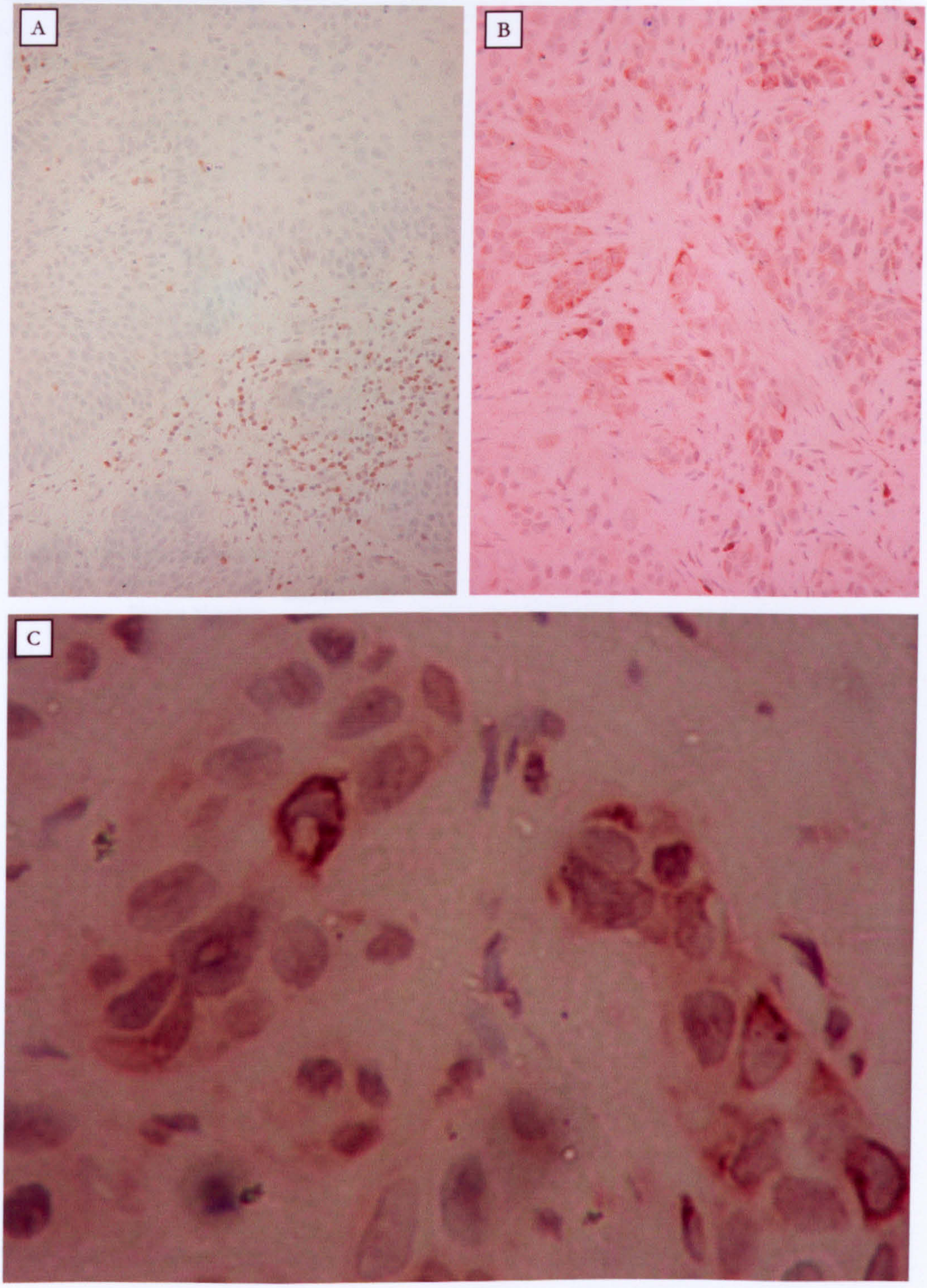

Figure 7.11 – bcl-2 immunostaining. **A** – A representative image of a tumour negative for bcl-2 staining (x100). bcl-2 immunoreactivity is absent from tumour cells but present within the cytoplasm of infiltrating lymphocytes and stromal cells. **B** – A representative image of a tumour positive for bcl-2 (x100). **C** – High power magnification of the same tumours identifies bcl-2 within the cytoplasm of tumour cells (x400). Counterstain – Haematoxylin.

Radio-resistant patients

Patient Number	Diploid/Non-diploid	DNA index (Dominant Clone)	Other Clones
01	Diploid	1.09	
02	Non-diploid	1.51	2.04
03	Diploid	1.08	
04	Non-diploid	1.64	2.37
05	Non-diploid	1.30	
06	Non-diploid	1.46	
07	Non-diploid	1.81	
08	Non-diploid	1.36	
		Mean = 1.42	

Radio-sensitive patients

Patient Number	Diploid/Non-diploid	DNA index (Dominant Clone)	Other Clones
09	Non-diploid	1.40	
10	Non-diploid	1.88	
11	Non-diploid	1.65	
12	Non-diploid	1.53	
13	Non-diploid	1.47	
14	Diploid	1.10	
15	Non-diploid	1.35	
16	Non-diploid	1.61	
17	Non-diploid	1.54	
18	Non-diploid	2.01	
19	Non-diploid	1.43	1.87
20	Diploid	0.91	
21	Diploid	1.07	2.12
		Mean = 1.46	

Table 7.6 – DNA ploidy index of the RR and RS tumours as determined by image cytometry. Tumours were classified as diploid if the DNA index was 1.0 ± 0.1. No difference was noted between the distribution of non-diploid tumours between the two groups (RR – 6/8; RS 10/13).

expression being restricted to resistant tumours (5/8 – 63%). None of the other markers investigated demonstrated a significant relationship with radiotherapy resistance with expression detected at similar levels in the two groups.

7.3.9 DNA ploidy

DNA diploid tumours were defined as those that demonstrated a single major peak with a DNA index within the diploid range (1.0 ± 0.1). This cut-off value reflects the recommendations of the CAS200 manufacturers (Becton Dickinson) and has been applied in other similar studies (Zatterstrom *et al*, 1991). No difference was noted in the mean DNA index of the two groups (RR- 1.42; RS- 1.46) (Table 7.6). Diploid tumours were identified at similar frequencies in both groups (RR- 25%; RS- 23%).

7.4 Discussion

Immunohistochemistry successfully localised the antigens chosen for this study. bcl-2 expression was the only marker to correlate significantly with the radio-resistant phenotype in this small sample of resistant and sensitive tumours. bcl-2 is known to be located within the mitochondrial membrane and can also be detected in nuclear envelope membranes and endoplasmic reticulum (Lithgow *et al*, 1994). In a mixed population of HNSCC (n=85) bcl-2 expression was detected at 24% and a significant correlation (p=0.002) was identified between bcl-2 detection, abnormal p53 and locoregional radiotherapy failure (Gallo *et al*, 1999). bcl-2 levels have been shown previously to be elevated in tumours resistant to drug therapy suggesting a dual role in both chemo- and radiotherapy resistance (Makin and Hickman, 2000).

Interactions between the two key apoptotic proteins bcl-2 and bax appear to be very influential in determining the balance between inhibition and induction of the apoptotic response. Both bcl-2 and bax exist as active homo-dimers or (inactive) hetero-dimers. Elevated levels of bcl-2 block apoptosis whilst elevated levels of bax induce apoptosis. Enhancement of radio-sensitivity has been observed in HNSCC cell line models treated with an anti-EGFR monoclonal antibody (Huang *et al*, 1999). This amplification of radiation induced apoptosis was associated with an increase in bax expression and concurrent decrease in bcl-2 expression. Transfection of bax into a HNSCC cell line has also demonstrated an enhancement of response to cisplatin suggesting a similar role for bax in improving the efficacy of chemotherapy (Sugimoto *et al*, 1999).

The significant correlation of bcl-2 over-expression and local recurrence after radiotherapy is more evidence highlighting the key role apoptosis has in most forms of therapeutic tumour regression. The apoptotic complex interacts with many other proteins and loss of regulation of several key molecules is highly likely to alter the fine balance of the apoptotic response. Transfection of bcl-2 antisense oligonucleotides has led to restoration of drug susceptibility in lung cancer cell lines (Zangemeister *et al*, 1998; Koty *et al*, 1999) and has been proposed as a therapeutic stratergy in lung and prostate cancers (Worden and Kalemkerian, 2000; Dipaola and Aisner, 1999). Interestingly antisense mRNA to bcl-xL, another apoptotic inhibitory molecule, has also demonstrated the same restoration of drug induced apoptotic cell death in lung and colon cell lines (Leech *et al*, 2000; Nita *et al*, 2000).

Wild type p53 normally inhibits bcl-2 expression, encouraging apoptosis, however, abnormal p53 expression was detected at similar frequencies in the resistant (36%) and sensitive (48%) tumours not supporting a role for p53 in radio-resistance. Several reports have attempted to define a role for p53 in radiotherapy failure based on its pivotal role in the detection of DNA damage and cell cycle arrest. Failure to successfully recognise genotoxic damage effected by ionising radiation is potentially a crucial determinant of radio therapy response. Several studies have reported correlation between abnormal p53 and radio-resistance (Raybaud-Diogene *et al*, 1997, Bristow *et al*, 1996) and restoration of p53 function into HNSCC induced mouse xenografts has been shown to restore the G1 block and sensitise cells to radiotherapy *in vivo* (Chang *et al*, 1997). However the literature remains divided. A recent study utilising full length gene sequencing of the p53 gene identified several genetic alterations in 48% of tumours with no correlation between p53 status in pre-treatment biopsies (n=42) and local recurrence after radiation therapy (Saunders *et al*, 1999).

The similar distribution of abnormal p53 between radio-resistant and sensitive tumours identified in this study suggests that p53 alone cannot explain radio-resistance and indicates that additional mechanisms are involved. Indeed the frequency of p53 mutations detected in HNSCC tumours (ranging from 37 to 91%; Smith and Haffty, 1999; Kropveld *et al*, 1999) is far greater than the incidence of radio-resistance, at most 30%, indicating that the majority of tumours with mutant forms of p53 are still able to undergo some form of cell death after radiotherapy. One explanation for the lack of p53 correlation is that different p53 mutations may affect function in different ways giving rise to protein products with varying capabilities. Alternatively, additional pathways designed to ensure apoptosis after

DNA damage might compensate for p53 deficiencies in sensitive tumours. Disruptions in these additional pathways are likely therefore to contribute also to radio-resistance.

p21 loss in tandem with abnormal p53 has been correlated with radio-resistance in colorectal cancer (Fu *et al*, 1998). No evidence for p21 involvement in radio-resistance was identified in this study with only 1 resistant and 2 sensitive tumours demonstrating loss of p21 protein product. Neither was their any significant correlation with Cyclin D1 or her2 and radiotherapy response.

Radio-resistant and sensitive tumours did not differ significantly in their expression of either marker of proliferation studied. It has long been known that ionising radiation is more effective against actively dividing cells. Low proliferation rate (as determined by Ki-67 immunohistochemistry) has demonstrated a relative risk of radiotherapy failure of 3.8 in a large study of HNSCC patients (n=101) (Raybaud-Diogene *et al*, 1997). No correlation was detected in the cohort reported in this study, possibly due to the small number of tumours included. One discrepancy which remained unexplained was the detection of high levels of PCNA in 4 tumours that demonstrated low levels of Ki-67. Ki-67 is expressed throughout the active stage of the cell cycle and absent only in G0, the resting phase (Figure 2.1). The expression of PCNA is limited to the S phase of the cell cycle, therefore PCNA expression would be expected to always be co-expressed with Ki-67, whilst Ki-67 expression could occur independent of PCNA expression. Tissue heterogeneity is unlikely to explain this discrepancy as the limitations of the small biopsies analysed ensured that the area of tumour analysed in each case was consistent. Two main patterns of PCNA staining were identified in samples categorised as positive, immunoreactivity in the majority of cells and immunoreactivity in cells at the periphery of tumour cell islands. The PCNA immunoreactivity detected at the periphery identified in some specimens may actually represent some artefact of the technique or antibody clone employed and may explain the discrepancy between the Ki-67 and PCNA proliferation indices.

7.5 Future directions

The mechanism of action of bcl-2 in cancer still remains to be fully elucidated and requires a larger study on HNSCC radio-resistant and sensitive tumours. A focussed study on key components of apoptosis in a larger series of HNSCC patients is warranted. bcl-x, bax, bid, bak and bik are all candidates for inclusion as are downstream effectors of the apoptotic response such as the Caspase system.

The original aim of this chapter was to investigate the issue of radio-resistance in laryngeal tumours at both the chromosomal and protein level. CGH may identify chromosomal loci of genetic abnormalities associated with the resistant phenotype. Conventional CGH could not be performed on the specimens due to the small size of the pre-treatment biopsies and universal amplification of the DNA contained within the specimens was required to generate enough labelled DNA for CGH. The technique of Degenerate oligonucleotide primed PCR (DOP-PCR) described by Telenius *et al* (Telenius *et al*, 1992) was attempted, however major complications were encountered with PCR contamination. At the time of this study, facilities were not available for performing DNA extractions and PCR reactions in a 'clean room'. Due to the nature of the degenerate primer, which is designed to amplify DNA throughout the genome without biasing a particular locus, it is inherently susceptible to contamination by extraneous DNA. As this technique was not satisfactorily optimised the methodology was omitted from Chapter 3. Combined with the emerging technology of laser capture microdissection (Emmert-Buck *et al*, 1996), DOP-PCR based CGH could potentially describe the genomic aberrations present in a minimal number of cells from the smallest neoplasm. Using this approach it is intended to pursue the question of radio-resistance in a larger cohort of tumours. Only one of the radio-resistant patients included in this cohort of tumours was confirmed as dead of disease at the time of writing this thesis. As the tumours studied were all early stage tumours this excellent survival rate, despite the initial failure of the radiotherapy, is to be expected with today's surgical techniques. However, the challenge of identifying radio-resistant tumours prior to therapy is still an important goal as the additional morbidity associated with 'salvage' surgery remains a major problem for patients who do not respond to initial radiotherapy.

Chapter 8

Statistical Analysis of CGH Data – Importance of 3q25-q27 in HNSCC

8.1 Introduction

The analysis of HNSCC clinical specimens by CGH, reported in Chapters 5 and 6, has successfully demonstrated the presence of chromosomal aberrations within samples of malignant tissue. More significantly, this analysis has demonstrated a specific pattern of aberrations in head and neck cancer indicating a 'non-random' distribution of the loci of DNA copy number change. This consistent pattern provides strong evidence for the chromosomal location of important genes, and alterations in these genes are likely to be important in the development of HNSCC. This poses the obvious question: can a combination of genetic aberrations predict the biological characteristics of the individual tumour and does knowledge of these aberrations impart diagnostic or prognostic information? In order to evaluate the potential clinical application of these genetic alterations, all the malignant specimens studied during the course of this thesis were compiled and statistical analysis was performed to identify correlations between specific genetic alterations and the clinical behaviour of the HNSCC tumours studied.

8.2 Materials and Methods

8.2.1 Patient details

In total CGH was performed as described in Section 3.8 on clinical specimens obtained from 51 patients including 46 primary tumours and 23 LNM. Both tumour and LNM specimens were obtained from 18 patients, specimens of LNM alone from 5 patients and specimens of tumour alone from 28 patients. All tumours analysed were squamous cell carcinomas. One patient (Pt. 8) had previous carcinoma of the lung whilst the remainder had no previous malignancies. All patients were treated with curative intent by surgical excision and all but 4 patients received post-operative radiotherapy. The clinicopathological details of all the patients are summarised in Table 8.1. The majority of patients were male (male:female ratio 2.9:1) with oropharyngeal/hypopharyngeal being the most common (41%), followed by laryngeal (35%) and oral cavity tumours (16%). Two tumours originated in the maxillary sinus and a further 2 were of unknown primary origin (only specimens of LNM were obtained from these two patients). Advanced tumours (T3/T4) predominated the cohort of specimens (73%) as did tumours with pathologically proven nodal metastases (69%). These values indicate the cohort of tumours studied were broadly representative of HNSCC cancer in the UK.

Follow up of patients lasted until 1 August 2001. The Mean duration of follow up was 41 months (Median = 44 months, range 7-65 months). During this period 23 tumours

	Number
Clinical Specimens [1]:-	
Primary Tumour	46
Nodal Metastasis	23
Sex:-	
Male	38
Female	13
Primary Site [2]:-	
Larynx	18
Oro/Hypopharynx	21
Oral Cavity	8
Maxillary Sinus	2
Unknown Primary	2
T Stage [2]:-	
T1	4
T2	8
T3	14
T4	23
Nodal Status:-	
Node Positive	35
Node Negative	16
Differentiation:-	
Well Differentiated	4
Moderately Differentiated	18
Poorly Differentiated	26
Un Differentiated	3
Recurrences [3]:-	
Local	7
Regional	16
Distant	4

Table 8.1 – Clinicopathological details of patients studied. Specimens were received from 51 patients in total. [1]For 18 patients tumour and LNM were obtained, for 28 patients tumour alone was obtained and for 7 patients LNM alone was obtained. [2]For 2 patients the site of the primary was unknown (only nodal specimens were received). [3]Tumour recurrence occurred in 23 patients including 3 cases of recurrence at more than one site (1 case of local and regional recurrence, 1 case of local and distant recurrence and 1 case of local, regional and distant recurrence).

recurred (45.1%) of which 4 were local recurrences, 14 were regional, 2 were distant and 3 patients recurred at more than one site. Twenty patients died (39%) of which 19 cases were confirmed as dying of HNSCC disease including one death due to post-operative complications after surgery for a T_4N_0 postcricoid carcinoma extending to the upper oesophagus. The remaining deceased patient died in hospital after subsequently undergoing a bowel resection for diverticulitis and the exact cause of death was unclear.

8.2.2 CGH

Specimens were collected and CGH performed as described in Section 3.6 to 3.8.

8.2.3 Statistical analysis

Statistical analysis was performed using SPSS version 10. The department of Applied Statistics, University of Hull provided advice on the statistical analysis. Survival analysis was performed using the Kaplan-Meier method. Survival analysis was performed in February 2002 and all patients alive at the time of analysis were censored accordingly. The difference in the survival curves was tested for statistical significance using the log rank test. The differences in the frequencies of aberrations between the population of tumours and nodes, and between the node positive and node negative primary tumours was tested for significance using Fisher's exact test. In all cases values of $p<0.05$ were considered to be statistically significant.

8.3 Results

8.3.1 Survival analysis of clinicopathological details

Survival analysis was performed on the clinicopathological parameters of tumour site, T stage, N stage, tumour differentiation, and tumour recurrence. Unsurprisingly, tumour recurrence demonstrated the strongest association with survival ($p<0.0001$ – log rank test) with a mean survival for recurrent tumours of 26.0 months compared with 55.1 months for those tumours that did not recur (Figure 8.1). Tumours of the Oral cavity (n=8) demonstrated a reduced survival (mean = 31.0 months) compared with tumours of other sites (mean 44.3 months) however this association was not significant ($p=0.1033$ – log rank test). No association was demonstrated for laryngeal or oro-hypopharyngeal tumours. Tumours with pathologically proven LNM at time of diagnosis had a mean survival of 39.4 months compared with 45.6 months for those without. This association was not significant (Figure 8.2; $p=0.3366$ – log rank test). When tumours which subsequently developed LNM were included in the node positive group this association was stronger but

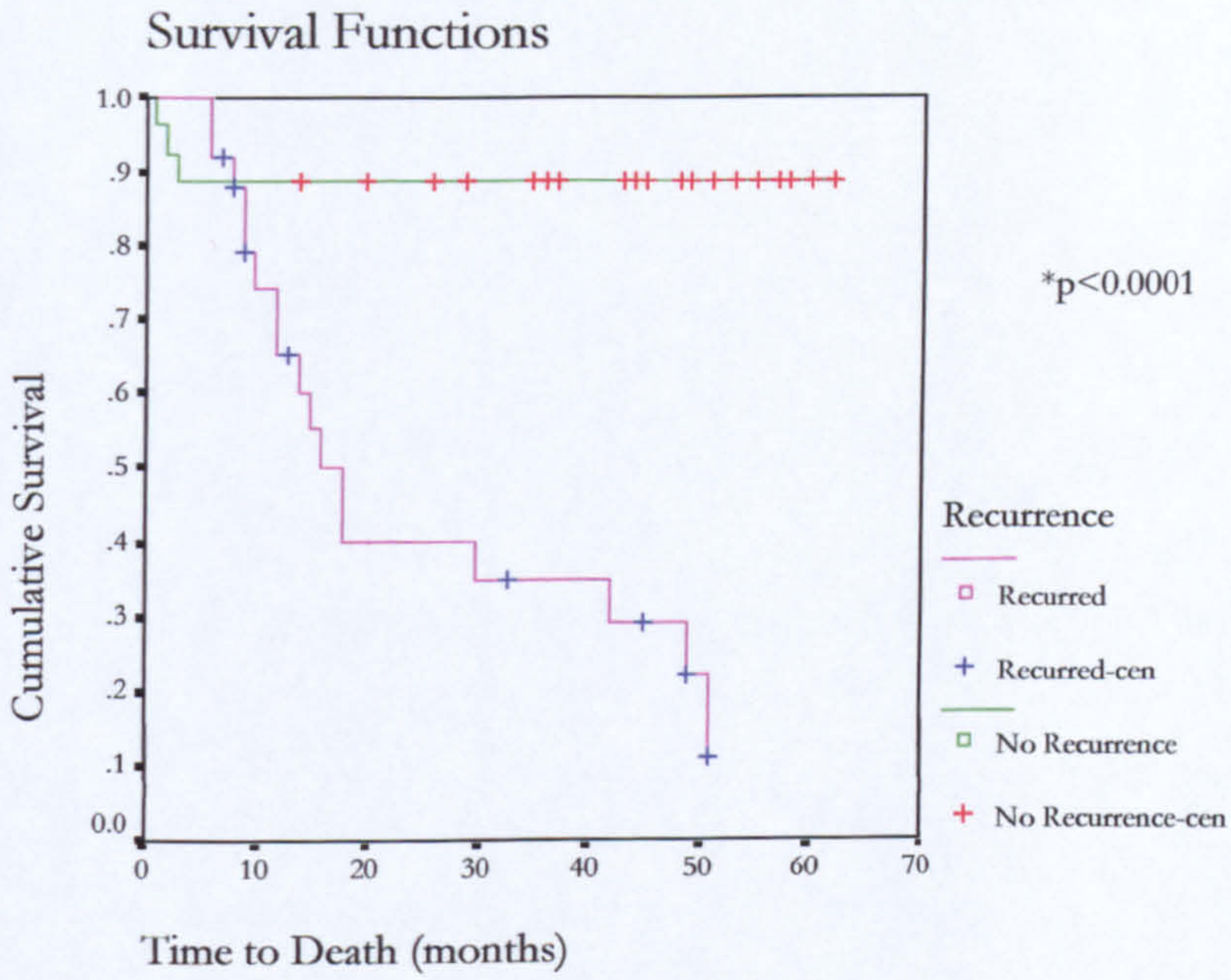

Figure 8.1 – Kaplan-Meier survival analysis for recurrent tumours. A highly significant association was identified between tumour recurrence and reduced survival. The purple line represents tumours which recurred (with censored events indicated by blue crosses) and the green line represents tumours which did not recur (censored events indicated by red crosses). Survival is expressed as the proportion of patients

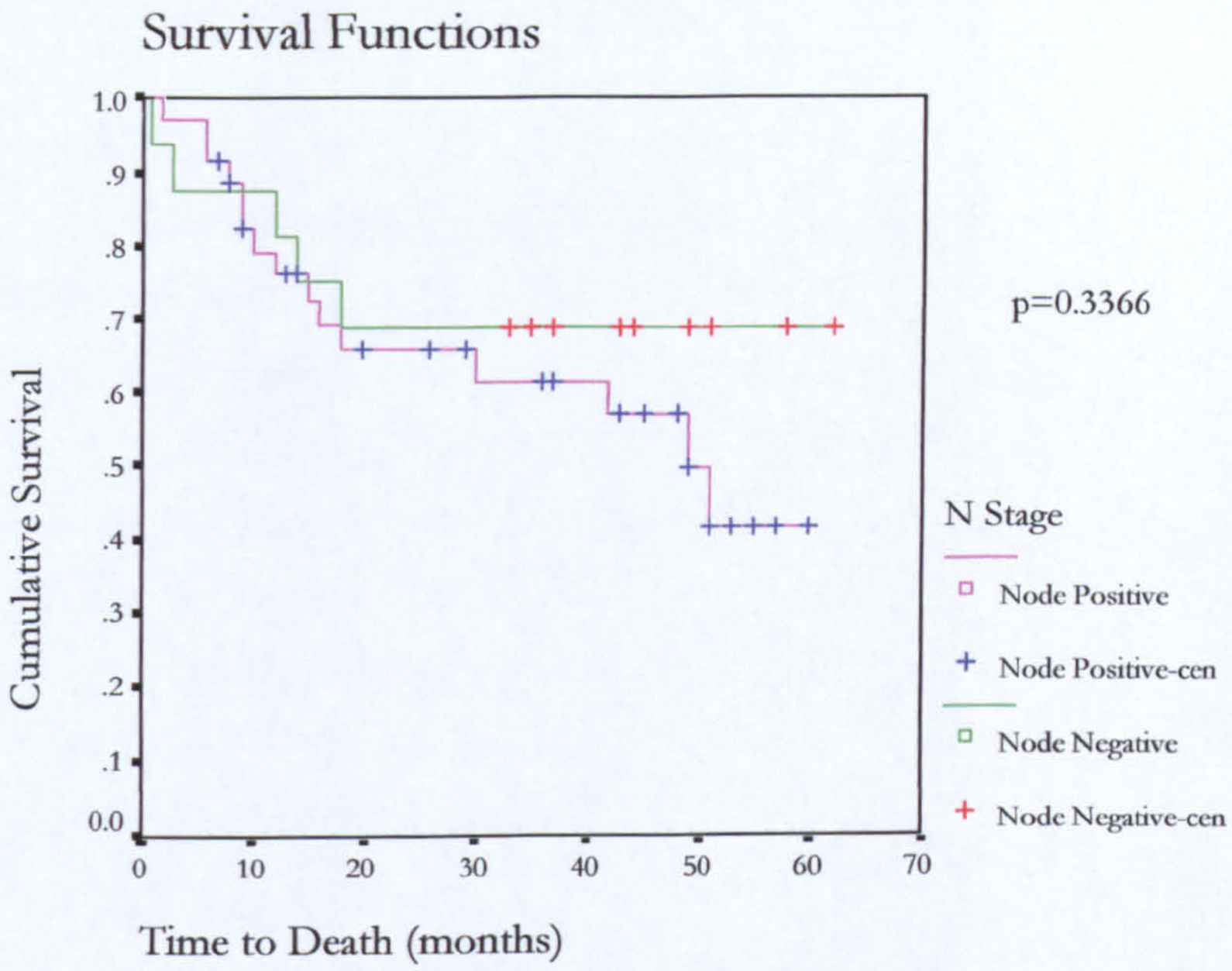

Figure 8.2 – Kaplan-Meier survival analysis for nodal stage. An association was identified between positive lymph nodes at diagnosis (n=35; upper plot) and reduced survival, however this did not reach significance. When those tumours which subsequently developed nodal metastases were included (n=37 total) this association was stronger but still not significant.

again failed to reach significance (p=0.2812 – log rank test). No significant correlation between tumour stage or differentiation and survival was noted.

8.3.2 CGH Data

Chromosomal aberrations were detected in 39 of the 46 tumour specimens (85%) and 22 of 23 nodal specimens (95.6%). DNA deletions were identified at a slightly higher frequency than gains with an average of 7.2 losses detected in the 46 tumours (range 0-23) and 5.9 gains (range 0-21). This resulted in an average of 13.1 loci of copy number change in this cohort of tumours. Chromosomal aberrations were identified at a slightly higher frequency in the population of 23 nodal specimens with an average of 16.2 copy number changes per specimen (8.3 deletions (range 0-20) and 7.9 gains (range 0-16). No significant difference was noted between the mean number of aberrations detected within the pathological subtypes of HNSCC studied with a mean of 13.4 aberrations in the laryngeal tumours, 13.4 in the oro/pharyngeal tumours and 11.4 in the oral cavity tumours. A linear increase was noted in the mean number of aberrations and the pathological differentiation of the tumours and this is depicted in Figure 8.3. Well-differentiated tumours contained the fewest aberrations (mean = 9.0; n=3) followed by moderately differentiated tumours (mean = 12.65; n=17), poorly differentiated tumours (mean = 13.4; n=24) and finally un-differentiated tumours (mean = 19.0; n=2). When tumours were categorised using T stage this trend was not as clear, T1 tumours contained the fewest aberrations (mean = 6.8; n=4) however T4 tumours contained the next fewest aberrations (mean = 11.9; n=23). T2 tumours contained a mean of 14.6 aberrations (n=8) and T3 a mean of 16.7 aberrations (n=11). The mean number of aberrations in node positive tumours was slightly higher with an average of 14.0 aberrations per tumour (n=33) compared with 11.3 for node negative tumours (n=13).

8.3.3 Frequent loci of copy number change identified by CGH

Figures 8.4 to 8.8 depict the loci of frequent copy number aberration identified in all the 69 tumours and nodes (Figure 8.4), in the primary tumours alone (Figure 8.5), in the node positive tumours (Figure 8.6), in the node negative tumours (Figure 8.7) and in the LNM (Figure 8.8). These data are also tabulated and presented in Table 8.2. Gains of DNA were frequently detected (>20% of all 69 malignant specimens) on chromosome 1q, 2q, 3q, 4q, 5p, 6q, 7p, 7q, 8q, 11q, 13q, 18p and 18q and losses of DNA on chromosomes 1p, 2q, 3p, 4q, 5q, 7q, 8p, 9q, 10q, 11p, 11q, 13q, 17p, 18q, 19p, 21 and 22.

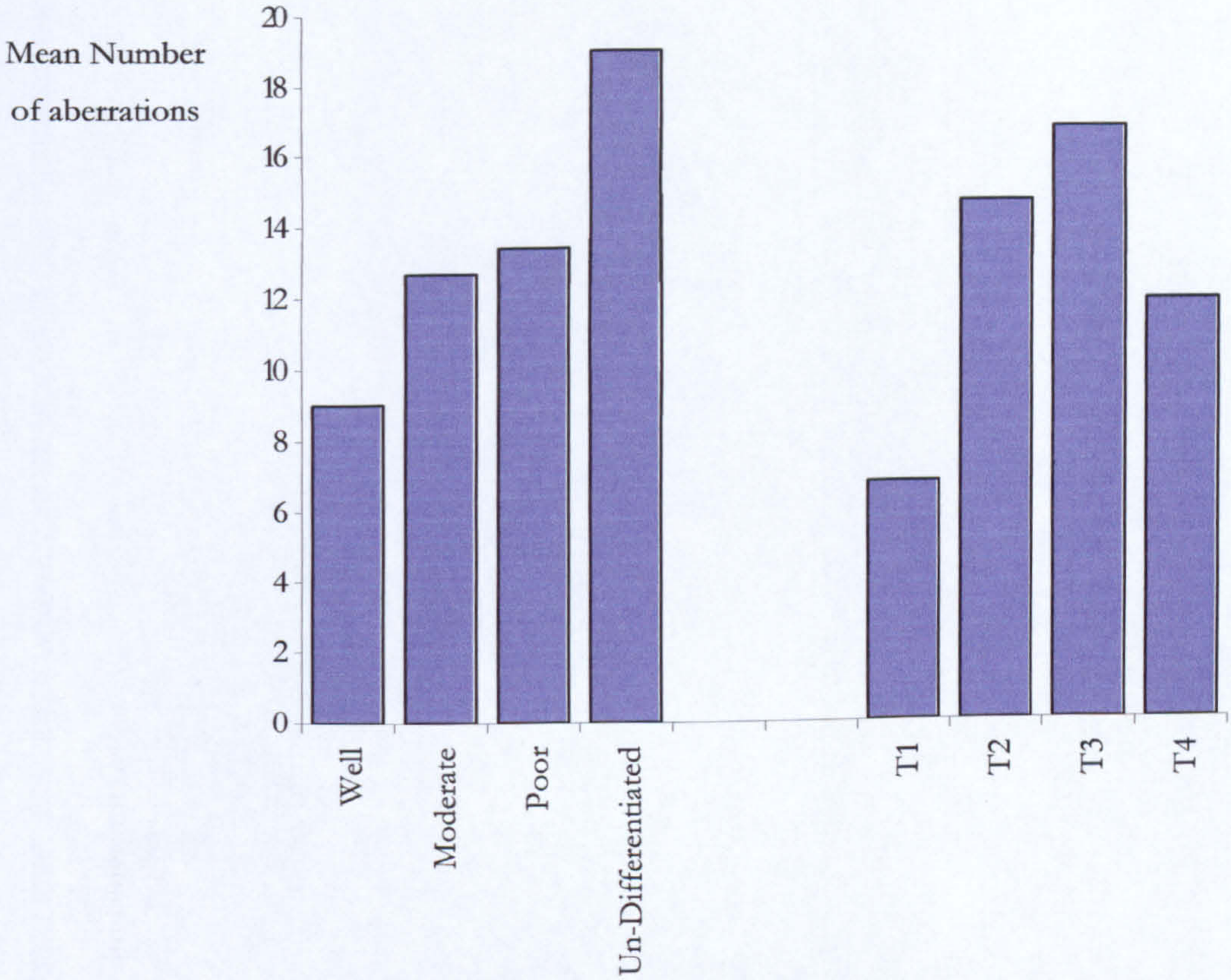

Figure 8.3 – Mean number of aberrations identified by CGH stratified according to pathological grade and staging. When tumours were categorised by pathological staging a linear increase in the mean number of aberrations was identified, however this trend was not as clear when tumours were grouped by T stage.

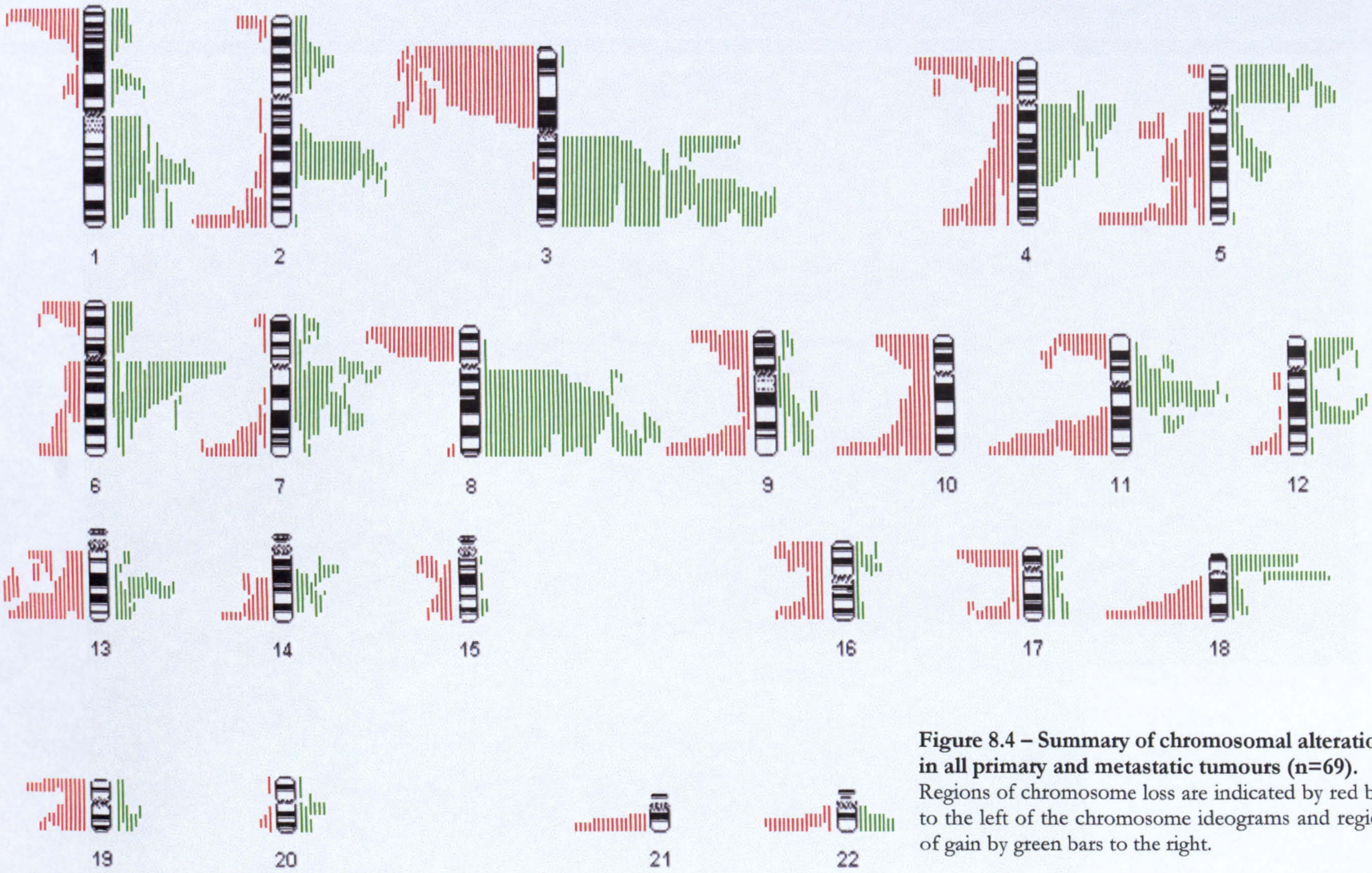

Figure 8.4 – Summary of chromosomal alterations in all primary and metastatic tumours (n=69).
Regions of chromosome loss are indicated by red bars to the left of the chromosome ideograms and regions of gain by green bars to the right.

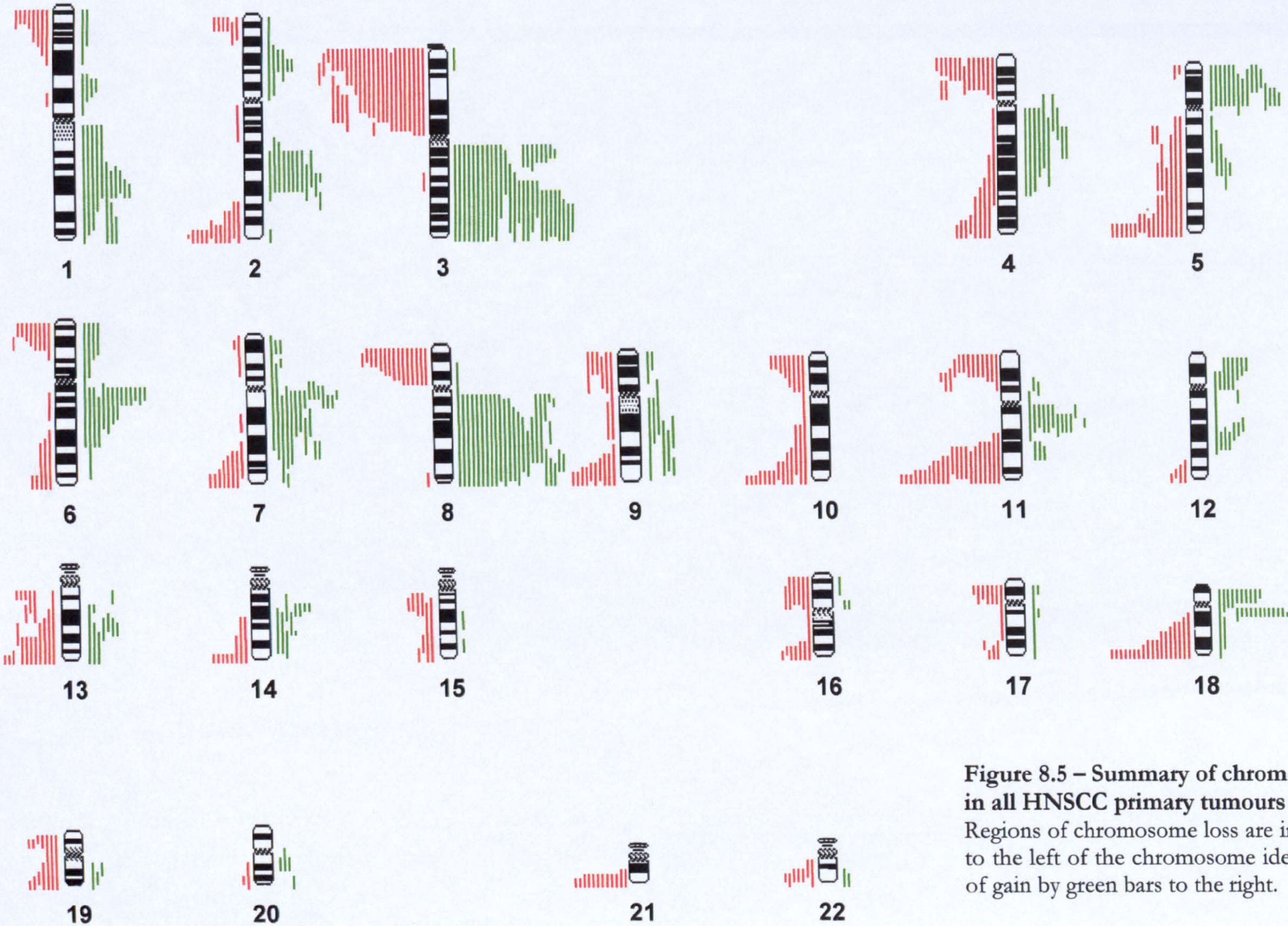

Figure 8.5 – Summary of chromosomal alterations in all HNSCC primary tumours (n=46).
Regions of chromosome loss are indicated by red bars to the left of the chromosome ideograms and regions of gain by green bars to the right.

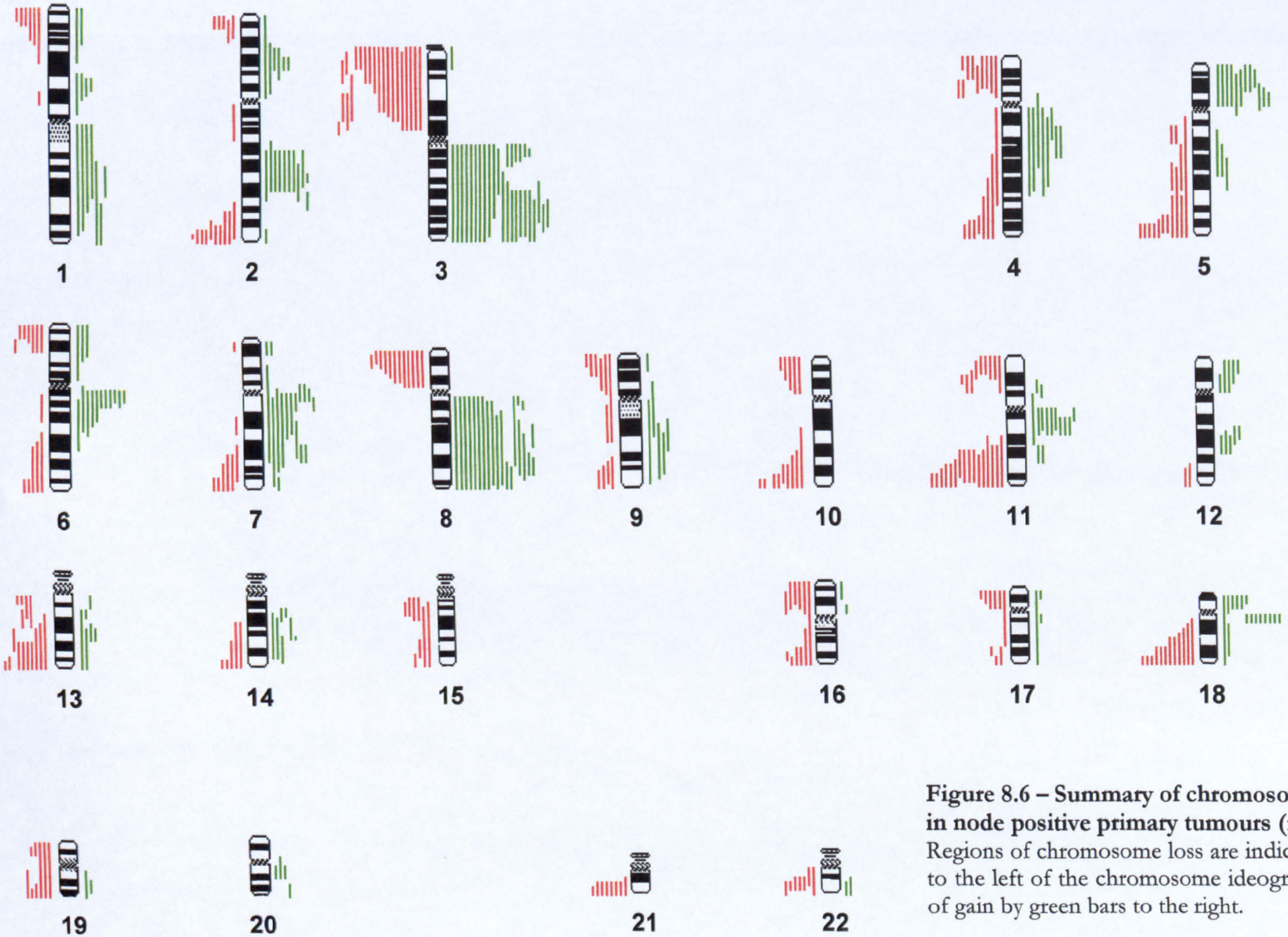

Figure 8.6 – Summary of chromosomal alterations in node positive primary tumours (n=33).
Regions of chromosome loss are indicated by red bars to the left of the chromosome ideograms and regions of gain by green bars to the right.

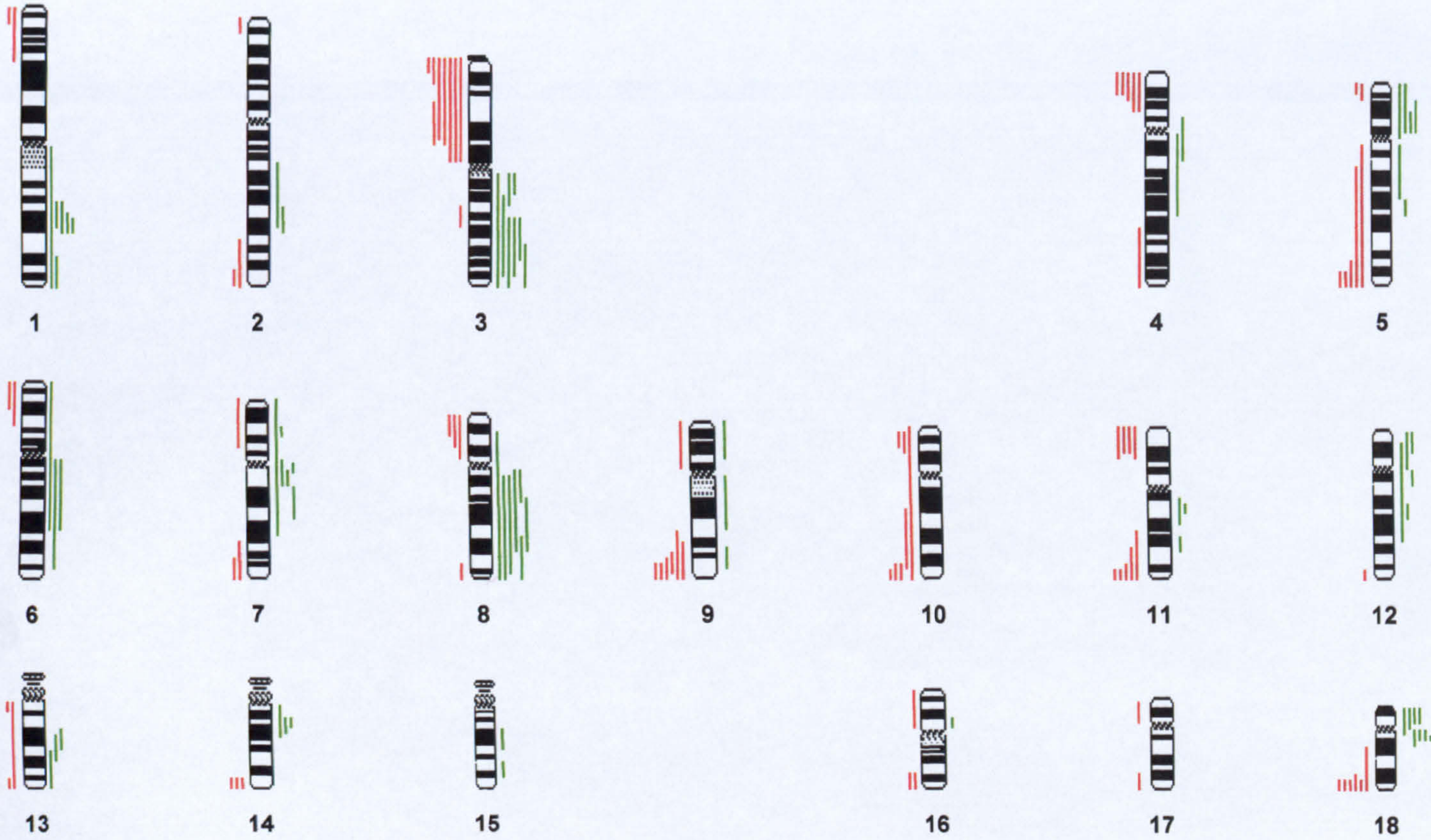

Figure 8.7 – Summary of chromosomal alterations in node negative primary tumours (n=13).
Regions of chromosome loss are indicated by red bars to the left of the chromosome ideograms and regions of gain by green bars to the right.

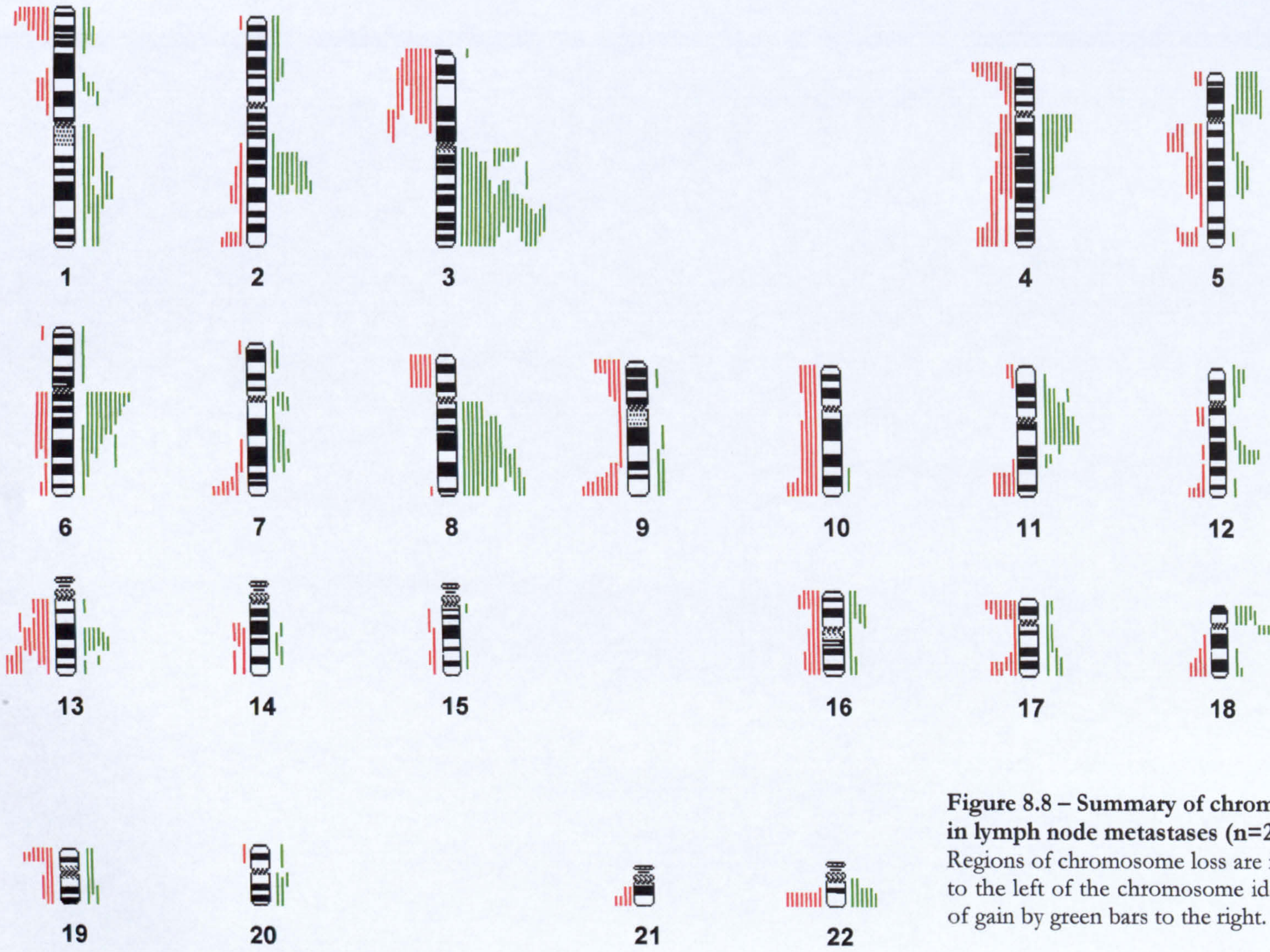

Figure 8.8 – Summary of chromosomal alterations in lymph node metastases (n=23).
Regions of chromosome loss are indicated by red bars to the left of the chromosome ideograms and regions of gain by green bars to the right.

Loci	Gain/ Loss	All Tumours and Nodes (n=69)	All Primary Tumours (n=46)	Node -ve Tumours (n=13)	Node +ve Tumours (n=33)	LNM (n=23)
1p34.2-pter	Loss	24.6	17.4	15.4	18.2	34.8
1q31-q32	Gain	26.1	23.9	38.5	18.2	30.4
2p14-p22	Gain	13.0	13.0	0.0	18.2	13.0
2q22-q32.1	Gain	30.4	26.1	15.4	30.3	39.1
2q36-qter	Loss	24.6	26.1	15.4	30.3	21.7
3pter-p22	Loss	44.9	52.2	53.8	51.5	34.8
3p21	Loss	39.1	45.7	46.2	45.5	30.4
3p14-cen	Loss	39.1	41.3	38.5	42.4	34.8
3qcen-q13	Gain	46.4	45.7	30.8	51.5	47.8
3q25-q27	Gain	65.2	56.5	38.5	63.6	82.6
4qcen-q21	Gain	31.9	30.4	38.5	27.3	39.1
4p15-pter	Loss	11.6	6.5	0.0	9.1	21.7
4q26-q28	Loss	18.8	17.4	7.7	21.2	26.1
4q31.3-qter	Loss	24.6	21.7	15.4	24.2	30.4
5p	Gain	33.3	34.8	30.8	36.4	30.4
5q12-q13	Loss	15.9	10.9	15.4	9.1	26.1
5q21-q23	Loss	14.5	13.0	15.4	12.1	17.4
5q32-qter	Loss	31.9	34.8	38.5	33.3	21.7
6qcen-q16	Gain	36.2	30.4	23.1	33.3	43.5
6q25qter	Loss	10.1	10.9	0.0	15.2	8.7
7p12-q11.2	Gain	27.5	32.6	30.8	33.3	17.4
7q22-31	Gain	23.2	19.6	15.4	21.2	30.4
7q32-qter	Loss	20.3	21.7	15.4	24.2	17.4
8p	Loss	29.0	32.6	23.1	36.4	21.7
8q	Gain	40.6	41.3	30.8	45.5	39.1
8q23-qter	Gain	55.1	52.2	46.2	54.5	60.9

Table 8.2 – Frequency of Genetic Aberrations in HNSCC. The loci of all the genetic aberrations identified are listed along with the frequency of detection in each of the tumour groups. (LNM – Lymph Node Metastasis; pter – p-telomere; qter – q-telomere; cen – centromere)

Loci	Gain/ Loss	All Tumours and Nodes (n=69)	All Primary Tumours (n=46)	Node -ve Tumours (n=13)	Node +ve Tumours (n=33)	LNM (n=23)
9p	Loss	18.8	15.2	7.7	18.2	26.1
9q32-qter	Loss	26.1	21.7	46.2	12.1	34.8
10p	Loss	17.4	17.4	23.1	15.2	17.4
10q25-qter	Loss	30.4	30.4	38.5	27.3	30.4
11p	Loss	21.7	28.3	30.8	27.3	8.7
11q12-q13	Gain	29.0	26.1	15.4	30.3	34.8
11q22-qter	Loss	39.1	45.7	38.5	48.5	21.7
12p	Gain	15.9	17.4	23.1	15.2	13.0
12q21-q22	Gain	18.8	15.2	15.4	15.2	26.1
12q24.1-qter	Loss	10.1	6.5	7.7	6.1	17.4
13q12-q14	Loss	15.9	15.2	15.4	15.2	17.4
13q21-q22	Loss	15.9	10.9	7.7	12.1	30.4
13q21-q22	Gain	20.3	15.2	23.1	12.1	26.1
13q31-qter	Loss	26.1	26.1	15.4	30.3	30.4
14q21-q23	Gain	14.5	17.4	23.1	15.2	8.7
14q24-qter	Loss	15.9	17.4	23.1	15.2	8.7
16p	Loss	15.9	15.2	7.7	18.2	21.7
16q22-qter	Loss	15.9	17.4	15.4	18.2	17.4
17p	Loss	20.3	15.2	7.7	18.2	30.4
17q24-qter	Loss	15.9	10.9	7.7	12.1	26.1
18p	Gain	21.7	21.7	30.8	18.2	21.7
18q11	Gain	23.2	28.3	30.8	27.3	13.0
18q21-qter	Loss	31.9	39.1	46.2	36.4	17.4
19p	Loss	20.3	15.2	15.4	15.2	30.4
19q13-qter	Loss	15.9	15.2	7.7	18.2	13.0
21	Loss	23.2	28.3	38.5	24.2	17.4
22	Gain	11.6	4.3	0.0	6.1	26.1
22	Loss	21.7	17.4	7.7	21.2	34.8

Table 8.2 – Frequency of Genetic Aberrations in HNSCC (continued).

8.3.4 Structural manifestation of chromosomal aberrations

Many of the aberrations identified consisted of the gain or loss of entire chromosomes (chromosomal aneuploidy) or chromosome arms. 26 incidences of whole chromosome aneuploidy were identified in the 69 malignant specimens with losses outnumbering gains. These included complete loss of chromosomes 19 (5 cases), 10 (4), 21 (4), 16 (3), 13 (2), 15 (1), 17 (1) and 22 (1) and complete gain of chromosomes 17 (2 cases), 22 (2), 18 (1) and 19 (1). Gain of the entire chromosome arm was identified on chromosomes 8q (14 cases), 3q (12), 5p (11), 18p (7), 12p (5), 1q (2), 2p (2), 6p (2), 7q (1), 20p (1) and 20q (1). Loss of the entire arm was identified on chromosomes 8p (12 cases), 3p (9), 17p (8), 4p (7), 9p (5), 16p (3), 18q (3), 5q (2), 10p (2), 19q (2), 4q (1), 11p (1), 16q (1), 20p (1) and 20q (1). Simultaneous gain of material from one arm and losses of material from the other was identified in a substantial number of cases. These included 3p loss/3q gain (28 cases), 8p loss/8q gain (13), 5p gain/5q loss (9) and 18p gain/18q loss (5). Several of these cases constituted the simultaneous gain of the entire arm and loss of the other, suggestive of isochromosome formation, including 3p loss/3q gain (13 cases), 8p loss/8q gain (10) and 18p gain/18q loss (1). A distinct pattern of gain and loss was also noted on chromosome 11 however in this instance the centromeric breakage was not involved, instead simultaneous gain of 11q13 and loss of 11q23-qter was consistently detected in 15 cases.

The distribution of chromosomal abnormalities identified by CGH depicted in Figures 8.4 to 8.8 demonstrates the non-random nature of the chromosome aberrations. Several regions of DNA gain and loss were seen to overlap allowing the delineation of minimal regions of gain and loss (MRG and MRL respectively).

8.3.4.1 Chromosomal regions of gain identified by CGH

The most frequent locus of chromosomal gain in all 69 malignant specimens was identified on chromosome 3q. In 12 specimens (17.5%) the entire long arm of chromosome 3 was found to show an increase in copy number. In a further 8 specimens (11.6%) gain of the whole arm was suggested however the CGH ratio for the sub-centromeric region of 3q (3qcen-3q13) did not exceed the threshold for copy number increase. Two distinct MRG were identified on 3q: 3q25-q27 (65.2%) and 3qcen-q13.3 (46.4%). The second most common DNA gain was localised to 8q. In a pattern similar to 3q, gain of the whole arm was identified in 14 cases (20.3%) and a MRG localised to 8q23-qter (55.1%). Gain of material on 4q and 6q followed a similar pattern with the size of gain ranging from small (10-20Mb) regions of DNA at the centromere, to gains encompassing the majority of the

arm. Because of this, the MRG for both chromosomes was limited to a short, sub-centromeric region specifically 6qcen-q16 (36.2%) and 4qcen-q21 (31.9%). However, detection of gains at the centromeres of chromosomes by CGH is notoriously unreliable and should be interpreted with caution. The MRG 2q31-q32.1 was gained in 30.4% of cases with the majority of these cases (15/21) demonstrating gain of a consistent sized chromosomal region 2q23-q32.1. Gain of material on 11q13, a frequent finding in classical G-banding analysis of HNSCC (Meredith *et al*, 1995; Akerval *et al*, 1995), was identified in 29.0% of cases. Gain of material on chromosome 7 apparently overlapped the centromeric portion with a MRG mapping to 7p12-q11.2 (27.5%). The MRG on chromosome 1q was mapped to 1q31-q32 and detected in 26.1% of cases. Other MRG included 18q11 (23.2%), 7q22-q31 (23.2%), 18p (21.7%), 13q21-q22 (20.3%), 12q21-q22 (18.8%), 12p (15.9%) and 2p14-p22 (13%).

8.3.4.1.1 High level gains (amplifications)

Several regions of high level gain, indicative of gene amplification, were identified in the cohort of specimens. High level gains were defined as a fluorescent ratio of >1.5, a value adopted in other CGH studies (Hermesen *et al*, 2001). The chromosomal loci of these amplifications are depicted in Figure 8.9 and were limited to relatively few regions of the genome. The most common site of amplification, occurring in 12 primary tumours and 9 LNM, was chromosome 3q with a region of common overlap localised to 3q25-q27. Copy number alterations on 3q demonstrated several distinct patterns of manifestation and are detailed in Figure 8.10 and Table 8.3. Figure 8.10 (A) demonstrates a low level gain of the entire long arm of chromosome 3q suggestive of a duplication. Figure 8.10 (B) represents gain of the entire arm with additional high level gain (amplification) of the region 3q22-qter. Conversely, some tumours demonstrated amplification within the region 3q25-qter without concomitant gain of the entire long arm (Figure 8.10 (C)). Finally, low level gains restricted to the region 3q25-qter were also identified (Figure 8.10 (D)).

Amplification of chromosome band 11q13 was detected in 4 primary tumours and 3 LNM. Other regions of high level gain included 5p, 7p12-q11.2, 8q24-24.3 (2 primary tumours each), 6p22-cen, 12p (1 primary tumour each) and 6q21-22 (1 LNM).

8.3.4.2 Chromosomal regions of loss identified by CGH

The chromosomal material deleted most frequently in the cohort of tumours (n=69) was located on chromosome 3p. The majority of losses were seen to involve the majority of the chromosomal arm, however three MRL were identified: 3p24 (44.9%), 3p21 (39.1%)

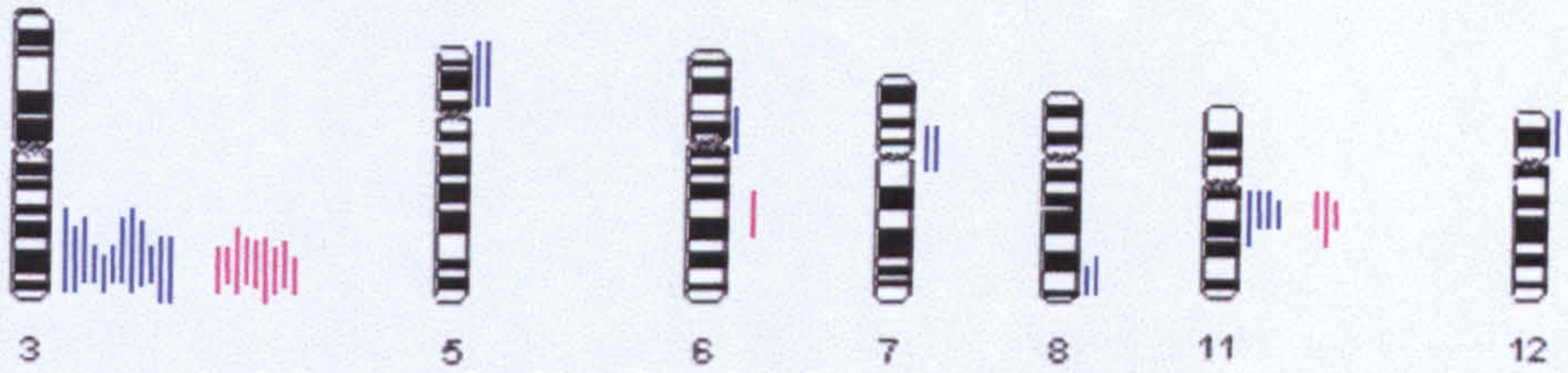

Figure 8.9 – Chromosomal location of regions of high level gain (amplification). High level gains (CGH colour ratio >1.5) were identified at several chromosomal loci. Those identified in the primary tumours are represented by a blue bar to the right of the chromosome ideograms and those in the lymph node metastases by a purple bar. The most common site of amplification was 3q26-27 (21 cases), followed by 11q13 (7 cases) and 5p, 7p12-q11.2, 8q24-24.3 (2 cases each). Amplifications on 6p22-cen, 6q21-22 and 12p were each identified in a single case.

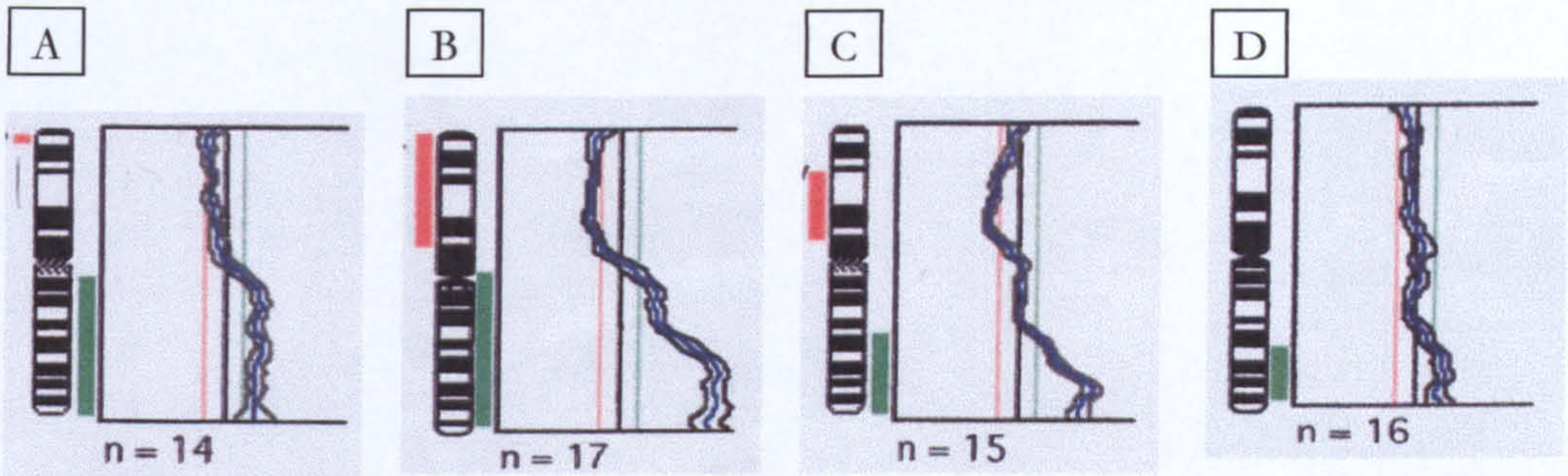

Figure 8.10 – Differences in the manifestation of gain of material on 3q.
3q was the most common site of both gain of DNA and amplification. Representative CGH profiles are depicted for the different scenarios encountered. These included gain of the entire long arm (A), gain of the entire long arm with amplification of the region encompassing 3q25-qter (B), amplification of 3q25-qter without concomitant gain of the rest of 3q (C) and gain of the 3q25-qter region alone (D).

	3q arm gain (A or B)	3q25-qter amplification (B or C)	3q25-qter gain alone (D)	3q25-qter amplification or gain of 3q25-qter alone (C or D)
T_1	0.0 (*0.0*)	0.0 (*0.0*)	0.0 (*0.0*)	0.0 (*0.0*)
T_2	50.0 (*50.0*)	37.5 (*37.5*)	12.5 (*12.5*)	50.0 (*50.0*)
T_3	27.2 (*30.0*)	18.2 (*20.0*)	27.2 (*30.0*)	45.5 (*50.0*)
T_4	21.7 (*26.3*)	30.4 (*36.8*)	34.8 (*42.1*)	65.2 (*79.0*)
N_0	23.0 (*30.0*)	15.4 (*20.0*)	23.0 (*30.0*)	38.5 (*50.0*)
N_+	27.3 (*31.0*)	30.3 (*34.5*)	27.3 (*31.0*)	57.6 (*65.5*)

Table 8.3 – Frequency of the different manifestations of 3q gains. Frequencies are expressed as percentages of tumours demonstrating the different patterns of gain and/or amplification of material on 3q. Figures in bracket represent the frequencies when only the 39 tumours demonstrating chromosomal abnormalities were considered (n=39).

and 3p13-p14 (39.1%). Other deletions which frequently encompassed the entire arm were detected on 8p (29.0%); 21 (23.2%); 22 (21.7%); 17p and 19p (both 20.3%); 9p (18.8%); 10p (17.4%) and 16p 15.9%). Many of the other regions of deletion identified extended to the telomere of the involved chromosome arm. These included deletion of 11q22-qter (39.1%); 5q32-qter and 18q21-qter (both 31.8%); 10q25-qter (30.4%); 9q32-qter and 13q31-qter (both 26.1%); 1p34.2-pter, 2q36-qter and 4q31.3-qter (all 24.6%); 11p14-pter (21.7%); 7q32-qter (20.3%); 14q24-qter, 16q22-qter, 17q24-qter, 19q13-qter (all 15.9%) and 6q25-qter, 12q24-qter (both 10.1%). Other MRL included 4q26-q28 (18.8%) and 5q12-q13 (15.9%).

8.3.4.3 Comparison of chromosomal aberrations identified in node positive tumours and node negative tumours

Copy number changes identified at several chromosomal loci were found at differing frequencies between the node positive (N+ve; n=33) and node negative (N-ve; n=13) tumours (Table 8.2). Aberrations found at a higher frequency in the tumours with lymph node involvement pathologically proven at the time of treatment included:

- 2p14-p22 gain (18.2% of N+ve vs. 0.0% of N-ve)
- 2q22-q32.1 gain (30.3% of N+ve vs. 15.4% of N-ve)
- 2q36-qter gain (30.3% of N+ve vs. 15.4% of N-ve)
- 3q25-q27 gain (63.6% of N+ve vs. 38.5% of N-ve)
- 4q26-q28 loss (21.2% of N+ve vs. 7.7% of N-ve)
- 4q31.3-qter loss (24.2% of N+ve vs. 15.4% of N-ve)
- 6q25-qter loss (15.2% of N+ve vs. 0.0% of N-ve)
- 9p loss (18.2% of N+ve vs. 7.7% of N-ve)
- 11q12-q13 gain (30.3% of N+ve vs. 15.4% of N-ve)
- 13q31-qter loss (30.3% of N+ve vs. 15.4% of N-ve)
- 22q loss (21.2% of N+ve vs. 7.7% of N-ve)

Fewer regions of copy number change were identified at a higher frequency in the node negative tumours:

- 1q31-q32 gain (38.5% of N-ve vs. 18.2% of N+ve)
- 9q32-qter loss (46.2% N-ve vs. 12.1% N+ve; *p=0.020*)

The increased frequency of 9q32-qter deletion in node negative tumours was statistically significant (p=0.020 – Fishers exact test).

8.3.4.4 Comparison of chromosomal aberrations identified in primary tumours and lymph node metastases

When the incidence of aberrations detected in the primary tumours (n=46) was compared with the lymph node metastases (LNM; n=23) several regions were identified more frequently in the lymph node metastases.

- 3q25-q27 gain (82.6% of LNM vs. 56.5% of primary tumours; *p=0.0215*)
- 8q23-qter (60.9% of LNM vs. 52.2% of primary tumours
- 1p34.2-pter loss (34.8% of LNM vs. 17.4% of primary tumours)
- 4q15-pter loss (21.7% of LNM vs. 6.5% of primary tumours)
- 5q12-q13 loss (26.1% of LNM vs. 10.9% of primary tumours)
- 13q21-q22 loss (30.4% of LNM vs. 10.9% of primary tumours; *p=0.049*)
- 17p loss (30.4% of LNM vs. 15.2% of primary tumours)
- 17q24-qter loss (26.1% of LNM vs. 10.9% of primary tumours)
- 19p loss (30.4% of LNM vs. 15.2% of primary tumours)
- 22q gain (26.1% of LNM vs. 4.3% of primary tumours; *p=0.014*)
- 22q loss (34.8% of LNM vs. 17.4% of primary tumours)

The most frequent aberration identified in both groups was gain of material on 3q, specifically 3q25-q27. However the frequency of 3q25-q27 gain was dramatically increased in the LNM compared with the primary tumours. This increase was statistically significant (p=0.0215 – Fishers exact test). Gain of 8q23-qter, the second most common region of gain in both groups, was also detected at a slightly increased frequency in the LNM. Interestingly both gain and loss of material from chromosome 22 was detected more frequently in the LNM (The increase in gain of material from 22q in the LNM was statistically significant (p=0.014 – Fishers exact test).

Fewer regions of increased copy number change were detected in the primary tumours. Gain of 7p12-q11.2 was identified at approximately a two-fold greater frequency in the primary tumours compared with LNM (32.6% and 17.4% respectively). Deletion of material on 11p demonstrated the greatest difference in frequency with 28.3% of primary tumours demonstrating a decreased copy number compared with only 8.7% of LNM. The

small, sub-centromeric, gain of material on 18q11 was identified in 28.3% of primary tumours and 13.0% of LNM.

8.3.5 Statistical analysis of CGH data

8.3.5.1 Survival Analysis – correlation of chromosomal aberrations with survival

Kaplan-Meier survival analysis was performed for the chromosomal aberrations identified in the 39 tumours demonstrating chromosomal copy number changes. Initially, survival analysis was performed for gains and losses of DNA on each chromosomal arm. Patients were divided into two groups (aberration/no aberration) and copy number increases and decreases analysed separately. Any regions demonstrating significance (at the level $p<0.05$) were then re-analysed, with the analysis restricted to aberrations demonstrating a minimal region of overlap, i.e. only aberrations covering the same chromosomal region were scored as positive. Where more than one distinct minimal region of copy number change was identified on a single chromosome arm, the regions were analysed separately. In total 48 initial analyses were performed.

Chromosomal aberrations which demonstrated a statistically significant ($p<0.05$ – log rank test) association with survival are detailed in Table 8.4. Figures 8.11 to 8.14 depict representative Kaplan-Meier survival curves. Initial survival analysis of gain of material on chromosome 3q identified a trend towards decreased survival in tumours with gains on 3q however this did not reach significance (Figure 8.11 (A) $p=0.2329$ – log rank test). When the two minimal regions of gain on chromosome 3q (3qcen-q13 and 3q5-q27) were analysed separately a significant association between gain of material at 3q25-q27 and reduce survival was identifed (Figure 8.11 (B) $p=0.0196$ – log rank test). The mean survival for tumours with gain of material in this region was 36.3 months (standard error 4.5) compared with 57.5 months (standard error 4.3) for those without. Other regions of frequent copy number change demonstrating a significant association with reduced survival included deletion of 7q32-qter (Figure 8.12; $p=0.0141$ – log rank test), and deletion of 19p (Figure 8.13 (A) $p=0.0239$ – log rank test) and deletion of 19q (Figure 8.13 (B) $p=0.0271$ – log rank test). Other regions which have recently been reported in the literature to associate with reduced survival, but which did not reach significance in this cohort of tumours, are also listed in Table 8.4 (Bockmuhl *et al*, 2000). Figure 8.14 depicts survival curves for deletion of 8p and deletion of 18q, both of which failed to reach significance.

Locus	Gain/Loss	No. of cases with / without aberration	Censored cases with / without aberration	Significance (Log rank)
7q	Deletion	9/30	3/22	0.0141
4p	Gain	1/38	0/25	0.0166
3q25-27	Gain	26/13	14/11	0.0196
19p	Deletion	7/32	3/23	0.0239
11p	Gain	2/37	0/25	0.0250
19q	Deletion	7/32	3/22	0.0271
17q	Deletion	5/34	2/23	0.0286
2q	Gain	14/25	7/18	0.0590
18q	Deletion	18/21	9/16	0.0816
8p	Deletion	16/23	9/16	0.2036
3q	Gain	30/9	18/7	0.2329

Table 8.4 – Chromosomal loci of copy number change associated with reduced disease specific survival in order of significance. All chromosomal loci demonstrating a statistically significant association with reduced survival are listed for the 39 primary tumours in which chromosomal aberrations were detected. Significance was tested using the log rank test. The lower half of the table lists interesting chromosomal loci that did not demonstrate a significant association with survival in this cohort of tumours. These loci include several reported in the literature as associating with survival (2q, 18q, 8p - see text). In addition, the p value for the survival association for tumours demonstrating gains anywhere on 3q is listed to highlight the significance of gains specifically in the region 3q25-27.

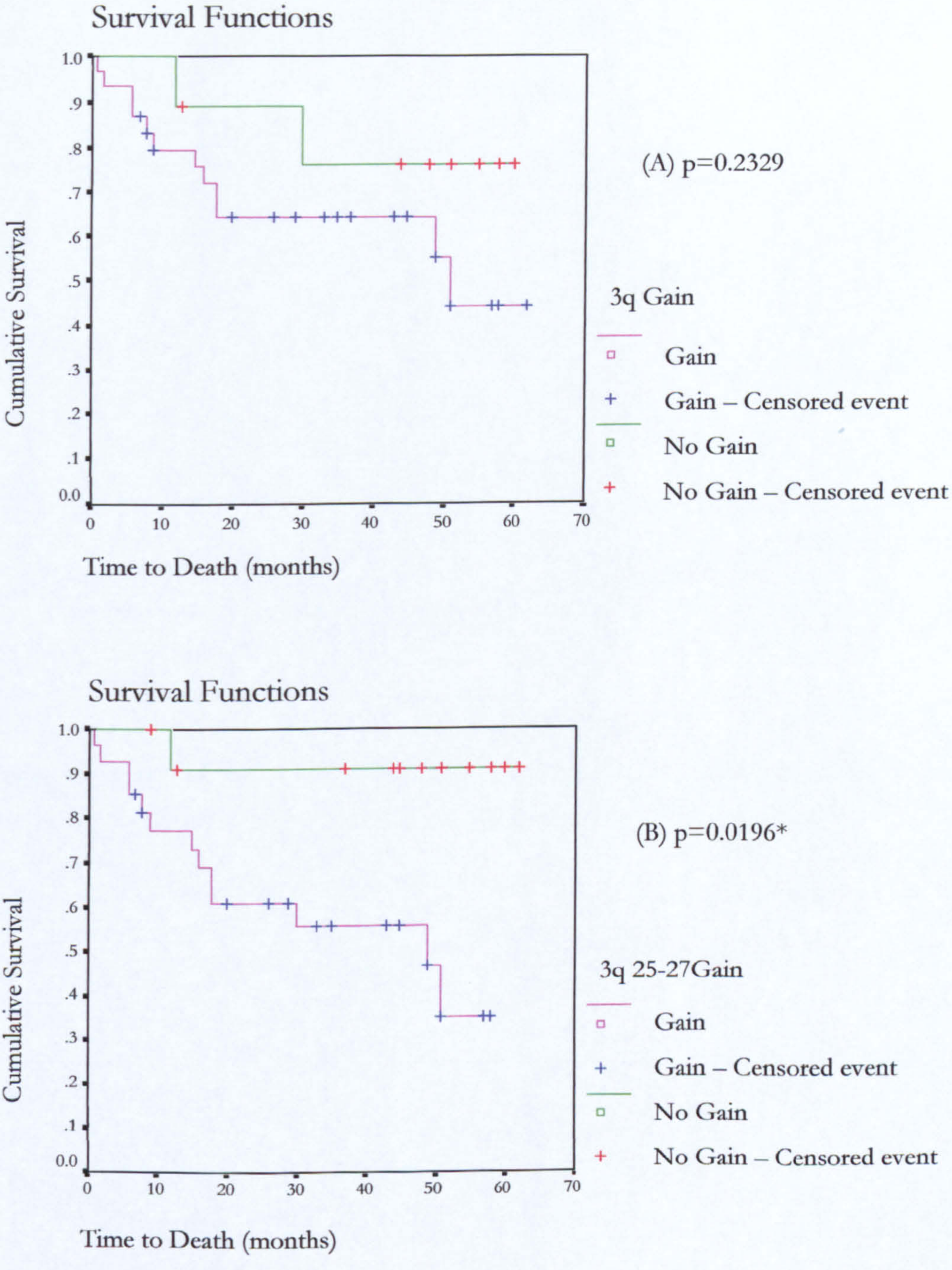

Figure 8.11 – Kaplan Meier survival analysis for copy number changes on chromosome 3q. When survival analysis was performed for all tumours demonstrating gain of material on 3q a trend was noted between reduced overall survival and gain of material on 3q (A). This association was not significant. However, when specific regions of 3q were analysed individually a significant association was identified for gain of material at 3q25-27 and a reduction in overall survival (B).

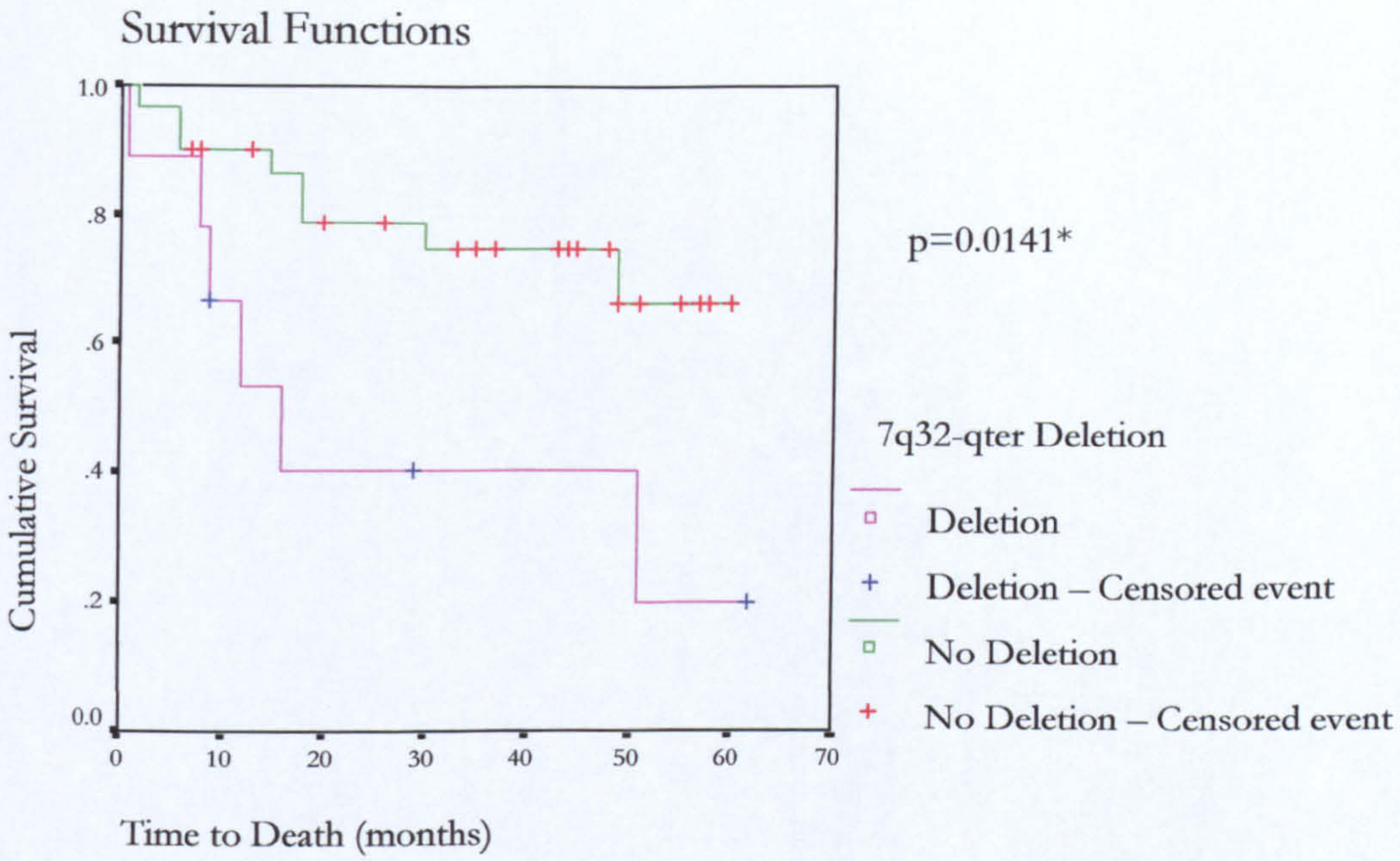

Figure 8.12 – Kaplan Meier survival analysis for deletion of 7q32-qter. A significant association was identified between reduced survival and a minimal region of deletion encompassing 7q32-qter.

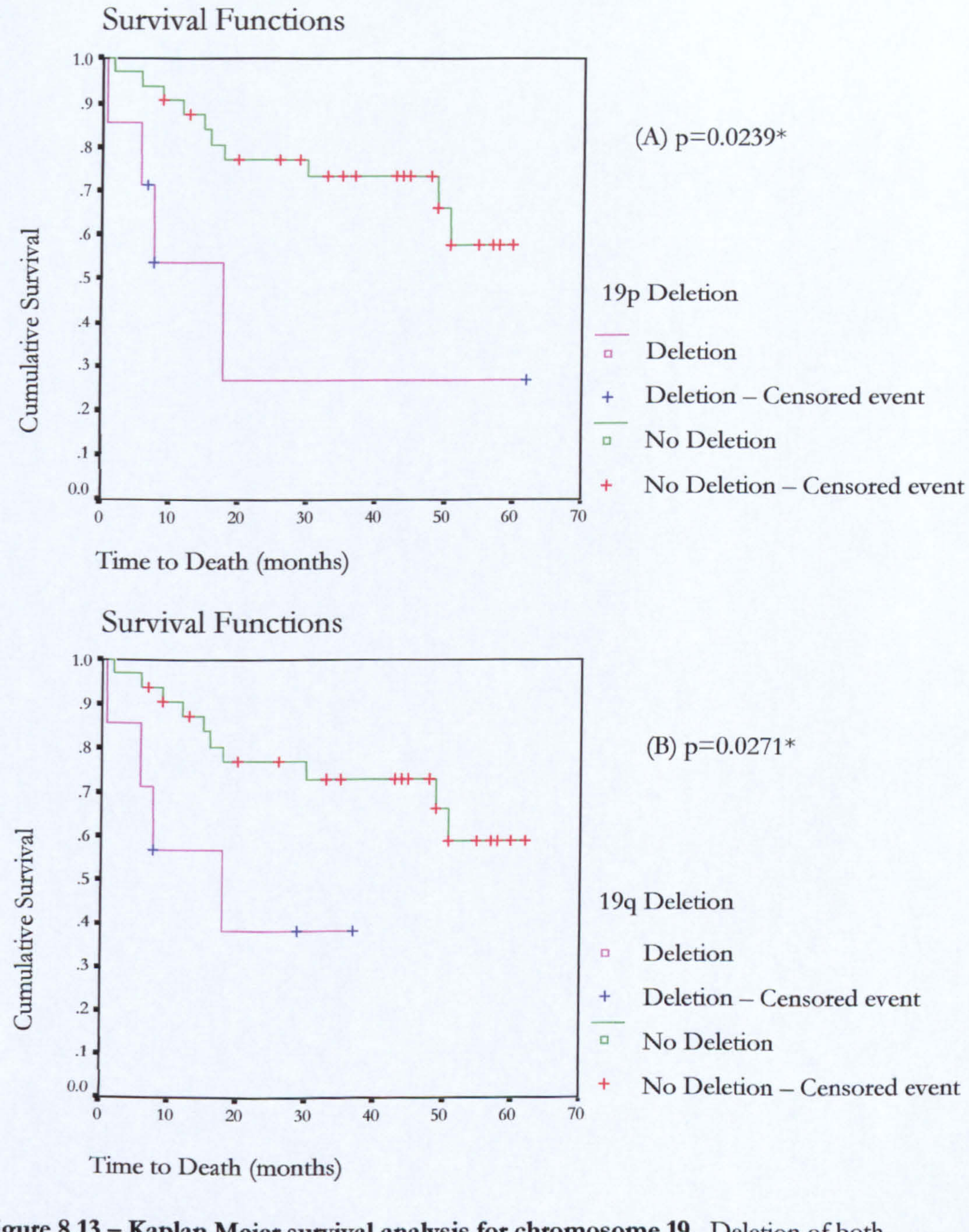

Figure 8.13 – Kaplan Meier survival analysis for chromosome 19. Deletion of both 19p (A) and 19q (B) were significantly associated with reduced overall survival.

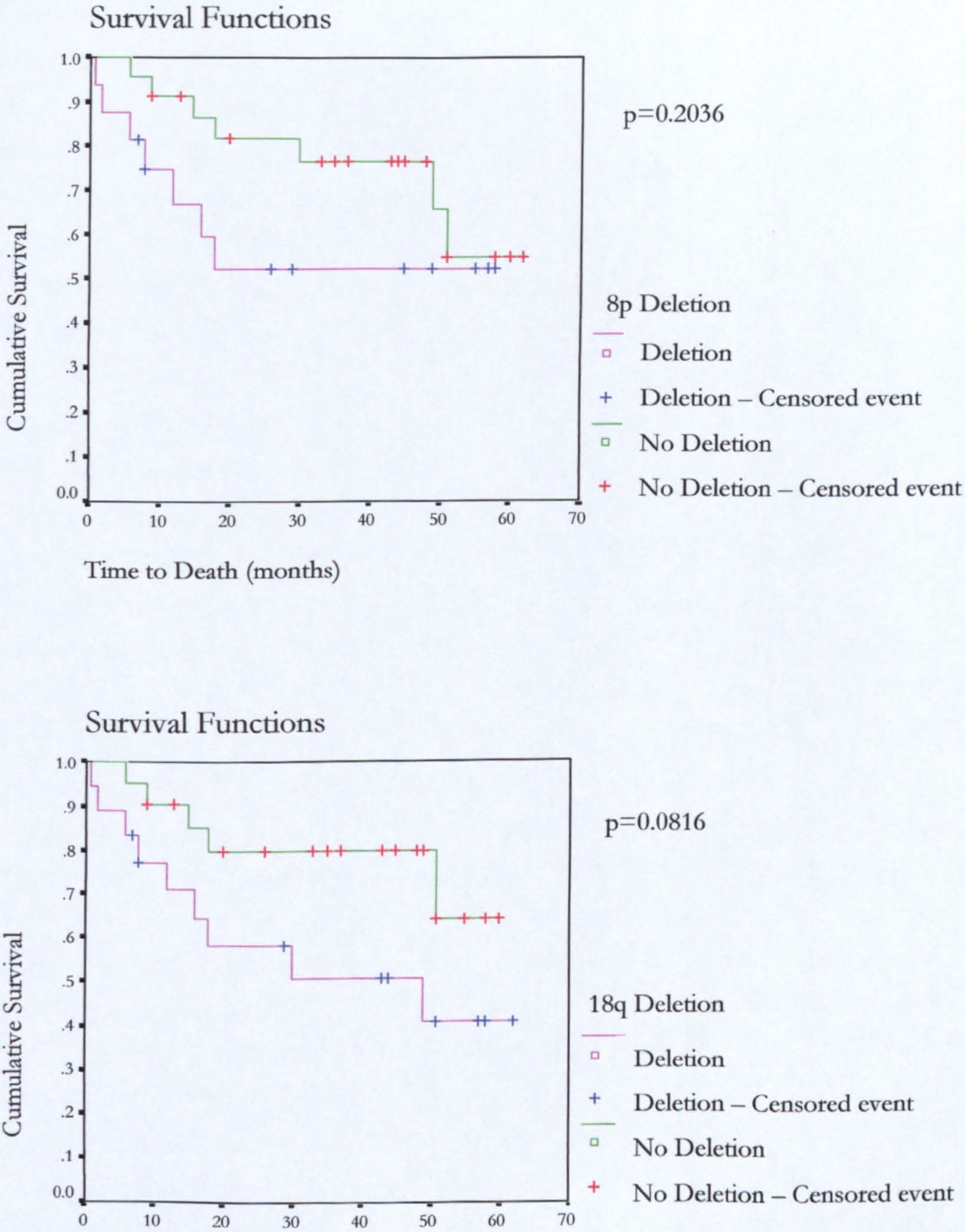

Figure 8.14 – Kaplan Meier Survival analysis for regions of copy number change reported in the literature as associating with survival. In this cohort of tumours neither deletion of 8p or deletion of 18q demonstrated a significant association with reduced survival.

8.4 Discussion

The most interesting result emerging from the analysis of CGH data was the association of gains of material located within 3q25-27 with the progression of HNSCC. Gain of this region was the most prevalent gain detected. A higher frequency was demonstrated in tumours with pathologically proven lymph node involvement and a significantly higher frequency in metastatic tumours compared with primary tumours. In addition, Kaplan-Meier survival analysis demonstrated a significant association of gain of this region and reduced overall survival. Several other CGH studies have identified 3q as a consistent site of both gain of DNA and amplification (Bockmuhl *et al*, 2000; Bergamo *et al* 2000; Singh *et al*, 2001; Hermesen *et al*, 2001; Hashimoto *et al*, 2001). A similar association with survival has recently been identified by Bockmuhl *et al* (2000). In their study of 113 primary HNSCC tumours gain of material at 3q21-q29 demonstrated a strong significance (p=0.007 – log rank test) with a reduced overall survival. The significance of the difference between the region of chromosome 3q identified in this thesis (3q25-27) and Bockmuhl's study (3q21-29) is unclear but may reflect the different methods of statistical analysis employed. Bockmuhl *et al* employed a superior CGH analysis software package that allowed integrated statistical analysis of chromosomal alterations at each chromosomal band throughout the genome (at the ISCN 400 band resolution). This software was not available for the analysis of the tumours presented here and manual statistical calculations had to be performed for a limited number of chromosomal loci. The sheer magnitude and complexity of performing separate survival analyses for each chromosomal band for 46 independent data sets would have involved over 18,000 calculations and therefore was not feasible. The region 3q25-27 represents the minimal region of overlap present in all tumours demonstrating a gain on 3q2. Many of these gains extended further, however every case included this minimum region. Bockmuhl *et al* also identified several other regions of copy number change as independent prognostic markers carrying a higher significance than conventional clinicopathological parameters. None of these other regions were confirmed in this study. Associations with reduced survival were seen for some regions, however these did not reach statistical significance, for example the deletion of 18q depicted in Figure 8.14. The explanation for this discrepancy is unclear, however it may reflect differences in the cohorts of tumours employed, or regional variation in the genetic aberrations involved in HNSCC tumourigenesis.

Gain of 3q has been reported in numerous tumour types, most frequently in those of squamous origin including HNSCC and cervical carcinoma. (Gebhart and Liehr, 2000). In

SCC of the uterine cervix, gain of 3q has been shown to define the transition from severe dysplasia to invasive carcinoma (Hesselmeyer *et al*, 1997). Data on the timing of 3q gain in HNSCC remains limited. One small study of 10 primary tumours and matched 'normal' buccal mucosa identified gain of chromosome 3 material in 6/10 tumours and 2/10 samples of buccal mucosa using FISH analysis with centromeric probes (Ai *et al*, 1999). The high frequency of 3q gains identified in the present study is consistent with 3q gain being an early event in HNSCC tumourigenesis and may reflect a situation similar to that identified in cervical SCC. However, an early genetic requirement for tumourigenesis would be unlikely to carry prognostic value as demonstrated here and elsewhere (Bockmuhl *et al*, 2000). In contrast, the failure to identify a prognostic significance for deletions of 3p, a very common event, in the tumours reported in this thesis is consistent with 3p deletions being early genetic requirements for HNSCC, detectable in premalignant tissues (Califano *et al*, 1996). The apparent conflict regarding 3q gains in HNSCC may indicate the presence of multiple genes associated with tumourigenesis in this region. Alterations in a gene required early in the development of HNSCC may arise through chromosomal alterations below the resolution of CGH, while mutations which drive the progression of the disease towards a more aggressive phenotype may involve amplification of a putative tumour gene (high level copy number gain).

Recently Hashimoto *et al* (2001) have further delineated the involvement of 3q gains in HNSCC tumourigenesis by demonstrating a correlation between amplification, as opposed to low level gain, of 3q26-qter and tumour progression (n=32). Hashimoto identified gain of 3q26-qter in 91% of tumours, and amplification at a significantly higher frequency in T4 tumours (70%) when compared with T2 and T3 tumours (both 27%; $p<0.05$ – Fishers exact test). This amplification was not significantly associated with histopathological grade or nodal stage. In the cohort of tumours reported here this association was not as clear. Amplification was found more frequently in Node positive tumours (Table 8.3) but a linear association with tumour stage was not identified. One possible explanation for this can be hypothesised when the different manifestations of 3q gain are considered (Figure 8.10). When tumours demonstrating either amplification of 3q25-qter or gain of 3q25-qter alone (Table 8.3) are grouped together a pattern similar to that described by Hashimoto *et al* is observed. This situation represents tumours that exhibit a relative over-representation of genes within the critical region of 3q25-q27 when compared with other loci on 3q. More importantly, this analysis would include tumours with amplification of 3q25-q27 which may have been masked by signal dilution either due to normal cell contamination or the clone containing an amplification constituting only a minority of the tumour cells, i.e. Figure 8.10

D may represent dilution of the CGH signal depicted in Figures 8.11 B or C. When tumours are analysed based on this assumption, copy number aberrations at 3q25-q27 are demonstrated at a higher frequency in T4 tumours in a pattern similar to that reported by Hashimoto *et al.*

Several candidate genes have been localised to 3q25-27. One known oncogene within this locus is the human telomerase gene (*hTR*). Telomerase activity is absent in normal somatic cells but is almost universally detectable in human tumours and thought to be a key factor in the immortalisation of cancer cells (Soder *et al*, 1997). Interestingly the gene for the catalytic subunit of telomerase (*hTERT*) is located at 5p15, another frequent site of DNA gain and amplification identified in this thesis. Other genes of interest at 3q25-q27 include the *FGF12* growth factor and *PIK3CA*, which encodes the p110 catalytic subunit of phosphatidylinositol-3'-kinase, a critical component of many cell signalling pathways including those of *EGF* and *PDGF* (Volina *et al*, 1994). Increased copy number of the *PIK3CA* gene has been identified in cervical cancer and a similar amplification of the gene in ovarian cancer has been shown to be associated with increased expression (Ma *et al*, 2000, Shayesteh *et al*, 2001). More recently, targeted FISH experiments using yeast artificial chromosomes (YACs) have demonstrated amplification of the *PIK3CA* gene in a panel of HNSCC cell lines (Singh *et al*, 2001). It appears likely that several genes within the region of 3q gain identified in this thesis are important for HNSCC progression. Gain of some may be essential for tumorigenesis such as the potential immortalizing role of telomerase genes whereas amplification of growth stimulatory genes may occur later in the progression of HNSCC and perhaps identify more aggressive tumours with a worse prognosis.

Another region of interest demonstrating prognostic significance was deletion of 7q32-qter. Occurring in approximately one quarter of primary tumour specimens, this region demonstrated the strongest significance for reduced disease specific survival using the log rank test. Prognostic importance of this region had not previously been reported in the literature. At least one candidate tumour suppressor gene resides within this location: *CATR1*. *CATR1* remains to be fully characterised, however, suppression of endogenous CATR1 expression by transfection with *CATR1* antisense was shown to convert an oral squamous cell line (SCC83-01-82) to a tumourigenic phenotype in host nude mice (Li *et al*, 1996). The untreated cell line was non-tumourigenic. Therefore loss of CATR1 expression in an already cancerous cell appears to convert the tumour to a more aggressive phenotype, consistent with the significant association of deletion of the 7q32-qter region and reduced survival.

Interrogation of the Online Mendelian Inheritance in Man (OMIM) database (http://www.ncbi.nlm.nih.gov/Omim/) identified other genes involved in growth stimulatory pathways within other frequent loci of DNA gain. These included the fibroblast growth factors 3 and 4 (*FGF3*, *FGF4*) both located at 11q13 and the epidermal growth factor receptor (*EGFR*) at 7p11-p12. Overexpression of these gene products may stimulate tumour progression by initiating autocrine or paracrine growth stimulatory loops and may play a role in HNSCC carcinogenesis. Interestingly both these sites were loci of amplification. Other oncogenes implicated in HNSCC mapping to loci identified as frequent site of DNA gain included *c-myc* (8q24), *cyclin-D1* (11q13) and *k-ras* (12p). Several chromosomal loci were also identified which, to date, no oncogenes have yet been mapped including 2q22-32, 8q12-q21.3, 18p and 18q11. The importance of chromosomal loci of several known TSGs was also confirmed in this study: deletion of DNA was frequently identified at the site of *fhit* (3p14), *vhl*, *dlc1* (3p22-pter), *nat1* (8p), *mts1(p16)* (9p), *ing1* (13q31-qter), *p53* (17p) and *dcc* (18q21-qter).

Chromosomal aberrations were detected in 39 of the 46 tumour specimens (85%) and 22 of 23 nodal specimens (95.6%). These figures are in concordance with other CGH studies on HNSCC using similar methodology (Bergamo *et al*, 2000; Brzoska *et al*, 1995). However, it is important to note that other CGH studies on HNSCC which employed serial sectioning of tumour specimens and DNA extraction of micro-dissected tissue identified aberrations in 100% of specimens (Speicher *et al*, 1995; Bockmühl *et al*, 1996; Hashimoto *et al*, 2001). In this work, as in the studies presented by Bergamo and Brzoska, normal tissue was carefully removed from the specimen at the time of collection and DNA extracted from a piece of tumour taken directly adjacent to the specimen used for histopathological diagnosis. Examination of this specimen confirmed the presence of >60% of tumour cells in the cases studied however this method does not guarantee that the value is true throughout the entire sample from which DNA was extracted. The superior method (employed by Speicher, Bockmühl and Hashimoto) of serial sectioning the sample used for DNA extraction allows histopathological examination throughout the entire biopsy and subsequent removal of areas of normal tissue from each section. This method better guarantees that DNA from malignant cells will constitute the vast majority of the DNA extracted from each specimen and therefore the sensitivity of detecting aberrations by CGH will be higher. This technical difference is the likeliest explanation for the discrepancy between the aberrations identified in the various CGH studies on HNSCC. This is the reason that tumours that did not demonstrate aberrations in the cohort under

study were excluded from later statistical analysis to avoid the inclusion of potentially false negatives.

As CGH is a global screening tool, each experiment generates data on a large number of variables. As a consequence of this, when performing both survival and correlation analysis between patterns of aberrations and clinical characteristics it is inevitable that some statistically significant correlations will arise by chance, especially when the frequency of a particular aberration is low. For example gain of 4p (n=1) demonstrated a strong association (p=0.0166) with reduced survival. To some extent the problem of comparing multiple variables can be overcome by applying statistical error correction tools, such as Bonferroni correction, however in this small cohort of tumours it was decided not to employ such techniques as CGH is essentially a screening tool to identify areas of the genome worthy of further analysis using higher resolution molecular techniques.

The mean number of copy number aberrations identified in this cohort of 46 patients (13.1) falls within the range of those reported in other HNSCC CGH studies (13.1-23.2) and is similar to those reported in lung CGH studies (7.9-16.9). The mean number of copy number aberrations reported in other tumours types (reviewed by Gebhart and Liehr, 1999) is significantly lower reflecting the complexity of HNSCC tumour karyotypes (stomach 3.1-9.1; colon 5.6-11.9; liver 6.7-9.9; kidney 2.9-8.2; bladder 4.3-12.2; prostate 2.9-5.6; breast 4.1-10.1)

The non-random nature of the regions of copy number change identified in this thesis, as well as the clinical significance of some of these regions, indicate that the genetic loci identified would be expected to contain genes important to the tumourigenesis of HNSCC. These aberrations have proven to have prognostic potential in a group of tumours for which the conventional clinicopathological parameters failed to significantly predict outcome. In addition, differences in the frequencies of chromosomal aberrations were seen between primary and metastatic tumours and primary tumours with local metastases compared with those that did not spread. The two most interesting regions demonstrating a prognostic potential, 3q25-27 and 7q32-qter, warrant further prospective analysis using higher resolution techniques such as allelic imbalance analysis using microsatellite markers or FISH analysis using chromosome probes for the affected regions. The identification of genes, or chromosomal regions, with prognostic potential will allow for better management of HNSCC patients as well as identifying new targets for therapeutic intervention.

Chapter 9

Concluding Remarks

9.1 Concluding Remarks

Head and neck squamous cell carcinoma remains a major health problem world-wide and contributes significantly to the morbidity and mortality associated with human cancer. Long term survival rates for HNSCC have reached a plateau, changing little over the last 20 years and novel molecular makers of prognosis diagnosis and therapeutic targets are now urgently required to advance the treatment of this disease. Definition of the genetic changes underlying HNSCC is underway but remains incomplete. This thesis evaluated the application of the molecular genetic technique of CGH both to the genomic characterisation of HNSCC and the identification of new prognostic markers. This thesis has demonstrated that HNSCC tumours are characterised by consistent, non-random genetic rearrangements. It has been shown that these chromosomal aberrations can be reliably detected within a clinical laboratory setting and that, even in a relatively small cohort of tumours, such genetic aberrations convey prognostic information. The main conclusions that can be drawn from these studies are summarised below:

1. HNSCC tumours are characterised by numerous, common regions of gross chromosomal gain and loss. None of these abnormalities are detectable in the mucosa surrounding the site of a primary HNSCC tumour, when analysed by CGH (Chapter 5). This indicates that these abnormalities detected are inherently related to the malignant characteristics of HNSCC and that any genetic abnormalities within the cells that constitute the histologically normal mucosa surrounding a primary tumour are below the resolution of CGH. The phenomenon of 'field cancerization' remains to be definitively proven, however several studies support the presence of abnormal cells in the mucosa adjacent to primary HNSCC. The current literature has so far only demonstrated subtle, discrete mutations, such as p53 mutation, and numerical chromosomal aberrations present in a minority of cells. Both scenarios are below the resolution of CGH therefore this technique would not be useful clinically for the screening of mucosa at risk of transformation in HNSCC patients.

2. The overall pattern of genetic aberrations present in primary HNSCC and local metastases is very similar, however there was discordance in every case analysed (Chapter 6). At least one chromosomal abnormality was found to be common to every pair of primary and metastatic tumours with some pairs of tumours demonstrating a high degree of clonal relationship. A subset of lymph node metastases, however, shared relatively few cytogenetic abnormalities indicating that a linear progression pathway may not satisfactorily

explain the progression to the metastatic genotype in all HNSCC. In these cases, the clones of cells that eventually established the metastatic deposit apparently diverge genetically from the cells that constitute the majority of the primary mass at a relatively early stage. It is established that early diagnosis and treatment of HNSCC reduces the likelihood of local metastases, therefore any cells with metastatic potential are likely to remain part of the primary tumour mass until another, as yet undefined, genetic event occurs. Several genetic aberrations were detected at a higher frequency in the nodal metastases, most notably copy number changes in chromosome 22. The role of chromosome 22 is currently under investigation in primary and metastatic HNSCC using the higher resolution technique of allelic imbalance using microsatellite markers. The aim of this study is to resolve whether chromosomal loci on 22 are involved in the process of metastases and more importantly, whether such information can be used prognostically in molecular examination of the primary tumour for evidence of cells with metastatic potential. Such information would be clinically valuable both in preventing unnecessary prophylactic neck dissections and also to allow closer monitoring of patients at risk from local metastases.

3. Radio-resistant glottic HNSCC tumours demonstrate different patterns of protein expression (Chapter 7). Most notable was the significantly higher frequency of over-expression of bcl-2 in glottic tumours resistant to radiotherapy. Bcl-2 is an anti apoptotic protein involved in triggering cell death after DNA damage by ionising radiation detected by the p53 tumour suppressor protein. Therefore dysregulation of bcl-2 expression is a logical mechanism by which tumour cells may acquire resistance to therapeutic radiotherapy. A similar finding has recently been demonstrated in the literature by others (Gallo *et al*, 1999). The small cohort of tumours studied in this chapter make this essentially a hypothesis generating study. The decision to limit the study to a pure population of early glottic tumours naturally restricted the number of resistant specimens available, however this did ensure that any differences in marker expression was not a result of molecular differences of HNSCC from different anatomical sub-sites. Efforts are now underway to obtain additional samples from multiple centres in order to substantiate these findings in a larger series of patients.

The involvement of bcl-2 in radio-resistance raises an interesting question of the mechanism of overexpression of bcl-2. The bcl-2 gene was discovered as one of the first chromosomal rearrangements to be involved in cancer. The t(14;18) translocation characteristic of B cell lymphoma causes the bcl-2 gene to translocate from chromosome

18 to chromosome 14, adjacent to a strong immunoglobulin promotor. Balanced translocations such as this would not be detected by CGH, however PCR based technologies and FISH may be able to identify a similar mechanism of bcl-2 up-regulation in resistant tumours. Such techniques would be ideally suited to diagnostic application in a clinical laboratory. The involvement of bcl-2 in radio-resistance warrants further investigation as a diagnostic marker of radio-resistance would prevent the considerable morbidity associated with salvage surgery following failed radiotherapy. The identification of resistant tumours would allow surgery to be the primary therapy of choice in the small but significant proportion of patients who fail to respond to radio-therapy.

4. Some of the chromosomal aberrations identified have demonstrated prognostic significance, most notably gain of 3q25-27 and deletion of 7q32-qter (Chapter 8). In addition, differences in the frequency of copy number changes were identified between metastasising and non-metastasising tumours, and primary tumours and metastatic disease (Chapters 6 and 8). The demonstration of genetic aberrations exhibiting prognostic significance in this relatively small cohort of tumours, using a megabase-resolution technology, provides strong encouragement for the continued investigation of the molecular abnormalities underlying HNSCC. Such findings demonstrate evidence that molecular characterisation of HNSCC can provide additional markers of prognosis to supplement the classical pathological assessment of tumours. Many of the chromosomal regions identified in this thesis contain tumour genes already implicated in the tumourigenesis of HNSCC including 3p14 (*fhit*), 8q24 (*c-myc*), 9p (*p16*), 11q13 (*ccnd1*) and 17p (*p53*). The perturbed genes in other regions identified in this, and other studies, remain to be fully elucidated. Further characterisation of these regions is now required and will involve higher resolution mapping involving techniques such as LOH for the analysis of regions of deletion and positional cloning strategies for gains and amplifications (high copy number gains).

Analysis of several other tumour entities has led to the identification of putative tumour genes located within regions of copy number imbalance identified by CGH. CGH analysis of 33 thyroid tumours and cell lines demonstrated a previously unreported amplification of 2p21 (Chen *et al*, 1998). The subsequent hybridization of a dense array (n=43) of FISH mapped, chromosome 2p21, bacterial-artificial-chromosomes (BAC's) to metaphase chromosomes from a thyroid cell line narrowed the amplified region to 3-6Mb and identified a minimum amplicon size defined by a contig of 420kb. Sequencing analysis of this contig revealed a fragment of the protein kinase C epsilon (PKC$_\varepsilon$) gene. This

amplification was further shown to result in an overexpressed and truncated PKC$_\epsilon$ protein (Knauf *et al*, 1999). Cell lines expressing truncated PKC$_\epsilon$ demonstrated resistance to apoptosis, were associated with higher bcl-2 levels, reduced expression of bax and impairment of p53 stabilization suggesting a role in for PKC$_\epsilon$ in apoptosis signalling pathways in thyroid cells.

The chromosomal loci of copy number changes identified in this thesis are consistent with the reports of CGH analysis on HNSCC in the literature. Deletions of 3p and gains of 3q are consistently the most frequently reported CGH aberrations in HNSCC and the overall pattern of aberrations is relatively concordant. HNSCC karyotypes are known to be amongst the most complex of solid tumours, demonstrating numerous regions of genomic imbalance and this may reflect the diversity of this group of diseases. A recent analysis of laryngeal, oropharyngeal and hypopharyngeal tumours demonstrated a statistically significant higher frequency of amplification of oncogenes at 11q13 in hypopharyngeal tumours (Rodrigo *et al*, 2001). This highlights the potentially different biology of cancers arising from different sites. CGH analyses of distinct histological subtypes are rarely performed due to the availability of fresh tissue specimens. Improvements in DNA labelling methodology are beginning to allow CGH analysis of archival specimens (van Gijlswijk *et al*, 2001), however this technique still remains technically difficult and has not been widely applied. Recently, the National Center for Biotechnology Information has established an online CGH database (http://www.ncbi.nlm.nih.gov/sky/) allowing individuals to deposit CGH data making it freely available for other researchers. Such a resource may allow large scale CGH analysis of individual HNSCC histological subtypes by combining data generated by multiple institutions. It is intended to submit the data generated during the course of this thesis.

Therapy maybe a word on Cleeve

9.2 Molecular genetics and cancer – Future perspectives

Identification and characterisation of the chromosomal re-arrangements in different types of human neoplasms is a fundamental goal of cancer biology. Since the discovery of the Philadelphia chromosome in 1960 (Norwell & Hungerford, 1960), a substantial knowledge base has been established for the haematological malignancies and the identification of chromosomal translocations now forms an integral part of the diagnosis and classification of these diseases. In many respects the knowledge base on solid tumours lags several decades behind that of the leaukaemias and lymphomas. The clinical impact of cytogenetic findings in solid tumours is to date limited to the distinction between benign and malignant

epithelial tumours of several anatomical sites including the ovary, salivary glands and the kidney (Mitelman *et al*, 1997b). The main reason for this significant difference in cytogenetic data is the technical difficulties associated with working with solid tumour chromosomes by conventional cytogenetic methods. CGH has been applied to a wide range of tumour types and has proven to be a valuable tool for the detection of copy number aberrations. The routine diagnostic use of CGH has been predicted (Zitzelberger *et al*, 1997) but has so far failed to be realised. At present the application of CGH is mainly restricted to research laboratories due to the labour intensive nature of the technique and the need for specialised analysis equipment and skilled operators. In addition, improvements in the resolution of CGH are required before its transition from research laboratory to diagnostic laboratory. In my opinion, CGH in the form described in this thesis is unlikely to become a part of routine cancer pathology. Recent methodological developments in CGH have replace the conventional metaphase chromosome targets with immobilised target DNA arrayed in small spots onto glass 'chips' (Solinas-Toldo *et al*, 1997, Wessendorf *et al*, 2002). These chips consist of an ordered set of DNA fragments derived from either BAC clones or flow sorted chromosomal libraries. Whilst CGH by this method still requires specialized instrumentation, the analysis procedure can be fully automated as the technically demanding aspect of metaphase chromosome identification is no longer required. At present, the availability of such chips and the repertoire of DNA targets is limited and still at the research stage. The distinction between using ordered arrays derived from chromosomal libraries and arrays consisting of known genes is important. Using whole chromosome library chips dramatically increases the resolution of CGH to the range of 40-130kb and still enables the identification of novel regions of copy number change as the full genome is screened in every experiment (however several chips may be required to contain all the clones). Arrays consisting of known genes limit the data acquired to the genes loaded onto the chip. Until the genomic aberrations characterising the cancer of interest are fully described it is essential that the full genome screening capability of CGH is maintained. Whilst the technology is still 'young', array based technologies are beginning to generate vast amounts of data and it is expected that many of the genes whose expression is abnormal in HNSCC will be characterised over the next few years. The ultimate goal of chip based CGH in a diagnostic setting will involve customised chips for each of the major cancer types allowing the molecular pathological assessment and accurate classification of an individual patients tumour biopsy.

Will a tumour diagnostic biopsy/ by ...ment

9.2.1 Molecular Pathology

During the past century, the clinical behaviour of cancer has been predicted based on its microscopic appearance predominately using histological assessment of H&E staining on tissue biopsies. One of the major roles of cancer pathology is classification of the tumour type including the cellular origin, histological grade and the stage of the disease. These assessments are essential in determining the cancer prognosis and treatment approach. Nevertheless, there are limitations to this approach including the subjectivity of pathological assessment and variation between observers for certain categories of pathological diagnosis. In addition, the morphology of the tumour cells often does not always reveal the underlying biology reflected in patients with the same tumour type exhibiting completely different courses of disease. The revolution in molecular biology has in many ways been driven by the persistent need for better methods for accurately characterizing and subcategorising cancer and to understand its biological diversity.

It is unlikely that CGH alone would be sufficient for the molecular diagnosis of cancer. CGH is a method for evaluating the copy number of DNA sequences throughout the genome. However, it is the biological consequence of the expression of the proteins coded within these abnormal regions of DNA that is responsible for the malignant characteristics of cancer. Whilst the presence of genetic abnormalities in genomic DNA and the resulting aberrant protein expression are inherently linked, analysis of the DNA alone does not take into account additional abnormalities at the level of mRNA transcription and splicing and translation. For this reason, the technologies most likely to play a major role in the diagnosis and prognosis of cancer alongside CGH will be the rapidly growing specialty of cDNA microarrays. cDNA arrays are similar to the CGH arrays mentioned above in that they consist of ordered arrays of known DNA oligonucleotides bonded to glass microscope slides. However, the main difference is that instead of hybridising genomic DNA fragments to the target array, RNA is isolated from the tissue of interest and reverse transcribed to cDNA. These cDNA fragments are competitively hybridised to the arrays with a differentially labelled reference sample. The fundamental difference between CGH arrays and cDNA arrays is that the latter provides a snapshot of the genes actively being transcribed at the time of analysis. The power of this technique has rapidly become clear with studies on breast cancer, lymphoma and neural tumours predicting clinical outcome based on different gene expression profiles identified through cDNA arrays (van 't Veer *et al*, 2002; Shipp *et al*, 2002; Pomeroy *et al*, 2002).

The transfer of molecular pathology to the clinic will rely on the persistence of the academic head and neck oncologist to drive research forward, and to provide the clinical specimens essential for the unravelling of the complex molecular interactions which underlie this disease. It is envisaged that clinical advances will occur in phases, dependant on the extent of the knowledge of the molecular changes in HNSCC. Initial successes may lie in the early detection of the disease with the screening of high-risk individuals likely to be amongst the first technologies transferred from the laboratory to the clinic. These techniques do not require a complete understanding of the molecular biology of a disease, however they are dependent on the acquisition of markers of suitable specificity and sensitivity. At present, prostate specific antigen (PSA) is the most successful molecular marker in use in screening programs and whilst the impact of PSA screening on mortality remains controversial, most studies show a benefit to prostate cancer screening (Cookson, 2001). More detailed characterisation of HNSCC tumours will hopefully allow tailoring of therapy based on a genetic profile of the genetic characteristics of an individual patients tumour. Two clinical situations addressed in this thesis that would benefit greatly from the ability to predict the biological behaviour of a tumour include determining the optimum primary therapy for a tumour resistant to radio-therapy and the prevention of elective neck dissection in the pathologically node negative neck. Long term goals of cancer genetics include to identification of novel targets for chemotherapy and, perhaps the 'holy grail' of cancer therapy, gene therapy for the molecular restoration of defective apoptotic pathways.

In summary, this thesis has identified several areas of the genome important to the tumourigenesis of HNSCC. Some of these regions have demonstrated the prognostic potentials of molecular genetic analysis of HNSCC tumours. Further characterisation of these regions is now required to identify the genes whose expression is altered and such characterisation will allow this diverse group of diseases to be classified to a degree of accuracy far higher than current pathological practices allow. In addition, a greater understanding of the biology of HNSCC would be expected to lead to novel molecular therapeutic strategies targeted against these molecular abnormalities. To a large degree, HNSCC remains a preventable disease. The evidence linking cigarette smoking to HNSCC development is indisputable, however smokers have been reluctant to change their habits despite pressure from health care workers and more recently directly from the government in the form of increased taxation. Added to this, the several decade time lag between initiation of smoking and the development of HNSCC means that this disease will remain to be a significant cause of the morbidity and mortality for many years to come.

References

Adams JM, Gerondakis S, Webb E, Corcoran LM and Cory S. Cellular myc oncogene is altered by chromosome translocation to an immunoglobulin locus in murine plasmacytomas and is rearranged similarly in human Burkitt lymphomas. *Proc Nat Acad Sci*, **80**:1982-1986 (1983).

Agur AMR and Lee MJ (Eds). *Grants Atlas of Anatomy 10th Edition.* Lippincott Williams & Wilkins, Philadelphia (1999).

Ah-See KW, Cooke TG, Pickford IR, Soutar D and Balmain A. An allelotype of squamous carcinoma of the head and neck using microsatellite markers. *Cancer Research*, **54**(7):1617-1621 (1994).

Ahomadegebe JC, Barrois M, Fogel S, Le Bihan ML, Douc-Rasy S, Duvillard P, Armand JP and Riou G. High incidience of p53 alterations (mutation, deletion, overexpression) in head and neck primary tumours and metastases; absence of correlation with clinical outcome. Frequent protein overexpression in normal epithelium and in early non-invasive lesions. *Oncogene*, **10**:1217-1227 (1995).

Ai H, Barrera JE, Pan Z, Meyers AD and Varella-Garcia M. Identification of individuals at high risk for head and neck carcinogenesis using chromosome aneuploidy detected by fluorescence in situ hybridization. *Mutation Research*, **439**(2):223-232 (1999).

Akerval JA, Jin Y, Wennerberg JP, Zatterstrom UK, Kjellen E, Mertens F, Willen R, Mandahl N, Heim S and Mitelman F. Chromosomal abnormalities involving 11q13 are associated with poor prognosis in patients with squamous cell carcinoma of the head and neck. *Cancer*, **74**:152-158 (1995).

Akerval JA, Michalides RJ, Minerta H, Balm A, Borg A, Dictor MR, Jin Y, Loftus B, Mertens F and Wennerberg JP. Amplification of cyclin D1 in squamous cell carcinoma of the head and neck and the prognostic value of chromosomal abnormalities and cyclin D1 overexpression. *Cancer*, **79**:380-389 (1997).

Ali S, Tiwari RM, and Snow GB. False positive and false negative neck nodes. *Head Neck*, 8:78-82 (1985).

Andrews NA, Jones AS, Helliwell TR and Kinsella AR. Expression of the E-cadherin-catenin cell adhesion complex in primary squamous cell carcinomas of the head and neck and their nodal metastases. *British Journal of Cancer*, **75**(10):1474-1480 (1997).

Anwar K, Nakakuki K, Naiki H and Inuzuka M. ras gene mutations and HPV infection are common in human laryngeal carcinoma. *International Journal of Cancer*, **53**(1):22-28 (1993).

Apte SS, Mattei M-G and Olsen BR. Cloning of the cDNA encoding human tissue inhibitor of metalloproteinases-3 (TIMP-3) and mapping of the TIMP3 gene to chromosome 22. *Genomics*, **19**:86-90 (1994).

Atchley WR and Fitch WM. Myc and Max: molecular evolution of a family of proto-oncogene products and their dimerization partner. *Proc. Nat. Acad. Sci*, **92**:10217-10221 (1995).

Auerbach O, Stout AP, Hammond EC and Garfinkle I. Changes in bronchial epithelium in relation to cigarette smoking and in relation to lung cancer. *New England Journal of Medicine* **256**:253-267 (1961).

Azemar M, Schmidt M, Arlt F, Kennel P, Brandt B, Papadimitriou A, Groner B and Wels W. Recombinant ntibody toxins specific for ErbB2 and EGF receptor inhibit the in vitro growth of human head and neck cancer cells and cause rapid tumor regression in vivo. *International Journal of Cancer*, **86**(2):269-275 (2000).

Baillie-Johnson H, Twentyman PR, Fox NE, Walls GA, Workman P, Watson JV, Johnson N, Reeve JG and Bleehen NM. Establishment and characterisation of cell lines from patients with lung cancer (predominantly small cell carcinoma). *British Journal of Cancer*, **52**(4):495-504 (1985).

Balmain A and Birnie GD. Nick translation of mammalian DNA. *Biochimica et Biophysica Acta*, **561**(1):155-66 (1979).

Baross-Francis A, Andrew SE, Penney JE and Jirik FR. Tumors of DNA mismatch repair-deficient hosts exhibit dramatic increases in genomic instability. *Proceedings of the National Academy of Sciences of the United States of America*, **95**(15):8739-8743 (1998).

Barth TF, Benner A, Bentz M, Dohner H, Moller P and Lichter P. Risk of false positive results in comparative genomic hybridization. *Genes, Chromosomes & Cancer*, **28**(3):353-357 (2000).

Bedi GC, Westra WH, Gabrielson E, Koch W and Sidransky D. Multiple head and neck tumors: evidence for a common clonal origin. *Cancer Research*, **56**(11):2484-2487 (1996).

Bellacosa A, Almadori G, Cavallo S, Cadoni G, Galli J, Ferrendina G, Scambia G and Neri G. Cyclin D1 gene amplification in human laryngeal squamous cell carcinomas: prognostic significance and clinical implications. *Clin Cancer Res*, **2**:175-180 (1996).

Bentz M, Plesch A, Stilgenbauer S, Dohner H and Lichter P. Minimal sizes of deletions detected by comparative genomic hybridization. *Genes, Chromosomes & Cancer*, **21**(2):172-175 (1998).

Bergamo NA, Rogatto SR, Poli-Frederico RC, Reis PP, Kowalski LP, Zielenska M and Squire JA. Comparative genomic hybridization analysis detects frequent over-representation of DNA sequences at 3q, 7p, and 8q in head and neck carcinomas. *Cancer Genetics & Cytogenetics*, **119**(1):48-55 (2000).

Blons H, Cabelguenne A, Camot F, Laccourreye O, de Waziers I, Hamelin R, Brasnu D, Beaune P and Laurent-Puig P. Microsatellite analysis and response to chemotherapy in head-and-neck squamous-cell-carcinoma. *International Journal of Cancer*, **84**(4):410-415 (1999).

Blot WJ, McLaughlin JK, Winn DM, Austin DF, Grumbers RS, Preston-Martin S, Bernstein L, Schoenberg JB, Stemhagen A and Fraumeni JF Jr. Smoking and drinking in relation to oral and pharyngeal cancer. *Cancer Res*, **48**: 3282-3287 (1988).

Bockmühl U, Petersen I, Schwendel A and Dietel M. Genetic screening of head-neck carcinomas using comparative genomic hybridization (CGH). *Laryngo- Rhino- Otologie*, **75**(7):408-414 (1996).

Bockmühl U, Wolf G, Schmidt S, Schwendel A, Jahnke V, Dietel M and Petersen I. Genomic alterations associated with malignancy in head and neck cancer. *Head and Neck*, **20**(2):145-151 (1998).

Bockmühl U, Schluns K, Kuchler I, Petersen S and Petersen I. Genetic imbalances with impact on survival in head and neck cancer patients. *American Journal of Pathology*, **157**(2):369-375 (2000).

Bouchard C, Staller P and Eilers M. Control of cell proliferation by myc. *Trends in Cell Biology*, 8:202-206 (1998).

Bouquot JE and Whitaker SB. Oral leukoplakia--rationale for diagnosis and prognosis of its clinical subtypes or "phases". *Quint Internat*, **25**:133-140 (1994).

Boveri T. Zur frage der entstehung maligner tumoren, *Gustav Fischer*, Jena (1914).

Boyle JO, Hakim J, Koch W, van der Riet P, Hruban RH, Roa RA, Correo R, Eby YJ, Ruppert JM and Sidransky D. The incidence of p53 mutations increases with progression of head and neck cancer. *Cancer Research*, **53**(19):4477-4480 (1993).

Breasted JH. *The Edwin Smith Papyrus*. p403, University of Chicago Press, Chicago. (1970)

Brennan JA, Boyle JO, Koch WM, Goodman SN, Hruban RH, Eby YJ, Couch MJ, Forastier AA and Sidransky D. Association between cigarette smoking and mutation of the p53 gene in squamous cell carcinoma of the head and neck. *New England Journal of Medicine*, **332**:712-717 (1995a).

Brennan JA, Mao L, Hruban RH, Boyle JO, Eby YJ, Koch WM, Goodman SN and Sidransky D. Molecular assessment of histopathological staging in squamous-cell carcinoma of the head and neck. *New England Journal of Medicine*, **332**(7):429-35 (1995b).

Bristow RG, Benchimol S and Hill RP. The p53 gene as a modifier of intrinsic radiosensitivity: implications for radio therapy. *Radiotherapy and Oncology*, **40**:197-223 (1996).

Brzoska PM, Levin NA, Fu KK, Kaplan MJ, Singer MI, Gray JW and Christian MF. Frequent novel DNA copy number increase in squamous cell head and neck tumours. *Cancer Research*, **55**:3055-3059 (1995).

Burns JE, Baird MC, Clark LJ, Burns PA, Edington K, Chapman C, Mitchell R, Robertson G, Soutar D and Parkinson EK. Gene mutations and increased levels of p53 protein in human squamous cell carcinomas and their cell lines. *British Journal of Cancer*, **67**(6):1274-1284 (1993).

Cachin Y. Management of cervical nodes in head and neck cancer. In: Rhys Evans PH, Robin PE, Fielding JWL, (Eds). *Head and neck cancer.* Castle House Publications Ltd, London. England, pp168-177 (1983).

Cahill DP, Lengauer , Yu J, Riggins GJ, Willson JK, Markowitz SD, Kinzler KW and Vogelstein B. Mutations of mitotic checkpoint genes in human cancers. *Nature*, **392**:223-224 (1998).

Califano J, van der Reit P, Westra W, Narwoz H, Clayman G, Piantadosi S, Corio R, Lee D, Greenberg B, Koch W and Sidransky D. Genetic progression model for head and neck cancer: Implications for field cancerization. *Cancer Research*, **56**:2488-2492 (1996).

Callender T, el-Naggar AK, Lee MS, Frankenthaler R, Luna MA and Batsakis JG. PRAD-1 (CCND1)/cyclin D1 oncogene amplification in primary head and neck squamous cell carcinoma. *Cancer*, **74**:152-158 (1994).

Capaccio P, Pruneri G, Carboni N, Pagliari AV, Quatela M, Cesana BM and Pignataro L. Cyclin D1 expression is predictive of occult metastases in head and neck cancer patients with clinically negative cervical lymph nodes. *Head & Neck*, **22**(3):234-240 (2000).

Carey TE, Van Dyke DL and Worsham MJ. Non random chromosome aberrations and clonal populations in head and neck cancer. *Anti cancer Research*, **13**:2561-2568 (1993).

Carothers AM. DNA damage, mutation, and repair. In: Bertino JR Ed. *Encyclopedia of Cancer*, Academic Press, New York and London, pp484 (1997).

Carriot F and Sasco AJ. Cannabis and cancer. *Revue d Epidemiologie et de Sante Publique*, **48**(5):473-83, (2000).

Caspersson T, Zech L and Johansson C. Analysis of human metaphase chromosome set by aid of DNA-binding fluorescent agents. *Experimental Cell Research*, **62**(2):490-492 (1970).

Cattani P, Hohaus S, Bellacosa A, Genuardi M, Cavallo S, Rovella V, Almadori G, Cadoni G, Galli J, Maurizi M, Fadda G and Neri G. Association between cyclin D1 (CCND1) gene amplification and human papillomavirus infection in human laryngeal squamous cell carcinoma. *Clinical Cancer Research*, 4(11):2585-2589 (1998).

Cerezo L, Millan I, Torre A Aragon G and Otero J. Prognostic factors for survival and tumour control in cervical lymph node metastases from head and neck cancer: a multivariant study of cases. *Cancer*, 69:1224-1234 (1992).

Chang EH, Jang YJ, Hao Z, Murphy G, Rait A, Fee We Jr, Sussman HH, Ryan P, Chaing Y and Pirollo KF. Restoration of the G1 checkpoint and the apoptotic pathway mediated by wild type p53 sensitises squamous cell carcinoma of the head and neck to radiotherapy. *Archives of Otolaryngology – Head and Neck Surgery*, 123(5):507-512 (1997).

Charuruks N, Shin DM, Voravud N. Ro JY, Hong WK and Hittelman WN. Genetic instabilities of chromosome 9, 17 and accumulation of p53 overexpression during multistage tumorigesis in head and neck cancer. *Journal of the Medical Association of Thailand*, 79 (Suppl 1):S104-112 (1996).

Chen XN, Knauf A, Gonsky R, Wang M, Lai EH, Chissoe S, Fagin JA and Korenburg JR. From amplification to gene in thyroid cancer: A high resolution mapped bacterial-artificial-chromosome resource for cancer chromosome aberrations guides gene discovery after comparative genomic hybridization. *Am J Human Genetics*, 63:625-637 (1998).

Cheng L, Sturgis EM, Eicher SA, Char D, Spitz MR and Wei Q. Glutathione-S-transferase polymorphisms and risk of squamous-cell carcinoma of the head and neck. *International Journal of Cancer*, 84(3):220-224 (1999).

Choi G and Chung K. Polysomies of chromosomes 7 and 17 in head and neck squamous cell carcinomas. *Arch Otolaryngology Head and Neck Surgery*, 122:1062-1067 (1996).

Chung KY, Mukhopadhyay T, Kim J, Casson A, Ro JY, Goepfert H, Hong WK and Roth JA. Discordant p53 gene mutations in primary head and neck cancers and corresponding second primary cancers of the upper aerodigestive tract. *Cancer Research*, 53(7):1676-1683 (1993).

Clark LJ, Edington K, Swan IR, McLay KA, Newlands WJ, Wills LC, Young HA, Johnston PW, Mitchell R and Robertson G. The absence of Harvey ras mutations during development and progression of squamous cell carcinomas of the head and neck. *British Journal of Cancer*, **68**(3):617-620 (1993).

Clayman GL, Stewart MG, Weber RS, el-Naggar AK and Grimm EA. Human papillomavirus in laryngeal and hypopharyngeal carcinomas. Relationship to survival. *Archives of Otolaryngology -- Head & Neck Surgery*, **120**(7):743-748 (1994).

Clayman GL, el-Naggar AK, Lippman SM, Henderson YC, Frederick M, Merritt JA, Zumstein LA, Timmons TM, Liu TJ, Ginsberg L, Roth JA, Hong WK, Bruso P and Goepfert H. Adenovirus-mediated p53 gene transfer in patients with advanced recurrent head and neck squamous cell carcinoma. *Journal of Clinical Oncology*, **16**(6):2221-2232 (1998).

Cloos J, Spitz SP, Hsu TC, Zhang ZF, Tobi H, Braakhuis BJ and Snow GB. Genetic susceptibility to head and neck squamous cell carcinoma. *Journal of the National Cancer Institute*, **88**(8):530-535 (1996).

Cookson MM. Prostate cancer: screening and early detection. *Cancer Control*, **8**(2):133-40 (2001).

Cope C, Rowe D, Delbridge L, Philips J and Friedlander M. Comparison of image analysis and flow cytometric determination of cellular DNA content. *Journal of Clinical Pathology*, **44**(2):147-151 (1991).

Copper MP, Jovanovic A, Nauta JJ, Braakhuis BJ, de Vries N, van der Waal I and Snow GB. Role of genetic factors in the etiology of squamous cell carcinoma of the head and neck. *Curr Probl Cancer*, **17**:69-141 (1993).

Cowan JM, Beckett MA and Weichselbaum RR. Chromosome changes characterizing in vitro response to radiation in human squamous cell carcinoma cell lines. *Cancer Research*, **53**:5542-5547 (1993).

Craven JM, Pavelic ZP, Stambrook PJ, Pavelic L, Gapany M, Kelley DJ, Gapany S and Gluckman JL. Expression of c-erbB-2 gene in human head and neck carcinoma. *Anticancer Research*, **12**(6B):2273-2276 (1992).

Crissman JD, Liu WY, Gluckman JL and Cummings G. Prognostic value of histopathologic parameters in squamous cell carcinoma of the oropharynx. *Cancer*, **54**: 2995-3001 (1984).

Cunningham C, Dunlop GM, Wylie AH and Bird CC. Deletion mapping in colorectal cancer of a putative tumour suppressor gene in 8p22-p21.3. *Oncogene*, 8(5):1391-1396 (1993).

Czepulkowski B. *Analysing Chromosomes.* Bios Scientific Publishers Limited (2001).

Das N, Majumder J and DasGupta UB. ras gene mutations in oral cancer in eastern India. *Oral Oncology*, **36**(1):76-80 (2000).

DavidsonTM, Haghighi P, Astarita R, Baird S and Seagrean S. Microscopically orientated histological surgery for head and neck mucaosal cancer. *Cancer*, 60:1865-1861 (1987).

Davidson BJ, Lydiatt WM, Abate MP, Schantz SP and Chaganti RS. Cyclin D1 abnormalities and tobacco exposure in head and neck squamous cell carcinoma. *Head & Neck*, **18**(6):512-521 (1996).

de Meulemeester M, Vink A, Jakobs M, Hermsen M, Steenman M, Slater R, Dietrich A and Mannens M. The application of microwave denaturation in comparative genomic hybridization. *Genetic Analysis*, **13**(5):129-133 (1996).

Deitch A. Cytophotometry of nucleic acids. In: Weid GL (Ed). *Introduction to Quantitive Cytochemistry*. pp327-354, Academic Press, New York and London (1966).

DiPaola RS and Aisner J. Overcoming bcl-2- and p53-mediated resistance in prostate cancer. [Review] *Seminars in Oncology*, **26**(1 Suppl 2):112-116 (1999).

Donald PJ. Marijuana smoking - possible cause of head and neck carcinoma in young patients. *Otolaryngol Head Neck Surg*, **94**: 517-521 (1986).

du Manoir S, Schrock E, Bentz M, Speicher MR, Joos S, Ried T, Lichter P and Cremer T. Quantitative analysis of comparative genomic hybridization. *Cytometry*, **19**(1):27-41 (1995).

El-Naggar AK, Lai S, Luna MA, Zhou XD, Weber RS, Goepfert H and Batsakis JG. Sequential p53 mutation analysis of pre-invasive and invasive head and neck squamous cell carcinoma. *International Journal of Cancer*, **64**:196-201 (1995).

El-Naggar AK, Lai S, Clayman G, Lee JK, Luna MA, Goepfert H and Batsakis JG. Methylation, a major mechanism of p16/CDKN2 gene inactivation in head and neck squamous carcinoma. *American Journal of Pathology*, **151**(6):1767-1774 (1997a).

El-Naggar AK, Hurr K, Luna MA, Goepfert H, Hong WK and Batsakis JG. Intratumoral genetic heterogeneity in primary head and neck squamous carcinoma using microsatellite markers. *Diagnostic Molecular Pathology*, **6**(6):305-308 (1997b).

Emmert-Buck MR, Bonner RF, Smith PD, Chuaqui RF, Zhuang Z, Goldstein SR, Weiss RA and Liotta LA. Laser capture microdissection. *Science*, **274**(5289):998-1001 (1996).

Erber R, Klein W, Andl T, Enders C, Born AI, Conradt C, Bartek J and Bosch FX. Aberrant p21(CIP1/WAF1) protein accumulation in head-and-neck cancer. *International Journal of Cancer*, **74**(4):383-389 (1997).

Erber R, Conradt C, Homann N, Enders C, Finckh M, Dietz A, Weidauer H and Bosch FX. TP53 DNA contact mutations are selectively associated with allelic loss and have a strong clinical impact in head and neck cancer. *Oncogene*, **16**(13):1671-1679 (1998).

Fearon ER and Vogelstein B. A genetic model for colorectal tumorogenesis. *Cell*, **61**:759-767 (1990).

Fedder M and Gonzalez MF. Nasopharyngeal carcinoma: brief review. *Am J Med*, **79**: 365 (1985).

Fidler IJ and Kripke ML. Metastasis results from preexisting variant cells within a malignant tumor. *Science*, **197**(4306):893-895 (1977).

Field JK, Spandidos DA, Stell PM, Vaughan ED, Evan GI and Moore JP. Elevated expression of the c-myc onco-protein correlates with poor prognosis in head and neck squamous cell carcinoma. *Oncogene*, **4**:1463-1468 (1989).

Field JK and Spandidos DA. The role of ras and myc oncogenes in human solid tumours and their relevance in diagnosis and prognosis. A review. *Anticancer Research*, **10**:1-22 (1990).

Field JK, Risk JM, Tsiriyotis C, Adamson R, Zoumpourlis V, Rowley H, Taylor K, Whittaker J, Howard P, Beirne JC, Gosney JR, Woolgar J, Vaughan ED, Spandidos DA and Jones AS. Allelotype of squamous cell carcinoma of the head and neck: fractional allele loss correlates with survival. *British Journal of Cancer*, **72**(5):1180-1188 (1995).

Flaitz CM, Hicks MJ. Molecular piracy: the viral link to carcinogenesis. *Oral Oncol.* **34**(6):448-53 (1998).

Ford CE, Jones KW, Miller OJ, Mittwoch U, Penrose LS, Ridler M and Shapiro A. The chromosomes in a patient showing both mongolism and the Klinefelter syndrome. *Lancet* **i**:709-710 (1959).

Fortin A, Guerry M, Guerry R, Talbot M, Praise O, Schwaab G, Bosq J, Bourhis J, Salvatori P, Janot F and Busson P. Chromosome 11q13 gene amplifications in oral and oropharangeal carcinomas: no correlation with subclinical lymph node invasion and disease recurrence. *Clin Cancer Res*, **3**:1609-1614 (1997).

Freije JM, MacDonald NJ and Steeg PS. Nm23 and tumour metastasis: basic and translational advances. *Biochemical Society Symposia*, **63**:261-271 (1998).

Fu CG, Tominaga O, Nagawa H, Nita ME, Masaki T, Ishimaru G, Higuchi Y, Tsuruo T and Muto T. Role of p53 and p21/Waf1 detection in patient selection for preoperative radiotherapy in rectal cancer patients. *Diseases of the Colon and Rectum*, **54**:3361-3364 (1998).

Gallo O, Chiarelli I, Boddi V, Bocciolini C, Bruschini L and Porfirio B. Cumulative prognostic value of p53 mutations and bcl-2 protein expression in head-and-neck cancer treated by radiotherapy. *International Journal of Cancer*, **84**(6):573-579 (1999).

Gannon JV, Greaves R, Iggo R and Lane DP. Activating mutations in p53 produce a common conformational effect. A monoclonal antibody specific for the mutant form. *EMBO Journal*, **9**:1595-1602 (1990).

Garkavtsev I, Kazarov A, Gudkov A and Riabowol K. Suppression of the novel growth inhibitor p33ING1 promotes neoplastic transformation. *Nature Genetics*, **14**(4):415-420 (1996).

Garkavtsev I, Demetrick D and Riabowol K. Cellular localization and chromosome mapping of a novel candidate tumor suppressor gene (ING1). *Cytogenetics & Cell Genetics*, **76**(3-4):176-178 (1997).

Gasparotto D, Maestro R, Barzan L, Vukosavljevic T, Doglioni C, Sulfaro S, Piccinin S and Boiocchi M. Recurrences and second primary tumours in the head and neck region: differentiation by p53 mutation analysis. *Annals of Oncology*, **6**(9):933-939 (1995).

Gebhart E, Liehr T, Wolff E, Ries J, Fiedler W, Steininger H, Koscielny S and Girod S. Pattern of genomic imbalances in oral squamous cell carcinomas with and without an increased copy number of 11q13. *International Journal of Oncology*, **12**(5):1151-1155 (1998).

Gebhart E and Liehr T. Patterns of genomic imbalances in human solid tumours (Review). *International Journal of Oncology*, **16**:385-399 (2000).

Giannoudis A and Herrington CS. Human papillomavirus variants and squamous neoplasia of the cervix. [Review] *Journal of Pathology*, **193**(3):295-302 (2001).

Glaab WE and Tindall KR. Mutation rate at the hprt locus in human cancer cell lines with specific mismatch repair-gene defects. *Carcinogenesis*, **18**(1):1-8 (1997).

Gotte K, Hadaczek P, Coy JF, Wirtz HW, Riedel F, Neubauer J and Hormann K. Fhit expression is absent or reduced in a subset of primary head and neck cancer. *Anticancer Research*, **20**(2A):1057-1060 (2000).

Grandis JR and Tweardy DJ. Elevated levels of transforming growth factor alpha and epidermal growth factor receptor messenger RNA are early markers of carcinogenesis in head and neck cancer. *Cancer Research*, **53**:3579-3584 (1993).

Grandis JR and Tweardy DJ. Elevated levels of transforming growth factor alpha and epidermal growth factor receptor messenger RNA are early markers of carcinogenesis in head and neck cancer. *Cancer Research*, **53**(15):3579-3584 (1993).

Grandis JR, Melhem MF, Gooding WE, Day R, Holst VA, Wagener MM, Drenning SD and Tweardy DJ. Levels of TGF-alpha and EGFR protein in head and neck squamous cell carcinoma and patient survival. *Journal of the National Cancer Institute*, **90**(11):824-832 (1998).

Greenblatt MS, Bennet WP, Hollstein M and Haris CC. Mutations in the p53 tumor suppressor gene: Clue to cancer etiology and molecular pathogenesis. *Cancer Research*, **54**:4855-4878 (1994).

Greenman J, Ashman JNE, Brankin V V, McDonald AW, Duthie GS, Lee PWR, Kerin MJ and Monson JRT. Multiple cell populations in colorectal carcinomas: analysis by 3-colour fluorescence in situ hybridization. *International Journal of Oncology*, **12**(1):75-80 (1998).

Griffin BE. Epstein-Barr virus (EBV) and human disease: facts, opinions and problems. *Mutation Research*, **462**(2-3):395-405 (2000).

Gronbank M, Becker U, Johansen DHT, Jensen G and Tia S. Population based cohort study of the association between alcohol intake and cancer of the upper digestive tract. *BMJ*, **317**:844-848 (1998).

Gupta VK, Schmidt AP, Pashia ME, Sunwoo JB and Scholnick SB. Multiple regions of deletion on chromosome arm 13q in head-and-neck squamous-cell carcinoma. *International Journal of Cancer*, **84**(5):453-457 (1999).

Gutman M, Ravia Y, Assaf D, Yamamoto T, Rozin R and Shiloh Y. Amplification of c-myc and c-erbB-2 protooncogenes in human solid tumours: frequency and clinical significance. *International Journal of Cancer*, **44**:802-805 (1989).

Hager G, Formanek M, Gedlicka C, Knerer B and Kornfehl J. Ethanol decreases expression of p21 and increases hyperphosphorylated pRb in cell lines of squamous cell carcinomas of the head and neck. *Alcoholism: Clinical & Experimental Research*, **25**(4):496-501 (2001).

Hardman RA, Afshari CA and Barrett JC. Involvement of mammalian MLH1 in the apoptotic response to peroxide-induced oxidative stress. *Cancer Research*, **61**(4):1392-1397 (2001).

Harwood AR, Beale FA, Cummings BJ, Keane T and Rider WT. T2 glottic cancer: an analysis of time dose-volume factor. *Int J of Radiat. Oncol Biol. Phys*, **7**:1501-1505 (1981).

Huang SM, Bock JM and Harari PM. Epidermal growth factor receptor blockade with C225 modulates proliferation, apoptosis, and radiosensitivity in squamous cell carcinomas of the head and neck. *Cancer Research*, **59**(8):1935-1940 (1999).

He Y, Zeng Q, Drenning SD, Melhem MF, Tweardy DJ, Huang L and Grandis JR. Inhibition of human squamous cell carcinoma growth in vivo by epidermal growth factor receptor antisense RNA transcribed from the U6 promoter. *Journal of the National Cancer Institute*, **90**(14):1080-1087 (1998).

Heim S and Mitelman F. Nineteen of 26 cellular oncogenes precisely localized in the human genome map to one of the 83 bands involved in primary cancer-specific rearrangements. *Hum Genet*, **75**:70-72 (1987).

Hemmer J, Kraft K and Polackova J. Representativity of incisional biopsies for the assessment of flow cytometric DNA content in head and neck squamous cell carcinoma. *Pathology, Research & Practice*, **194**(2):105-109 (1998).

Hemmer J, Nagel E and Kraft K. DNA aneuploidy by flow cytometry is an independent prognostic factor in squamous cell carcinoma of the oral cavity. *Anticancer Research*, **19**(2B):1419-1422 (1999).

Henderson BE, Louie E, SooHoo Jing J, Buell P and Gardner MB. Risk factors associated with nasopharyngeal carcinoma. *N Engl J Med*, **295**: 1101-1106 (1977).

Henegariu O, Heerema NA, Wright LL, Bray-Ward P, Ward DC and Vance GH. Improvements in Cytogenetic Slide Preparation: Controlled Chromosome Spreading, Chemical Aging and Gradual Denaturing. *Cytometry*, **43**:101–109 (2001).

Hermsen M, Guervos MA, Meijer G, Baak J, van Diest P, Marcos CA and Sampedro A. New chromosomal regions with high-level amplifications in squamous cell carcinomas of the larynx and pharynx, identified by comparative genomic hybridization. *Journal of Pathology*, **194**(2):177-182 (2001).

Hibi K, Takahashi T, Yamakawa K, Ueda R, Sekido Y, Ariyoshi Y, Suyama M, Takagi H, Nakamura Y and Takahashi T. Three distinct regions involved in human lung cancer. *Oncogene*, **7**:445-449 (1992).

Hinds PW, Dowdy SF, Eaton EN, Arnold A and Weinberg RA. Function of a human cyclin gene as an oncogene. *Proceedings of the National Academy of Sciences of the United States of America*, **91**(2):709-713 (1994).

Hittelman WN, Voravud N, Shin DM, Lee JS, Ro JY and Hong WK. Early genetic changes during upper aerodigestive tract tumorigenesis. *Journal of Cellular Biochemistry – Supplement*, **17F**:233-236 (1993).

Hollstein MC, Peri L, Mandard AM, Welsh JA, Montesano R, Metcalf RA, Bak M and Harris CC. Genetic analysis of human esophageal tumors from two high incidence geographic areas: frequent p53 base substitutions and absence of ras mutations. *Cancer Research*, **51**(15):4102-4106 (1991).

Hoffman HT, Karnell LH, Funk GF, Robinson RA and Menck HR. The National Cancer Data Base report on cancer of the head and neck. *Archives of Otolaryngology - Head & Neck Surgery*, **124**(9):951-962 (1998).

Homer JJ, Greenman J and Stafford ND. Angiogenesis in head and neck squamous cell carcinoma. *Clin Otolaryngol*, **25**:169-180 (2000).

Hsu SM, Raine L and Fanger H. The use of antiavidin antibody and avidin-biotin-peroxidase complex in immunoperoxidase techniques. *American Journal of Clinical Pathology*, **75**(6):816-21 (1981a).

Hsu SM, Raine L and Fanger H. Use of avidin-biotin-peroxidase complex (ABC) in immunoperoxidase techniques: a comparison between ABC and unlabeled antibody (PAP) procedures. *Journal of Histochemistry & Cytochemistry*, **29**(4):577-80 (1981b).

Hsu TC. Mammalian chromosomes in vitro. I. The karyotype of man. *J Hered*, **43**:167-172 (1952).

Hussussian CJ, Struewing JP, Goldstein AM, Higgins PA, Ally DS, Sheahan MD, Clark WH Jr, Tucker MA and Dracopoli NC. Germline p16 mutations in familial melanoma. *Nature Genetics*, 8(1):15-21 (1994).

Ishitoya J, Toriyama M, Oguchi N, Kitamura K, Ohshima M, Asano K and Yamamoto T. Gene amplification and overexpression of EGF receptor in squamous cell carcinomas of the head and neck. *British Journal of Cancer*, **59**:559-562 (1989).

Jacob R, Welkoborsky HJ, Mann WJ, Hofken F, Dienes HP and Freije JE. Heterogeneity of squamous cell carcinomas of the head and neck--analysis of tumor biologic factors and proliferation rates. *Laryngoscope*, **106**(9Pt 1):1170-1175 (1996).

Jafek BW and Stark AK (Eds). *ENT Secrets*. Hanley and Belfus, Inc. Philadelphia (1996).

Jahnke V, Matthias C, Fryer A and Strange R. Glutathione S-transferase and cytochrome-P-450 polymorphism as risk factors for squamous cell carcinoma of the larynx. *American Journal of Surgery*, **172**(6):671-673 (1996).

Jahnke V, Matthias C, Bockmuhl U and Strange RC. Genetic predisposition for the development of head and neck carcinomas. [German] *Laryngo- Rhino- Otologie*, **78**(1):24-27 (1999).

James LA. Comparative genomic hybridization as a tool in tumour cytogenetics. *Journal of Pathology*, **187**(4):385-395 (1999).

Jang M, Cai L, Udeani GO, Slowing KV, Thomas CF, Beecher CW, Fong HH, Farnsworth NR, Kinghorn AD, Mehta RG, Moon, RC and Pezzuto JM. Cancer chemopreventive activity of resveratrol, a natural product derived from grapes. *Science*, **275**:218-20 (1997).

Janot F, Klijanienko J, Russo A, Mamet JP, de Braud F, El-Naggar AK, Pignon JP, Luboinski B and Cvitkovic E. Prognostic value of clinicopathological parameters in head and neck squamous cell carcinoma: a prospective analysis. *British Journal of Cancer*, **73**(4):531-538 (1996).

Jin Y, Mertens F, Mandahl N, Heim S, Olegard C, Wennerberg J, Biorklund A and Mitelman F. Chromosome abnormalities in eighty-three head and neck squamous cell carcinomas: influence of culture conditions on karyotypic pattern. *Cancer Research*, **53**(9):2140-2146 (1993).

Jin Y, Mertens F, Jin C, Akervall J, Wennerberg J, Gorunova L, Mandahl N, Heim S and Mitelman F. Nonrandom chromosome abnormalities in short-term cultured primary squamous cell carcinomas of the head and neck. *Cancer Research*, **55**(14):3204-3210 (1995).

Jin C, Jin Y, Wennerberg J, Dictor M and Mertens F. Nonrandom pattern of cytogenetic abnormalities in squamous cell carcinoma of the larynx. *Genes, Chromosomes & Cancer*, **28**(1):66-76 (2000).

Jones AS, Morar P, Phillips DE, Field JK, Husband D and Helliwell TR. Second primary tumours in patients with head and neck squamous cell carcinoma. *Cancer*, **75**:1343-1353 (1995).

Jones AS, Houghton DJ, Beasley NJ and Husband DJ. Improved survival in patients with head and neck cancer in the 1990's. *Clin Otolaryngol*, **23**:319-325 (1998).

Jones JW, Raval JR, Beals TF, Worsham MJ, Van Dyke DL, Esclamado RM, Wolf GT, Bradford CR, Miller T and Carey TE. Frequent loss of heterozygosity on chromosome arm 18q in squamous cell carcinomas: Identification of 2 regions of loss – 18q11.1-q12.3 and 18q21.1-q23. *Archives of Otolaryngology and Head and Neck Surgery*, **123**:610-614 (1997).

Joos S, Scherthan H, Speicher MR, Schlegel J, Cremer T and Lichter P. Detection of amplified DNA sequences by reverse chromosome painting using genomic tumor DNA as probe. *Human Genetics*, **90**(6):584-589 (1993).

Kallioniemi A, Kallioniemi OP, Sudar D, Rutovitz D, Gray JW, Waldman and Pinkle D. Comparative genomic hybridization for molecular cytogenetic analysis of solid tumours. *Science*, **258**:818-821 (1992).

Kallioniemi OP, Kallioniemi A, Piper J, Isola J, Waldman FM, Gray JW and Pinkel D. Optimizing comparative genomic hybridization for analysis of DNA sequence copy number changes in solid tumors. *Genes, Chromosomes & Cancer*, **10**(4):231-243 (1994).

Kamb A, Gruis NA, Weaver-Feldhaus J, Liu Q, Harshman K, Tavtigian SV, Stockert E, Day RS III, Johnson BE and Skolnick MH. A cell cycle regulator potentially involved in genesis of many tumor types. *Science*, **264**: 436-440 (1994).

Kapranos N, Stathopoulos GP, Manolopoulos L, Kokka E, Papadimitriou C, Bibas A, Yiotakis J and Adamopoulos G. p53, p21 and p27 protein expression in head and neck cancer and their prognostic value. *Anticancer Research*, **21**(1B):521-528 (2001).

Karhu R, Kahkonen M, Kuukasjarvi T, Pennanen S, Tirkkonen M and Kallioniemi O. Quality control of CGH: impact of metaphase chromosomes and the dynamic range of hybridization. *Cytometry*, **28**(3):198-205 (1997).

Katoh T, Kaneko S, Boissy R, Watson M, Ikemura K and Bell DA. A pilot study testing the association between N-acetyltransferases 1 and 2 and risk of oral squamous cell carcinoma in Japanese people. *Carcinogenesis*, **19**(10):1803-1807 (1998).

Kearsley JH, Leonard JH, Walsh MD and Wright GR. A comparison of epidermal growth factor receptor (EGFR) and c-erbB-2 oncogene expression in head and neck squamous cell carcinomas. *Pathology*, **23**(3):189-194 (1991).

Kendall MJ, Toescu V and Wallace DM. QED: quick and early diagnosis. *Lancet*, **348**(9026):528-529 (1996).

Kerbel RS, Waghorne C, Korczak B, Lagarde A and Breitman ML. Clonal dominance of primary tumours by metastatic cells: genetic analysis and biological implications. [Review] *Cancer Surveys*, **7**(4):597-629 (1988).

Kiaris H, Spandidos DA, Jones AS, Vaughan ED and Field JK. Mutations and genomic instability of the H-ras proto-oncogene in squamous cell carcinomas of the head and neck. *Br J Cancer*, **72**:123-128 (1995).

Kiaris H, Spanakis N, Ergazaki M, Sourvinos G and Spandidos DA. Loss of heterozygosity at 9p and 17q in human laryngeal tumors. *Cancer Letters*, **97**(1):129-134 (1995).

King R, *Cancer Biology 2nd Edition*. Prentice Hall, London (2000)

Kinzler KW and Vogelstein B. Lessons from hereditary colon cancer. *Cell*, **87**:159-170 (1996).

Kinzler KW and Vogelstein B. Gatekeepers and caretakers. *Nature*, **386**:761-763 (1997).

Kim J, Shin DM, El-Naggar A, Lee JS, Corrales C, Lippman SM, Hong WK and Hittelman WN. Chromosome polysomy and histological characteristics in oral premalignant lesions. *Cancer Epidemiology, Biomarkers & Prevention*, **10**(4):319-325 (2001).

Kirchhoff M, Geredes T, Rose H, Maahr J, Ottesen AM and Lundsteen C. Detection of chromosomal gains and losses in comparative genomic hybridization analysis based on standard reference intervals. *Cytometry*, **31**:163-173 (1998).

Kirchhoff M, Gerdes T, Maahr J, Rose H, Bentz M, Döhner H and Lundsteen C. Deletions below 10 megabasepairs are detected in comparative genomic hybridizations by standard reference intervals. *Genes, Chromosomes and Cancer*, **25**:410-413 (1999).

Knauf JA, Elisei R, Mochly-Rosen D, Liron T, Chen XN, Gonsky R, Korenberg JR, Fagin JA. Involvement of protein kinase Cepsilon (PKCepsilon) in thyroid cell death. A truncated chimeric PKCepsilon cloned from a thyroid cancer cell line protects thyroid cells from apoptosis. *J Biolog Chem*, **274**(33):23414-23425 (1999).

Knudson AG Jr. Mutation and cancer: statistical study of retinoblastoma. *Proceedings of the National Academy of Sciences of the United States of America*, **68**(4):820-823 (1971).

Kocabas NA. Karahalil B. Karakaya AE. Sardas S. Influence of GSTM1 genotype on comet assay and chromosome aberrations after induction by bleomycin in cultured human lymphocytes. *Mutation Research*, **469**(2):199-205 (2000).

Koty PP, Zhang H and Levitt ML. Antisense bcl-2 treatment increases programmed cell death in non-small cell lung cancer cell lines. *Lung Cancer*, **23**(2):115-127 (1999).

Kraus J, Weber RG, Cremer M, Seebacher T, Fischer C, Schurra C, Jauch A, Lichter P, Bensimon A and Cremer T. High-resolution comparative hybridization to combed DNA fibers. *Human Genetics*, **99**(3):374-380 (1997).

Krishnamurthy J, Kannan K, Feng J, Mohanprasad BK, Tsuchida N and Shanmugam G. Mutational analysis of the candidate tumor suppressor gene ING1 in Indian oral squamous cell carcinoma. *Oral Oncology*, **37**(3):222-224 (2001).

Kropveld A, van Mansfield AD, Nabben N, Hordijk GJ and Slootweg PJ. Discordance of p53 status in head and neck squamous cell carcinoma patients. *European Journal of Cancer, Part B, Oral Oncology*, **32B**(6):388-393 (1996).

Kropveld A, Rozemuller EH, Leppers FGJ, Scheidel KC, de Weger RA, Koole R, Hordijk GJ, Slootweg PL and Tilanus MGJ. Sequencing analysis of RNA and DNA of Exons 1 through 11 shows p53 gene alterations to be present in almost 100% of head and neck squamous cell cancers. *Laboratory Investigations*, **79**:347-353 (1999).

Kunkel TA. DNA-mismatch repair. The intricacies of eukaryotic spell-checking. *Current Biology*, **5**(10):1091-1094 (1995).

Kurzrock R, Gutterman JU and Talpaz M. The molecular genetics of Philadelphia chromosome-positive leukemias. *New England Journal of Medicine*, **319**(15):990-998 (1988).

Kuukasjarvi T, Karhu R, Tanner M, Kahkonen M, Schaffer A, Nupponen N, Pennanen S, Kallioniemi A, Kallioniemi OP and Isola J. Genetic heterogeneity and clonal evolution underlying development of asynchronous metastasis in human breast cancer. *Cancer Research*, **57**(8):1597-1604 (1997).

Kyomoto R, Kumazawa H, Toda Y, Sakaida N, Okamura A, Iwanaga M, Shintaku M, Yamashita T, Hiai H and Fukumoto M. Cyclin D1 gene amplification is a more potent prognostic factor that is protein overexpression in human head and neck squamous cell carcinoma. *Int J Cancer*, **74**:576-581 (1997).

Lai S and El-Naggar AK. Differential expression of key cell cycle genes (p16/cyclin D1/pRb) in head and neck squamous carcinomas. *Laboratory Investigations*, **79**(3):255-260 (1999).

Lasko D and Cavenee W. Loss of constitutional heterozygosity in human cancer. *Annu Rev Genet*, **25**:281-314 (1991).

Lazar AD, Winter MR, Nogueira CP, Larson PS, Finnemore EM, Dolan RW, Fuleihan N, Chakravarti A, Zietman A and Rosenberg CL. Loss of heterozygosity at 11q23 in squamous cell carcinoma of the head and neck is associated with recurrent disease. *Clinical Cancer Research*, 4(11):2787-2793 (1998).

Lee NK, Ye YW, Li X, Schweitzer C and Nisen PD. Allelic loss on chromosome 13 can preceed histological changes in head and neck cancer. *International Journal of Oncology*, **5**:205-210 (1994).

Leech SH, Olie RA, Gautschi O, Simoes-Wust AP, Tschopp S, Haner R, Hall J, Stahel RA and Zangemeister-Wittke U. Induction of apoptosis in lung-cancer cells following bcl-xL anti-sense treatment. *International Journal of Cancer*, **86**(4):570-576 (2000).

Lejeune J, Gautier M and Turpin R. Etudes des chromosomes somatiques de neuf enfants mongoliens. *Compt Rend*, **248**:1721-1722 (1959).

Lenz C, Dietz A, Pfuhl A, Finckh M, Conradt C, Weidauer H and Bosch FX. Detection of numerical chromosome aberrations in leukoplakia and squamous epithelial carcinomas of the head-neck area using fluorescence in situ hybridization. [German] *HNO*, 48(5):367-371 (2000).

Leon X, Quer M Diez S, Orus C, Lopez-Pousa A and Burgues J. Second neoplasm in patients with head and neck cancer. *Oncol Rep*, 5:955-958 (1999).

Levan A. The effect of colchicine on root mitosis in Allium. *Heredity* **24**:471-486 (1938).

Levy A, Zucman J, Delattre O, Mattei MG, Rio MC and Basset P. Assignment of the human stromelysin 3 (STMY3) gene to the q11.2 region of chromosome 22. *Genomics*, **13**(3):881-883 (1992).

Li R, Waga S, Hannon GJ, Beach D, and Stillman B. Differential effects by the p21 cdk inhibitor on PCNA-dependent DNA replication and repair. *Nature*, **371**:534-537 (1994).

Li D, Yan H, Chen J, Casto BC, Theil KS and Milo GE. Malignant conversion of human cells by antisense cDNA to a putative tumor suppressor gene. *Carcinogenesis*, **17**(8):1751-1755 (1996).

Licciardello JTW, Spitz MR and Hong WK. Multiple primary cancer in patients with cancer of the head and neck: second cancer of the head and neck, esophagus and lung. *International Journal of Radiation Oncology Biol. Phys*, **17**:467-476 (1989).

Lithgow T, van Driel R, Bertram JF and Strasser A. The protein product of the oncogene bcl-2 is a component of the nuclear envelope, the endoplasmic reticulum, and the outer mitochondrial membrane. *Cell Growth & Differentiation*, **5**(4):411-417 (1994).

Little M and Wainwright B. Methylation and p16: suppressing the suppressor. *Nature Medicine*, **1**(7):633-634 (1995).

Lleonart ME, Martin-Duque P, Sanchez-Prieto R, Moreno A, Ramon Y and Cajal S. Tumor heterogeneity: morphological, molecular and clinical implications. [Review] *Histology & Histopathology*, **15**(3):881-898 (2000).

Loeb LA. Mutator phenotype may be required for multistage carcinogenesis. *Cancer Research*, **51**(12):3075-3079 (1991).

Looser KG, Shah JP and Strong EW. The significance of 'positive' margins in surgically resected epidermoid carcinoma. *Head Neck Surg*, **1**:107-111 (1978).

Lukas J, Parry D, Aagaard L, Mann DJ, Bartkova J, Strauss M, Peters G and Bartek J. Retinoblastoma-protein-dependent cell-cycle inhibition by the tumour suppressor p16. *Nature*, **375**(6531):503-506 (1995).

Luo Y, Hurwitz J and Massague J. Cell-cycle inhibition by independent cdk and PCNA binding domains in $p21^{Cip1}$. *Nature*, **375**:159-161 (1995).

Lydiatt WM, Anderson PE, Bazzana T, Casale M, Hughes CJ, Huvos AG, Lydiatt DD and Schantz SP. Molecular support for field cancerization in the head and neck. *Cancer*, 82(7):1376-1380 (1998).

Lydiatt WM, Davidson BJ, Schantz SP, Caruana S and Chaganti RS. 9p21 deletion correlates with recurrence in head and neck cancer. *Head & Neck*, 20(2):113-118 (1998).

Maestro R, Gasparotto D, Vukosavljevic T, Barzan L, Sulfaro S and Boiocchi M. Three discrete regions of deletion at 3p in head and neck cancers. *Cancer Research*, 53(23):5775-5779 (1993).

Maestro R, Piccinin S, Doglioni C, Gasparotto D, Vukosavljevic T, Sulfaro S, Barzan L and Boiocchi M. Chromosome 13q deletion mapping in head and neck squamous cell carcinomas: identification of two distinct regions of preferential loss. *Cancer Research*, 56(5):1146-1150 (1996).

Magnano M, De Stefani A, Lerda W, Usai A, Ragona R, Bussi M and Cortesina G. Prognostic factors of cervical lymph node metastasis in head and neck squamous cell carcinoma. *Tumori*, 83(6):922-926 (1997).

Makin G and Hickman JA. Apoptosis and cancer chemotherapy. [Review] *Cell & Tissue Research*, 301(1):143-152 (2000).

Mao L, Fan YH, Lotan R and Hong WK. Frequent abnormalities of FHIT, a candidate tumor suppressor gene, in head and neck cancer cell lines. *Cancer Research*, 56(22):5128-5131 (1996).

Mao L and el-Naggar AK. Molecular changes in the multistage pathogenesis of head and neck cancer. In: Srivastava et al (Eds), *Molecular Pathology of Early Cancer*, IOS Press, Amsterdam, Netherlands, pp189-205 (1999).

Martiat P, Michaux JL and Rodhain J. Philadelphia-negative (Ph-) chronic myeloid leukemia (CML): comparison with Ph+ CML and chronic myelomonocytic leukemia. *Blood*, 78(1):205-211 (1991).

Maurizi M, Almadori G, Ferrandina G, Distefano M, Romanini ME, Cadoni G, Benedetti-Panici P, Paludetti G, Scambia G and Mancuso S. Prognostic significance of epidermal growth factor receptor in laryngeal squamous cell carcinoma. *British Journal of Cancer*, **74**(8):1253-1257 (1996).

McKaig RG, Baric RS and Olshan AF. Human papillomavirus and head and neck cancer: epidemiology and molecular biology. *Head & Neck*, **20**(3):250-265 (1998).

Meredith SD, Levine PA, Burns JA, Gaffey MJ, Boyd JC, Weiss LM, Erickson NL and Williams ME. Chromosome 11q13 amplification in head and neck squamous cell carcinoma. Association with poor prognosis. *Archives of Otolaryngology -- Head & Neck Surgery*, **121**(7):790-794 (1995).

Merlo A, Herman JG, Mao L, Lee DJ, Gabrielson E, Burger PC, Baylin SB and Sidransky D. 5' CpG island methylation is associated with transcriptional silencing of the tumour suppressor p16/CDKN2/MTS1 in human cancers. *Nature Medicine*, **1**(7):686-692 (1995).

Mertens F, Johansson B, Höglund M and Mitlemann F. Chromosomal imbalance map of malignant solid tumours: A cytogenetic survey of 3,185 neoplasms. *Cancer Research*, **57**:2765-2780 (1997).

Michalides RJ, van Veelen NM, Kristel PM, Hart AA, Loftus BM, Hilgers FJ and Balm AJ. Overexpression of cyclin D1 indicates a poor prognosis in squamous cell carcinoma of the head and neck. *Archives of Otolaryngology -- Head & Neck Surgery*, **123**(5):497-502 (1997).

Milroy CM, Ferlito A, Devaney KO and Rinaldo A. Role of DNA measurements of head and neck tumors. *Annals of Otology, Rhinology & Laryngology*, **106**(9):801-804 (1997).

Mitelman F, Mertens F and Johansson B. A breakpoint map of recurrent chromosomal rearrangements in human neoplasia. *Nature Genetics*, **15**:417-474 (1997).

Mitelman F, Johansson B, Manadahl N and Mertens F. Clinical significance of cytogenetic findings in solid tumours. *Cancer Genet Cytogenet*, **95**(1):1-8 (1997b).

Morton RP and McIvor NP. Tumours of the hypopharynx. In: Kerr, AG (Ed). *Scott-Brown's Otolaryngology 6th Edition*, pp5/15/1-5/15/17, Butterworth-Heinmann (1997).

Myers JN. Molecular pathogenesis of squamous cell carcinoma. In: Myers EN and Suen JY (Eds), *Cancer of the head and neck, 3rd edition*, WB Saunders, Philadelphia, pp5-15 (1996).

Nacheva EP, Grace CD, Bittner M, Ledbetter DH, Jenkins RB and Green AR. Comparative genomic hybridization: a comparison with molecular and cytogenetic analysis. *Cancer Genetics & Cytogenetics*, **100**(2):93-105 (1998).

Nakanishi H, Wang XL, Imai FL, Kato J, Shiiba M, Miya T, Imai Y and Tanzawa H. Localization of a novel tumor suppressor gene loci on chromosome 9p21-22 in oral cancer. *Anticancer Research*, **19**(1A):29-34 (1999).

Nawroz H, van der Riet P, Hruban RH, Koch W, Ruppert JM and Sidransky D. Allelotype of head and neck squamous cell carcinoma. *Cancer Research*, **54**(5):1152-1155 (1994).

Nees M, Homann N, Discher H, Andl T, Enders C, Herold-Mende C, Schuhmann A and Bosch FX. Expression of mutated p53 occurs in tumor-distant epithelia of head and neck cancer patients: a possible molecular basis for the development of multiple tumors. *Cancer Research*, **53**(18):4189-4196 (1993).

Nemunaitis J, Swisher SG, Timmons T, Connors D, Mack M, Doerksen L, Weill D, Wait J, Lawrence DD, Kemp BL, Fossella F, Glisson BS, Hong WK, Khuri FR, Kurie JM, Lee JJ, Lee JS, Nguyen DM, Nesbitt JC, Perez-Soler R, Pisters KM, Putnam JB, Richli WR, Shin DM and Walsh GL. Adenovirus-mediated p53 gene transfer in sequence with cisplatin to tumors of patients with non-small-cell lung cancer. *Journal of Clinical Oncology*, **18**(3):609-622 (2000).

Nita ME, Ono-Nita SK, Tsuno N, Tominaga O, Takenoue T, Sunami E, Kitayama J, Nakamura Y and Nagawa H. Bcl-X(L) antisense sensitizes human colon cancer cell line to 5-fluorouracil. *Japanese Journal of Cancer Research*, **91**(8):825-832 (2000).

Nowell PC and Hungerford DA. A minute chromosome in human chronic granulocytic leukemia. *Science*, **132**:1497 (1960).

Nylander K, Nilsson P, Mehle C and Roos G. p53 mutations, protein expression and cell proliferation in squamous cell carcinomas of the head and neck. *British Journal of Cancer*, **71**(4):826-830 (1995).

Nylander K, Dabelsteen E and Hall PA. The p53 molecule and its prognostic role in squamous cell carcinomas of the head and neck. [Review] *Journal of Oral Pathology & Medicine*, **29**(9):413-425 (2000).

O'Brien CJ, Smith JW, Soong SJ, Urist MM and Maddox WA. Neck dissection with and without radiotherapy: prognostic factors, patterns of recurrence, and survival. *American Journal of Surgery*, **152**(4):456-463 (1986).

O'Connor AFF and Lund VJ. Ear Nose and Throat. In: Burnand KG and Young AE (Eds). *The new Aird's companion in surgical studies 2nd Edition*, pp499-528, Churchill Livingstone, London (1998).

Ogawara K, Miyakawa A, Shiba M, Uzawa K, Watanabe T, Wang XL, Sato T, Kubosawa H, Kondo Y and Tanzawa H. Allelic loss of chromosome 13q14.3 in human oral cancer: correlation with lymph node metastasis. *International Journal of Cancer*, **79**(4):312-317 (1998).

Ono K, Miyakawa A, Fukuda M, Shiiba M, Uzawa K, Watanabe T, Miya T, Yokoe H, Imai Y and Tanzawa H. Allelic loss on the short arm of chromosome 8 in oral squamous cell carcinoma. *Oncology Reports*, **6**(4):785-789 (1999).

Osella P, Carlson A, Wyandt H and Milunsky A. Cytogenetic studies of eight squamous cell carcinomas of the head and neck: Deletion of 7q possible primary event. *Cancer Genetics and Cytogenetics*, **59**:73-78 (1992).

Partridge M, Emilion G and Langdon JD. LOH at 3p correlates with a poor survival in oral squamous cell carcinoma. *British Journal of Cancer*, **73**:366-371 (1996).

Partridge M, Emilion G, Falworth M, A'Hern R, Phillips E, Pateromichelakis S and Langdon J. Patient-specific mutation databases for oral cancer. *International Journal of Cancer*, 84(3):284-292 (1999).

Partridge M, Li SR, Pateromichelakis S, Francis R, Phillips E, Huang XH, Tesfa-Selase F and Langdon JD. Detection of minimal residual cancer to investigate why oral tumors recur despite seemingly adequate clearance. *Clinical Cancer Research*, (7):2718-2725 (2000).

Pavelic ZP, Li YQ, Stambrook PJ, McDonald JS, Munck-Wikland E, Pavelic K, Dacic S, Danilovic Z, Pavelic L and Mugge RE. Overexpression of p53 protein is common in premalignant head and neck lesions. *Anticancer Research*, **14**(5B):2259-2266 (1994).

Pearlstein RP, Benninger MS, Carey TE, Zarbo RJ, Torres FX, Rybicki BA and Dyke DL. Loss of 18q predicts poor survival of patients with squamous cell carcinoma of the head and neck. *Genes, Chromosomes & Cancer*, **21**(4):333-339 (1998).

Pegram MD, Konecny G and Slamon DJ. The molecular and cellular biology of HER2/neu gene amplification/overexpression and the clinical development of herceptin (trastuzumab) therapy for breast cancer. [Review] *Cancer Treatment & Research*, **103**:57-75 (2000).

Petruzzelli GJ, Benefield J and Yong S. Mechanism of lymph node metastases: current concepts. *Otolaryngologic Clinics of North America*, **31**(4):585-599 (1998).

Piccinin S, Gasparotto D, Vukosavljevic T, Barzan L, Sulfaro S, Maestro R and Boiocchi M. Microsatellite instability in squamous cell carcinomas of the head and neck related to field cancerization phenomena. *British Journal of Cancer*, **78**(9):1147-1151 (1998).

Pignataro L, Pruneri G, Carboni N, Capaccio P, Cesana BM, Neri A and Buffa R. Clinical relevance of cyclin D1 protein overexpression in laryngeal squamous cell carcinoma. *J Clin Oncol*, **16**:3069-3077 (1998).

Pinkle D, Straume T and Gray JW. Cytogenetic analysis using quantitative, high sensitivity fluorescence hybridization. *Proceedings of the National Academy of Sciences of the USA*, **83**:2394-2398 (1986).

Piper J, Rutovitz D, Sudar D, Kallioniemi A, Kallioniemi OP, Waldman FM, Gray JW and Pinkel D. Computer image analysis of comparative genomic hybridization. *Cytometry*, **19**(1):10-26 (1995).

Pirollo KF, Hao Z, Rait A, Jang YJ, Fee WE Jr, Ryan P, Chiang Y and Chang EH. p53 mediated sensitization of squamous cell carcinoma of the head and neck to radiotherapy. *Oncogene*, **14**:1735-1746 (1997).

Poli-Frederico RC, Bergamo NA, Reis PP, Kowalski LP, Zielenska M, Squire JA and Rogatto SR. Chromosome 22q a frequent site of allele loss in head and neck carcinoma. *Head & Neck*, **22**(6):585-590 (2000).

Pomeroy SL, Tamayo P, Gaasenbeek M, Sturla LM, Angelo M, McLaughlin ME, Kim JY, Goumnerova LC, Black PM, Lau C, Allen JC, Zagzag D, Olson JM, Curran T, Wetmore C, Biegel JA, Poggio T, Mukherjee S, Rifkin R, Califano A, Stolovitzky G, Louis DN, Mesirov JP, Lander ES and Golub TR. Prediction of central nervous system embryonal tumour outcome based on gene expression. *Nature*, **415**(6870):436-442 (2002).

Potten CS, Chadwick CA, Cohen AJ, Nikaidos O, Matsunaga T, Schipper NW and Young AR. DNA damage in UV-irradiated human skin in vivo: automated direct measurements by image analysis (thymine dimers) compared with indirect measurements (unscheduled DNA synthesis) and protection by methoxypsoralen. *International Journal of Radiation Biology*, **63**:313-324 (1993).

Press MF, Pike MC, Hung G, Zhou JY, Ma Y, George J, Dietz-Band J, James W, Slamon DJ, Batsakis JG and el-Naggar AK. Amplification and overexpression of Her-2/neu in carcinomas of the salivary gland: correlation with poor prognosis. *Cancer Research*, **54**:5675-5682 (1994.).

Ransom DT, Leonard JH, Kearsley JH, Turbett GR, Heel K, Sosars V, Hayward NK and Bishop JF. Loss of heterozygosity studies in squamous cell carcinomas of the head and neck. *Head & Neck*, **18**(3):248-253 (1996).

Raybaud-Diogene H, Tetu B, Morency R, Fortin A and Monteil RA. p53 overexpression in head and neck squamous cell carcinoma: a review of the literature. [Review] *European Journal of Cancer, Part B, Oral Oncology*, **32B**(3):143-149 (1996).

Raybaud-Diogene H, Fortin A, Morency R, Roy J, Monteil RA and Tetu B. Markers of radioresistance in squamous cell carcinomas of the head and neck: a clinicopathological and immunohistochemical study. *Journal of Clinical Oncology*, **15**:1030-1038 (1997).

Reed AL, Califano J, Cairns P, Westra WH, Jones RM, Koch W, Ahrendt S, Eby Y, Sewell D, Nawroz H, Bartek J and Sidransky D. High frequency of p16 (CDKN2/MTS-1/INK4A) inactivation in head and neck squamous cell carcinoma. *Cancer Research*, **56**(16):3630-3633 (1996).

Redon R, Muller D, Caulee K, Wanherdrick K, Abecassis J and du Manoir S. A simple specific pattern of chromosomal aberrations at early stages of head and neck squamous cell carcinomas: PIK3CA but not p63 gene as a likely target of 3q26-qter gains. *Cancer Research*, **61**(10):4122-4129 (2001).

Renan MJ. How many mutations are required for tumourigenesis? Implications from human cancer data. *Molecular Carcinogenesis*, **7**(3):139-146 (1993).

Resto VA, Caballero OL, Buta MR, Westra WH, Wu L, Westendorf JM, Jen J, Hieter P and Sidransky D. A putative oncogenic role for MPP11 in head and neck squamous cell cancer. *Cancer Research*, **60**(19):5529-5535 (2000).

Rieder CL and Palazzo RE. Colcemid and the mitotic cycle. *Journal of Cell Science*, **102**(3):387-92 (1992).

Riese U, Dahse R, Fiedler W, Theuer C, Koscielny S, Ernst G, Beleites E, Claussen U and von Eggeling F. Tumour suppressor gene p16 (CDKN2A) mutation status and promoter inactivation in head and neck cancer. *International Journal of Molecular Medicine*, **4**(1):61-65 (1999).

Rizos E, Sourvinos G and Spandidos DA. Loss of heterozygosity at 8p, 9p and 17q in laryngeal cytological specimens. *Oral Oncology*, **34**(6):519-523 (1998).

Rizos E, Sourvinos G, Arvanitis DA, Velegrakis G and Spandidos DA. Low incidence of H-, K- and N-ras oncogene mutations in cytological specimens of laryngeal tumours. *Oral Oncology*, **35**(6):561-563 (1999).

Rodrigo JP, Garcia LA, Ramos S, Lazo PS and Suarez C. EMS1 gene amplification correlates with poor prognosis in squamous cell carcinomas of the head and neck. *Clin Cancer Res*, **6**(8):3177-3182 (2000).

Rodrigo JP, Suarez C, Gonzalez MV, Lazo PS, Ramos S, Coto E, Alvarez I, Garcia LA, Martinez JA. Variability of genetic alterations in different sites of head and neck cancer. *Laryngoscope*, **111**(7):1297-1301 (2001).

Rosen EM, Fan S, Rockwell S and Goldberg ID. The molecular and cellular basis of radiosensitivity: Implications for understanding how normal tissues and tumours respond to therapeutic radiation. *Cancer Investigation*, **17**(1):56-72 (1999).

Rousseau A, Lim MS, Lin Z and Jordan RC. Frequent cyclin D1 gene amplification and protein overexpression in oral epithelial dysplasias. *Oral Oncology*, **37**(3):268-275 (2001).

Rowley H, Jones AS and Field JK. Chromosome 18: a possible site for a tumour suppressor gene deletion in squamous cell carcinoma of the head and neck. *Clinical Otolaryngology & Allied Sciences*, **20**(3):266-271 (1995).

Rowley H, Jones A, Spandidos D and Field J. Definition of a tumor suppressor gene locus on the short arm of chromosome 3 in squamous cell carcinoma of the head and neck by means of microsatellite markers. *Archives of Otolaryngology - Head & Neck Surgery*, **122**(5):497-501 (1996).

Rowley JD. Molecular cytogenetics: Rosetta stone for understanding cancer - Twenty-ninth G.H.A. Clowes Memorial Award Lecture. *Cancer Research*, **50**(13):3816-3825 (1990).

Rubin JS, Qui L and Etkind P. Amplification of the int-2 gene in head and neck squamous cell carcinoma. *J Laryngol Otology*, **109**:72-76 (1995).

Sambrook J, Fritsch EF and Maniatis T (Eds). *Molecular cloning: A laboratory manual 2nd Edition*. New York: Cold Spring Laboratory Press (1989).

Sanchez-Cespedes M, Okami K, Cairns P and Sidransky D. Molecular analysis of the candidate tumor suppressor gene ING1 in human head and neck tumors with 13q deletions. *Genes, Chromosomes & Cancer*, **27**(3):319-322 (2000).

Santini J, Formento JL, Francoual M, Milano G, Schneider M, Dassonville O and Demard F. Characterization, quantification and potential clinical value of the epidermal growth factor receptor in head and neck squamous cell carcinomas. *Head Neck*, **13**:132-139 (1991).

Saranath D, Chang SE, Bhoite LT, Panchal RG, Kerr IB, Mehta AR, Johnson NW and Deo MG. High frequency mutation in codons 12 and 61 of H-ras oncogene in chewing tobacco-related human oral carcinoma in India. *British Journal of Cancer*, **63**(4):573-578 (1991).

Saunders ME, MacKenzie R, Shipman R, Fransen E, Gilbert R and Jordan RC. Patterns of p53 gene mutations in head and neck cancer: full-length gene sequencing and results of primary radiotherapy. *Clinical Cancer Research*, **5**(9):2455-2463 (1999).

Sauter ER, Cleveland D, Trock B, Ridge JA and Klein-Szanto AJ. p53 is overexpressed in fifty percent of pre-invasive lesions of head and neck epithelium. *Carcinogenesis*, **15**(10):2269-2274 (1994).

Sauter ER, Ridge JA, Trock B, Cleveland D, Whitley KV, Mohr RM and Klein-Szanto A. Overexpression of p53 gene in primary and metastatic head and neck carcinomas. *Laryngoscope*, **105**(6):653-656 (1995).

Schecter AL, Stern DF, Vaidyanathan L, Decker SJ, Drebin JA, Greene MI and Weinberg RA. The neu oncogene: an erbB-related gene encoding a 185000 Mr tumour antigen. *Nature*, **312**:513-516 (1984).

Schnitt SJ. Breast cancer in the 21st century: neu opportunities and neu challenges. [Review] *Modern Pathology*, **14**(3):213-218 (2001).

Scholzen T and Gerdes J. The Ki-67 protein: from the known and the unknown. [Review] *Journal of Cell Physiology*, **182**(3):311-322 (2000).

Schraml P, Kononen J, Bubendorf L, Moch H, Bissig H, Nocito A, Mihatsch MJ, Kallioniemi OP and Sauter G. Tissue microarrays for gene amplification surveys in many different tumor types. *Clinical Cancer Research*, **5**(8):1966-1975 (1999).

Schuuring E, Verhoeven E, Litvinov S and Michalides RJ. The product of the EMS1 gene, amplified and overexpressed in human carcinomas, is homologous to a v-src substrate and is located in cell-substratum contact sites. *Molecular & Cellular Biology*, **13**(5):2891-2898 (1993).

Shayesteh L, Lu Y, Kuo WL, Baldocchi R, Godfrey T, Collins C, Pinkel D, Powell B, Mills GB and Gray JW. PIK3CA is implicated as an oncogene in ovarian cancer. *Nature Genetics*, **21**(1):99-102 (1999).

Shin DM, Voravud N, Ro JY, Lee JS, Hong WK and Hittelman WN. Sequential increases in proliferating cell nuclear antigen expression in head and neck tumorigenesis: a potential biomarker. *Journal of the National Cancer Institute*, **85**(12):971-978 (1993).

Shin DM, Ro JY, Hong WK and Hittelman WN. Disregulation of epidermal growth factor receptor expression in premalignant lesions during head and neck tumourigenesis. *Cancer Research*, **54**:3153-3159 (1994).

Shin DM, Charuruks N, Lippman SM, Lee JJ, Ro JY, Hong WK and Hittelman WN. p53 protein accumulation and genomic instability in head and neck multistep tumorigenesis. *Cancer Epidemiology, Biomarkers & Prevention*, **10**(6):603-609 (2001).

Shipp MA, Ross KN, Tamayo P, Weng AP, Kutok JL, Aguiar RC, Gaasenbeek M, Angelo M, Reich M, Pinkus GS, Ray TS, Koval MA, Last KW, Norton A, Lister TA, Mesirov J, Neuberg DS, Lander ES, Aster JC and Golub TR. Diffuse large B-cell lymphoma outcome prediction by gene-expression profiling and supervised machine learning. *Nat Med*, 8(1):68-74 (2002).

Sidransky D, Frost P, Von Eschenbach A, Oyasu R, Preisinger AC and Voglestein B. Clonal origin of bladder cancer. *New England Journal of Medicine*, **56**:2484-2487 (1992).

Sidransky D. Molecular genetics of head and neck cancer. [Review] *Current Opinion in Oncology*, **7**(3):229-233 (1995).

Silberstein DL and Shows TB. Gene for glutathione S-transferase-1 (GST1) is on human chromosome 11. *Somatic Cell Genetics*, 8(5):667-675 (1982).

Singh B, Gogineni SK, Sacks PG, Shaha AR, Shah JP, Stoffel A and Rao PH. Molecular cytogenetic characterization of head and neck squamous cell carcinoma and refinement of 3q amplification. *Cancer Research*, **61**(11):4506-4513 (2001).

Slaughter DP, Southwick HW and Smeijkal W. Field cancerization in oral stratified squamous epithelium: Clinical implications of multicentric origin. *Cancer*, **6**:963-968 (1953).

Smith BD and Haffty BG. Molecular markers as prognostic factors for local recurrence and radioresistance in head and neck squamous cell carcinoma. *Radiation Oncology Investigations*, **7**:125-144 (1999).

Snijders PJ, Scholes AG, Hart CA, Jones AS, Vaughan ED, Woolgar JA, Meijer CJ, Walboomers JM and Field JK. Prevalence of mucosotropic human papillomaviruses in squamous-cell carcinoma of the head and neck. *International Journal of Cancer*, **66**(4):464-469 (1996).

Snow GB. Cancer of the head and neck region. In: Veronesi U, (Ed). *Surgical oncology*. pp476-494, Springer-Verlag, New York (1989).

Snow GB, Patel P, Lemma's CR and Toward R. Management of cervical lymph nodes in patients with head and neck cancer. *Errata Otorhinolaryngol*, **249**:187-194 (1992).

Solinas-Toldo S, Lampel S, Stilgenbauer S, Nickolenko J, Benner A, Dohner H, Cremer T and Lichter P. Matrix-based comparative genomic hybridization: biochips to screen for genomic imbalances. *Genes, Chromosomes & Cancer*, **20**(4):399-407 (1997).

Song AU, Mais DD, Groo S, Wright JR and Yoshida GY. Expression of nm23 antimetastatic gene product in head and neck squamous cell carcinoma. *Otolaryngology - Head & Neck Surgery*, **122**(1):96-99 (2000).

Soria JC, Morat L, Commo F, Dabit D, Perie S, Sabatier L and Fouret P. Telomerase activation cooperates with inactivation of p16 in early head and neck tumorigenesis. *British Journal of Cancer*, 84(4):504-511 (2001).

Speicher MR, Owe C, Crotty P, du Manoir S, Costa J and Ward DC. Comparative genomic hybridization detects novel deletions and amplifications in head and neck squamous cell carcinomas. *Cancer Research*, **5**:1010-1013 (1995).

Speicher MR, Gwyn Ballard S and Ward DC. Karyotyping human chromosomes by combinatorial multi-fluor FISH. *Nature Genetetics*, **12**: 368-375 (1996).

Speight PM, Farthing PM and Bouquot JE. The pathology of oral cancer and precancer. *Curr Diag Path*, **3**:165-177 (1996).

Spitz MR, Fueger JJ, Halabi S, Schantz SP, Sample D and Hsu TC. Mutagen sensitivity in upper aerodigestive tract cancer: a case-control analysis. *Cancer Epidemiology, Biomarkers & Prevention*, **2**(4):329-33 (1993).

Squier CA. Smokeless tobacco and oral cancer: a cause for concern? *CA: a Cancer Journal for Clinicians* **34**: 242 (1984).

Sreekantaiah C, Rao PH, Xu L Sacks PG, Schantz SP and Chaganti RS. Consistent chromosomal losses in head and neck squamous cell carcinoma cell lines. *Genes, Chromosomes and Cancer*, **11**:29-39 (1996).

Staplers LJA, Verbeek ALM and van Daal WAJ. Results of radiotherapy and surgery for glottic carcinoma. *Cancer Treat Rev*, **14**:131-141 (1987).

Stein WD. Analysis of cancer incidence data on the basis of multistage and clonal growth models. *Advances in Cancer Research*, **56**:161-213 (1991).

Stell PM, Laryngology. In: Kerr, AG (Ed). *Scott-Brown's Otolaryngology 6th Edition*, Butterworth-Heinmann (1997).

Storkel S, Reichert T, Reiffen KA and Wagner W. EGFR and PCNA expression in oral squamous cell carcinomas-a valuable tool in estimating the patient's prognosis. *Eur J Cancer B Oral Oncol*, **29B**(4):273-277(1993).

Strauss BS, Sagher D and Acharya S. Role of proofreading and mismatch repair in maintaining the stability of nucleotide repeats in DNA. *Nucleic Acids Research*, **25**(4):806-813 (1997).

Stoecklie SJ, Pawlik AB, Lipp M, Huber A and Schmid S. Salvage surgery after failure of nonsurgical therapy for carcinoma of the larynx and hypopharynx. *Archives of Otolaryngology - Head & Neck Surgery*, **126**(12):1473-1477 (2000).

Su YA, Wang XQ, Hu N, Pei XF and Wu M. G-banded chromosome analyses of mucosal epithelium adjacent to esophageal cancer – Some consistent changes. *Scienta Sinica*, **31**(6):710-718 (1988).

Sugimoto C, Fujieda S, Seki M, Sunaga H, Fan GK, Tsuzuki H, Borner C, Saito H and Matsukawa S. Apoptosis-promoting gene (bax) transfer potentiates sensitivity of squamous cell carcinoma to cisplatin in vitro and in vivo. *International Journal of Cancer*, **82**(6):860-867 (1999).

Tabor MP, Brakenhoff RH, van Houten VM, Kummer JA, Snel MH, Snijders PJ, Snow GB, Leemans CR and Braakhuis BJ. Persistence of genetically altered fields in head and neck cancer patients: biological and clinical implications. *Clinical Cancer Research*, **7**(6):1523-1532 (2001).

Takes RP, Baatenburg de Jong RJ, Wijffels K, Schuuring E, Litvinov SV, Hermans J and van Kreiken JH. Expression of genetic markers in lymph node metastases compared with their primary tumours in head and neck cancer. *Journal of Pathology*, **194**(3):298-302 (2001).

Takebayashi S, Ogawa T, Jung KY, Muallem A, Mineta H, Fisher SG, Grenman R and Carey TE. Identification of new minimally lost regions on 18q in head and neck squamous cell carcinoma. *Cancer Research*, **60**(13):3397-3403 (2000).

Tanaka H, Shimada Y, Harada H, Shinoda M, Hatooka S, Imamura M and Ishizaki K. Methylation of the 5' CpG island of the FHIT gene is closely associated with transcriptional inactivation in esophageal squamous cell carcinomas. *Cancer Research*, **58**(15):3429-3434 (1998).

Taverna P, Liu L, Hanson AJ, Monks A and Gerson SL. Characterization of MLH1 and MSH2 DNA mismatch repair proteins in cell lines of the NCI anticancer drug screen. *Cancer Chemotherapy & Pharmacology*, **46**(6):507-516 (2000).

Telenius H, Carter NP, Bebb CE, Nordenskjold M, Ponder BA and Tunnacliffe A. Degenerate oligonucleotide-primed PCR: general amplification of target DNA by a single degenerate primer. *Genomics*, **13**(3):718-725 (1992).

Terhaard CH, Snippe K, Ravasz LA, van der Tweel I and Hordijk GJ. Radiotherapy in T1 laryngeal cancer: prognostic factors for locoregional control and survival, uni- and multivariant analysis. *Int J of Radiat. Oncol Biol. Phys*, **21**:1179-1186 (1991).

Tjio JH and Levan A. The chromosome number of man. *Am J Obstet Gynecol*, **130**:723-724 (1956).

Tosios KI, Kapranos N and Papanicolaou SI. Loss of basement membrane components laminin and type IV collagen parallels the progression of oral epithelial neoplasia. *Histopathology*, **33**(3):261-268 (1998).

Tsuchida S and Sato K. Glutathione transferases and cancer. *CRC Crit Rev Biochem Mol*, **27**:337-384 (1996).

Twentyman PR, Wright KA, Mistry P, Kelland LR and Murrer BA. Sensitivity to novel platinum compounds of panels of human lung cancer cell lines with acquired and inherent resistance to cisplatin. *Cancer Research*, **52**(20):5674-80 (1992).

Tytor M, Franzen G and Olofsson J. DNA ploidy in oral cavity carcinomas, with special reference to prognosis. *Head & Neck*, **11**(3):257-263 (1989).

Tytor M and Olofsson J. Prognostic factors in oral cavity carcinomas. *Acta Oto-Laryngologica – Supplement*, **492**:75-78 (1992).

Uhlman DL, Adams G, Knapp D, Aeppli DM and Niehans G. Immunohhistochemical staining for future neoplastic progression in the larynx. *Cancer Research*, **56**:2199-2205 (1996).

Uzawa K, Yoshida H, Suzuki H, Tanzawa H, Shimazaki J, Seino S and Sato K. Abnormalities of the adenomatous polyposis coli gene in human oral squamous-cell carcinoma. *International Journal of Cancer*, **58**(6):814-817 (1994).

Uzawa K, Yoshida MA, Oshimura M and Ikeuchi T. Suppresion of tumourigenicity in three different cell lines of human oral squamous cell carcinoma by introduction of chromosome 3p via micro-cell mediated chromosome transfer. *Oncogene*, **11**:1997-2004 (1995).

van der Riet P, Nawroz H, Hruban RH, Corio R, Tokino K, Koch W and Sidransky D. Frequent loss of chromosome 9p21-22 early in head and neck cancer progression. *Cancer Research*, **54**(5):1156-1158 (1994).

van Oijen MG, Tilanus MG, Medema RH and Slootweg PJ. Expression of p21 (Waf1/Cip1) in head and neck cancer in relation to proliferation, differentiation, p53 status and cyclin D1 expression. *Journal of Oral Pathology & Medicine*, **27**(8):367-375 (1998).

Van Dyke DL, Worsham MJ, Benninger MS, Krause CJ, Baker SR, Wolf GT, Drumheller T, Tilley BC and Carey TE. Recurrent cytogenetic abnormalities in squamous cell carcinomas of the head and neck region. *Genes, Chromosomes and Cancer*, **9**:192-206 (1994).

van Gilsjwick RPM, Talman EG, Jannsen PJA, Snojeijers SSS, Killian J, Tanke HJ, Heetebrij RJ. Universal linkage system: versatile nucleic acid labelling technique. *Expert Rev Mol Diagn*, **1**(1):81-91 (2001).

van Heerden WF, Swart TJ, van Heerden MB, van Rensburg EJ, Engelbrecht S, Dreyer L and Huebner K. Immunohistochemical evaluation of Fhit protein expression in oral squamous cell carcinomas. *Journal of Oral Pathology & Medicine*, **28**(10):433-437 (1999).

van Oijen MG, Leppers Vd, Straat FG, Tilanus MG and Slootweg PJ. The origins of multiple squamous cell carcinomas in the aerodigestive tract. *Cancer*, **88**(4):884-893 (2000).

van't Veer LJ, Dai H, van de Vijver MJ, He YD, Hart AA, Mao M, Peterse HL, van der Kooy K, Marton MJ, Witteveen AT, Schreiber GJ, Kerkhoven RM, Roberts C, Linsley PS, Bernards R, Friend SH. Gene expression profiling predicts clinical outcome of breast cancer. *Nature*, **415**(6871):530-536 (2002).

Vasef MA, Ferlito A and Weiss LM. Nasopharyngeal carcinoma, with emphasis on its relationship to Epstein-Barr virus. *Annals of Otology, Rhinology & Laryngology*, **106**(4):348-56 (1997).

Virgilio L, Shuster M, Gollin SM, Veronese ML, Ohta M, Huebner K and Croce CM. FHIT gene alterations in head and neck squamous cell carcinomas. *Proceedings of the National Academy of Sciences of the USA*, **93**:9770-9775 (1996).

Veltman JA, Hopman AH, van der Vlies SA, Bot FJ, Ramaekers FC and Manni JJ. Double-target fluorescence in situ hybridization distinguishes multiple genetically aberrant clones in head and neck squamous cell carcinoma. *Cytometry*, **34**(3):113-120 (1998).

Vennstrom B and Bishop JM. Isolation and characterization of chicken DNA homologous to the two putative oncogenes of avian erythroblastosis virus. *Cell*, **28**(1):135-143 (1982).

Vogelstein B, Fearon ER, Hamilton SR Kern SE, Preisinger AC, Leppert M, Nakamura Y, White R, Smits AM and Bos JL. Genetic alterations during colorectal tumor development. *New England Journal of Medicine*, **319**:525-532 (1998).

Vokes EE, Weichselbaum RR, Lippman SM and Hong WK. Head and Neck cancer. *N Engl J Med*, **328**:184-194 (1993).

Volinia S, Hiles I, Ormondroyd E, Nizetic D, Antonacci R, Rocchi M and Waterfield MD. Molecular cloning, cDNA sequence, and chromosomal localization of the human phosphatidylinositol 3-kinase p110 alpha (PIK3CA) gene. *Genomics*, **24**(3):472-477 (1994).

Voravud N, Shin DM, Ro JY, Lee JS, Hong WK and Hittelman WN. Increased polysomies of chromosomes 7 and 17 during head and neck multistage tumorigenesis. *Cancer Research*, **53**(12):2874-2883 (1993).

Waber PG, Lee NK and Nisen PD. Frequent allelic loss at chromosome arm 3p is distinct from genetic alterations of the Von-Hippel Lindau tumor suppressor gene in head and neck cancer. *Oncogene*, **12**(2):365-369 (1996).

Wang XD, Liu C, Chung J, Stickel F, Seitz HK and Russell RM. Chronic alcohol intake reduces retinoic acid concentration and enhances AP-1 (c-Jun and c-Fos) expression in rat liver. *Hepatology*, **28**(3):744-50 (1998).

Wattre P, Bert V and Hober D. Apoptosis and human viral infections. [Review] [French] *Annales de Biologie Clinique*, **54**(5):189-97 (1996).

Weber JL and May PE. Abundant class of human DNA polymorphisms which can be typed using the polymerase chain reaction. *Am J Hum genet*, **44**:388-396 (1989).

Weinberg RA. How cancer arises. *Scientific American*, **275**(3):62-70 (1996).

Wessendorf S, Fritz B, Wrobel G, Nessling M, Lampel S, Goettel D, Kuepper M, Joos S, Hopman T, Kokocinski F, Dohner H, Bentz M, Schwaenen C, Lichter P. Automated screening for genomic imbalances using matrix-based comparative genomic hybridization. *Lab Invest*, **82**(1):47-60 (2002).

Wells D, Sherlock JK, Handyside AH and Delhany JD. Detailed chromosomal and molecular genetic analysis of single cells by whole genome amplification and Comparative genomic hybridisation. *Nucleic Acids Research*, **27**(4):1214-1218 (1999).

Wolff E, Girod S, Liehr T, Vorderwulbecke U, Ries J, Steininger H and Gebhart E. Oral squamous cell carcinomas are characterized by a rather uniform pattern of genomic imbalances detected by comparative genomic hybridisation. *Oral Oncology*, **34**(3):186-190 (1998).

Wong-Staal F, Dalla-Favera R, Franchini G, Gelmann EP and Gallo RC. Three distinct genes in human DNA related to the transforming genes of mammalian sarcoma retroviruses. *Science*, **213**:226-228 (1981).

Wood GS and Warnke R. Suppression of endogenous avidin-binding activity in tissues and its relevance to biotin-avidin detection systems. *Journal of Histochemistry & Cytochemistry*, **29**(10):1196-204 (1981).

Worden FP and Kalemkerian GP. Therapeutic advances in small cell lung cancer. [Review] *Expert Opinion on Investigational Drugs*, **9**(3):565-579 (2000).

Worsham MJ, Wolman SR, Carey TE, Zarbo RJ, Benninger MS and Van Dyke DL. Chromosomal aberrations identified in culture of squamous carcinomas are confirmed by fluorescence in situ hybridisation. *Molecular Pathology*, **52**(1):42-46 (1999).

Xia W, Lau YK, Zhang HZ, Liu AR, Li L, Kiyokawa N, Clayman GL, Katz RL and Hung MC. Strong correlation between c-erbB-2 overexpression and overall survival of patients with oral squamous cell carcinoma. *Clinical Cancer Research*, **3**(1):3-9 (1997).

Xia W, Lau YK, Zhang HZ, Xiao FY, Johnston DA, Liu AR, Li L, Katz RL and Hung MC. Combination of EGFR, HER-2/neu, and HER-3 is a stronger predictor for the outcome of oral squamous cell carcinoma than any individual family members. *Clinical Cancer Research*, **5**(12):4164-4174 (1999).

Yoo GH, Xu HJ, Brennan JA, Westra W, Hruban RH, Koch W, Benedict WF and Sidransky D. Infrequent inactivation of the retinoblastoma gene despite frequent loss of chromosome 13q in head and neck squamous cell carcinoma. *Cancer Research*, **54**(17):4603-4606 (1994).

Yoshida K, Yoshitomo-Nakagawa K, Seki N, Sasaki M and Sugano S. Cloning, expression analysis, and chromosomal localization of BH-protocadherin (PCDH7), a novel member of the cadherin superfamily. *Genomics*, **49**:458-461 (1998).

Yoshida MC, Wada M, Satoh H, Yoshida T, Sakamoto H, Miyagawa K, Yokota J, Koda T, Kakinuma M and Sugimura T. Human HST1 (HSTF1) gene maps to chromosome band 11q13 and coamplifies with the INT2 gene in human cancer. *Proceedings of the National Academy of Sciences of the United States of America*, **85**(13):4861-4864 (1988).

Young B and Heath JW (Eds). *Wheater's Functional Histology – A text and colour atlas.* Churchill Livingston, London (2000).

Yu MC. Diet and nasopharyngeal carcinoma. *Prog Clin Biol Res*, **346**:93-105 (1990).

Zangemeister-Wittke U, Schenker T, Luedke GH and Stahel RA. Synergistic cytotoxicity of bcl-2 antisense oligodeoxynucleotides and etoposide, doxorubicin and cisplatin on small-cell lung cancer cell lines. *British Journal of Cancer*, **78**(8):1035-1042 (1998).

Zatterstrom UK, Wennerberg J, Ewers SB, Willen R and Attewell R. Prognostic factors in head and neck cancer: histologic grading, DNA ploidy, and nodal status. *Head & Neck*, **13**(6):477-487 (1991).

Manuals and web pages

AJCC Cancer Staging Manual 5th Edition. Lippincott Williams & Wilkins, Philadelphia (1997).

Effective Head and Neck Cancer Management: Second Consensus Document, BAO-HNS Document 4 Autumn (2000).

Northern and Yorkshire Cancer Registry Information service online (www.nycris.org.uk)

Mitelman Database of Chromosome Aberrations in Cancer (2001). Mitelman F, Johansson B and Mertens F (Eds.), http://cgap.nci.nih.gov/Chromosomes/Mitelman

U.S. Department of Health and Human Services. *Reducing the Health Consequences of Smoking: 25 Years of Progress—A Report of the Surgeon General.* DHHS publication (CDC) 89-8411. Washington DC: Government Printing Office, (1989).

Appendices

Suppliers Names and Addresses

Amersham Pharmacia Biotech UK Limited
Amersham Place, Little Chalfont, Buckinghamshire HP7 9NA.

Appligene Oncor (Qbiogene)
Salamsnder Quay West, Park Lane, Harefield, Middlesex UB9 6NZ.

Becton Dickinson UK Ltd
Between Towns Road, Cowley, Oxford, OX4 3LY.

BDH Laboratory Supplies
Broom Road, Poole, Dorset BH13 1TP.

Chance Propper Ltd
Spoon Lane, Smethwick, Warley.

Dako Ltd
Denmark House, Angel Drove, Ely, Cambridgeshire CB7 4ET.

Decon Laboratories Ltd
Conway Street, Hove East Sussex BN3 3LY.

Digital Scientific Ltd
Sheraton House, Cambridge CB3 0AX.

ECACC (European Collection of Cell Cultures, Centre for Applied Microbiology & Research)
Salisbury, Wiltshire SP4 0JG.

Life Technologies Ltd
3 Fountain Drive, Inchinnan Business Park, Paisley PA4 9RF.

Ludl Electronic Products Ltd
171 Brady Avenue, Hawthorn, New York, 10532 USA.

Menzel-Glaser (Apogent Technologies Inc)
48 Congress Street, Portsmouth, New Hampshire, New Hampshire 03801, USA.

National Diagnostics
Unit 4 Fleet Business Park, Itlings Lane, Hessle, East Riding of Yorkshire HU13 9LX.

Nikon UK Limited
Nikon House, 380 Richmond Road, Kingston upon Thames, Surrey KT2 5PR.

Photometrics
USA West Coast, 3440 East Britannia Drive, Tucson, Arizona 85706 USA.

Promega Corporation
Delta House, Chilworth Research Centre, Southampton SO16 7NS.

Rathburn Chemicals Limited
Walkerburn, Scotland EH43 6AU.

Scientific Laboratory Supplies (SLS) Ltd
Units 26-27, Wilford Industrial Estate, Ruddington Lane, Wilford, Nottingham NG11 7EP.

Serotec Ltd
22 Bankside, Station Approach, Kidlington, Oxford OX5 1JE.

Sigma Chemical Company Limited
Fancy Road, Poole Dorset BH12 4QH.

Vector Laboratories Ltd
3 Accent Park, Bakewell Road, Orton Southgate, Peterborough PE2 6BR.

Vysis (UK) Ltd
Rosedale House, Rosedale Road, Richmond, Surrey TW9 2SZ.

Walker Safety Cabinets Ltd
Unit 2, Howard Town Mills, Mill St, Glossop SK13 8PT.

Abbreviations used in this thesis

AJCC	-	American Joint Committee on Cancer
CAS	-	Cell Analysis System
CGH	-	Comparative Genomic Hybridization
CNA	-	Copy Number Aberration
DNA	-	Deoxyribonucleic Acid
EBV	-	Epstein-Barr Virus
GST	-	Glutathione S-Transferase
H&E	-	Haematoxylin and Eosin
HNPCC	-	Hereditary Non-Polyposis Colorectal Cancer
HNSCC	-	Head and Neck Squamous Cell Carcinoma
HPV	-	Human Papilloma Virus
ISCN	-	International System for Cytogenetic Nomenclature
LNM	-	Lymph Node Metastases
LOH	-	Loss Of Heterozygosity
MMP	-	Matrix Metalloproteinases
MMR	-	Mis-match Repair
MRG	-	Minimal Region of Gain
MRL	-	Minimal Region of Loss
NAT	-	N-AcetylTransferase
PCNA	-	Proliferating Nuclear Cellular Antigen
RNA	-	Ribonucleic Acid
RR	-	Radio-Resistant
RS	-	Radio-Sensitive
TIMP	-	Tissue Inhibitor of Metalloproteinase
TNM	-	Tumour, Nodal metastases and Distant metastases system
UADD	-	Upper Aero-Digestive Tract
UICC	-	Union International Contre le Cancer
YAC	-	Yeast Artificial Chromosome